CELLULAR SIGNALLING BY TISSUE FACTOR AND LIPOPROTEINS IN THE PATHOGENESIS OF ATHEROSCLEROSIS

A PhD thesis submitted to the University of London

by Nicola J. James,

Department of Biochemistry and Molecular Biology,

Royal Free and University College Hospital Schools of Medicine,

University College London

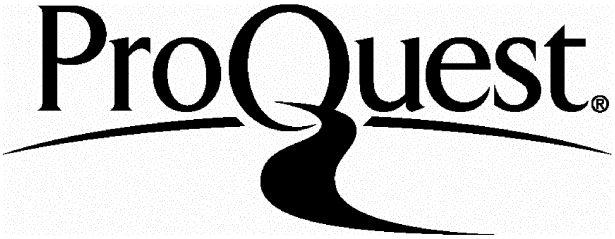

Dedicated to
my mother and father

ABSTRACT

Atherosclerosis is a chronic disease advanced by repeated episodes of endothelial injury. Upon endothelial injury, tissue factor: factor VIIa complexes (TF: FVIIa) are formed that promote production of fibrin and induce intracellular signalling.

A role for the cytoplasmic domain of TF in the induction of cytosolic Ca^{2+} transients was investigated. Wild type TF was cloned and a cytoplasmic deletion mutant was generated. Wild type and mutant TF were successfully expressed in Chinese Hamster Ovary K1 cells (CHO K1), however, unstable basal cytosolic Ca^{2+} levels precluded determination of the role of the cytoplasmic domain of TF in signalling.

The procoagulant activity of TF is inhibited by the apolipoprotein B100 moiety of native low density lipoprotein (LDL). The inhibitory motif is located in a 6-mer region of apo B100 (KRAD6). KRAD6 exhibited concentration-dependent inhibition of TF: FVIIa-induced cellular signalling. Furthermore, a 14-mer peptide, containing the KRAD6 sequence, decreased the formation of cellular networks in an *in vitro* model of angiogenesis.

The KRAD6 peptide inhibits both the procoagulant and signalling functions of TF: FVIIa. The KRAD6 may thus be of therapeutic use in diseases whose pathologies are linked with angiogenesis, such as atherosclerosis and metastasis.

TF activity and oxLDL are important risk factors for atherosclerosis. Activation of TF: FVIIa by oxLDL may contribute to the proatherogenic activity of oxLDL. The involvement of TF in the induction of cytosolic Ca^{2+} transients by LDL was investigated. Ca^{2+} responses to nLDL were independent of TF and a role for TF in Ca^{2+} signalling by oxLDL was equivocal. In addition, the data show that Ca^{2+} elevations to nLDL were transient, whereas oxLDL elicited sustained Ca^{2+} elevations. These distinct patterns of cytosolic Ca^{2+} flux enable cells to respond appropriately, in accordance with the oxidation status of LDL.

PUBLICATIONS AND PRESENTATIONS

Parts of this work have previously been published as;

- *James N.J., Ettelaie C., Prothero L.S., Richards C.D. and Bruckdorfer K.R. Inhibition of factor VIIa-induced cytosolic Ca^{2+} transients in Madin-Darby Canine kidney cells by an apolipoprotein B100-derived peptide Blood Coagulation and Fibrinolysis, Autumn 1998, P9
- James N.J., Ettelaie C., Briddon S., Watson S.P. and Bruckdorfer K.R. Inhibition of factor VIIa-induced Ca^{2+} transients by an apolipoprotein B100-derived peptide in monocytic THP-1 cells 5th European Vascular Biology Association meeting, Leuven 1998 H3
- James N.J., Briddon S., Ettelaie C., Watson S.P. and Bruckdorfer K.R. Potentiation of FVIIa induced cytosolic Ca^{2+} transients by factor X in monocytic THP-1 cells 5th EVBA meeting, Leuven 1998 H4
- James N.J., Ettelaie C. and Bruckdorfer K.R. (2001) Inhibition of TF activity reduces the density of cellular network formation in an *in vitro* model of angiogenesis Biochem Soc Trans (*in press*)
- James N.J., Ettelaie C., Richards C.D., and Bruckdorfer K.R. Inhibition of FVIIa-induced cytosolic Ca^{2+} transients in Madin-Darby canine kidney cells by an apolipoprotein B100-derived peptide (*submitted to FEBS Letters*)
- James N.J., Byrne D., Ettelaie C., Richards C.D., and Bruckdorfer K.R. The effects of lipid peroxidation on the ability of low density lipoprotein to induce Ca^{2+} transients in T24 bladder carcinoma cells (*manuscript in preparation*)

*Awarded Young Investigator's prize

Part of this work has been presented orally;

- James N.J. The role of tissue factor in the formation of tubular network structures in an *in vitro* model of angiogenesis. International Conference on "Thrombosis and hemostasis issues in cancer", Bergamo, Italy, November 2001
- James N.J. Inhibition of tissue factor activity reduces the density of cellular network formation in an *in vitro* model of angiogenesis. Biochemical Society Meeting, York, England, December 2001

ACKNOWLEDGEMENTS

I would like to thank my principal supervisor Richard Bruckdorfer for his guidance and the British Heart Foundation for their financial support. I would also like to thank Tony Michael and Annette Graham for their input. I am indebted to Chris Richards and Steve Watson for kindly granting me access to their fluorescence kinetic imaging equipment and to Nicholas Bradley for helping with the statistical analysis.

I would especially like to thank my partner, Camille Ettelaie, Dianne James and Claire Shannon-Lowe for their confidence in me. Thanks also to family and friends; Jim Butcher, Colin James, Stephen Butcher, Caroline Coleman, Sheila Simmonds, Leanne Court, Rammile and Carol Ettelaie, Maria and John Young, Janet and Terry Petersen, Judy and Mervyn Robbins, Les Wilkins, Dean Norgate, Matt Locke, Mike Rodenas, Kerissa Lawson, Carol Tate, Dan Wallace and Rhadi Anand for their interest and encouragement.

TABLE OF CONTENTS

1.2 Cardiovascular disease

1.3 The role of tissue factor in the progression of atherosclerosis

1.4 Calcium and cellular signaling mechanisms 59

1.5 Aims 60

CHAPTER 2: GENERAL METHODS

2.1 Mammalian cell culture methodology

2.2 Coagulation methods

2.3 Kinetic imaging methods

2.4 General molecular biology methods

CHAPTER 3: THE ROLE OF THE INTRACELLULAR DOMAIN OF TISSUE FACTOR IN THE INDUCTION OF CA^{2+} TRANSIENTS BY THE FVIIA : TISSUE FACTOR COMPLEX

3.1 Introduction

3.2 Aims

3.3 Methods

CHAPTER 4: INHIBITION OF TISSUE FACTOR :FVIIA-MEDIATED INDUCTION OF CA^{2+} TRANSIENTS BY AN APOLIPOPROTEIN B100-DERIVED PEPTIDE

4.6 Discussion

CHAPTER 5: THE ROLE OF TISSUE FACTOR IN THE FORMATION OF TUBULAR NETWORK STRUCTURES IN AN *IN VITRO* MODEL OF ANGIOGENESIS

5.1 Introduction

5.2 Aims

5.3 Methods

5.4 Results

6.4 Results

CHAPTER 7: GENERAL DISCUSSION

LIST OF FIGURES

LIST OF APPENDICES

LIST OF ABBREVIATIONS

Amino acids;

Alanine	Ala	A
Arginine	Arg	R
Aspartic acid	Asp	D
Asparagine	Asn	N
Cysteine	Cys	C
γ-carboxyglutamic acid	Gla	-
Glutamic acid	Glu	E
Glutamine	Gln	Q
Glycine	Gly	G
Histidine	His	H
Isoleucine	Ile	I
Leucine	Leu	L
Lysine	Lys	K
Methionine	Met	M
Phenylalanine	Phe	F
Proline	Pro	P
Serine	Ser	S
Threonine	Thr	T
Tryptophan	Trp	W
Tyrosine	Tyr	Y
Valine	Val	V

11-HETE	11-hydroxy-5,8,12,14-eicosatetraenoic acid
12-HETE	12-hydroxy-5,8,10,14-eicosatetraenoic acid
13-HODE	13-hydroxy-9,11,-octadecadienoic acid
15-HETE	15-hydroxy-5,8,11,13-eicosatetraenoic acid
18:1	Oleic acid
18:2	Linoleic acid
20:4	Arachidonic acid
5-HT	Serotonin
8-HETE	8-hydroxy-5,9,11,14-eicosatetraenoic acid
9-HETE	9-hydroxy-5,7,11,14-eicosatetraenoic acid

9-HODE	9-hydroxy-10,12,-octadecadienoic acid
Å	Angströms
ABP-280	Actin binding protein 280, filamin
ACAT	Acyl: cholesterol acyltransferase
ADP	Adenosine diphosphate
Apo B100	Apolipoprotein B100
AR	Amphiregulin
Bam H1	Restriction endonuclease
BTEB2	Basic transcription element binding protein 2
CHD	Coronary heart disease
CHO K1 cells	Chinese Hamster Ovary cells
CHO K1 (+TF*wt*)	CHO K1 cells expressing exogenous *wild-type* tissue factor
CHO K1(pVgRXR)	CHO cells transfected with pVgRXR plasmid
CTGF	Connective tissue growth factor
DEGRck	1,5-dansyl-Glu-Gly-Arg chloromethyl ketone
DMEM	Dulbecco's modified Eagle's medium
DMSO	Dimethyl sulphoxide
dNTP	Deoxynucleoside triphosphate
ECACC	European cell and animal culture collection
EGF1	FVII epidermal growth factor-like domain 1
EGF2	FVII epidermal growth factor-like domain 2
FACS	Fluorescence-activated cell sorter
FBS	Foetal bovine serum
$F_c\varepsilon$ RI	Immunoglobulin E receptor type I
FGF-5	Fibroblast growth factor 5
fra-1	fos-related antigen 1
Fura2AM	Fura2 acetoxymethylester
GD-FVIIa	Gla-domainless factor VIIa
Gla domain	γ-carboxyglutamic acid-rich domain
GM-CSF	granulocyte macrophage colony stimulating factor
GpIb	Platelet glycoprotein Ib
GpIIb/IIIa	Platelet glycoprotein IIb/IIIa
HaCaT	Human keratinocyte cell line
hbEGF	Heparin binding epidermal growth factor-like growth factor
Hind III	Restriction endonuclease

HMWK	High molecular weight kininogen
HMW-UK	High molecular weight urokinase
ICAM	Intercellular adhesion molecule
IGF-1	Insulin-like growth factor 1
IIb/IIIa	Fibrinogen receptor
KRAD 14	Lysine rich apolipoprotein B-100 derived 14-mer peptide
KRAD6	Lysine rich apolipoprotein B-100 derived 6-mer peptide
LCAT	Lecithin: cholesterol acyl transferase
LDL	Low-density lipoprotein
LMW-UK	Low molecular weight urokinase
LRP	LDL receptor related protein
M.I.	Myocardial infarction
MCP-1	Monocyte chemoattractant protein 1
M-CSF	Monocyte colony stimulating factor
MDCKI	Madin-Darby Canine kidney cells
mmLDL	Minimally oxidised LDL
MMP	Matrix metalloproteinases
nLDL	Native low-density lipoprotein
oxLDL	Fully oxidised LDL
PAI	Plasminogen activator inhibitor
PAR	Protease activated receptor
PBS	Phosphate buffered saline
PCR	Polymerase chain reaction
PD-ECGF	platelet derived endothelial cell growth factor
PDGF	Platelet derived growth factor
PI3K	Phosphatidylinositol 3-kinase
pIND(+TF*wt*)	Wild-type tissue factor cloned into pIND plasmid
pIND(+TF*del241-263*)	pIND plasmid containing mutant tissue factor
pIND(+TF*S253A*)	pIND plasmid containing mutant tissue factor
pIND(+TF*S258A*)	pIND plasmid containing mutant tissue factor
pIND(+TF*S263A*)	pIND plasmid containing mutant tissue factor
PI-PLC	Phosphatidylinositol phospholipase C
Pro C	Protein C
Pro S	Protein S
PUFA	Polyunsaturated fatty acid

Rac	GTPase
Rho	GTPase
RT-PCR	Reverse transcription polymerase chain reaction
SRA	Scavenger receptor A
sTF	Soluble tissue factor; the extracellular domain
THP-1	Human monocytic cell line
T24 cells	Human bladder carcinoma cells
tAP	Tick anticoagulant protein
TF	Tissue factor
TFPI	Tissue factor pathway inhibitor
TGFα and β	Transforming growth factor α and β
tPA	Tissue type plasminogen activator
TTP	Tristetraproline
uPA	Urokinase type plasminogen activator
uPAR	Urokinase plasminogen activator receptor
VCAM	Vascular cell adhesion molecule
VEGF	Vascular endothelial growth factor
vWF	von Willebrand factor

CHAPTER 1

GENERAL INTRODUCTION

1.1 Haemostasis

Haemostasis is a physiological response that is invoked to minimise blood loss in the event of vascular injury. Haemostasis involves five main mechanisms, namely, vasoconstriction, platelet plug formation, blood coagulation, permanent closure of the injured surface, dissolution of the clot and vascular remodelling. These processes serve to promote healing of injured arteries, however, chronic activation of haemostasis promotes the progression of cardiovascular disease.

1.1.1 Initial responses to vascular damage

The recruitment of circulating platelets to collagen exposed at the site of insult comprises the initial response to vascular injury. Collagen exposed upon endothelial injury binds von Willebrand factor (vWF) and changes its conformation, rendering it capable of binding and activating platelets via the platelet receptor glycoprotein Ib (GpIb) (Girma J.P., 1987 and Ruggeri Z.M., 1987). Upon activation, discoid platelets extend pseudopodia and become 'sticky'. The activated platelets aggregate and form a soft platelet plug that reduces or temporarily stems bleeding.

Figure 1.1: Factors released from activated platelets

Release product	Biological activity
Dense granules	
ADP	Platelet aggregation
Serotonin	Platelet aggregation, vasoconstriction, TF induction
α granules	
Platelet factor 4	Inhibition of heparin
PDGF	Proliferation of smooth muscle, endothelial and fibroblast cells
Thrombospondin	Reinforcement of fibrinogen-mediated platelet: platelet links
Thrombin	Platelet aggregation
Thromboxane A2	Platelet aggregation
Fibrinogen	Platelet aggregation
PAF	Platelet aggregation
PAI-1	Inhibition of the fibrinolytic pathway
TFPI	Inhibition of the extrinsic pathway
PD-ECGF	Proliferation of endothelial cells
VEGF	Induction of angiogenesis

ADP; adenosine diphosphate, PDGF; platelet derived growth factor, TGFα; transforming growth factor α, TGFβ; transforming growth factor β PAI-1; plasminogen activator inhibitor 1, TFPI; tissue factor pathway inhibitor, PD-ECGF; platelet-derived endothelial cell growth factor

Collagen-activated platelets release factors that accelerate the formation of the platelet plug, enhance vasoconstriction and initiate wound healing responses (figure 1.1). ADP released from activated platelets leads to the activation and recruitment of circulating platelets to the site of injury. Platelets also release serotonin (5-HT), a potent vasoconstrictor that acts locally to reduce blood flow to the injured area. The initial platelet response is a rapid and effective method of limiting blood loss, however the prevention of bleeding, attained in this manner, cannot be maintained indefinitely.

Damage to the endothelium also leads to the exposure of tissue factor (TF), that results in the initiation of the coagulation cascade and leads to the formation of fibrin (figure 1.2). Fibrin serves to provide structural reinforcement of the soft platelet plug. Fibrin forms bridges between platelets, by binding to the platelet cell surface receptors IIb/IIIa (GpIIb/IIIa) expressed on activated platelets.

Many of the blood coagulation reactions occur on a phospholipid surface. The phospholipid provided by activated platelets and damaged endothelial cells ensures that the coagulation process is restricted to the site of injury.

1.1.2 Overview of the coagulation cascade

The formation of fibrin has traditionally been divided into the extrinsic, intrinsic and common pathways (figure 1.2). The contact pathway leads to the activation of the intrinsic pathway.

The formation of fibrin ensues from a sequential cascade of activation of a series of circulating proteins. The proteins comprising the cascade mechanism were postulated to exist as inactive precursors that become activated by proteolysis (Davie E.W., 1964 and MacFarlane R.G., 1964) to enable stepwise activation of the proteolytic cascade. Many of these proteins were identified in patients with bleeding complications whose conditions were rectified by a protein present in normal plasma.

The extrinsic pathway and intrinsic pathway were once thought to act independently of one another. However, this strict hypothetical dichotomy is inconsistent with clinical observations. The blood of patients with deficiency of the contact pathway retains the ability to coagulate, demonstrating that the intrinsic pathway is not absolutely essential for blood clotting. On the other hand, haemophiliacs lacking coagulation factors belonging to the intrinsic pathway, bleed suggesting that the extrinsic pathway alone is not sufficient to support haemostasis. The classification of the coagulation cascade into two separate branches is thus an oversimplification of a more complex series of reactions. The extrinsic pathway is important in the initiation of fibrin formation and interacts with the intrinsic pathway, which is important in the amplification and maintenance of fibrin formation. Although the strict intrinsic/extrinsic

dichotomy of classification does not exist *in vivo*, for the purposes of discussion the pathways will be initially considered as two separate branches. A revised concept of coagulation is considered in the subsequent section.

1.1.2a The extrinsic pathway of blood coagulation

Initiation of the extrinsic pathway requires the presence of TF. Anatomically, TF is expressed in a pattern that forms an envelope surrounding the vascular tree (Drake T.A., 1989) and ensures that TF only comes in to contact with the blood in the event of vascular injury. TF is an integral membrane glycoprotein that is tightly associated with phospholipid and has a high affinity for circulating factor VII (FVII). Binding of the FVII ligand to its co-factor TF, in the presence of Ca^{2+} ions, facilitates the proteolytic conversion of the zymogen factor VII to an active serine protease (denoted FVIIa). Cleavage occurs at the Arg152-Ile peptide bond (Hagen F.S., 1986). The precise molecular nature of the interaction of TF with FVII, which facilitates the activation of FVII by TF is presented in chapter 4.

Formation of the TF: FVIIa complex enables the docking of factor X (FX) to a binding site, which extends across both TF and FVIIa. FX is then converted to a serine protease (denoted FXa) by the cleavage of a single Arg52-Ile peptide bond (DiScipio R.G., 1977).

1.1.2b The intrinsic pathway of blood coagulation

Activation of XI by thrombin in the presence of a negatively charged surface, such as heparin or dextran sulphate, occurs due to cleavage of the Arg369-Ile peptide bond in each of the two subunits (Naito K., 1991). FXIa autoactivates FXI in the presence of dextran sulphate (Naito K., 1991) and activates FIX in the presence of Ca^{2+} ions (DiScipio R.G., 1978).

Factor XIIa (FXIIa) activates FXI and is generated by the activity of kallikrein. Kallikrein is produced by the action of high molecular weight kininogen (HMWK) upon plasma prekallikrein. Patients deficient in FXI experience bleeding episodes, in contrast to patients deficient in FXII, prekallikrein or HMWK. These latter three proteins are, however, involved in the activation of FXI when plasma encounters a surface such as glass or kaolin *in vitro*.

If the amount of TF is limiting following vascular injury, the activation of factor FX by the intrinsic pathway, rather than by the TF: FVIIa complex may play a significant role in the initiation of coagulation (Bauer K.A., 1990). The activation of FIX by the TF: FVIIa complex occurs by proteolysis of the Arg145-Ala and the Arg180-Val peptide bonds (DiScipio R.G, 1978 and Yoshitake S., 1985). The FIXa forms a complex with the co-factor FVIIIa in the presence of Ca^{2+} ions and phospholipid. FVIIIa is itself activated by proteolysis of the Arg372-Ser, Arg470-Ser and Arg1689-Ser peptide bonds (Toole J.J., 1984, Vehar G.A.,

1984 and Eaton D., 1986). The initial cleavage of FVIII occurs in the presence of factor Xa, Ca^{2+} ions and phospholipid, or by thrombin alone once it has formed (Eaton D., 1986). The FIXa:FVIIIa complex activates FX by proteolysis of the same peptide bonds that are cleaved by the TF: FVIIa complex.

1.1.2c The common pathway of blood coagulation

FXa formed by both the intrinsic and extrinsic pathways comprises the first step in the initiation of the common pathway. FXa binds FVa in the presence of Ca^{2+} ions and phospholipid (Tracy P.B., 1981). The prothrombinase complex converts the zymogen prothrombin to the proteolytically active serine protease, α-thrombin. The activation of FV is initially catalysed by FXa, in the presence of Ca^{2+} and phospholipid (Monkovic D.D., 1990) and also later, by thrombin (Nesheim M.E., 1979, Esmon C.T., 1979 and Suzuki K., 1982). In either case, activation results from the cleavage of two internal peptide bonds, Arg170-Ser and Arg1545-Ser (Guinto E.R., 1982 and Laue T.M., 1989).

Prothrombin activation results from cleavage of two internal peptide bonds; Arg271-Thr and Arg320-Ile. The formation of thrombin facilitates the conversion of fibrinogen to fibrin by limited proteolysis. Fibrin is formed by the cleavage of a peptide bond (Arg18-Gly) in each of the two α chains and the Arg16-Gly bond in each of the two β chains (Blomback B., 1972). The new amino terminal sequences bind to domains in adjacent fibrin monomers resulting in the side-by-side polymerisation of fibrin.

Further strengthening of the clot arises from the cross-linking of monomers by FXIIIa, a transglutamidase forming ε-(γ-glutamyl)-lysine bonds between two adjacent molecules (Folk J.E., 1977). FXIIIa also incorporates other plasma proteins, including fibronectin and α2-anti-plasmin, into the clot in a similar manner. Thrombin cleaves FXIII at the Arg37-Gly peptide bond in each of the two α chains of the molecule (Takagi T., 1974, Ichinose A., 1986, Curtis C.G., 1974 and Hornyak T.J., 1991).

1.1.2d The revised coagulation theory

Both the intrinsic and extrinsic pathways generate FXa that leads to the activation of the common pathway. Although the division of the coagulation cascade into two separate limbs eases the discussion of the subject the view is outmoded given the multiple interactions of the clotting factors. The current view of the coagulation mechanism is that the extrinsic pathway forms a small amount of thrombin that primes the coagulation system and leads to the induction and maintenance of a secondary burst of coagulation via feedback activation of the intrinsic pathway. Thrombin exerts positive feedback over the activation of coagulation

proteins higher in the cascade, including FXI (Roberts H.R., 1998), FVIII and FV. Thrombin-mediated activation of FXI, in the intrinsic pathway, results in the activation of FXa by FIXa. This mechanism explains why patients with factor XII, prekallikrein or HMWK deficiency do not experience abnormal bleeding.

It has recently been discovered that the TF: FVIIa activates both factors X and IX (Roberts H.R., 1998). The resulting FXa and FIXa play very distinct roles in the subsequent clotting reactions (Monroe D.M., 1994 and Hoffman M., 1995). FXa remains in the vicinity of the TF bearing cell where it interacts with its co-factor, FV. The FXa:FVa complex converts prothrombin to thrombin, but the amount of thrombin formed is very small. The FIXa resulting from TF: FVIIa activation is mobile and finds its way to the surface of activated platelets, where it binds with high affinity (Kd of 0.2nM) in the presence of FVIIIa. The activation of FVIII, on the platelet surface, results from the ability of thrombin to dissociate of vWF from FVIII. The platelet bound FIXa:FVIIIa complex recruits and activates solution phase FX. Platelet bound FXa converts prothrombin to thrombin in quantities sufficient to result in the formation of a stable fibrin clot.

Amplification of the intrinsic pathway by thrombin generated during activation of the extrinsic pathway is important in sustaining coagulation since the extrinsic pathway is quickly inhibited by tissue factor pathway inhibitor (TFPI). TFPI prevents the activation of FX by the TF: FVIIa complex by forming a complex with the ternary complex of TF: FVIIa:FXa (Girard T.J., 1989). TFPI is the main physiological inhibitor of TF-induced coagulation (Broze G.J. Jr., 1990). The discovery that the generation of thrombin in baboons causes acute release of TFPI demonstrates the importance of thrombin in initiating inhibition of the extrinsic pathway (Lupu C., 1999), since the binding of TFPI to TF results in the endocytosis of TF.

Haemophiliacs exhibit deficiency of the intrinsic pathway proteins; either FVIII (haemophilia A), (Sadler J.E., 1987) or factor IX (haemophilia B), (Hedner U., 1987). However, these patients have normal circulating levels of FVII, FX and abundant TF at the site of injury. Upon inhibition of the TF-mediated coagulation response by TFPI, coagulation is normally sustained via the intrinsic pathway however, since haemophiliacs lack an essential intrinsic factor, bleeding persists. Notwithstanding, blood from patients completely deficient in FVII remains able to form a fibrin clot albeit slowly implying that there is redundancy of function in the coagulation system.

Figure 1.2: The coagulation cascade

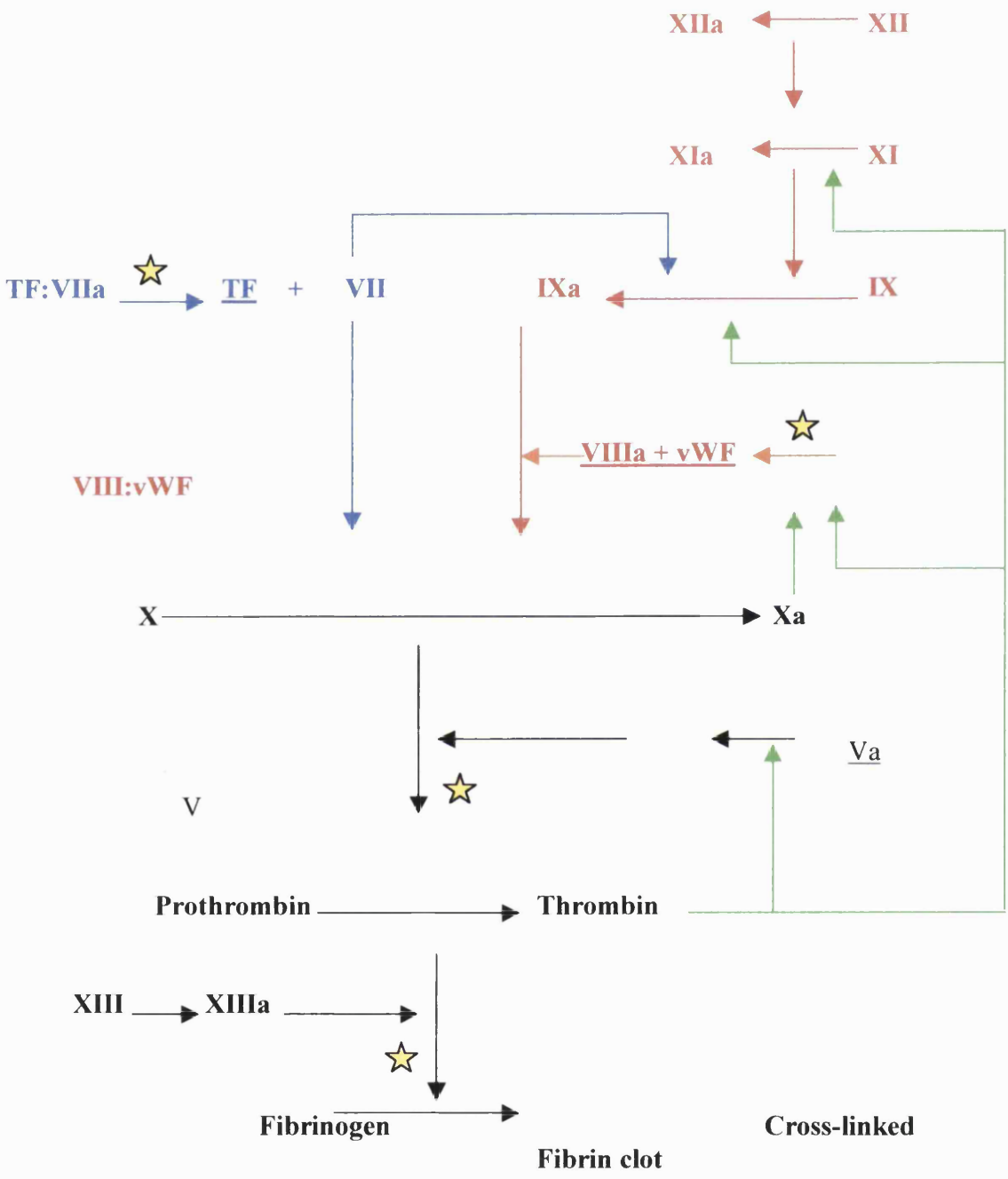

Legend:
Pathways: Intrinsic, Extrinsic, Common, positive feedback
☆; Ca^{2+} and phospholipid co-factors. Protein co-factors are underlined.
Coagulation factors shown as Roman numerals, activated forms denoted with 'a'
TF; tissue factor, vWF; von Willebrand factor.

1.1.3 The fibrinolytic pathway

Fibrinolysis prevents fibrin clots from becoming too large, induces wound healing and prevents thrombosis in undesirable locations (figure 1.3). Activation of the fibrinolytic pathway ultimately results in the activation of plasminogen to plasmin. Tissue-type plasminogen activators (tPA) and urokinase-type plasminogen activators (uPA) are two important extrinsic plasminogen activators. Studies of plasmin knock-out mice reveal impairment of wound healing. Wound healing is essentially a vascular remodelling process that involves the formation of a fibrin clot, which contracts to close the wound and is eventually degraded by plasmin. In addition, connective tissue is degraded to allow the migration of cells during the angiogenic phase of vascular remodelling. Plasmin has been implicated in vasculogenesis and angiogenesis. The activities of plasmin are a key feature of vascular remodelling and include the lysis of fibrin clots and degradation of the extracellular matrix via activation of matrix metalloproteinases that digest elastin and collagen.

Figure 1.3: Fibrinolysis - the protein C pathway

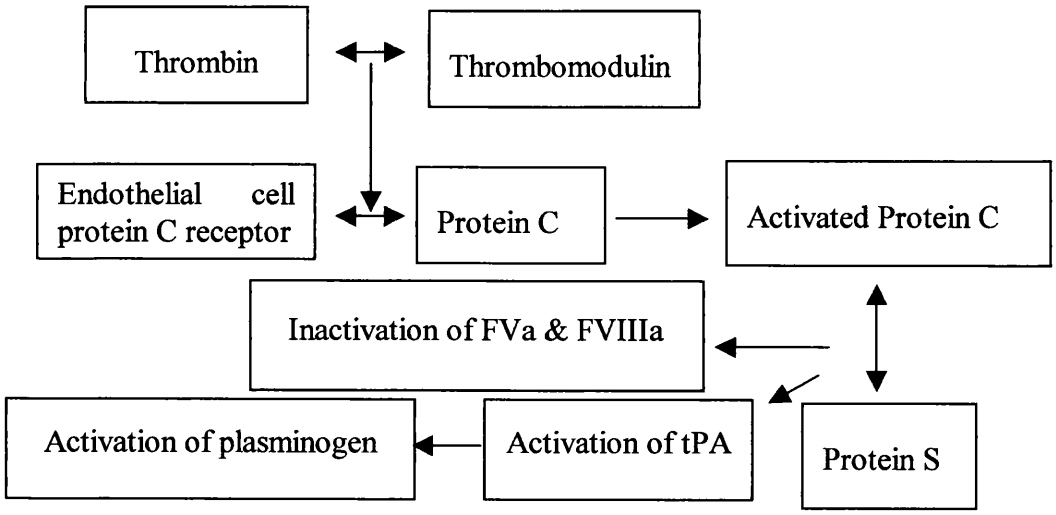

Legend; tPA, tissue plasminogen activator, ◄—► = interaction

The contact pathway of coagulation, consisting of high molecular weight kininogen (HMWK), prekallikrein and factor XII, induces the activation of uPA (Bell W.R., 1996). Activation of the contact pathway leads to the generation of kallikrein, which then activates pro-uPA. uPA then induces the formation of plasmin from the proenzyme plasminogen.

tPA is generated via the activation of the protein C pathway (Narayanan S., 1999). The binding of thrombin to thrombomodulin, that itself is bound to the endothelial cell protein C receptor, abolishes its procoagulant activity and induces the activation of protein C (Pro C), (Esmon C.T., 1997, Stubbs M.T., 1993 and Esmon C.T., 1987). Activated protein C (APC) then binds to protein S (Pro S) on platelet and endothelial cell membranes. The Pro C:Pro S

complex activates tissue plasminogen activator (tPA). In addition, the Pro C:Pro S complex inactivates plasminogen activator-inhibitor 1 and the coagulation co-factors V and VIII. The thrombin-thrombomodulin complex also activates an inhibitor of fibrinolysis, called the thrombin-activatable fibrinolysis inhibitor (TAFI).

1.1.4 Regulation of coagulation and fibrinolysis

The activation of the extrinsic pathway of coagulation is self down-regulated, since thrombin generation leads to the release of TFPI. The substrate specificity of thrombin is determined by thrombomodulin and influences the balance between coagulation and fibrinolysis. Since thrombin generation is related to the amount of exposed tissue factor (van't Veer C., 1994) the equilibrium between the processes of coagulation and fibrinolytic pathways may be indirectly determined by TF. Furthermore, TF suppresses fibrinolysis by inhibiting the pro C-mediated inactivation of FVa (Varadi K., 1999). In contrast, TF may directly activate fibrinolysis (Fan Z., 1990) via the interaction of the extracellular domain with plasminogen kringle domains. The overall balance between these two opposing activities of TF has not been explored.

1.2 Cardiovascular disease

The underlying cause of cardiovascular disease is inextricably linked with the blood coagulation system. Activation of the coagulation pathway is a protective measure to prevent severe haemorrhage upon injury. The subsequent induction of the fibrinolytic pathway promotes healing of the wound. However, chronic activation of the blood coagulation system and fibrinolytic pathway, due to episodic pathologic insult to the endothelium, contributes to the progression of cardiovascular disease. The following text provides a review of the literature pertaining to the incidence and pathobiology of cardiovascular disease in humans. The role of the coagulation and fibrinolytic systems in the development and progression of atherosclerosis is discussed.

1.2.1 Overview

Atherosclerosis is a chronic disease of the vascular system, almost exclusive to humans, that is responsible for considerable morbidity and mortality in industrialised nations. Since the disease is typically manifest after the procreational period of life, selective genetic pressures are not exerted upon factors predisposing humans to heart disease. Both genetic and environmental risk factors associated with atherosclerosis have been identified (figure 1.4).

The early stages of atherosclerosis are broadly characterised by lipid deposition in the arterial wall. Over time, these lesions may be induced to develop into complicated fibrolipid lesions

that may elicit a severe symptomatic disease state. Complicated lesions exhibiting particular characteristics (see 1.2.9) are predisposed to rupture. Rupture of lesions tends to be responsible for the majority of the morbidity and mortality arising from cardiovascular disease (Stary H.C., 1995). Cardiovascular disease may manifest as either stable or unstable angina and can ultimately lead to myocardial or cerebral ischaemia resulting in myocardial infarction or cerebral infarction (stroke). The factors that determine whether lesions progress into an unstable or stable type are complex and not fully understood but are outlined in section 1.2.9.

Figure 1.4: Risk factors for cardiovascular disease

Elevated levels of LDL/VLDL	High-fat diet
Reduced levels of HDL	Smoking
Hypertension	Low antioxidant levels
Diabetes	Lack of exercise
Obesity	Infectious agents
Elevated levels of haemostatic factors	Contraceptive pills
Depression	Maleness

1.2.2 Histological classification of the development of atherosclerotic lesions

Atherosclerotic lesions may either be silent with no gross effect on normal physiology or may indeed cause morbidity and/or mortality. In order to treat patients with atherosclerosis effectively, knowledge of the factors relating to the propensity of lesions to cause detriment is necessary. To this end, a histological classification of the stages of atherosclerosis as well as a correlation of lesion type with clinical syndromes have been documented by the American Heart Association (Stary H.C, 1995). Lesions are designated by Roman numerals that signify the usual sequence of lesion progression (figure 1.5).

Figure 1.5a: The histological classification of type I and type II atherosclerotic lesions

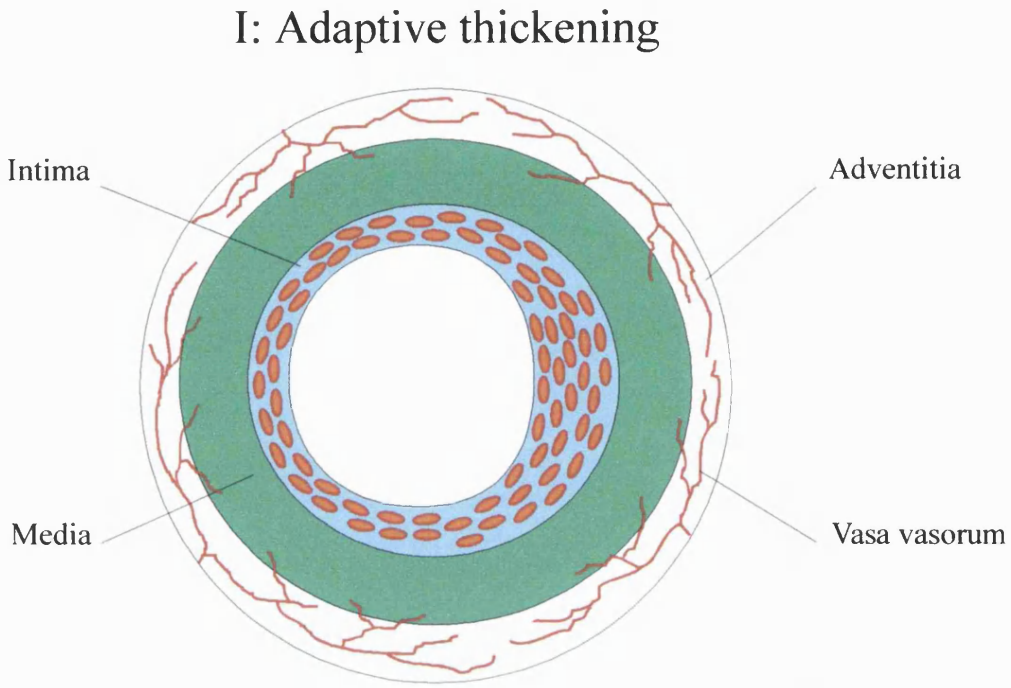

Adaptive thickenings are present at birth especially at arterial bifurcations and result from adaptations to local mechanical forces.

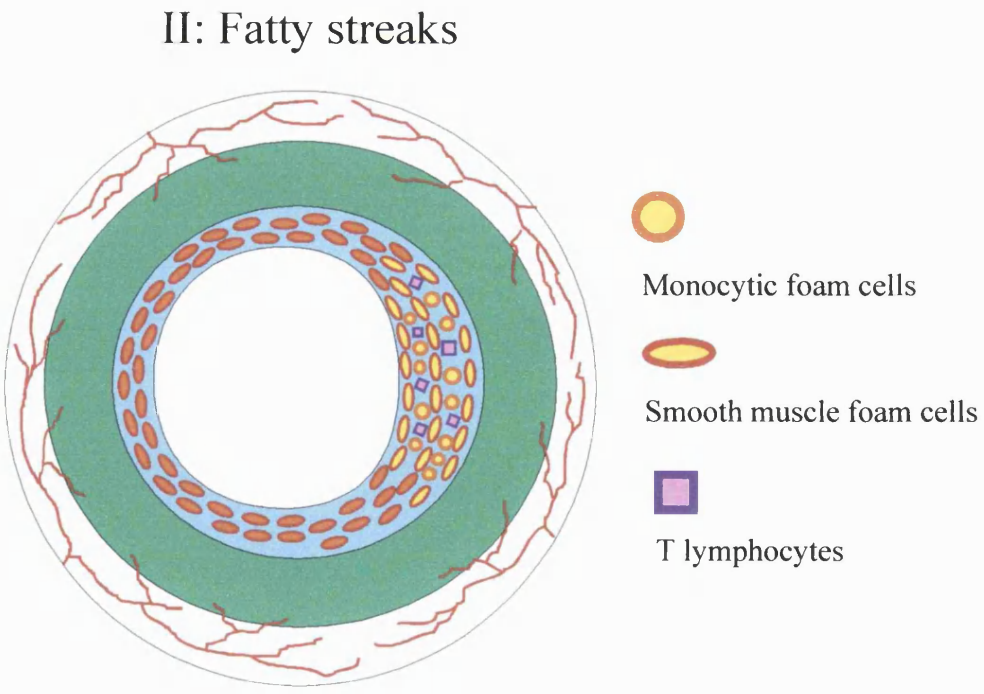

Fatty streaks consist of layers of macrophages foam cells and smooth muscle foam cells. T-lymphocytes are also present.

Figure 1.5b:The histological classification of type III and type IV atherosclerotic lesions

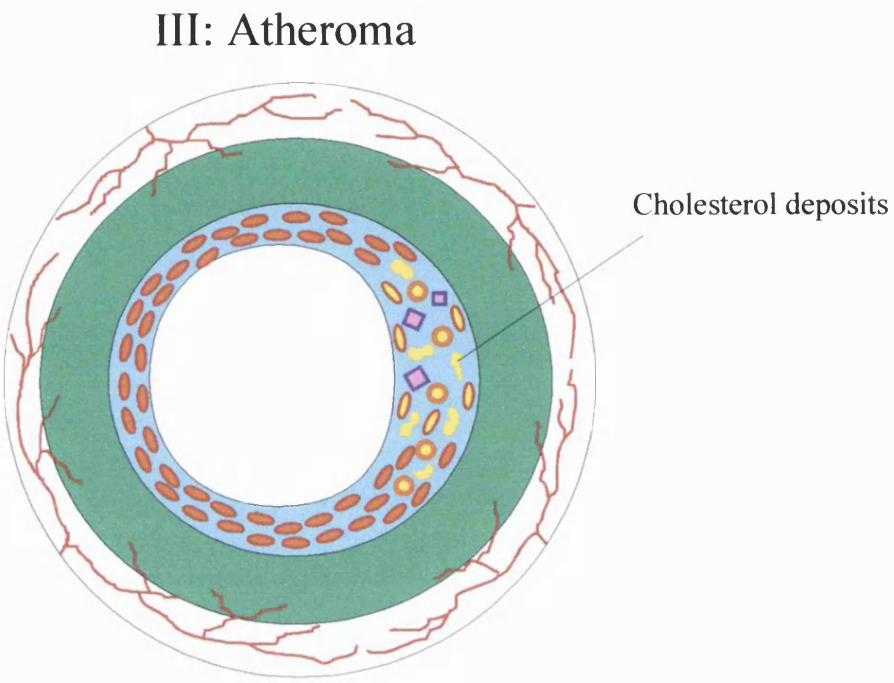

Scattered collections of extracellular lipid deposits disrupt the coherence of smooth muscle cells

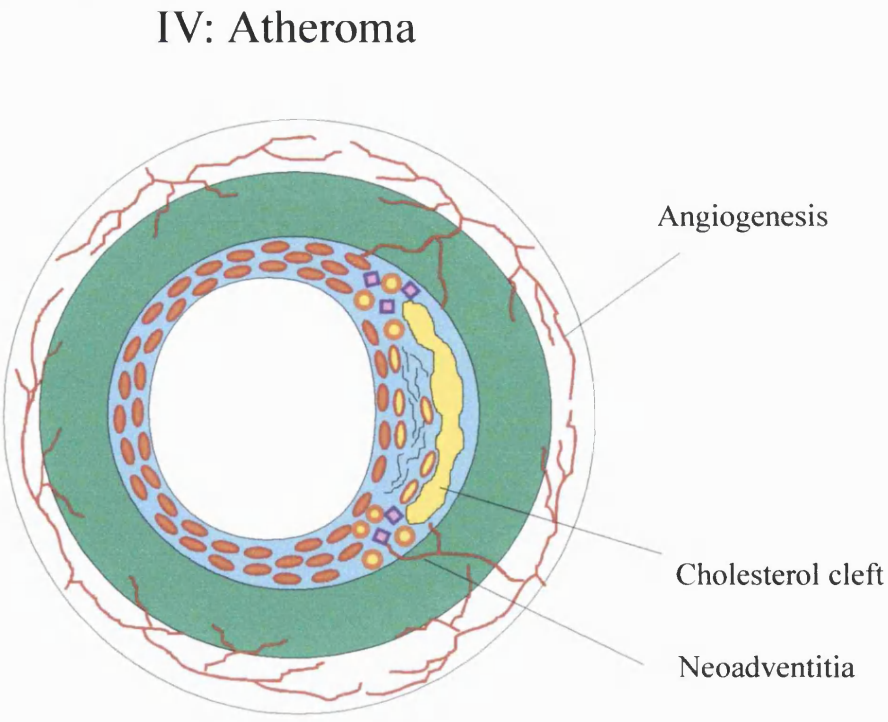

Smaller deposits of lipid coalesce to form large cholesterol clefts. Neovascular capillaries border the lipid core. Macrophages and lymphocytes tend to associate with these capillaries.

Figure 1.5c: The histological classification of type V and type VI atherosclerotic lesions

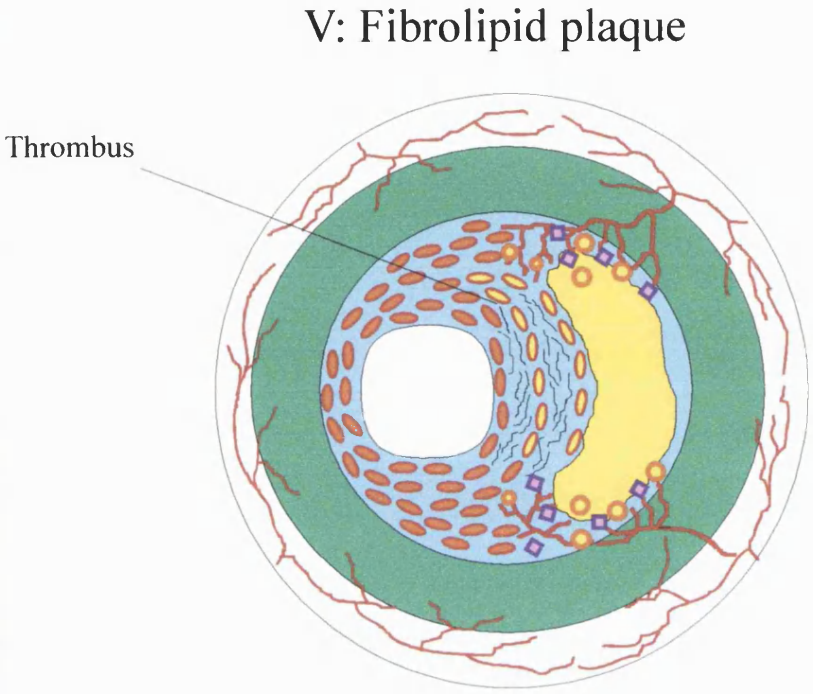

Thick layers of collagenous fibrous connective tissue forms above the lipid core. Layers of thrombi and smooth muscle cells are present. Neovascular capillaries increase in number and size.

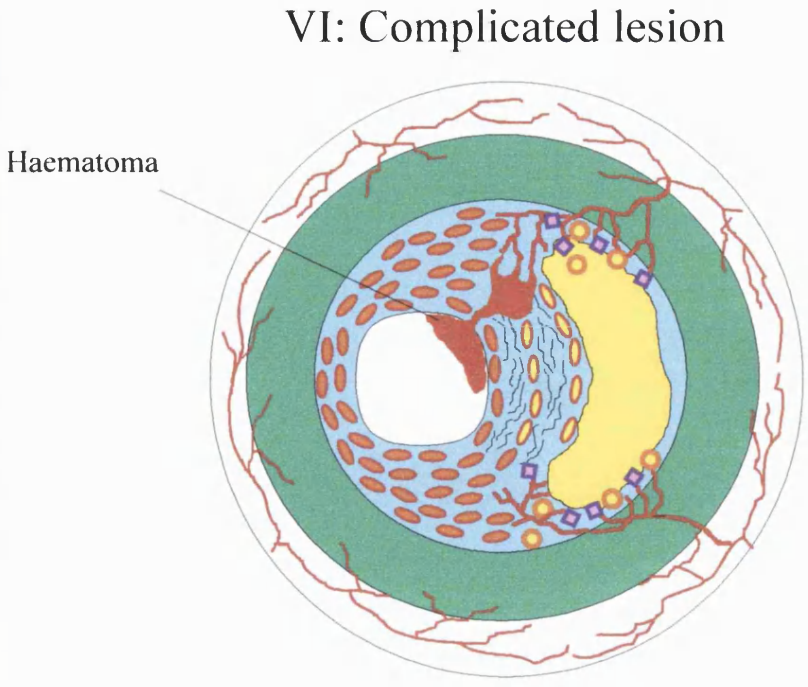

Complicated lesions may contain fissures, haematoma or thrombus.

Type I lesions contain atherogenic lipoprotein that results in an increase in macrophages. Macrophages internalise and accumulate these modified lipids in an unregulated manner (Steinbrecher U.P., 1984 and Morel D.W., 1984) resulting in the formation of scattered foam cells. Type I lesions tend to be more marked in areas of adaptive thickening. Adaptive thickenings do not obstruct the lumen, are present at birth and result from adaptations to local mechanical forces. Type II lesions are grossly designated as 'fatty streaks' and consist of layers of macrophage foam cells and lipid–laden smooth muscle cells. Type II lesions also contain T lymphocytes. Type III lesions, are potentially symptom-producing. Scattered collections of extracellular lipid droplets are evident and may disrupt the coherence of intimal smooth muscle cells. The scattered lipid droplets are the precursors of a larger core of lipid that characterises type IV lesions, or atheroma. Formation of the lipid core precedes an increase in fibrous tissue that changes the nature of the intima above the lipid core. Around the fourth decade of life, type IV lesions or fibrolipid plaques may progress to type V lesions or directly to type VI lesions. Type V lesions contain thick layers of fibrous connective tissue. Type VI lesions result from plaque fissure and contain haematoma and thrombus (type VI lesion). Type V lesions consist of multi-layers of lipid separated by fibrous connective tissue. These multi-layered fibroatheroma are classes as type Va lesions. Alternatively, calcium may predominate in type V lesions (type Vb) or may consist mainly of connective tissue and little or no lipid or calcium (type Vc). Both type IV and type V lesions may be complicated by disruption of the lesion surface, haematoma or thrombotic deposits. Type VI lesions may contain fissures (type VIa), haematoma (type VIb) or thrombosis (type VIc). The flow diagram in figure 1.6 indicates the pathways in the evolution and progression of atherosclerotic lesions.

1.2.3 The 'response-to-injury' hypothesis of the initiation of atherosclerosis

Ross integrated earlier hypotheses (von Rokitansky 1852, Virchow 1856 and Duguid J.B., 1946) into a unified 'response-to-injury' hypothesis (Ross R., 1986 and Ross R., 1993). The 'response-to-injury' hypothesis of atherogenesis proposes that injury to the endothelium is the critical initiating event. Endothelial cells have tight intercellular junctional complexes and function as a selectively permeable barrier between blood and tissues. The orientation of endothelial cells in areas of arterial branching or curvature become misaligned and become permeable to macromolecules such as LDL. Such areas are preferential sites for lesion formation. Fatty streaks are found at bifurcations in the arterial tree, often coincident with areas of intimal thickening. Vascular injury has been classified into classes that represent increasing stages of severity (figure 1.7, Fuster V., 1992a).

Figure 1.6:
Pathways in the evolution and progression of atherosclerosis

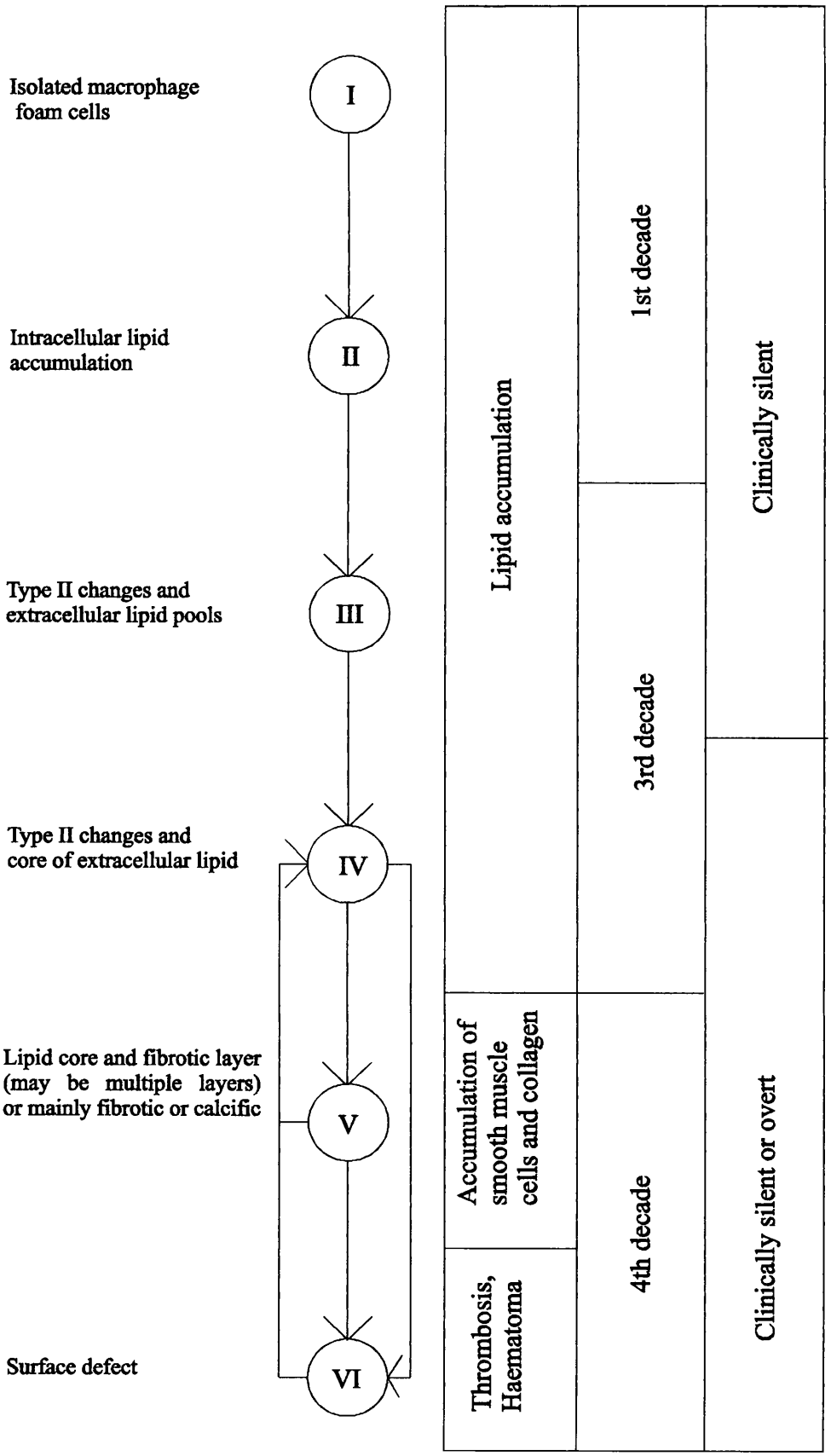

Figure 1.7: Classification and outcome of endothelial injuries

Injury type	Mediator of injury
1	Arterial bifurcation
	Infection
	Vasoactive amines
	Immuno-complexes
	Chemical irritants e.g. tobacco smoke
2	Oxidised LDL
	Release of toxic products by macrophages
	Adhesion of platelets to subendothelial collagen
3	Rupture of plaques

Type 1 injuries result in functional but not morphologic changes in endothelial cells and may be potentiated by hypercholesterolaemia.
Type 2 injury leads to the release of growth factors that induce migration and proliferation of smooth muscle cells to produce fibrointimal lesions.
Type 3 injury is the most serious type of injury and results in thrombus formation.

Manifestations of the dysfunction of the endothelium caused by injury include increased trapping of lipoprotein in the artery (Mora R., 1987) and the appearance of specific adhesive glycoproteins on the endothelial surface. Monocytes and T-lymphocytes attach to these glycoproteins and migrate between the endothelial cell under the influence of growth regulatory molecules and chemotactic factors released by the endothelium, the adherent leukocytes and underlying smooth muscle cells.

1.2.4 The progression of atherosclerosis

The processes invoked by endothelial injury, in normal circumstances are a protective response. However, chronic episodic insult to the endothelium leads to the formation of atherosclerotic lesions due to activation of an inflammatory-fibroproliferative response. The subendothelial migration of monocytes and T cells coupled with the deposition of subendothelial lipid give rise to the conditions for the oxidation of subendothelial deposits of lipoprotein by monocytes, smooth muscle cells and endothelial cells (Morel D.W., 1984 and Cathcart M.K., 1985). The nature of the initiating radical is discussed in section 6.1.2. Evidence suggests that oxLDL is a key component in endothelial injury (Cathcart M.K., 1985, Rosenfeld M.E., 1990 and Steinbrecher U.P., 1990).

OxLDL leads the to expression of the scavenger receptor by monocytes and smooth muscle cells (Fogelman A.M., 1981). Expression of the scavenger receptor leads to the endocytosis of oxLDL. Since the scavenger receptor pathway does not exhibit negative feedback, macrophages and smooth muscle cells accumulate lipid and become foam cells. These foam cells are responsible for the visual appearance of the fatty streaks of type II lesions. The

ubiquity and early onset of the atherosclerotic process is supported by the finding of fatty streaks in the coronary arteries of half the autopsy specimens from children aged 10 to 14 years (WHO, 1985, Stary H.C., 1989 and McGill H.C. Jr, 1984).

In type III lesions deposits of lipid in the extracellular milieu disrupt the organisation of smooth muscle cells (Stary H.C., 1995). The scattered lipid droplets may coalesce to form a larger, more disruptive lipid core that characterises type IV lesions (Stary H.C., 1989). It has been suggested that foam cell-derived oxidised lipids constitute a significant proportion of the core of advanced lesions (Mitchison M.J., 1985, Rosenfeld M.E., 1990 and Ball R.Y., 1995). OxLDL has a central role in the progression of atherosclerosis due to its ability to elicit an array of proatherogenic responses by arterial cells (figure 1.8).

Newly-formed capillaries surrounding the lipid cores in type IV lesions are derived from the adventitial vasa vasorum by neovascularisation or angiogenesis. The neovascular capillaries grow towards the boundary of the lipid core. Macrophages and T cells tend to associate with the capillaries and are also more prevalent at the periphery of the lipid core (Stary H.C., 1995 and Mitchell J.R.A., 1965). The presence of these cells at the plaque periphery in type IV lesions may allude to a role for these cells in the development of neovascularisation. The extent of angiogenesis is positively correlated with the severity of the plaque (Kamat B.R., 1987). In addition, plaque regression is accompanied by regression of neovascularisation (Williams J.K., 1988). A link between angiogenesis and intimal hyperplasia has been established (Stabb M.E., 1997). The appearance of new capillaries in areas of vascular thickening prior to the development of plaques (Kwon H.M., 1998) suggests that angiogenesis facilitates intimal hyperplasia. The observation that inhibitors of angiogenesis limit plaque growth in apolipoprotein E deficient mice supports this interpretation (Moulton K.S., 2000).

The formation of capillaries at the margins of the lipid core becomes pronounced in type V plaques. The progression of type IV to type V lesions also corresponds to an increase in fibrous tissue, mainly collagen, above the lipid core. Collagen is secreted from an expanded population of differentiated smooth muscle cells originating from the media. The growth of smooth muscle cells narrows the artery leading to intimal thickening. Reparative connective tissue forms at sites where accumulations of extracellular lipid disrupt the normal tissue structure. Apoptosis in the lipid core of lesions leads to the formation of necrotic cores. Type V lesions consist of a large lipid core beneath a fibrous cap. Plaque instability may lead to fissure of the lesion and haematoma or thrombus. The presence of haematoma or thrombus defines type VI plaques. Haematoma may also result from haemorrhage of angiogenic capillaries (Paterson J.C., 1936, Barger A.C., 1984 and Beeuwkes R III., 1990).

Figure 1.8: Proatherogenic responses of arterial cells to oxidatively modified LDL

Cell type	Direct effect	Indirect effect
Endothelial	Synthesis of adhesion molecules ELAM-1. ICAM-1, GMP-140	Adhesion of monocytes
	Synthesis of chemoattractants; MCP-1	Transendothelial migration of monocytes
	Synthesis of colony stimulating factors; M-CSF, GM-CSF	Proliferation of smooth muscle cells
	Synthesis of growth factors; bFGF, PDGF	Proliferation of smooth muscle cells
	Impaired NO secretion	Vasoconstriction and platelet adhesion
	Secretion of EDRF	Vasoconstriction
	Secretion of prostaglandins	Platelet aggregation
	Impaired protein C synthesis	Thrombin generation, platelet aggregation and coagulation
	Enhanced TF synthesis	Thrombin generation, platelet aggregation and coagulation
	Inhibition of tPA synthesis	Defective fibrinolysis
	Stimulation of PAI-1 synthesis	Defective fibrinolysis
Monocytes/macrophages	Synthesis of MCP-1	Chemoattraction of monocytes
	Endocytosis of oxLDL	Foam cell generation
	Increased presentation of antigens	Activation of immune responses
Smooth muscle	Direct chemoattraction	Migration of smooth muscle cells
	Synthesis of PDGF	Migration of smooth muscle cells
	Synthesis of bFGF	Proliferation of smooth muscle cells
		Scavenger receptor expression and foam cell generation

The progression of atheromatous plaques is mediated by the expression of a variety of growth factors and cytokines. Classically the former are involved in chemotaxis and proliferation while the latter are involved in inflammatory responses. However, with respect to atherosclerosis these two roles are closely inter-related. The growth regulatory molecules elicit the migration, proliferation and differentiation of monocytes, endothelial cell and smooth muscle cells. A table of these complex interactions detailing the cellular sources and targets, of various growth factors is presented in figure 1.9. Many of these growth factors elicit the secretion of further growth factors by other cells. Thus, induction of the healing response is transmitted across different arterial cell types to elicit a co-ordinated response.

1.2.5 Lipoproteins and atherosclerosis

Lipids are transported in the blood as a component of globular particles called lipoproteins. Lipoproteins also have a role in immune reactions, coagulation and tissue repair (Durrington P.N., 1994). Lipoproteins generally consist of a hydrophobic core of lipids encapsulated by polar phospholipids. Proteins, known as apolipoproteins, are associated with the lipoproteins and serve structural and regulatory functions. The composition of lipoproteins is outlined in figure 1.10 and the metabolic pathway is depicted in figure 1.11.

The LDL of human plasma is composed of a heterogeneous mixture of discrete particle subspecies that differ in their physicochemical and biological properties. LDL isolated from individual subjects is heterogeneous in terms of its density (Nelson C.A. 1977). Plasma LDL has been subfractionated on the basis of density into three major subclasses, namely, light density LDL (1.018-1.030g/ml), intermediate density LDL (1.030-1.040g/ml) and small dense LDL (1.040-1.065g/ml), (Chapman M.J., 1988). Each of the subclasses differs in their physicochemical and biological properties (Lindgren F.T., 1969, Ghosh S., 1993, Nelson C.A., 1977, Rubenstein B., 1978, Shen M.M.S., 1982, Teng B.A., 1985, Patsch W.R., 1982 and Lee D.M., 1970).

Hydrodynamic analysis demonstrates that individual LDL subfractions have distinct peak flotation rates and particle sizes, which vary inversely in proportion to density. The flotation rates of subspecies with average densities of 1.0260 to 1.0409 g/ml range from 9.3 to 5.2. Subspecies with average densities of 1.024 to 1.049 g/ml range from 229 to 214 Angstroms in diameter respectively. The molecular weights also decrease progressively with increased density. Individual LDL subclasses typically resolve as unique narrow bands using polyacrylamide gradient gel electrophoresis and each band correlates with a unimodal refractometric profile upon examination by analytical centrifugation.

Examination of the net electrical charge by agarose gel electrophoresis revealed that each subspecies has discrete mobility and thus unique net negative charge. Intermediate density LDL (1.0297 to 1.0327 g/ml) had the lowest negative charge, while dense LDL (1.0393 to 1.0483g/ml) displayed slightly increased net negative charge.

Analysis of the composition of LDL subclasses revealed some common features. Cholesteryl ester is the predominant lipid ester (38.3-42.8%) in all LDL subclasses and tends to diminish as density increases. Triglycerides are a minor component (3-5%). The proportion of free cholesterol tends to diminish within a narrow range between subclasses (8.5-11.6%). The ratios of cholesteryl ester to free cholesterol or phospholipid increase with density whereas the free cholesterol to phospholipid ratio is constant. The phospholipid to protein ratio was constant in light density LDL (1.0260 to 1.0314 g/ml) but was reduced 0.2-fold as density increased.

Apolipoprotein B-100 was the major protein in all subfractions and was slightly more than 1 molecule per LDL particle. Apo B100 is the sole apoprotein in all subspecies of LDL from 1.0271-1.0393g/ml, however, Apo E and apo(a) were detected in subspecies of LDL above and below these densities. Trace amounts of Apo CIII were detected at densities greater than 1.0358g/ml.

Intermediate density LDL binds with higher affinity to the LDL receptor than either light or dense LDL (Nigon F., 1991). As a consequence, intermediate LDL is degraded *in vivo* more quickly than the light or dense subspecies of LDL.

The differences in the physicochemical properties of human LDL probably arises due to differences in their origins and metabolism and possibly predicts their fate and may further be indicative of their atherogenicity.

A landmark lipid intervention trial (Steinberg D., 1997a) conclusively showed a cause-and-effect relationship between blood cholesterol levels and risk of coronary heart disease. However, myocardial infarction is evident in people with low cholesterol levels (<200) and patients with high cholesterol levels (>300) may show no clinical signs of CHD (Steinberg D., 1997a). Further studies indicate that it is the oxidation status of LDL that modulates the impact of hypercholesterolaemia on the blood vessel wall.

An association has been established between the titre of antibodies to oxLDL and the rate at which atherosclerosis progresses (Khoo J.C., 1990). The antioxidant, probucol, reduces plasma and aortic wall oxysterol levels in cholesterol-fed rabbits (Hodis H.N., 1992 and Stalenhoef A.F.H., 1993). Results derived from several different animal models using several different antioxidants (probucol, butylated hydroxytoluene, diphenylphenylenediamine and

vitamin E) confirm the role of oxidation in atherogenesis (Carew T.E., 1987 and Kita T., 1987, Steinberg D., 1997a). The efficacy of the compounds in inhibiting LDL from oxidation *ex vivo* and their ability to inhibit atherogenesis is correlated (Sasahara M., 1994). In addition, patients randomised to 400-800 IU vitamin E showed 47% fewer non-fatal myocardial infarctions and cardiovascular fatalities than the placebo group (Stephens N.G., 1996).

An increase in small dense LDL is associated with increased risk of cardiovascular disease (Austin M.A., 1988, Campos H., 1992 and Chapman M.J., 1998). Several mechanisms have been proposed to account for the increased atherogenicity of small, dense LDL. Penetration of small, dense LDL to the arterial is facilitated by their small particle size (~260 Angstroms). In addition, the subendothelial deposition of small, dense LDL may be exacerbated by their low affinity for the LDL receptor (Nigon F., 1991) and the consequent increase in plasma residence time (Packard C.J., 1997). Proteoglycans in the intimal intracellular matrix selectively bind small dense LDL, sequestering this lipoprotein in a pro-oxidative environment (Anber V., 1997). This may be an important factor contributing to the increased susceptibility of small, dense LDL to oxidative modification (Dejager S., 1993, Tribble D.L. 1992 and de Graaf J., 1991). The increased propensity of small dense LDL to oxidation may also arise from a relative deficit of lipophilic antioxidants (ubiquinol-10, vitamin E and oxygenated carotenoids), (Tribble D.L., 1994 and Goulinet S., 1997), an elevated proportion of polyunsaturated fatty acids (de Graf, 1991) and altered surface lipid monolayer (Tribble D.L., 1992).

The mechanism of oxidation of LDL deposited in the artery wall has been the subject of intense research. The ability of endothelial cell and smooth muscle cells to initiate peroxidation of LDL has been demonstrated *in vitro*. Cocultures of endothelial and smooth muscle cells convert LDL to mmLDL which then promotes the induction of monocyte chemotactic protein 1 which in turn, results in the transendothelial migration of monocytes (Navab M., 1991). In addition, monocytes and leukocytes oxidise LDL and render it cytotoxic (Cathcart M.K., 1985). Modification of LDL by endothelial cells involves lipid peroxidation and degradation of phospholipids (Steinbrecher U.P., 1984). Endothelial cell lipoxygenase has been implicated in the oxidative modification of LDL (Parthasarathay S., 1989). The nature of the initiating radical is discussed further in section 6.1.2.

Figure 1.9: Growth regulatory molecules in atherosclerosis

Growth regulator	Source	Target and outcome
bFGF	Macrophages, endothelial cells, smooth muscle cells	Endothelial and smooth muscle cell proliferation, endothelial chemotaxis
GM-CSF	Endothelial cells	Monocyte chemotaxis, proliferation and differentiation
hb-EGF	Endothelial cells	Smooth muscle cell proliferation
IGF	Fibroblasts	Smooth muscle cell proliferation
IL-1	Macrophages, endothelial cells, smooth muscle cells	Smooth muscle cell proliferation
MCP-1	Endothelial cells	Monocyte chemotaxis and transendothelial migration
M-CSF	Endothelial cells	Monocyte chemotaxis, proliferation and differentiation
PD-ECGF	Platelets	Proliferation of endothelial cells
PDGF	Endothelial cells	Smooth muscle cell proliferation and chemotaxis
TGFα	Macrophages, platelets	Endothelial cell proliferation
TGFβ	Platelets, endothelial cells, macrophages, smooth muscle cells	Smooth muscle cell proliferation. Inhibition of smooth muscle cell proliferation and increased deposition of matrix (fibronectin, collagen and glycosaminoglycans)
TNFα	Macrophages, endothelial cells, smooth muscle cells	Smooth muscle cell proliferation
VEGF	Macrophages, smooth muscle cells	Endothelial cell proliferation

Figure 1.10: The composition of plasma lipoproteins

	Chylo-microns	VLDL	LDL	IDL	HDL_2	HDL_3
% of total lipoprotein						
Protein	1-2	10	18	25	40	55
Lipid	98-99	90	82	75	60	45
% of total lipids						
Triglycerides	88	56	32	7	6	7
Cholesterol	3	17	41	59	43	38
Phospholipid	9	19	27	28	42	41
% of cholesterol esterified	46	57	66	70	74	81

Figure 1.11: Antioxidant and lipid composition of LDL

	mol/mol LDL
Fatty acids	
Palmitic acid	693
Palmitoleic acid	44
Stearic acid	143
Oleic acid	454
Linoleic acid	1100
Arachidonic acid	153
Docosahexanoic acid	29
Antioxidants	
α-tocopherol	6.37
γ-tocopherol	0.51
β-carotene	0.29
α-carotene	0.12
Lycopene	0.16
Cryptoxanthin	0.14
Cantaxanthin	0.02
Lutein + zeaxanthin	0.04
Phytofluene	0.05
Ubiquinol-10	0.10
Total PUFAs (mean)	1283
Total antioxidants (mean)	7.8

Taken from Esterbauer H. et al (1992)

Figure 1.12: Metabolism of lipoproteins

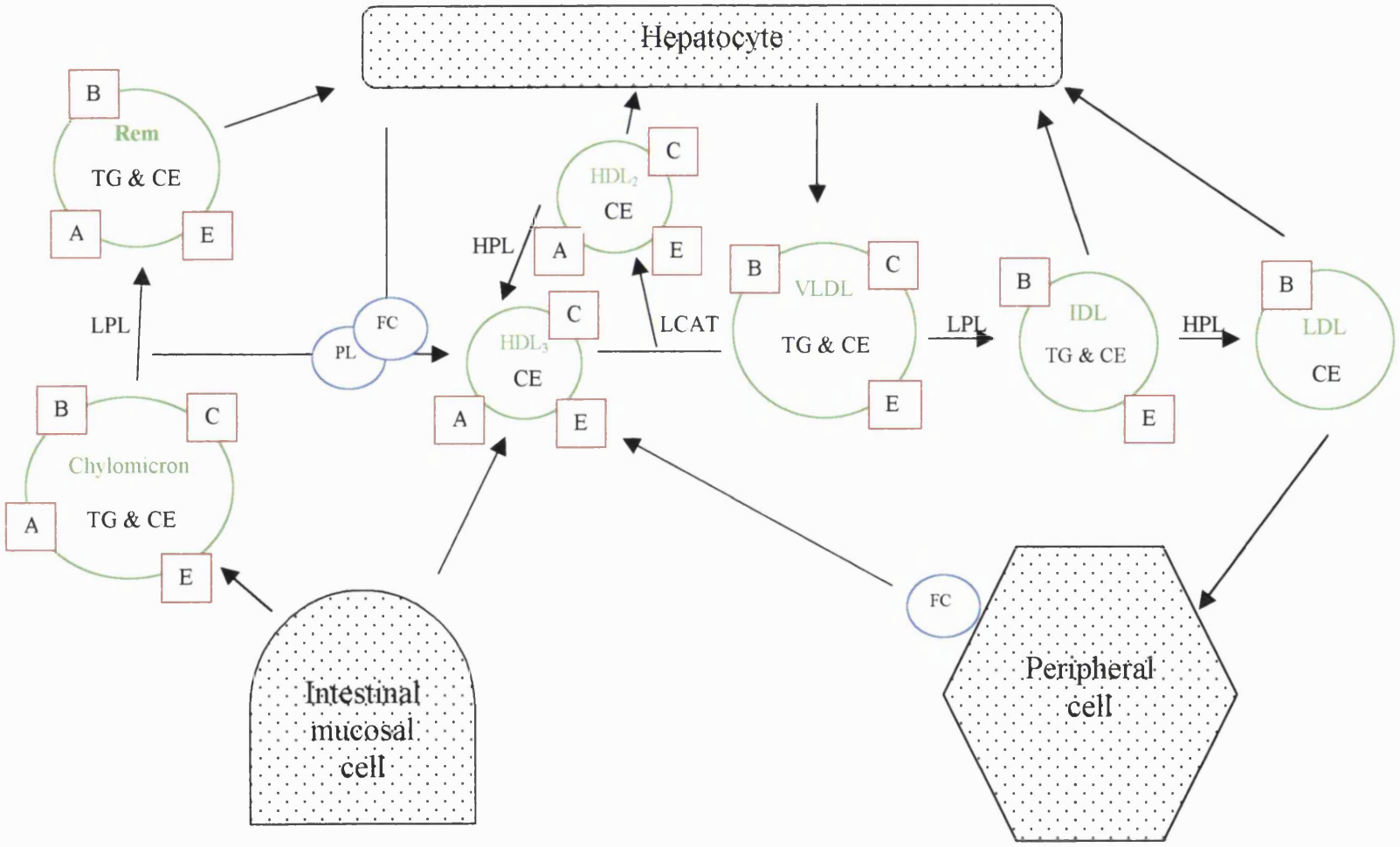

Legend: A, B, C and E refer to the corresponding apoproteins and FC, PL, CE and TG to free cholesterol, phospholipid, cholesterol ester and triglyceride respectively. Rem; chylomicron remnants, HDL; high density lipoprotein, VLDL; very low density lipoprotein, LDL; low density lipoprotein, LPL; lipoprotein lipase, HPL; hepatic lipase, LCAT; lecithin: cholesterol acyl transferase

Oxidised LDL represents a broad spectrum of modified particles that range from mildly (mmLDL) to extensively modified (oxLDL). Highly oxidised LDL (oxLDL) contains abundant lipid peroxidation products (Brown M.S., 1983) including aldehydes. The formation of aldehydes results in the loss of amino groups from apo B100, as a consequence oxLDL has increased electrophoretic mobility (Esterbauer H., 1992) and is recognised by the scavenger receptor (Parthasarathy S., 1986 and Henriksen T., 1983).

Minimally-modified LDL is LDL that has undergone antioxidant depletion and oxidation of arachidonate-containing phospholipid but much less linoleic oxidation. MmLDL has little or no protein modification and is taken up by the native LDL receptor (Berliner J.A., 1990 and Watson A. D., 1995). In addition, mmLDL induces differentiation factors (Rajavashisth T.B., 1990) as well as the transendothelial migration of monocytes via the induction of monocyte chemotactic protein-1 (MCP1) in smooth muscle and endothelial cells (Berliner J.A., 1990, Navab M., 1988 and Navab M., 1991).

Minimal modification of LDL is insufficient to alter its interaction with the LDL receptor or to make it a ligand for the acetyl LDL receptor (Berliner J.A., 1990). The impact of LDL oxidation upon the progression of atherosclerosis is in part due to the ability of mmLDL and oxLDL to induce a number of proatherogenic responses by arterial cells (figure 1.8).

The proatherogenic responses of arterial cells to the various LDL species include the induction of; increased permeability in endothelial cells, adhesion molecules, chemotactic factors, growth factors, haemostatic factors and cytotoxicity. Instigation of these responses contributes to the progression of atherosclerosis by enhancing the formation of subendothelial deposits of foam cells due to transendothelial migration, proliferation and differentiation of monocytes, lymphocytes and neutrophils. In addition, intimal hyperplasia results from the ability of oxidised LDL to promote migration and proliferation of smooth muscle cells. A prothrombotic status may result from the activation of platelet aggregation, the enhancement of thrombosis and reduction of fibrinolysis. Plaque instability results from an increase in the lipid: collagen ratio (Davies M.J., 1993). Oxidised LDL also contributes to plaque instability due to its cytotoxic effects upon smooth muscle cells and foam cells, which result in a reduction in collagen composition and increased lipid content of plaques, respectively.

Importantly, the studies tabulated in figure 1.8 also demonstrate that native, non-oxidised LDL induces proatherogenic responses including; the induction of the monocyte chemotactic factor MCP-1, endothelial adhesion molecules ICAM-1, VCAM-1, E-selectin and the cytokine PDGF and expression of the scavenger receptor CD36. Induction of these factors facilitates the progression of atherosclerosis as a result of the promotion of the adhesion and

transendothelial migration of monocytes and T-cells and their transformation to foam cells as well as the induction of smooth muscle cell proliferation.

Thus, both native and oxidised LDL are capable of promoting atherosclerosis, however, oxLDL is more precisely correlated with the risk of cardiovascular disease (Khoo J.C., 1990), This may arise from a differential in the response of cells to native versus oxidised LDL, for instance oxidised and not native LDL results in increased permeability in endothelial monolayers. Increased endothelial permeability is a critical factor in the initiation stages of atherosclerosis since it permits the deposition of lipid in the subendothelial space. Some studies have addressed the issue of differential responses to native and oxidised LDL, (although many have not), and this subject is discussed further in section 6.6.1.

1.2.6 Sources of oxidised LDL in atherosclerosis

The repertoire of proatherogenic activities of mmLDL is sufficient to initiate atherosclerosis. The induction of endothelial permeability by mmLDL (Essler M., 1999) facilitates the deposition of lipoproteins in the subendothelium. In addition transendothelial migration of monocytes and T-lymphocytes is mediated via the induction of ELAM-1 (an endothelial adhesion molecule for monocytes and T-lymphocytes) and chemotactic factors (Berliner J.A., 1990) in response to mmLDL. Moreover, once lipoproteins, either native or mildly oxidised, are deposited in the subendothelium, cell-mediated oxidation occurs and results in the formation of extensively modified LDL and the consequent induction of additional proatherogenic activities.

It has been proposed that oxidation of LDL occurring at sites remote from atherosclerotic plaques may be a source of oxLDL in plaques. Oxidised LDL has been identified at sites of inflammation (Exner M., 1996) and in this scenario it is possible that it may re-enter the circulation. It is accepted that oxidation of LDL circulating in plasma is unlikely, since the oxidative modification of LDL is inhibited in the presence of antioxidants and serum (Steinberg D., 1997a). However, recently the presence of oxidised lipoproteins has been detected in the blood of humans as a biochemical marker for coronary heart disease (Toshima S.I., 2000).

1.2.7 Mechanisms of arterial occlusion

The clinical symptoms of cardiovascular disease are diagnosed as stable angina, unstable exertional angina, crescendo angina, myocardial infarction, or cerebral ischaemia. Although the mechanisms precipitating the different clinical conditions vary, all the forms of

cardiovascular disease result from oxygen-starvation of tissues, due to the occlusion of the blood vessels that serve the tissue in question.

The means of obstruction may be due to episodic injury resulting in the activation of healing processes. The healing process involves the proliferation and migration of smooth muscle cells in the intimal layer of the lesion. Thrombi formed subsequent to injuries where coagulation is activated may become incorporated into the plaque during healing (Davies M.J., 1985 and Falk E., 1992). The presence of layers of cells and thrombi in plaques (Falk E., 1985) attest to the importance of episodic rupture, thrombosis and healing in the progression of atherosclerosis. After repeated cycles of injury and healing, the extent of occlusion may become critical such that a further thrombotic episode results in complete occlusion of the artery.

Occlusion may also occur if the cap of ruptured plaques lifts into the lumen of the artery and obstructs the flow of blood. In addition, occlusion may also occur at a remote site if a thrombotic embolism is released into the circulation upon plaque fissure. The emboli lodge in arteries with narrower bores e.g. the carotids, and cause cerebral ischaemia or stroke.

1.2.8 Plaque instability and the presentation of clinical symptoms

The severity of coronary artery stenosis in terms of the degree of occlusion and the number of diseased vessels serve as useful predictors of subsequent morbidity and mortality (Moise A., 1984) but lack precision. The degree of arterial occlusion by a lesion is not indicative of the likelihood of the lesion to precipitate an acute event (Brown G., 1990 and Brown B.G., 1993). On the contrary, lesions with less severe stenosis are more prone to rapid progression to severe stenosis or total occlusion and these cases may account for up to two thirds of acute myocardial infarction or unstable angina (Fuster V., 1990). Dangerous or vulnerable plaques often occur in angiographically normal segments of artery (Schleef R.R., 1988).

Severely stenotic plaques tend to be fibrotic and stable (Kragel A., 1991). Longstanding severe stenoses more commonly result in total vessel occlusion, with a small, silent or absent infarct, perhaps due to the presence of well-developed collateral vessels (Fuster V., 1979, Habib G.B., 1991 and Cohen M., 1989). Thrombotic occlusion of severely stenotic plaques may result from decreased blood flow (Davies M.J., 1988 and Woolf N., 1992).

Raised fibrolipid type lesions, IV and Va, are especially prone to disruptions of the surface (Constantinides P., 1966 and 1990, Davies M.J., 1985, Richardson P.D., 1989b, Falk E., 1989). An association between plaque fissure and/or ulceration and the development of unstable angina, acute myocardial infarction or sudden ischaemic death has been established (Richardson P.D., 1989b, Falk E., 1985, Davies M.J., 1989, Levin D.C., 1982, Ambrose

J.A., 1985, 1988a, 1988b & 1986 and Sherman C.T., 1986). Morbidity and mortality from atherosclerosis is largely due to type IV and V lesions in which disruptions of the lesion surface, haematoma or haemorrhage and thrombotic deposits have developed (Stary H.C., 1995). Lesion composition and morphology determines plaque stability and is a better predictor of clinical outcome than the degree of stenosis (Johnson J.M., 1985).

1.2.9 Plaque instability and lesion composition

The angiographic features associated with unstable symptoms include marked eccentricity, narrow neck or abrupt shoulders with overhanging edges and scalloped edges that represent areas of rupture (Thomas A.C., 1986, Levin D.C., 1982, Ambrose J.A., 1985, Ellis S., 1989). Lesions associated with chronic stable angina have a smooth outline, tapered shoulders, and appear symmetric or eccentric with a broad neck (Levin D.C., 1982).

Plaques that undergo disruption tend to be small and soft with high concentration of cholesterol and its esters (Richardson P.D., 1989b). The composition of advanced plaques is represented by a broad spectrum of variation in lipid and collagen content. At the extremes of the spectrum, the composition is represented on the one hand, by a thick collagenous cap and low lipid content, and on the other by a thin cap with high lipid content. The former plaque-type is white in appearance, while the latter type is yellow.

Destabilisation of plaques, leading to fissure, occurs when a high proportion of plaque volume is occupied by extracellular lipid and where there is preponderance of monocyte/macrophages and a lack of smooth muscle cells in the fibrous cap (Davies M.J., 1993). The absence of smooth muscle cells in the cap of rupture-prone plaques and the consequent lack of collagen contributes to a reduction in the tensile strength of the cap. Cells in lesions undergo apoptosis (Bennett M.R., 1995 and Geng Y.J., 1995). Apoptotic death of smooth muscle cells due to the cytotoxic effects of oxLDL is a major factor determining the reduction in collagen deposition in atherosclerotic plaques. Interestingly, 26-hydroxycholesterol, a product of LDL oxidation, is present in unstable macrophage-rich lesions not in their fibrous counterparts. A failure of macrophages to scavenge apoptotic cells in plaques may lead to instability due to the accumulation of extracellular lipid.

Computer modelling of tensile stresses across the vessel wall revealed high stresses on the plaque cap overlying a lipid pool. Weakness of the plaque cap favours redistribution of shear forces to the periphery of the plaque. Fissures frequently occur at the junction of the fibrous cap with the adjacent normal arterial wall (Richardson P.D., 1989b and Woolf N., 1992). Shear forces may arise due to disturbed patterns of blood flow in areas of stenosis (Karino T., 1987, Glagov S., 1988 and Weinberger J., 1988), sudden changes in intraluminal pressure or

tone (Nobuyoshi M., 1991 and Lin C.S., 1988), coronary spasm (Nobuyoshi M., 1991) and bending or twisting of arteries during contraction of the heart.

The induction of vasoconstriction resulting from the induction of expression of endothelin (Boulanger C.M., 1992) and the inactivation of endothelium-derived relaxing factor (EDRF), (Galle J., 1991 and Chin J.H., 1992) by oxLDL may be involved in precipitating rupture of destabilised plaques.

Neovascular capillaries tend to be more prevalent at the rupture-prone periphery of plaques (Stary H.C., 1995). The proximity of neovascular capillaries to the lumen of the artery increases as plaque severity increases (Kamat B.R., 1987). Proximity of the capillaries to the lumen renders severe plaques more prone to rupture. Neovascularisation is present in 50% of unstable plaques and in only 10% of patients with stable angina (Tenagalia A.N., 1998). The capillaries haemorrhage easily since they are fragile, and this may contribute to plaque instability and disruption (Barger A.C., 1990).

The weakening of plaque peripheries is associated with the predominance of macrophages and T cells at the plaque boundary, often associated with neovascular capillaries (Mitchell J.R.A., 1965). Inflammatory cells in lesions may facilitate intimal disruption (Tracy R.E., 1985 and van der Wal A.C., 1994). Furthermore, regions of lesions with increased foam cells tend to tear more readily (Davies M.J., 1993), due to the release of proteolytic enzymes such as elastase and collagenase by macrophages (Henney A.M., 1991) that digest the extracellular matrix of the vessel. Degradation of the matrix is part of vascular remodelling and provides the space required to allow the infiltration of endothelial cells during angiogenesis.

Components of lesions associated with thrombus formation can cause or facilitate fissures (Stary H.C., 1995). The fact that plaque disruption leads to thrombus formation has been known for some time (Constantinides P., 1966, Chapman I., 1965, Fulton W.F.M., 1965 and Friedman M., 1966). Unlysed non-fatal thrombotic deposits may initiate events that lead to a permanent increase in lesion thickness.

If only the endothelial surface of the lesion is disrupted, the thrombogenic stimulus is limited. At worst, a mural thrombus may be formed without clinical symptoms or further lesion growth. Deep rupture as seen in fissuring can lead to a thrombotic occlusion that may be recurrent (Falk E., 1989 and Falk E., 1992). Indeed, some patients with unstable angina may have intermittent or transient vessel occlusion and ischaemia (Fuster V., 1988). If the disruption is deep and exposes the lipid core and/or collagen a persistent occlusion may result in acute myocardial infarction (Fuster V., 1988). Exposure of type I collagen leads to extensive platelet activation and thus thrombosis (Badimon L., 1988). The severity of lesion disruption determines the size and nature of the thrombogenic

surface exposed by the rupture and thus the size of the ensuing thrombus. The gravity of the outcome of plaque rupture largely depends upon the severity of the rupture, the thrombogenicity of the plaque core and systemic factors.

1.2.10 Factors determining the thrombogenic potential of plaques

The formation of large thrombi leads to plaque destabilisation due to increases in plaque size and since components of thrombi lead to plaque rupture (Stary H.C., 1995). The lipid core is the most thrombogenic component of atherosclerotic plaques (Badimon L., 1986) probably due to the presence of TF. TF is expressed by macrophages, smooth muscle and endothelial cells in atherosclerotic plaques (figure 1.12). The impact of the presence of TF is compounded by the presence of oxLDL and phosphatidylserine, which both enhance TF activity (Ettelaie C., 1995 and Bach R., 1986). In addition, oxLDL indirectly leads to an increase in TF activity via its ability to induce cellular apoptosis (Morel D.W., 1983), which leads to the redistribution of phosphatidylserine to the external membrane layer (Martin S.J., 1995). Apoptotic cell surfaces elicit procoagulant activity (Casciola-Rosen L.A., 1996). Marked TF expression is detected in the acellular lipid core of plaques in close proximity to apoptotic macrophages and debris (Geng Y.J., 1995 and Mallat Z., 1999), probably due to its release in microparticles during apoptosis (Mallat Z.M., 1999). The induction of apoptosis by oxLDL is thus a critical factor determining plaque thrombogenicity upon rupture. In addition, oxLDL enhances the size of thrombus formed upon rupture via its ability to inhibit profibrinolytic factors including pro C (Weis J.R., 1991), tPA (Kugiyama K., 1993) and its enhancement of the anti-fibrinolytic factor PAI-1 (Kugiyama K., 1993).

Other factors also contribute to the thrombogenic potential of plaques. Haematomas arising from the rupture of capillaries formed during neovascularisation contain factors that enhance thrombogenesis (Paterson J.C., 1936, Barger A.C., 1984 and Beeuwkes R. III, 1990). Thrombotic occlusion tends to occur more readily at anatomical sites of vessel bifurcation and regions of arterial angulation because of reduced blood flow (Taeymans Y., 1992). Deformity of lesion surfaces arising from underlying or proximal lesions may also enhance the thrombogenic potential of the plaque via localised effects on blood flow. Other factors predisposing to thrombogenesis include high plasma fibrinogen levels, high levels of LDL and their resultant adverse effect upon platelet function (Aviram M., 1987), decreased fibrinolytic capacity (e.g. increased PAI–1), increased lp(a) interferes with the assembly of fibrinolytic proteins.

1.3 The role of tissue factor in the progression of atherosclerosis

Increased thrombogenic potential and plaque instability are major determinants of atherosclerotic progression. The following section presents functions of TF that support its role in the progression of atherosclerosis and the formation of unstable plaques.

Active TF is expressed in both early (Hatakeyama K., 1997) and late (Wilcox J.N., 1989) atherosclerotic lesions. TF antigen and activity in plaques are significantly higher in patients with unstable angina and myocardial infarction than in patients with stable angina (Ardissino D., 1997, Annex B.H., 1995 and Falciani M., 1998). Increased expression of TF is also increased in the plasma of patients with acute myocardial infarction (Suefuji H., 1997) or unstable angina (Misumi K., 1998) in comparison to those with stable angina.

1.3.1 Expression of tissue factor in cardiovascular disease

The expression of TF in normal and diseased vessels is depicted in figure 1.12. In normal vascular tissue, tissue factor is expressed in the tunica media and adventitia but is absent in endothelium, intima and media (Drake T.A., 1989 and Wilcox J.N., 1989). TF is selectively expressed to form an envelope that surrounds the periphery of the vascular tree. This pattern of TF expression ensures the initiation of coagulation in the event of vascular damage. TF has also been identified in organ capsules, epidermis, mucosal epithelium, cerebral cortex, renal glomeruli and cardiac myocytes (Drake T.A., 1989).

The induction of TF on endothelial cells and macrophages occurs in response to factors associated with vascular injury. Expression of TF is mediated by a variety of agonists including inflammatory cytokines, oxLDL, angiogenic factors, immune complexes, and lipopolysaccharide. A review of agents that either upregulate or inhibit TF expression is tabulated in appendix 1. Nearly all intimal smooth muscle cells, macrophages and endothelial cells were positive for TF in type I and type II lesions. In addition, TF is present in the later stages of the atherosclerotic plaque. TF positive cells were found scattered throughout the fibrous cap, the base and the shoulder region of plaques as well as in the core adjacent to cholesterol clefts (Wilcox J.N., 1989). In addition, the presence of significant quantities of TF in foam cell-rich regions, which tend to occur next to necrotic cores, was observed. Marmur et al (1996) also found TF in extracellular matrix and found particularly high levels in cholesterol-rich areas of plaques. Studies of type IV to VI type lesions (Stary H.C., 1995) confirmed that TF is particularly abundant in the lipid cores of such lesions but is also found in macrophages, smooth muscle cells, in the fibrous cap and in the endothelial cells overlying plaques (Thiruvikraman S.V., 1996). The expression of the TF inhibitor, TFPI, in relation to TF in atherosclerotic plaques has been recently investigated (Crawley J., 2000). TFPI

colocalises with TF in endothelial cells overlying plaques, in smooth muscle cells in the fibrous cap and in macrophages at the periphery of the necrotic core (Crawley J., 2000 and Kaikita K., 1999). The necrotic core itself contains TF but not TFPI. The latter observation is significant in terms of the potential to form occlusive thrombi since TF activity may occur unimpeded by TFPI subsequent to plaque rupture (Caplice N.M., 1998). Complicated plaques contain the greatest amounts of TF and TFPI. Furthermore, TFPI was found to be functionally active against TF: FVIIa-induced coagulation. In addition, the activity of TF and TFPI correlate with the distribution of the antigens detected immunohistochemically.

1.3.2 Tissue factor and plaque progression

Increased plaque thrombogenicity due to the presence of TF results in the generation of large thrombi. These thrombi become incorporated into the plaque structure and cause an increase in plaque size and instability (Stary H.C., 1995). The exposure of the thrombogenic core of plaques itself is dependent upon stability of the plaque. Thus, the progression of atherosclerosis persists due to a cycle of plaque rupture and thrombus formation where each promotes the onset of the other.

TF facilitates the intimal hyperplasia that underlies the progression of atherosclerotic plaques. The administration of either active site-inactivated FVIIa or TFPI to rabbits subsequent to injury of the femoral artery, results in attenuation of intimal hyperplasia and restenosis (Taubman M.B., 1997, Jang Y., 1995 and Brown D.M., 1996). Furthermore, inhibition of TF by TFPI *in vitro* leads to the inhibition of smooth muscle cell proliferation (Kamikubo Y., 1997) and migration (Sato Y., 1997). Smooth muscle cell proliferation and migration underlies the process of intimal hyperplasia which is in turn dependent upon neovascularisation (Kamat 1987, Stabb M.E., 1997, Kwon H.M., 1998, Moulton K.S., 1999). Since TF is involved in the mediation of angiogenesis (Zhang Y., 1994 and Carmeliet P., (1996), these studies suggest that a mechanism of involvement of TF in hyperplasia may be via its ability to promote angiogenesis. The induction of neovascular capillaries at the periphery of plaques leads to destabilisation.

In addition, TF mediates the activation of plasminogen, which leads to the secretion of matrix metalloproteinases. The observed involvement of macrophages in atherogenesis may, at least in part be due to the secretion of collagenase, elastase, stromelysin and matrix-metalloproteinases by these cells. Interestingly, macrophage infiltration is significantly increased in patients with unstable angina than those with stable angina (Kaikita K., 1997). Furthermore, 75% of the macrophages in those patients with unstable angina expressed TF in

contrast to 13% of macrophages in patients with stable angina and the extent of TF expression was related to the degree of macrophage infiltration.

TF promotes atherosclerosis via several mechanisms, including its ability to promote thrombosis, angiogenesis, cell proliferation and cellular apoptosis (figure 1.13). The induction of angiogenesis by TF results from the ability of the TF: FVIIa complex to elicit cellular signals that lead to the alteration of cellular phenotype. The array of genes induced by the TF: FVIIa complex is presented in section 3.1. In addition, signalling molecules that have been identified in the TF pathway are examined in section 5.1. In addition, the relationship between the signal transduction pathways and the role of TF in atherosclerosis is discussed in section 5.6.

1.3.3 The effect of native and oxidised LDL upon the activity of tissue factor

The data reviewed above demonstrate key roles for both tissue factor and oxidised LDL in the pathogenesis of atherosclerosis. The proatherogenic effects of oxidised LDL may, at least in part, result from the ability of oxidised LDL to enhance TF activity (Ettelaie C., 1995 and 1997). Interestingly, the effect of LDL upon TF activity is determined by its oxidation status. While oxidised LDL enhances TF activity, native LDL inhibits TF activity (Ettelaie C., 1995 and 1997). The ability of native LDL to inhibit TF activity results from a direct protein: protein interactions between the apolipoprotein B-100 (apo B100) component of LDL and the TF molecule (Ettelaie C., 1996). A lysine-rich region of apo B100 responsible for its inhibitory activity has been determined (KRAD6) and a proposed binding site in TF has been proposed (Ettelaie C., 1998). The identity of these domains and the experimental data leading to their discovery are discussed in further detail in chapter 3.

Aldehydes formed in LDL upon oxidation, result in the modification of ε-amino groups of lysine residues. Since lysine residues are of key importance in the inhibition of TF by apo B100 in native LDL, modification of the lysine residues in apo B100 abolishes the inhibitory activity of LDL towards TF activity. Moreover, the oxidation of LDL reverses its inhibitory effect and renders oxidised LDL capable of enhancing TF activity (Ettelaie C., 1995 and 1997). The mechanism by which oxidised LDL enhances TF activity may arise indirectly from the oxidation of tissue factor pathway inhibitor (TFPI), since the oxidation of LDL-associated TFPI results in loss of its inhibitory activity towards TF (Lesnik P., 1995).

Figure 1.13a: Localisation of tissue factor in normal artery and type I lesions

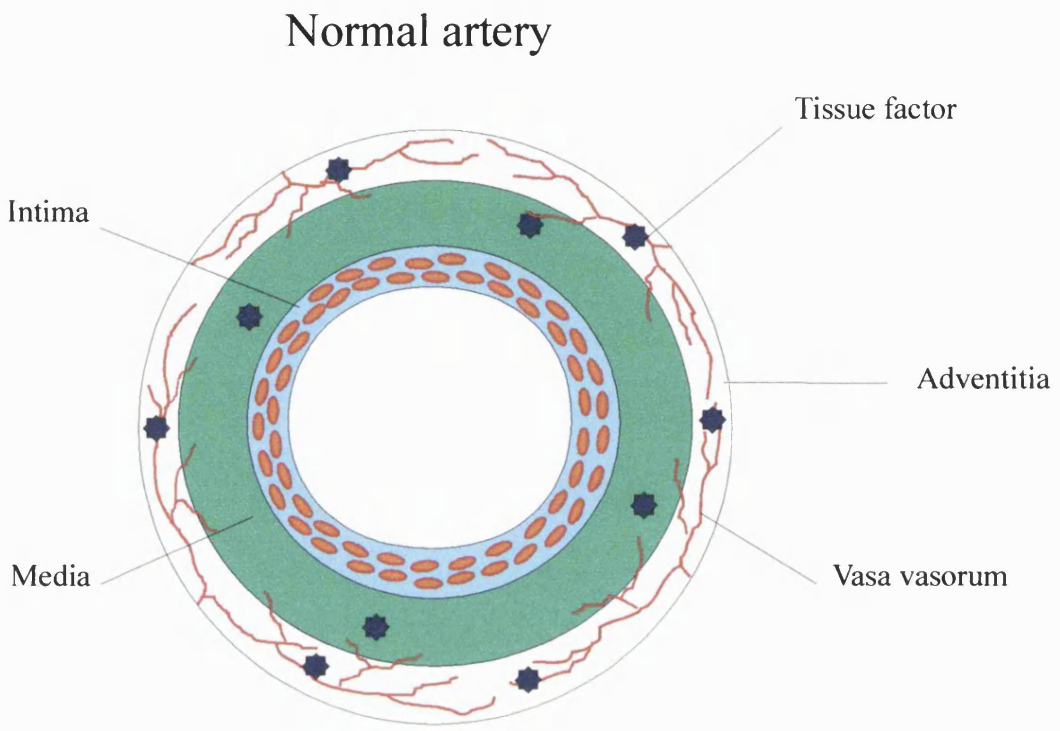

In normal vascular tissue, tissue factor is expressed in the tunica media and adventitia but is absent in endothelium, intima and media.

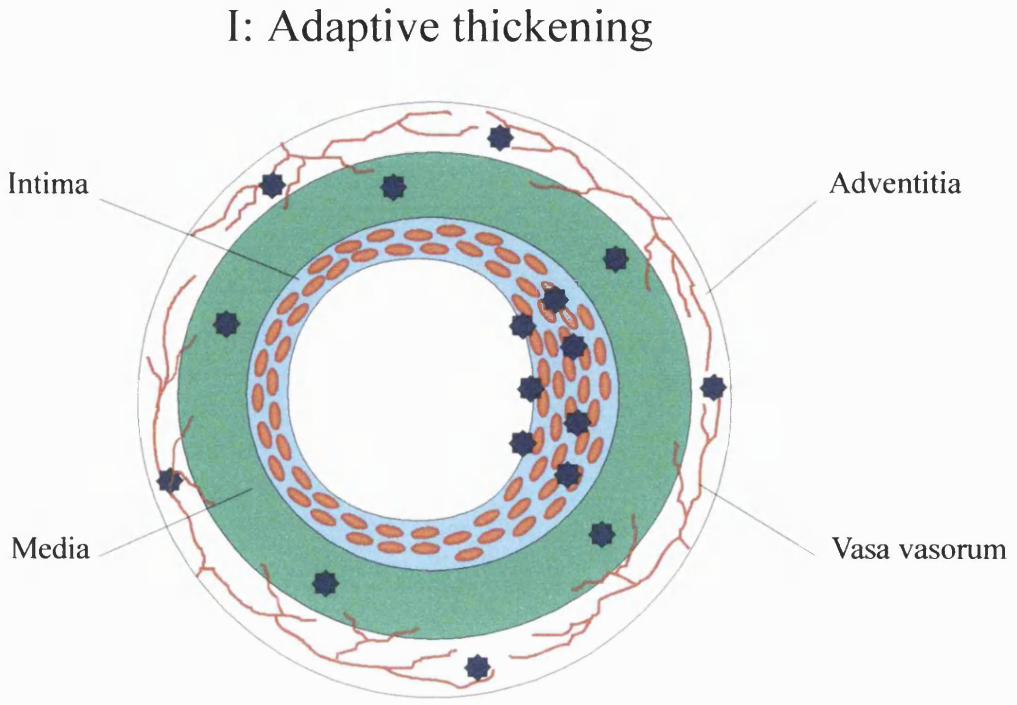

Figure 1.13b: Localisation of tissue factor in type II and type IV atherosclerotic lesions

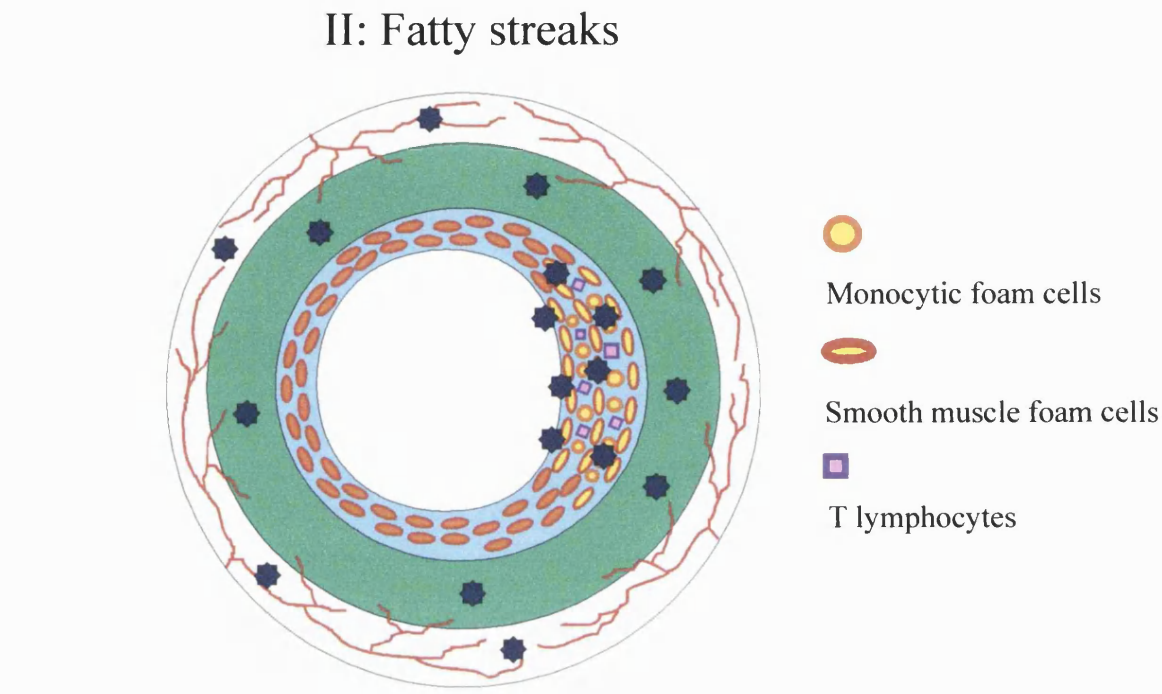

Nearly all intimal macrophages, endothelial and smooth muscle cells in plaques express tissue factor

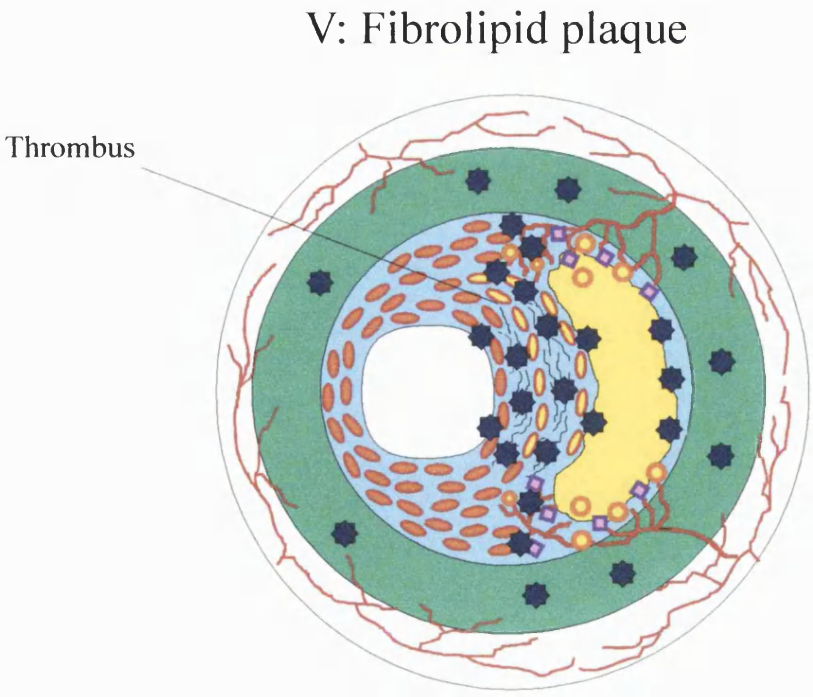

Tissue factor-positive cells are found adjacent to cholesterol clefts, throughout the fibrous cap and in the base and shoulder region of fibrolipid plaques.

Figure 1.14:

The involvement of tissue factor in the initiation and progression of atherosclerosis

TF-mediated response	Proatherogenic outcome	Reference
Activation of Rac kinase	Fatty streak formation via increased vascular permeability	Versteeg H.H., 2000
Transendothelial migration of monocytes	Fatty streak formation via monocyte extravasation	Randolph G.J., 1998 and Cunningham A., 1999
Induction of VEGF & FGF	Intimal hyperplasia via angiogenesis	Ollivier V., 1998
Activation of urokinase plasminogen activator receptor	Angiogenesis via extracellular matrix degradation	Taniguchi T., 1998, Fan Z., 1998
Smooth muscle cell migration and proliferation	Intimal hyperplasia via angiogenesis	Sato Y., 1997
Fibroblast chemotaxis	Intimal hyperplasia via angiogenesis	Siegbahn A., 2000
Induction of extracellular matrix signalling proteins CTGF and Cyr61	Intimal hyperplasia via cell adhesion, migration and proliferation	Pendurthi U.R., 2000
Induction of apoptosis	Plaque instability via enhanced thrombus formation	Hamuro T., 1998
Regulation of thrombin: thrombomodulin	Plaque instability via enhanced thrombus formation	Varadi K., 1999
Induction of wound healing responses (see figure 3.1)	Intimal hyperplasia, angiogenesis	Camerer E., 2000

Tissue factor activity is a key mediator of the progression of atherosclerosis. The ability of oxidised LDL to enhance the activity of TF may be of considerable importance in the mechanism mediating the proatherogenic effects of oxidised LDL. In addition, since native LDL inhibits TF activity, the loss of native LDL concomitant to its oxidation, may compound increases in TF activation by oxidised LDL.

1.4 Calcium and cellular signaling mechanisms

A diverse array of cellular biological responses are regulated by changes in cytosolic Ca^{2+} including; migration, metabolism, excitability, secretion, relaxation and contraction, proliferation, transcription and fertilisation. The versatility of Ca^{2+} signals is permitted by the ability of the ion to act in the context of space, time and amplitude (Berridge M.J., 1998).

Cellular Ca^{2+} is derived from external or internal sources. Ca^{2+} can enter through channels than span the plasma membrane. Alternatively Ca^{2+} can be released from internal Ca^{2+} stores through channels in the endoplasmic (Ca^{2+}_{ER}) or sarcoplasmic reticulum (Berridge M.J., 1993 and Clapham D.E., 1995). Ca^{2+} may enter through voltage-operated Ca^{2+} channels in excitable cells such as neurons or smooth muscle cells or receptor-operated channels in response to neurotransmitters. Store-operated channels are found in many non-excitable cells and are opened when internal Ca^{2+} stores are emptied. Ca^{2+}_{ER} is either released by the action of phospholipase C-generated inositol 1,4,5-trisphosphate (IP_3) (Lipp P., 1996) or via ryanodine receptors especially in excitable cells (Berridge M.J., 1997). In some cells, the production of IP_3 is modulated by the phosphatidyl inositol 3-OH kinase (PI3K) signaling pathway, which uses IP_2 to produce IP_3 that acts as a messenger to maintain the activity of PLC. Some of the Ca^{2+} rapidly sequestered by the mitochondria and is returned to the endoplasmic reticulum (Porter V.A., 1998), if the mitochondria become overloaded with Ca^{2+}, programmed cell death may become activated (Dolmetsch R.E., 1998).

The elevation of intracellular Ca^{2+} is tightly regulated since excessive cytosolic Ca^{2+} damages cells. Since Ca^{2+} does not undergo degradation or metabolism, excess Ca^{2+} is sequestered by the action of specific binding proteins and extrusion mechanisms. Intracellular Ca^{2+} in resting cells is tightly regulated between 10-100nM primarily by the actions of high affinity cytosolic binding proteins and ATP-dependent pumps on the plasma and endoplasmic reticulum membranes (Pozzan T., 2000). During excessive intracellular Ca^{2+}loads, low affinity mechanisms can also contribute to the buffering capacity of the cell including storage in the mitochondria and the Na^{+}/Ca^{2+} exchanger (Strehler 1995).

1.5 Aims

The activation of coagulation and cellular signalling mechanisms by the TF: FVIIa complex are central to the involvement of TF in the pathogenesis of atherosclerosis. The aim of these studies was to investigate various aspects of signalling by the TF: FVIIa complex.

- To determine the involvement of the cytoplasmic domain of TF in the induction of cytosolic Ca^{2+} transients by FVIIa
- To determine the involvement of each of the three serine residues in the cytoplasmic domain of TF in the induction of Ca^{2+} transients by FVIIa
- To investigate the effect of an apo B100 derived peptide inhibitor of TF activity, (KRAD6) upon the induction of Ca^{2+} transients by FVIIa
- To investigate the effect of inhibitors of TF activity, (KRAD6) upon the formation of cellular network structures in an *in vitro* model of angiogenesis
- To investigate the potential involvement of TF in the induction of Ca^{2+} transients by native and oxidised LDL

CHAPTER 2

GENERAL METHODS

2.1 Mammalian cell culture methodology

2.1.1 Preparation of sera

Foetal bovine serum (FBS) for use in the cloning of transfected mammalian cells was γ-irradiated in order to inactivate nanobacteria that survive heat inactivation and ultrafiltration (LabTech Int.). FBS to be used in all cell culture media was heat inactivated at 55°C for 30 minutes and was filtered sterilised through a 0.22μm pore filter.

2.1.2 Culture of human bladder carcinoma T24 cells

T24 cells were purchased from the European Cell and Animal Culture Collection (ECACC). Cells were maintained as monolayers in Dulbecco's Modified Eagle's Media (DMEM) containing Glutamax™ (Gibco BRL) and supplemented with 10% FBS. When the cell monolayers reached confluence, the cells were detached using a non-enzymatic procedure as described in section 2.1.7. Cells were split at a 1:15 ratio.

2.1.3 Culture of Madin-Darby Canine kidney cells

MDCK1 cells were the generous gift of Dr Christian Prydz (Biotechnology Centre, University of Oslo, Norway). Cells were maintained as monolayers in DMEM containing Glutamax™ and supplemented with 10% FBS. When the cells reached confluence the cells were detached using trypsin as described in 2.1.6. The cells were split at a 1:5 ratio.

2.1.4 Culture of Chinese Hamster Ovary K1 cells

Proline-dependent CHO K1 cells were obtained from ECACC. The cells were cultured in a 1:1 mix of DMEM and Ham's F12 media (Gibco) supplemented with 10% γ-irradiated FBS. The cells were maintained at 37°C, 5% CO2 in a humidified incubator. The cells were split 1:5 at confluence as described in 2.1.7.

2.1.5 Culture of myelomonocytic THP-1 cells

The monocytic cell line THP-1 exhibits characteristic features of monocytes (Tsuchiya, 1980). THP-1 cells were cultured in RPMI-1640 media (Gibco BRL) supplemented with penicillin (100U/ml), streptomycin (100μg/ml), (Gibco BRL) and 2mM glutamine (Gibco BRL). The cells were maintained at 37°C, 5% CO_2 in a humidified incubator.

2.1.6 Enymatic detachment of adherent cells

The supernatant was removed from the cell culture and the adherent cells were washed with Versene™ (Gibco BRL) to remove calcium. A volume of 0.25% trypsin/EDTA solution (Gibco BRL) sufficient to cover the base of the culture vessel was then added. The cells were incubated at 37°C and observed at 1-2 minute intervals. As soon as the cells were detached, the trypsin was inactivated by the addition of PBS (Gibco BRL) containing 5% FBS. The cell suspension was dispensed into centrifuge tubes and centrifuged at room temperature for 5 minutes at 300g. The supernatant was discarded and the cells were washed with PBS. The supernatant was again discarded and the cell pellet was resuspended.

2.1.7 Non-enzymatic detachment of adherent cells

Culture media was removed from the culture vessel and the adherent cells were rinsed with PBS. Versene™ (Gibco BRL) was added to the culture vessel to a depth of a few millimetres. The culture vessel was then incubated at 37°C. The culture vessel was removed at 5-minute intervals and tapped to release the cells. When the cells were released the cell suspension was pipetted into sterile centrifuge tubes. The culture vessel was then rinsed with sterile PBS (Gibco BRL) to ensure the collection of all the cells. The cells were then pelleted by centrifugation at 300g for 5 minutes.

2.1.8 Culture of cells on coverslips

2.1.8a Preparation of sterile coverslips for cell culture

16mm No2 coverslips were purchased from Raymond Lamb supplies. A beaker containing a solution of 70% ethanol was placed in the reservoir of a sonicator. The sonicator was switched on and the coverslips were individually dropped into the beaker of ethanol using autoclaved tweezers. The excess ethanol was removed from the beaker and the coverslips were individually placed onto tissue paper to dry inside a laminar airflow hood. After drying the coverslips were placed into a beaker and were autoclaved.

2.1.8b Growth of MDCK1, CHO K1 and T24 cells on glass coverslips

Cells in logarithmic phase were harvested from culture as described in section 2.1.6. and were resuspended to a concentration of 1 $x10^6$/ml in the appropriate culture media for the cells. Sterile coverslips were transferred to a 6cm diameter polypropylene petri-dishes.

Cells were added to the prepared culture vessels as follows; 3 x 10^6 MDCK1 cells were per petri-dish (D=9cm) for use after 36-48 hours. T24 cells were plated at a density of 1 x10^6 cells per petri-dish (D=6cm) for use after 36-48 hours. CHO K1 cells were plated at 0.6 x 10^6 cells per dish (D=6cm) for use after 36-48 hours, at 40-50% confluence in transfection studies. The cells were incubated at 37°C, 5% CO_2 in a humidified incubator for studies of cytosolic Ca^{2+} responses.

2.2 Coagulation methods

2.2.1 Prothrombin time assay

The prothrombin time assay was determined using a coagulometer (Helena Biosciences), which estimates coagulation via light transmission through the sample. The coagulometer was switched on and left to equilibrate to 37°C. 100µl of sample was added to the coagulometer cuvette, followed by 100µl of control plasma (Sigma). Coagulation was initiated by the addition of 100µl of 25mM $CaCl_2$. The time taken for the sample to clot was recorded and reported by the coagulometer.

2.2.2 Standard curve for prothrombin time test

A stock solution of recombinant human TF (Dade) was serially diluted with pyrogen-free water (Baxter) to produce a range of concentrations between 100 and 0.2 units/ml. 100µl aliquots were assayed and the prothrombin times produced by 8 independent samples of recombinant human TF (rTF) ranging from 0.02-20 units per assay were determined. A standard curve was constructed and is presented in figure 2.1. The calculated standard error was calculated and is too small to be visible on the graph. A trendline was fitted to the curve and the correlation value between the approximated curve and the observed clotting times is 0.99. The equation of the trendline, shown below, was expressed in terms of tissue factor units and this equation was used to calculate the TF units per assay from the prothrombin time of the sample.

TF units = EXP{ [ln (prothrombin time / 27.059) / -0.2838] }

Figure 2.1: Prothrombin time versus tissue factor activity

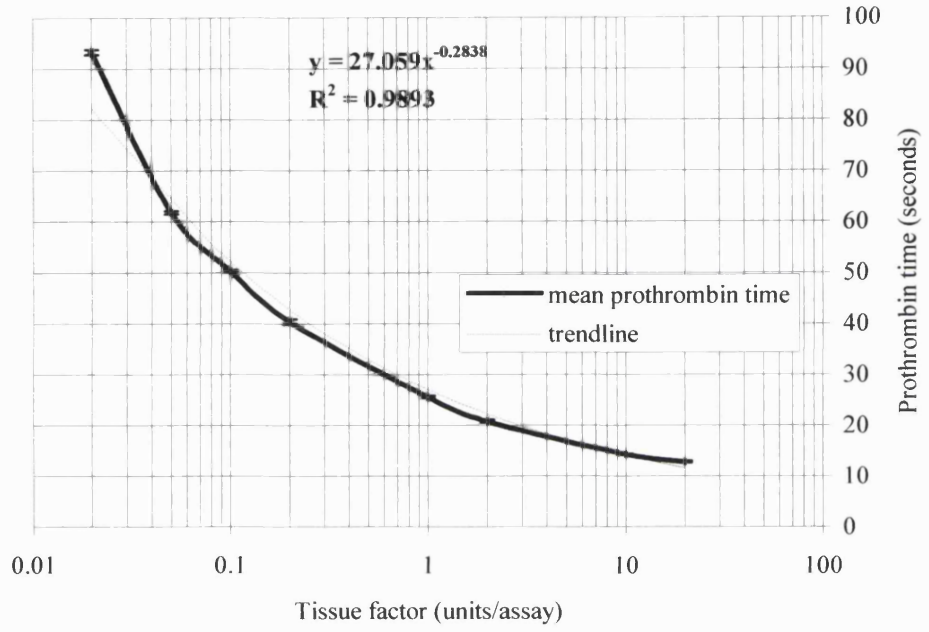

Recombinant human TF was reconstituted in water and a set of dilutions was set up ranging from 200U/ml to 0.02U/ml. 100µl samples were assayed for TF activity in a coagulometer (Helena Biosciences) using the prothrombin time test. All samples were assayed at 37°C. 100µl samples of TF were added to 100µl of control human plasma. Coagulation was initiated by the addition of 100µl of 25mM $CaCl_2$. The time taken for a clot to form was recorded for each sample. The data was used to construct a standard curve. A trendline was fitted to the standard curve and the equation of the trendline was rearranged to enable the calculation of TF units given the prothrombin clot time; TF units = EXP{ [ln (prothrombin time / 27.059) / -0.2838] }. The results are the mean ± S.E.M. for four independent experiments each assayed in duplicate.

2.3 Kinetic imaging methods

2.3.1 Principles of real-time imaging of Ca^{2+}-sensitive probes in live cells

Important advances in the measurement of ionic activity were brought about by the use of photoproteins such as the calcium-sensitive molecule aequorin, which emits light upon the binding of calcium ions. However, the introduction of such dyes into cells involved microinjection and dissociation constants were not always suited to the concentrations found in small cells. In 1982, the development of new fluorescent dyes revolutionised the ability of scientists to investigate ionic activity in single cells. Acetoxymethylester conjugates of the fluorescent dyes were developed enabling cells to be loaded with the dye rapidly in the test-tube. The ion-sensitive lipid-soluble dyes traverse the cell membrane and are hydrolysed by endogenous cellular esterases to a free acid form, which remains trapped inside the cell. Fluorescent compounds absorb light of particular wavelength (excitation wavelength). Absorption of the appropriate wavelength of light promotes the transition of electrons to a higher energy state. When the electron relaxes back to the ground state, photons of a particular wavelength (emission wavelength) are emitted. Since the energy of the emitted light is lower than the energy of the absorbed light, the emission wavelength of fluorescent light has a longer wavelength than the absorbed light. Fluorescent compounds thus have characteristic emission and absorption spectra. These spectra may be altered for example when an ion-sensitive dye binds to an ion and this property is exploited to detect changes in cellular ion levels.

Indicators used to measure Ca^{2+} may be single or dual wavelength dyes. The fluorescence intensity emitted from Fluo-3 upon binding Ca^{2+} is directly proportional to $[Ca^{2+}]i$. Although this indicates the changes in $[Ca^{2+}]i$, the intensity of the emitted fluorescence depends upon the initial concentration of the dye preventing the measurement of $[Ca^{2+}]i$ from fluorescence intensity. The dual excitation dye Fura2 displays a single emission peak at 510nm but has two absorption maxima, one at 340nm which increases with increasing ionised calcium and a second at 380nm which similarly decreases with a rise in ionised Ca^{2+} (figure 2.2). The 'spectral shift' property of ratiometric dyes makes them ideally suited for intracellular ion imaging. The ratio of the two wavelengths provides measurements of $[Ca^{2+}]i$ that are independent of light intensity, concentration of dye within the cell, cell thickness and dye loss due to bleaching of leakage. One essential problem with many of the fluorochromes used for ion measurement is the tendency for them to be taken up into intracellular compartments with time.

Figure 2.2: Excitation spectra of Fura2 in the presence of increasing ionised calcium

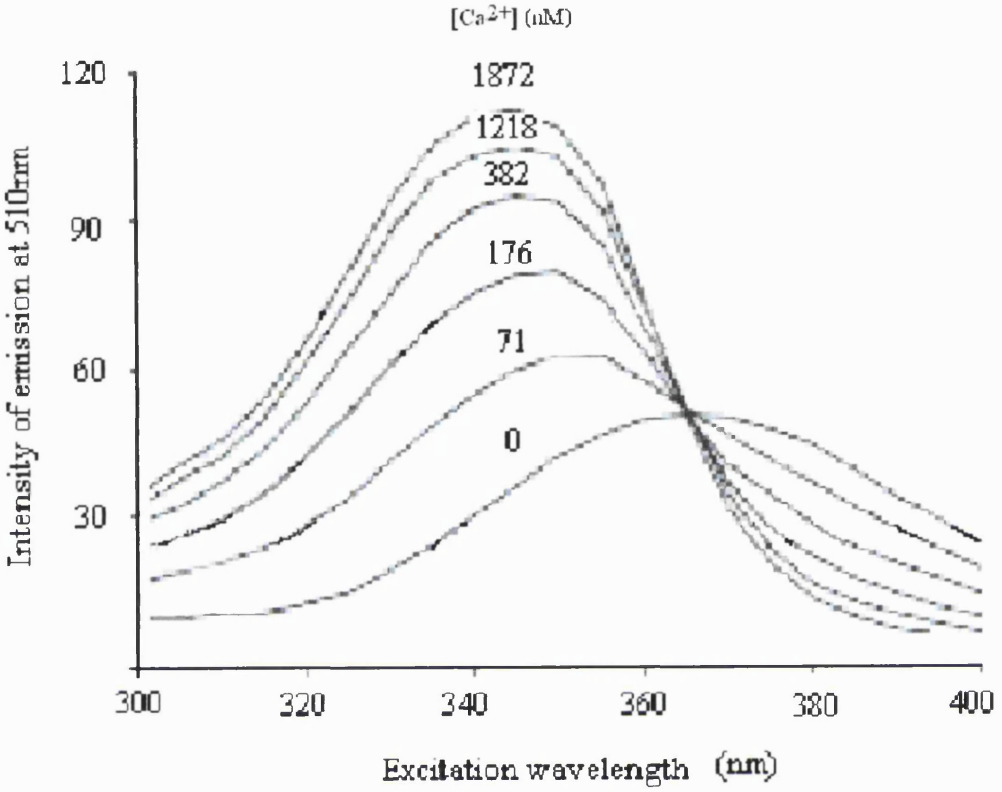

2.3.2 Loading of cells from monolayer cultures with Fura2AM

Cells grown on glass coverslips were rinsed in Hank's buffer (143mM NaCl, 5.6mM KCl, 2mM $MgCl_2$, 10mM Hepes, 10mM glucose and 1.2mM $CaCl_2$, pH 7.2). The excess buffer was removed and the coverslip was placed on top of an inverted microcentrifuge tube lid. 100µl of 1µM Fura2AM (Molecular Probes) was prepared by diluting a solution of 1mM Fura2AM in DMSO (Sigma) 1000-fold into Hank's buffer and was dispensed onto the cells. The cells were incubated in the dark at 37°C for 20-30 minutes to allow entry of the Fura2AM into the cells. The Fura2-loaded cells were then rinsed and washed for 20-30 minutes with 100µl Hank's buffer.

2.3.3 Imaging hardware

The imaging hardware set-up is shown in figure 2.3. The cells were visualised and fluorescent measurements obtained using an inverted Nikon Diaphot microscope with a range of fluorescent objective lenses (x40, x20, x10). A 75W Xenon arc lamp, which emits light across the ultra-violet (*uv*) and visible ranges, was used as the source of excitation light.

Figure 2.3: Digital imaging hardware

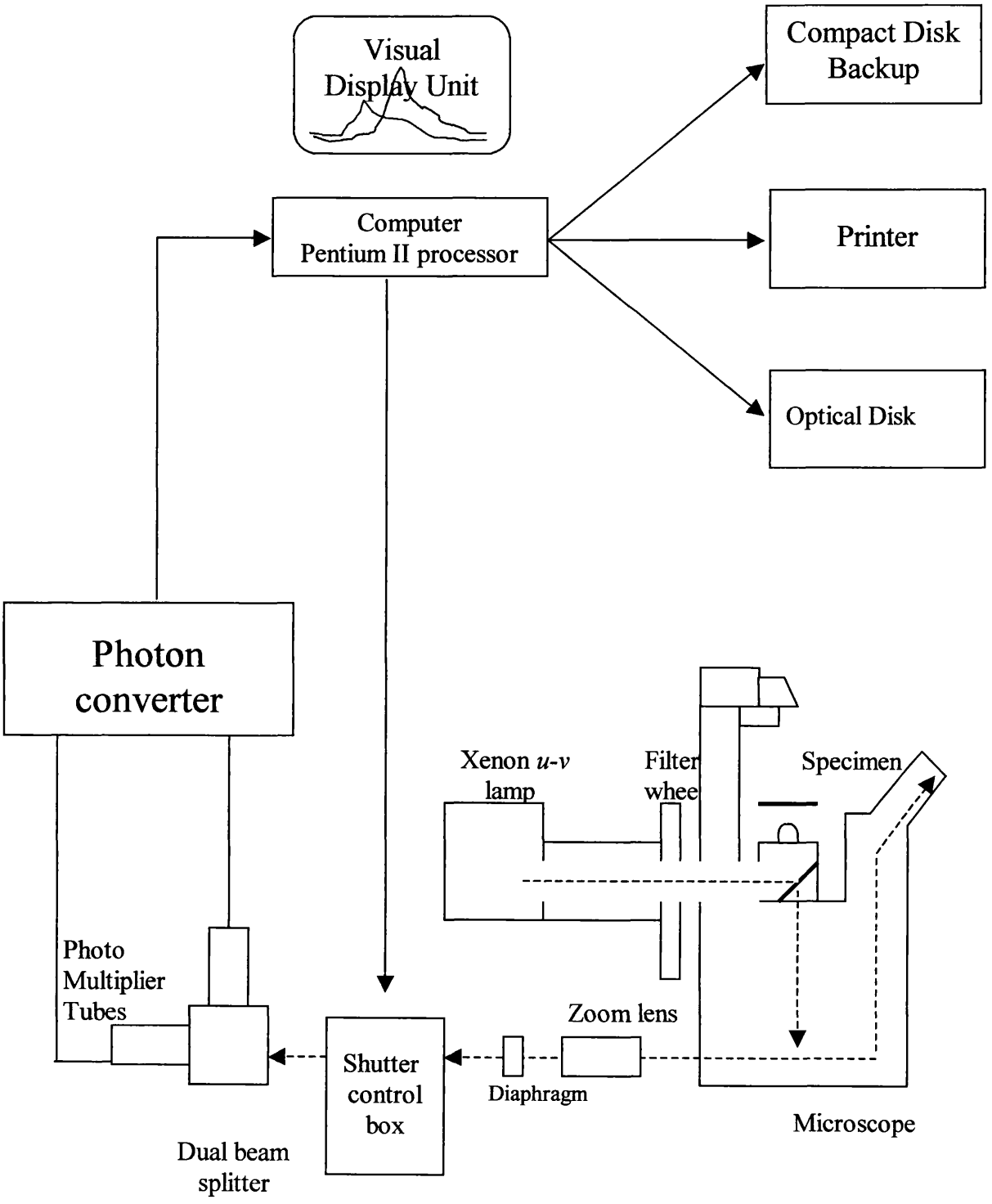

The cells were exposed alternating wavelengths of light of 340nm and 380nm using a rotating wheel (Sutter Instruments) that contained the appropriate filters. Cells were exposed to light only during the experimental runs to minimise the generation of oxygen free radicals and photodynamic cell damage by the *u-v* light. The dichroic mirror is positioned in the light path to separate excitation and emission wavelengths by reflecting the 340nm and 380nm excitation wavelength and transmitting the 510nm emission wavelength.

Emitted fluorescence was captured using a charge coupled device (CCD) camera (Digital Pixel), which was cooled to reduce thermal noise. The CCD consists of an outer layer of silicon, allowing light of longer wavelength to penetrate and a layer of silicon dioxide made up of pixels. Emitted fluorescence is absorbed by the silicon dioxide and is accumulated as charge. The quantity of charge in each pixel is proportional to the amount of light absorbed. At specified time points during the experimental sequence, the camera reads the charge. The camera and filter wheel were synchronised by a computer using software obtained from Kinetic Imaging.

2.3.4 Loading of coverslips into microscope attachment

A brass microscope stand adapter with a reservoir designed to accommodate a coverslip was removed from the microscope platform and cleaned. The phalange on which the coverslip was to be seated was smeared with petroleum jelly. The coverslip was seated onto the phalange and secured with a Teflon ring. The excess petroleum jelly was wiped away with a tissue. 200µl of Hank's buffer was then dispensed into the coverslip chamber.

The reservoir was then fitted with a drainage device to enable the coverslips chamber to be easily drained during an experimental run. The device consisted of a narrow l-shaped stainless steel tube connected to a syringe via flexible tubing. The device was seated at edge of the chamber with the end touching the coverslip and was held in place with plasticine.

2.3.5 Observation of cells

The cells were examined under a fluorescent objective and a suitable field of cells was selected. The fluorescence intensity of both the 340nm and 380nm images were observed to establish whether emission from the cells was within the optimal range. If the signal was near saturation, the intensity of the light source was decreased using neutral density filters (10-80% transmission) until the 340:380nm ratio of the cells was at least 400 units greater than for a cell-free area. Cells with a resting 340:380nm ratios of 0.8-1.5 were considered healthy. The time interval between the ratio measurements was selected and the duration of the experiment was assigned.

2.3.6 Measurement of background fluorescence

The background fluorescence was obtained subsequent to cell stimulation. The imaging chamber was drained and 200µl of 1% Triton X-100 was dispensed into the cell chamber. A total of five frames were collected at five-second intervals. The averages of the five frames at 340nm and 380nm were calculated and subtracted from the 340nm or 380nm emissions of the sample.

2.3.7 Data processing of image data files

2.3.7a Extraction of data from image data files

The data collected from kinetic imaging was analysed using Lucida analysis software (Kinetic Imaging). Grabbed images were split into 340nm and 380nm ratios, representing fluorescent emissions from Ca^{2+}-bound Fura2 and free Fura2 respectively. Background 340nm and 380nm fluorescences (section 2.3.6) were subtracted from the split ratios. The 340:380nm ratio was re-calculated, to exclude the background 340nm and 380nm fluorescences, and the image file was stored to optical disk. The program was then used to mark a region of interest within every cell collected in the image file, (>30). The software was used to calculate the 340:380nm ratios for each time frame in the region of interest and write the data to an Excel spreadsheet. The 340:380nm ratio is proportional to the relative level of cytosolic Ca^{2+}. Absolute values of cytosolic Ca^{2+} were estimated from the ratio of the fluorescent intensities at the two excitation wavelengths after calibration of the imaging equipment (section 2.3.8).

2.3.7b Selection of parameters to use as indices of the cytosolic Ca^{2+} response

Examination of 340:380nm ratios of cytosolic Ca^{2+} responses of cells in response to stimuli demonstrate a wide variation in the characteristics of the response produced. The variations occur in respect of the time period between the addition of the treatment and the onset of the response (latent period), the rate of increase of the calcium rise, the maximal level of the cytosolic rise in Ca^{2+} (peak amplitude) and the rate of decrease in Ca^{2+} levels after the peak amplitude (decay time), (figures 2.4 and 2.5). In addition, the integral of the response was used as an index of the overall duration and magnitude of the response.

Figure 2.4: Parameters defining the kinetics of cytosolic calcium flux

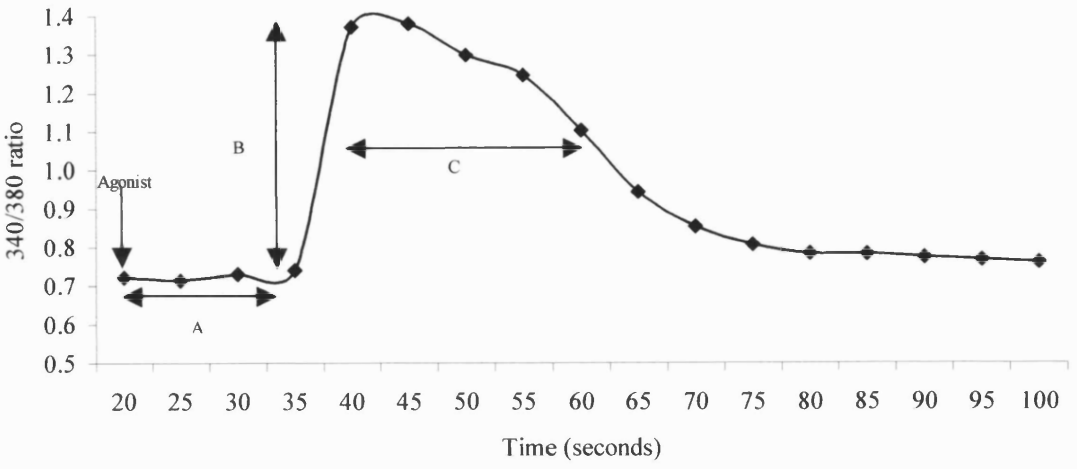

A: Lag time; time taken for induction of response
B: Peak amplitude; maximum increase in cytosolic calcium
C: Decay rate; time taken for calcium level to decrease to half the peak amplitude

Figure 2.5: Definition of indices used to measure cytosolic Ca^{2+} responses

- **Percent responders/response rate:**

  The percentage of the population of cells within the field of view that responded to the stimulus.

- **Peak amplitude:**

  The peak value of the post-treatment 340:380 ratio minus the mean of the pre-treatment 340:380 ratio

- **Decay time:**

  The time taken for the response to decay to half the value of the peak amplitude

- **Integral:**

  The area under the response curve

2.3.7c Visual Basic macro design for automation of file processing

In order to facilitate rapid analysis of the large data files, customised macros were written to automate data processing (appendix 2). The macro 'PlotXY' was used to reformat files and to plot and print graphical representations of the data in Microsoft Excel™. In addition another macro, 'MeanStDev' was written to perform calculation of the mean of the 340:380 ratio for each cell between given, user-defined time points specified in the user data sheet. This enables the user to compare the mean of the cytosolic calcium level before and after addition of the agonist or inhibitor. The macro 'PeakAmpDecay' was written to calculate the integral, the peak amplitude and the decay time of the cytosolic Ca^{2+} response of each cell. The calculation methods are defined in figure 2.5.

2.3.7d Definition of the criteria to assign cells as responsive to a stimulus

For the purpose of statistical analysis, a criterion was established classify cells as either responsive or non-responsive to a stimulus. A response was defined as a variation in the basal cytosolic Ca^{2+} levels of greater than 0.02, measured in terms of the standard error of the mean of the resting Ca^{2+} level.

2.3.7e Definition of the criteria to assign cells as exhibiting spontaneous Ca^{2+} transients

In order to analyse cellular responses to agonists and inhibitors, spontaneously firing cells were excluded from the statistical analysis. Spontaneously firing cells were defined as cells exhibiting a response, prior to the addition of agonist. The definition of a response is defined in 2.3.7d.

2.3.7f Statistical analysis of kinetic imaging data

Details of the statistical methods used to analyse the significance of the experimental results are described in the methods sections of each chapter.

2.3.8 Calibration of kinetic imaging apparatus

$[Ca^{2+}]_i$ was estimated from the ratio of the 510nm fluorescent intensities at the two excitation wavelengths (340nm and 380nm) as described by Grynkiewicz et al 1985. The maximum ratio value (R_{max}) was obtained by permeabilising the neurones with the Ca^{2+}-selective ionophore, 4-bromo A23187 (5μM) and discharging intracellular stores with thapsigargin (1μM) in buffer containing 50mM KCl and 2mM $CaCl_2$. The cells were then washed several times with buffer of a similar composition to the above but without $CaCl_2$ and containing

10mM EGTA. This provided the minimum ratio (R_{min}). Using this protocol, the constants R_{min} and R_{max} were 0.88 ± 0.047 and 4.23 ± 0.279 respectively (n=12). The $[Ca^{2+}]_i$ for intermediate values were then calculated from the following equation;

$$[Ca^{2+}]_i = K_d\,[(R - R_{min})/(R_{max} - R)][S_{f2}/S_{b2}]$$

where R is the ratio recorded under appropriate physiological conditions, S_{f2} is the signal at 380nm in Ca^{2+} -free buffer, S_{b2} is the signal in the presence of excess Ca^{2+}. The ratio of S_{f2}/S_{b2} was 3.12 ± 0.39 (n=12). K_d is the apparent dissociation constant for the indicator (usually 224nM for Fura2). Substitution of these values into the equation gives the formula;

$$[Ca^{2+}]_i = (698R\text{-}615.03) / (4.23 - R)$$

This formula was used to plot a graph of the 340:380nm fluorescence ratio versus the cytosolic Ca^{2+} levels (figure 2.6). Ca^{2+} is notoriously difficult to calibrate (see for example Tsien et al 1985). The graph in figure 2.6 demonstrates that a true minimum value was not obtained in this calibration. In these studies changes in Ca^{2+} are statistically analysed as fluorescence ratio changes rather than an absolute value. However, an estimate of the average absolute basal levels of cytosolic Ca^{2+} and the average increase in Ca^{2+} observed upon addition of agonists are presented in the text as a guideline. The estimate is derived from the equation of the trendline for the calibration curve, which is in the form y = mx + c. The equation was modified by setting the value for the intercept on the y axis (term c) to zero. Thus the equation for the calibration becomes;

Cytosolic $[Ca^{2+}]$ (nM) = 340:380nm fluorescence ratio / 0.0041

Figure 2.6: Instrument calibration
340: 380nm fluorescence ratio vs cytosolic $[Ca^{2+}]$

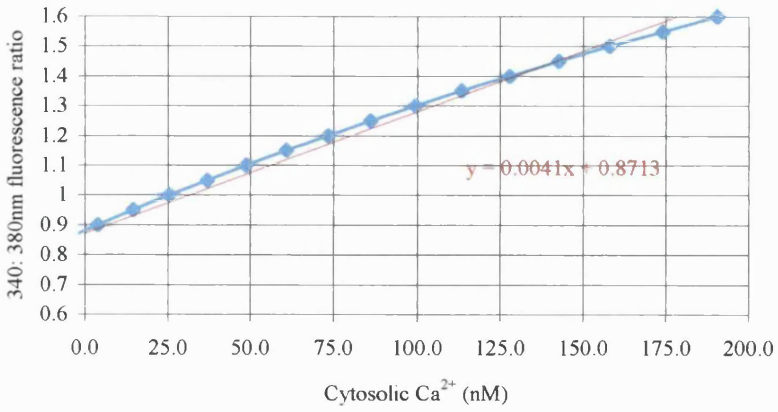

2.4 General molecular biology methods

2.4.1 Preparation of LB medium

10g of LB broth base (Sigma) was dissolved in a small Volume (~50ml) of sterile water. After thorough mixing the solution was made up to 500ml. The LB media was autoclaved and stored at room temperature for up to 3 months.

2.4.2 Preparation of low salt LB medium

10g of Tryptone, 5g yeast extract and 5g sodium chloride were dissolved in 1000ml of sterile pyrogen free deionised water (Baxter). The solution was then autoclaved for 20 minutes (15psi, 121°C). The solution was allowed to cool and stored below 30°C.

2.4.3 Preparation of LB agar/antibiotic plates

18.5g of LB agar was dissolved in a small volume (~50ml) of sterile water (Baxter). After thorough mixing of the LB agar, the solution was made up to 500ml with sterile water. The LB agar mix was then autoclaved and left to cool. Carbenicllin (Sigma) was added to a final concentration of 75μg/ml after allowing the LB agar media to cool to 55°C. The carbenicillin was mixed thoroughly and the LB agar poured into 6cm diameter polypropylene petri dishes to a depth of about 0.5cm. The plates were left to cool and were stored inverted for up to 3 months at 4°C.

2.4.4 Transformation of bacterial cells with plasmids

20-40ng of plasmid DNA in not more than 10μl was added to low efficiency JM109 cells (Promega). The bacteria and DNA were placed on ice for 10 minutes. The bacteria were heat shocked at 42°C for 50 seconds and immediately replaced on ice. 3ml of ice-cold SOC media (Gibco) was added prior to incubating the heat-shocked bacteria at 37°C for one hour. Transformants were selected by growth in media containing carbenicillin (75mg/ml). The transformed bacteria were either plated onto LB agar plates or inoculated into 50ml LB broth containing 75mg/ml carbenicillin. The success of the transformation was confirmed by isolation of plasmid from the overnight culture and agarose gel electrophoresis.

2.4.5 Isolation of plasmid DNA from transformed bacteria

5ml of cells were pelleted and the supernatant carefully removed. 3ml of cell resuspension solution was added to the cell pellet. 3ml of lysis solution was then added and the tube inverted several times. The pH of the suspension was then neutralised by the addition of 3ml of neutralisation buffer. The lysed cell suspension was then microcentrifuged at 13000rpm for

5 minutes. The supernatant was then collected. A syringe barrel was attached to a mini-column and the assembly was connected to a vacuum manifold. The supernatant was then pipetted into the syringe barrel followed by 1ml of resin. The vacuum was then applied to draw the supernatant/resin slurry into the mini-column. The mini-column was subsequently washed with 2ml column wash solution. The mini-column was vacuum dried for 30 seconds. The mini-column was then seated into the top of a microcentrifuge tube and spun for 2 minutes to remove residual column wash. The mini-column was then transferred to a fresh microcentrifuge tube and 50µl of water heated to 60°C was added to the column. The column was left for 1 minute prior to elution of the plasmid by centrifugation at 13000rpm for 30 seconds.

2.4.6 Spectroscopic determination of DNA and RNA concentrations

95µl of water was dispensed into a microcuvette. The absorbance of the blank sample was measured at 260 and 280nm in a spectrophotometer. 5µl of DNA/RNA sample was mixed with the water in the microcuvette and the absorption at 260nm and 280nm was determined. Background values were subtracted from the sample values at each wavelength.

The following formulae were used to convert to absorbance readings to concentrations;

$$[\text{dsDNA}]\ \mu g/ml = A_{260nm} \times \text{dilution factor} \times 50$$

$$[\text{ssRNA}]\ \mu g/ml = A_{260nm} \times \text{dilution factor} \times 40$$

2.4.7 Agarose gel electrophoresis

0.5g agarose (Promega) was added to 50ml 1X TBE (89nM Tris-borate, 2.5mM EDTA, pH 8.3 at 20°C) in a conical flask. The mixture was heated in a 750W microwave on medium power for 2 minutes to dissolve the agarose. The agarose was poured into a gel tray that was sealed with adhesive tape at the edges. A sample-loading comb was positioned into the agarose. The gel was left to set at room temperature for at least 2 hours. For electrophoresis of samples the comb and tape were removed and the gel was placed in the gel electrophoresis tank. The electrolyte reservoir of the tank was filled with 0.5X TBE sufficient to immerse the gel.

1µl of SYBRII and 8µl of sample loading solution (Sigma) was added to the samples. The samples were loaded into the sample wells alongside an appropriate DNA ladder (Sigma). Samples were resolved by electrophoresis at 1-5V/cm for 1-2 hours.

2.4.8 Decontamination of DNA samples using a PCR preparation kit

DNA samples were purified using the Wizard PCR Preps DNA purification system (Promega). 100µl of 'Direct Purification Buffer' was added to the samples in a 1.5ml microcentrifuge tube and the mixture was briefly vortexed. The resin mixture was warmed to 25°C for 10 minutes to ensure the crystals were dissolved. 1ml of resin mixture was added to the DNA sample and the mixture was vortexed briefly three times over a one-minute period. The mini-columns and the syringe barrels provided were assembled and the DNA/resin mixture was added to the syringe barrel. A vacuum was applied to draw the DNA/resin mixture into the mini-column. The column was washed with 2ml of 80% isopropanol under vacuum. The resin was dried under vacuum for a further 2 minutes. The mini-column was then transferred to a 1.5ml microcentrifuge to and centrifuged for 20 seconds at 12000g to remove any residual isopropanol. The mini-column was transferred to a fresh microcentrifuge tube and 50ul of TE buffer was added to the column. For DNA fragments greater than 3kb, the TE buffer was heated to 65-80°C. After 1 minute the mini-column was centrifuged at 12000g for 20 seconds to elute the cleaned DNA.

2.4.9 Determination of protein concentration using the Bradford assay

A standard curve was constructed for the Bradford protein assay. A series of dilutions of albumin ranging from 0.1mg/ml to 100mg/ml were prepared in duplicate. 1ml of each sample was incubated with 1ml of Bradford reagent (Sigma). In addition a blank solution was made up to determine the background absorbance of the Bradford reagent. The samples were left at room temperature for 30 minutes. The absorbance of the samples at a wavelength of 595nm was determined for each sample and the absorbance of the blank was subtracted from this value. The results were plotted on a graph of absorbance versus protein concentration (µg/ml). A linear regression line was fitted to the curve to provide an equation for the conversion of absorption readings into protein concentrations (r^2 = 0.94). The equation of the regression line was $y = 0.073x^{0.6758}$, where y is A_{595nm} and x is the protein concentration in µg/ml. To facilitate the ease of use of the standard curve, the equation was rearranged;

$$\text{Protein concentration (µg/ml)} = \{\text{EXP}\ [(\ln A_{595nm} - \ln 0.073)/0.6578]\}$$

CHAPTER 3

THE ROLE OF THE INTRACELLULAR DOMAIN OF TISSUE FACTOR IN THE INDUCTION OF CA^{2+} TRANSIENTS BY THE FVIIA : TISSUE FACTOR COMPLEX

3.1 Introduction

3.1.1 Tissue factor and cellular signalling

The ability of the TF: FVIIa complex to initiate the extrinsic pathway of coagulation (section 1.1) was established at the beginning of last century. More recently novel functions of the TF: FVIIa complex in cellular signalling have emerged. The initial data supporting a role for TF in cellular signalling was circumstantial in nature. The recognition of TF as a member of the cytokine receptor superfamily (Bazan J.F., 1990) suggested that TF might function in cellular signalling. In addition, the observation that phosphorylation of the serine residues occurs in the intracellular domain of TF (Zioncheck T.F. 1992 and Mody R.S., 1997) alludes to the existence of a TF-dependent signal transduction pathway. Further observations, demonstrating the involvement of TF in the alteration of cellular phenotype, confirmed a signalling function for TF.

The initial biological evidence that indicated a role for TF in cellular signalling was derived from studies *in vivo* that demonstrated the involvement of TF in angiogenesis. The first evidence to emerge that implicated a role for TF in angiogenesis was derived from studies of tumour genesis. The malignancy of tumours is synonymous with the ability of the tumour to metastasise and tumour metastasis is dependent upon angiogenesis at two stages of the pathogenic pathway (Folkman J., 1995). Firstly, metastatic cells are not shed from a primary tumour until after it has become vascularised. Second, upon arrival at the target organ metastatic cells must undergo neovascularisation to enable the metastasis to establish itself and grow.

A study in the early eighties that demonstrated the deposition of fibrin at the leading edge of breast tumours alluded to the involvement of TF in malignancy (Dvorak H.F., 1981). However, not until the next decade was a correlation between TF expression and metastatic capacity conclusively demonstrated (Mueller B.M., 1992). A number of subsequent studies confirm the association of TF with metastatic capacity in both humans (Contrino J., 1996, Vrana J.A, 1996, Pasqualini M.E. 1997, Koomagi R. 1998, Sawada M., 1999, Wojtukiewicz M.Z., 1999, Sawasda Y., 1999) and mice (Zhang Y., 1994 and Bromberg M.E., 1995) and also in cellular model systems (Kakkar A.K., 1999). A close correlation between the levels of VEGF and TF has been reported in neoplasia (Contrino J., 1996) furthermore, TF and VEGF co-localise in lung and breast cancer (Shoji M., 1998). VEGF is a cytokine that acts upon endothelial cells to promote vascular permeability, endothelial cell growth and angiogenesis (Connolly D.T., 1989 and Ferrara N., 1997). A significant relationship between TF expression, VEGF expression and microvessel density in human non-small cell lung

carcinoma has been reported (Koomagi M., 1998). The TF: FVIIa complex is capable of inducing VEGF (Ollivier V., 1998) and the existence of a positive feedback loop is suggested by the ability of VEGF to induce TF (Clauss M., 1996 and Camera M., 1999).

Increased TF activity accompanying angiogenesis has been also been observed in diabetic patients with retinopathic complications arising from neovascularisation of the retina (Zumbach M., 1997). The involvement of TF in the metastasis of tumours appears to result from the involvement of TF in angiogenesis. Metastasis of tumours and microvessel density are both linked to poor patient prognosis (Weidner N, 1991), thus TF activity may be indicative of the gravity of the disease. In addition, patients with malignant disease are at increased risk of thrombotic complications (Baron J.A., 1998), due to raised circulating levels of TF and excess thrombin generation (Kakkar A.K., 1995).

The ability of TF to support angiogenesis has been directly demonstrated. Enhancement of angiogenesis mediated by TF has been demonstrated in a diffusion chamber assay in rats, in an *in vitro* assay of bovine aortic endothelial cells in collagen gels (Watanabe T., 1999) and in tumours and in wounds (Nakagawa K., 1998). The role of TF in vasculogenesis during embryo development in mice has been recently recognised (Carmeliet P., 1996). Inactivation of the TF gene in mice resulted in abnormal circulation from yolk sac to embryo beyond embryonic day 8.5. TF deficiency compromises vascular development at a critical time when vessels develop a muscular wall in response to the physiological challenge of blood pressure load. This dysfunction seems to be related to a paucity of mesenchymal pericytes. This study demonstrates an intrinsic capacity for TF to function in *de novo* vascular modelling (vasculogenesis). The involvement of TF in vasculogenesis alludes to a potential for TF to be involved in the mechanisms of angiogenesis, where the circulatory network is extended from pre-existing vessels rather than occurring *de novo*.

More recently a number of studies have reported the activation of signalling pathways and the induction of genes by TF signalling. A list of genes induced by the TF: FVIIa complex is presented in figure 3.1. TF up-regulates several growth factors that have been reported to promote angiogenesis including, vascular endothelial growth factor (VEGF, Ollivier V., 1998), FGF-5, and CTGF (Camerer E., 2000a). CTGF and FGF-5 promote both the growth of connective tissue and angiogenesis and CTGF itself has been associated with atherosclerosis (Camerer E., 2000a). The binding of FVIIa to TF also induces expression of the poly(A) polymerase gene (PAP, Pendurthi U.R., 1997), a gene that is up-regulated in many human cancer tissues, particularly in colon carcinoma.

Not only does TF induce the expression of angiogenic proteins but it is itself up-regulated in response to recognised angiogenic stimuli including hypoxia (Lawson C.A., 1995 and

Amirkhosravi A., 1998), VEGF (Ollivier V., 1998), TGF-β (Ranganathan G., 1991) TNF-α (Martin N.B., 1993 and Camera E., 1999), PDGF-ββ (Xeureb, 1997), oestrogen (Quirk S.M., 1998) and bFGF (Camerer E., 2000). The mechanism of the involvement of TF in angiogenesis is explored further in chapter 5.

Figure 3.1: Activation of cellular responses by the tissue factor: FVIIa complex

- Transcriptional regulators
  p38 MAP kinase[a], p44/42 MAP kinase (erk1/2) [a,j,k], c-jun N-terminal kinase[a], c-fos [g], egr-1[a, g, h], ETR101[g], BTEB2[g], c-myc[g], fra-1[g], NFκB[e]
- Protein kinases
  Phospholipase C [a,c], PKC, G-proteins
- Growth factors
  Amphiregulin [g], hbEGF [g], FGF-5 [g], VEGF [h]
- Proinflammatory mediators
  IL-1β [g], IL-8 [g], LIF [g], MIP2α [g] , prostaglandin E2 receptor [g]
- Proteins involved in cellular reorganisation/ migration
  GTPases; RhoE[g], cdc42[d], Rac[d], urokinase receptor (uPAR)[b, g], PAI-2 [g], collagenases 1 and 3 [g], CTGF [f, g], Cyr61 [f], PDGF-BB-stimulated chemotaxis[c], Src-like kinases (c-src, lyn and yes)[d], c-Akt [d], IgE RI γ-chain[i], phosphatidylinositol 3-kinase [d]
- Intercellular communication
  Jagged1 [g]
- RNA processing
  Tristetraproline [g], cyclophilin [g], poly(A) polymerase[e]
- Stress/damage inducible gene
  GADD45 [g]

a: Camerer E., 1999, b: Taniguchi T., 1998, c: Siegbahn A., 2000, d: Versteeg H., 2000, e: Pendurthi U., 1997, f: Pendurthi U., 2000, g: Camerer E., 2000, h: Mechtcheriakova D., 1999, i: Masuda M., 1996, j: Sorensen B.B., 1999, k: Poulsen L.K., 1998

3.1.2 The proteolytic activity of TF: FVIIa and cellular signalling

The mechanism by which TF induces activation of the proteins listed in figure 3.1 is not fully understood, however, the proteolytic activity of the TF: FVIIa complex is known to be of importance in the signalling mechanism. Inactivation of FVIIa by a general serine protease inhibitor, benzamidine, inhibits induction of Ca^{2+} oscillations (Camerer E., 1996). In addition, inhibition of the active sites of FVIIa by 1,5-dansyl-Glu-Gly-Arg chloromethyl ketone (DEGRck) also abrogates the induction of Ca^{2+} signals (Camerer E., 1996). The involvement of thrombin as a mediator of the signalling pathway was excluded since the thrombin inhibitor hirudin had no significant effect upon cellular signalling elicited by FVIIa (Sorensen B.B., 1999). In addition, generation of FXa by FVIIa was excluded as a mechanism of signalling by FVIIa since TF: FVIIa-induced signalling was not quenched by tick anticoagulant protein (tAP), a specific inhibitor of FXa (Poulsen L.K., 1998).

Cellular signals induced by FVIIa are dependent upon proteolytic activity and its active site-inhibited counterpart is incapable of evoking Ca^{2+} signals. The requirement for the active site of FVIIa shows that ligand binding *per se* is not capable of mediating a cytosolic Ca^{2+} response. These results suggest the involvement of a factor other than TF in mediating FVIIa-induced cytosolic Ca^{2+} increases

It seems likely that a dual receptor mechanism exists that consists of a binding component and a proteolytically activated transducer. In this scenario, TF acts a co-factor that serves to tether the ligand to the cell surface. Since the protease activities of FVIIa and FXa are mandatory for the induction of the cytosolic Ca^{2+} signals, the potential involvement of protease activated receptors (PARs) 1-4 in the signalling responses to FVIIa and FXa was investigated. Protease activated receptors are the only receptors known to be activated by proteolysis (Camerer E., 1999). The PARs belong to a sub-group of the G-protein coupled receptor family. Agonist-induced activation of PARs leads to desensitisation of the Ca^{2+} response by a cleavage-independent mechanism that is thought to involve phosphorylation, internalisation and processing of the receptor. This mechanism renders the cells refractory to a second protease-induced response via the receptor.

The ability of thrombin to activate PARs 1, 3, and 4 and trypsin to activate PAR 2 was exploited to determine the potential involvement of PARs in FVIIa-induced signalling. In heterologous desensitisation experiments of the Ca^{2+} responses in MDCK cells, pre-treatment with thrombin did not impair the response to FVIIa or FXa (Camerer E., 1996). The inability of thrombin to desensitise the response to FVIIa and FXa excludes the involvement of PARs 1, 3 and 4 in the generation of cytosolic Ca^{2+} increases. In contrast, pre-treatment of HaCaT cells with the PAR2 agonist SLIGRL resulted in inhibition of the Ca^{2+} response induced by FVIIa by 57% (Camerer E., 1999). The desensitisation of the responses by SLIGRL suggests that PAR-2 or a close homologue is involved in the FVIIa- and FXa-evoked elevation of cytosolic Ca^{2+}. The involvement of the PAR-2 receptor in TF: FVIIa signalling has been confirmed recently (Camerer E., 2000b). Responses in keratinocytes and cytokine-treated endothelial cells suggests that PAR2 may be activated directly by TF: FVIIa and indirectly by TF: FVIIa-generated FXa.

3.1.3 Signalling molecules induced by TF: FVIIa

The ability of FVIIa to induce the transient tyrosine phosphorylation of cellular proteins was first observed in human monocytes (Masuda M., 1996). The electrophoretic mobility but not the specific identity of these tyrosine-phosphorylated proteins was determined. However, the association of TF with γ-chain homodimer of the IgE receptor type I ($F_c\varepsilon$ RI) in response to

occupation of TF by FVIIa was observed (Masuda M., 1996). The γ-chain of the $F_c\varepsilon$ RI is a signal-transducing protein. The significance of the association between TF and the γ-chain of $F_c\varepsilon$ RI has not been explored further.

It has been recently discovered that FVIIa leads to the activation of several proteins involved in cell signalling in a human keratinocyte cell line (HaCaT) (Camerer E., 1999). HaCaT cells constitutively express TF and respond to FVIIa with elevation of cytosolic Ca^{2+}, phosphorylation of p44/42 MAP kinase (erk 1/2), p38 MAP kinase and c-jun N-terminal kinase (c-JNK). FVIIa promotes the induction of the early response gene (egr-1) and this observation is the first known example of a transcription factor induced by a clotting factor. The induction of cytosolic Ca^{2+} elevations by FVIIa is sensitive to inhibition of PI-PLC in MDCK and HaCaT cells (Camerer E., 1996 and 1999). In addition, the induction of egr-1 in HaCaT by FVIIa is sensitive to inhibition of phosphatidyl-inositol phospholipase and inhibition of the p44/42 MAP kinase pathway (Camerer E., 1996 and 1999). Thus egr-1 induction is dependent upon PI-PLC and p44/42 MAP kinase. Furthermore, Ca^{2+} release is mediated by PI-PLC and therefore the Ca^{2+} signal probably lies on the pathway to induction of egr-1 expression.

The FVIIa-induced Ca^{2+} elevation in HaCaT cells is sensitive to pertussis toxin demonstrating that the signalling pathway is G-protein coupled (Camerer E, 1999). This result is consistent with a failure of the tyrosine kinase inhibitors herbimycin A, genistein and tyrphostin AG18 to inhibit FVIIa-induced Ca^{2+} response (Camerer E., 1996). Interestingly, although Ca^{2+} elevation probably lies on the pathway to induction of egr-1 by FVIIa, egr-1 induction was unaltered by pertussis toxin. This indicates that the initial part of the Ca^{2+} response is not required for the induction of egr-1.

3.1.4 Function of the extracellular and cytoplasmic domains of TF in signalling

The extracellular functions of the catalytically active TF: FVIIa complex co-operate with specific functions of the cytoplasmic domain to support metastasis (Fischer E.G., 1995, Mueller B.M., 1998, Bromberg M.E., 1999). Ligand binding *per se* is insufficient to support metastasis since active site-inhibited FVIIa does not support metastasis (Mueller B.M., 1998). The attenuation of metastasis by the blockade of the coagulation cascade at the levels of TF, FX and thrombin implicate a role for thrombin generation in the metastatic process (Fischer E.G., 1995). In addition, thrombin stimulates the adhesion of tumour cells to endothelium and subendothelium (Klepfish, 1993).

The ability of TF to promote metastasis of TF-transfected melanoma cells in severe combined immunodeficient (SCID) mice has been reported (Bromberg M.E., 1995). Metastasis of the

melanoma cells is abolished by loss of the cytoplasmic domain of TF. The requirement of the cytoplasmic domain in metastasis has been more specifically attributed to the requirement of the intracellular serine residues (Bromberg M.E., 1999). Phosphorylation of the cytoplasmic domain is required for the full metastatic effect of TF. Assembly of the TF: FVIIa complex is still required for metastasis even when the intracellular serine residues are mutated to aspartate residues, which mimic phosphorylated serine residues.

In contrast, other signalling functions of TF are reported to be independent of the cytoplasmic domain of TF. Signalling by TF: FVIIa through the PI-PLC, Ca^{2+}, p44/42 MAP kinase/egr-1 pathway occurs via the activation of PAR2. TF:FVIIa signalling via PAR2 (Camerer E., 2000), the activation of p44/42 MAP kinase (Sorensen B.B., 1999) and the induction of egr-1 by FVIIa and FXa in HaCaT cells (Camerer E., 1999) are all independent of the cytoplasmic domain of TF. Indeed, expression of TF lacking the cytoplasmic domain rescues embryonic lethality seen in TF knock-out mice (Melis E., 2001). Furthermore, it has recently been demonstrated that embryonic development, survival, fertility and coagulation are normal in mice engineered to express TF lacking the cytoplasmic domain (Melis E., 2001). These data demonstrate that the cytosolic domain is not essential for signal transduction in normal physiological processes.

Considered collectively, these data appear to present some contradictions. Tumour metastasis is dependent upon the cytoplasmic domain of TF (Bromberg M.E., 1995). The role of TF in tumour metastasis appears, at least in part, to be due to the ability of TF to promote angiogenesis. One of the mechanisms by which TF may induce angiogenesis is via its ability to induce VEGF (Ollivier V., 1998). The induction of VEGF is dependent upon the cytoplasmic domain of TF (Abe K., 1999). However, the induction of VEGF is also dependent upon egr-1, and yet egr-1 induction has been reported to be independent of the cytoplasmic domain of TF. Thus the involvement of the intracellular domain of TF in cellular signalling requires clarification. The data may reflect a functional redundancy of TF activity in normal physiological processes and an essential requirement for TF in pathological processes such as tumour metastasis.

3.2 Aims

- To investigate the induction of cytosolic Ca^{2+} transients by the TF: FVIIa complex in individual cells, using real-time fluorescence microscopy

- To determine the involvement of the cytoplasmic domain of TF in FVIIa-mediated Ca^{2+} signalling, using site-directed mutagenesis

- To investigate a potential role for each of the three serine residues in the cytoplasmic domain of the TF molecule in FVIIa-mediated Ca^{2+} signalling, by site-directed alanine replacement mutagenesis of TF (figure 3.2)

Figure 3.2: Point mutations in the cytoplasmic domain of TF

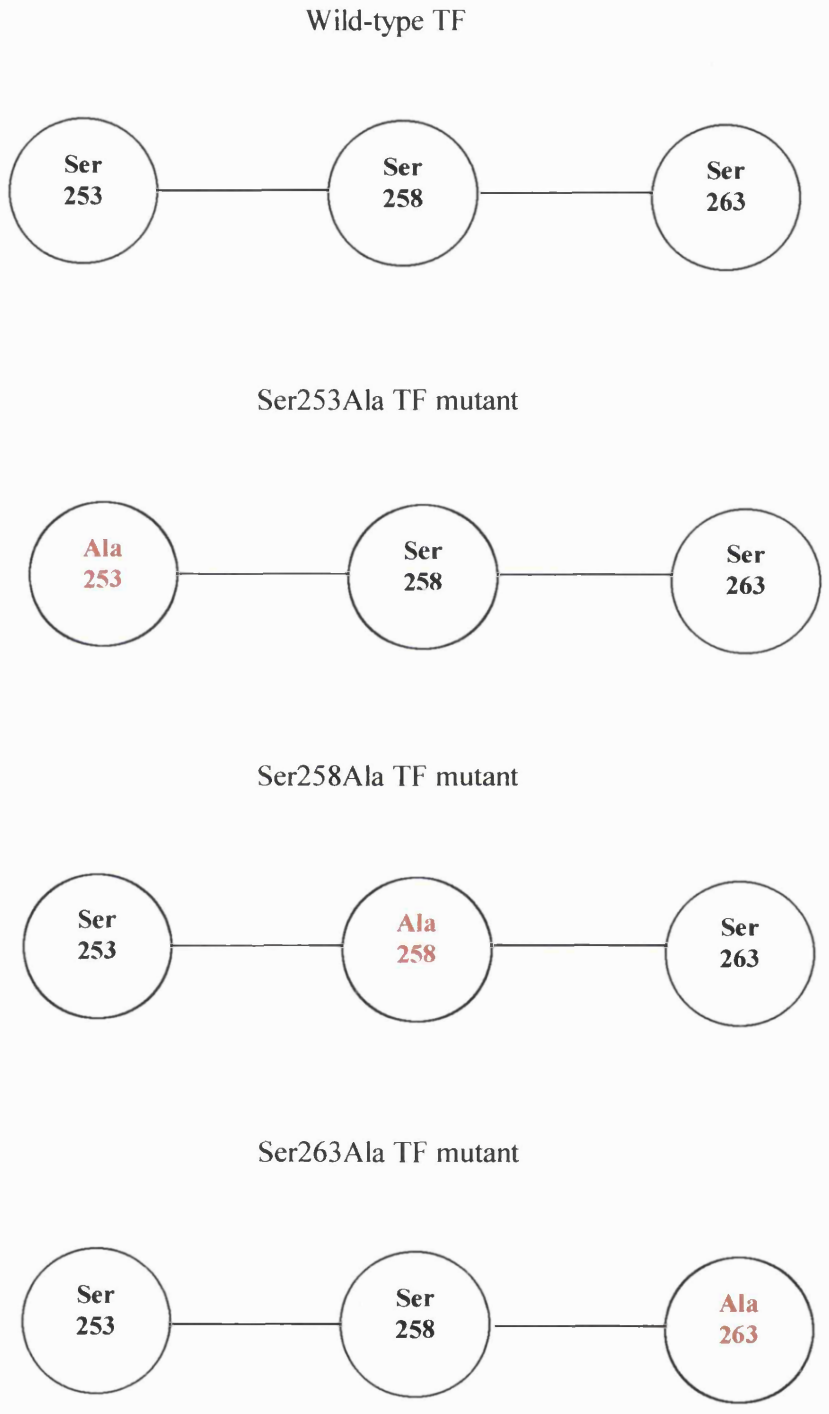

3.3 Methods

3.3.1 Overview of cloning and expression of wild-type tissue factor

3.3.1a The ecdysone-inducible expression vector system

The ecdysone-inducible expression vector system (Invitrogen) was selected as the cloning and eukaryotic expression vector for the following reasons. The ecdysone-inducible expression vector system (Invitrogen) expresses proteins in eukaryotic cells under the control of a concentration-dependent inducible promoter (figure 3.3). In addition, the expression system exhibits negligible basal expression with greater than 200-fold inducibility in mammalian cells (No D., 1996) since it uses an insect regulatory mechanism.

The pIND mammalian expression vector system consists of two plasmids; pIND and pVgRXR (Appendix 3). The gene of interest is cloned into the multiple cloning site of the pIND plasmid. Expression of the cloned gene is under the control of multiple copies (5) of the ecdysone-responsive element (E/GRE). The (E/GRE) element is located upstream of the multiple cloning site in the pIND subcloning vector. The (E/GRE) a hybrid DNA sequence located immediately upstream of the *Drosophila* minimal heat shock promoter pHSP. The E/GRE acts as a target site for the ecdysone receptor subunits, RXR and VgEcR, to bind and activate transcription from the pHSP. Both subunits of the heterodimeric ecdysone receptor, RXR and VgEcR, are constitutively expressed from the pVgRXR plasmid vector. In the presence of Muristerone^{TM}, an ecdysone homologue, the ecdysone receptor is activated and binds to the E/GRE. The receptor binding activates transcription from pHSP. The E/GRE prevents non-specific transcriptional activation since it is not recognised by endogenous mammalian regulatory molecules. Furthermore, multiple copies of the E/GRE sequence facilitate concentration-dependent induction of transcription by Muristerone^{TM}.

Both plasmids contain different antibiotic resistance genes to enable selection of successfully transfected mammalian cells. The pVgRXR vector (Appendix 3) contains Zeocin^{TM} resistance while the pIND vector produces neomycin resistance due to the expression of the APH gene, which detoxifies neomycin.

3.3.1b Cloning of *wild-type* TF and TF mutants

Wild-type tissue factor was cloned into the pIND expression vector system using the following methodology. Poly(A)+ mRNA was extracted from the myelomonocytic THP-1 cell line which expresses tissue factor constitutively. Reverse transcription of TF mRNA and the subsequent amplification of the TF cDNA were achieved using a single tube RT-PCR

Figure 3.3: The pIND expression vector system

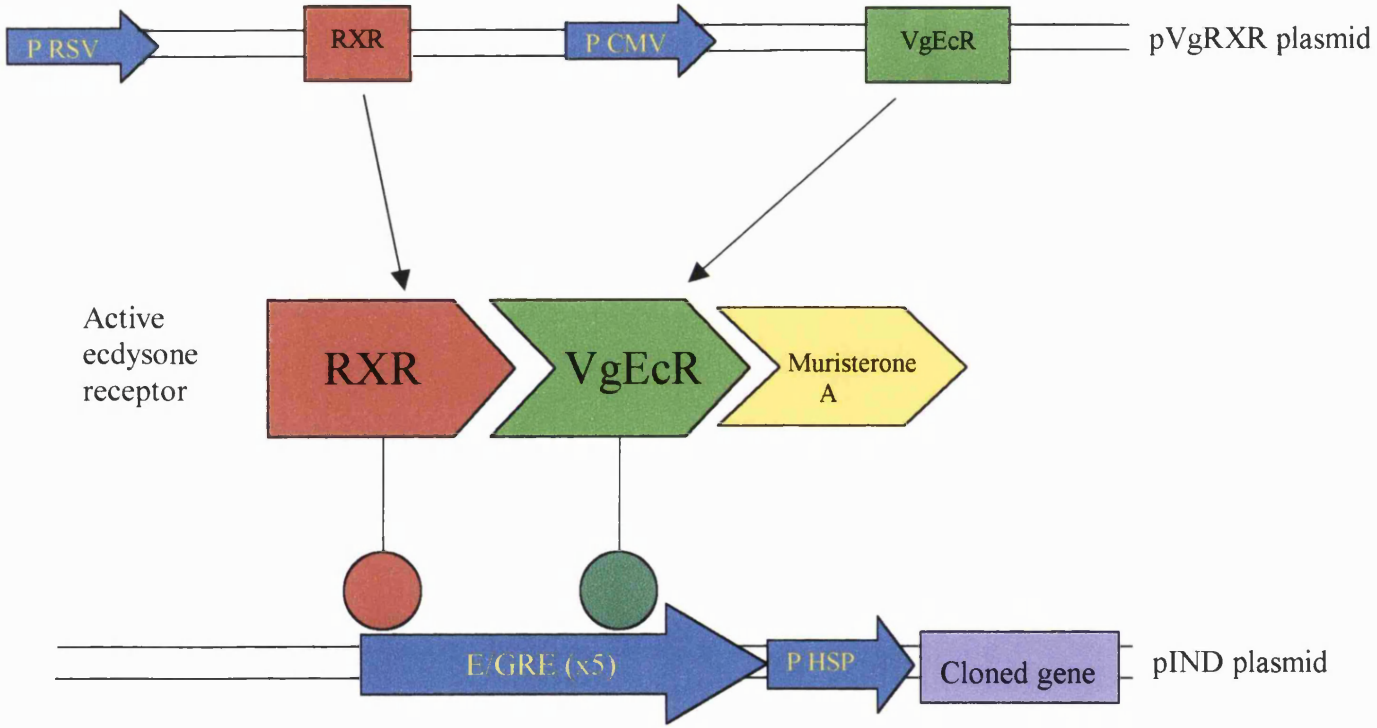

The gene of interest to be cloned is inserted into the multiple cloning site in the pIND plasmid The recombinant pIND plasmid is co-transfected with the pVgRXR plasmid into an appropriate mammalian cell. The pVgRXR plasmid expresses the two interacting subunits of the ecdysone receptor. When cells are treated with the ecdysone analogue, Muristerone A, the ecdysone receptor is activated and drives expression of the cloned gene from the pIND plasmid

P RSV & P CMV: Viral promoters, RXR & VgEcR: subunits of the heterodimeric ecdysone receptor, Muristerone A: ecdysone homologue, E/GRE: ecdysone and glucocorticoid response elements, P HSP: Drosophila minimal heat shock promoter.

technique (Promega). The RT-PCR primers were designed to introduce Bam H1 and Hind III restriction endonuclease sites flanking the RT-PCR product in order that the RT-PCR product could be uni-directionally cloned in-frame into the pIND expression vector (section 3.3.3). The pIND plasmid containing the cloned wild-type TF was then used as a template for site directed mutagenesis to produce TF mutants.

3.3.2 Isolation of poly(A)+ mRNA from THP-1 cells

Untreated THP-1 cells expressing TF were harvested for the preparation of poly(A) mRNA. The cells were washed with PBS and the supernatant removed. Poly(A)+ mRNA was extracted from the cells using the mini message maker kit (R & D Systems). 7 x 10^6 cells were resuspended in 1ml lysis buffer and the suspension was sheared using a 25-gauge needle. The sample was microcentrifuged for 3 minutes at 13000rpm. The supernatant was then transferred to a new tube and made up to 1.5ml with lysis buffer. 50µl of oligo dT-latex was then added to the supernatant. The tube was inverted 10 times and allowed to stand for 10 minutes. The suspension was then microcentrifuged for 5 minutes at 13000 rpm and the supernatant discarded. The pellet was resuspended in 350µl of lysis buffer before transfer to a spin column. The spin column was centrifuged at 13000 rpm for 2 minutes. The beads were then resuspended in 400µl of wash buffer and centrifuged for 1 minute at 13000 rpm. This wash step was repeated prior to the elution step. The poly(A)+ mRNA was released from the latex by the addition of 50µl of elution buffer heated to 70°C. The poly(A)+ mRNA was collected by centrifugation of the column for 1 minute at 13000 rpm. The concentration of the RNA was determined using spectroscopy as described in section 2.4.5.

3.3.3 RT-PCR of tissue factor from poly(A)+ mRNA

3.3.3a Primer design

The oligonucleotide primers for the RT-PCR of TF were purchased from PE-Applied Biosystems U.K., Warrington, Cheshire. The primers were supplied in 20% acetonitrile (v/v) in water. Immediately prior to use, aliquots of the oligonucleotides were freeze-dried and resuspended in nuclease-free water.

The 34-mer reverse primer (figure 3.4) was designed to be complementary to residues 99-32 of the TF mRNA. A Hind III restriction enzyme digestion site was incorporated 8-13 bases from the 5' terminus. The 7 bases flanking the 5' side of the Hind III site facilitate recognition by the restriction enzyme to ensure efficient digestion of the PCR product. This modification is unlikely to impair the DNA polymerase since base mismatches proximal to the 5' end are

far less critical for primer annealing than 3' mismatches. The forward primer was designed to anneal to residues 994-1028 of the TF mRNA species. This primer incorporated a BamH1 restriction enzymes site 8 bases from the 5' terminus to facilitate efficient digestion of the PCR product. Both primers were designed to have either a guanine or cytosine residue at the 3' terminus to optimise annealing of the mRNA template with the primers. In addition, the primers were designed to anneal at approximately identical temperatures and consisted of approximately 40% guanine or cytosine bases.

Figure 3.4: Primer design for RT-PCR of tissue factor mRNA

FORWARD PRIMER

5' **TCG ATC T*AA GCT T*CA ACT GGT AGA CAT GGA GAC C** 3'

REVERSE PRIMER;

5' **TCC AAC AGT *GGA TCC* TTT ATG AAA CAT TCA GTG G** 3'

Bases in italics denote Hind III and Bam H1 restriction enzyme sites respectively.

3.3.3b RT-PCR of tissue factor mRNA

The RT-PCR reaction was assembled as detailed in figure 3.5. The PCR was carried out using the 'hot start' method. DNA polymerase or forward primer was not added until after the reverse transcription reaction, during the first denaturation step of the PCR to minimise primer: dimer formation and false priming. The thermal cycling parameters for the TF RT-PCR reaction are tabulated in figure 3.6.

3.3.4 Extraction of the TF RT-PCR product from agarose gel

The RT-PCR reaction products were resolved by agarose gel electrophoresis (section 2.4.7). Siliconised glass wool was prepared by soaking glass wool in dimethyldichlorosilane and allowing the glass wool to dry. A 0.5ml microcentrifuge tube was prepared by puncturing the base with a hypodermic needle and transferring a sufficient amount of glass wool to form a plug at the base of the tube. The band of interest was excised from the gel under *u-v* illumination and was transferred to the microcentrifuge tube. The 0.5ml microcentrifuge tube was positioned inside a 1.5ml microcentrifuge tube. The assembly was then centrifuged for 15 minutes at 13000g and the eluate containing the DNA was collected.

Figure 3.5: Components of the RT-PCR reaction for tissue factor

Reaction component	Volume (µl)
AMV/Tfl buffer (10X)	10.0
Forward primer (4.7 pmol/µl)	5.0
Reverse primer (9.8 pmol/µl)	2.5
Template (poly(A)+ mRNA)	10
$MgSO_4$ (25mM)	2.0
dNTP (10mM each)	1.0
AMV reverse transcriptase (10U/µl)	1.0
Thermus *flavus* DNA polymerase (5U/µl)	1.0
Nuclease-free water	17.5
Total reaction volume (µl)	50.0

Figure 3.6: Thermal cycling protocol for RT-PCR of tissue factor

Step	Temperature (°C)	Time (minutes)
A. Reverse transcription	48	45
B. AMV inactivation	94	2
C. Template denaturation	94	1
D. Primer annealing	64	1
E. Primer extension	68	1
F. Repeat steps C to E 25 times	-	-
G. Extend all products	68	8

Figure 3.7: Restriction digestion of DNA with Bam H1 and Hind III

	Volume (µl)			
Reaction component	**A**	**B**	**C**	**D**
Buffer E (10X)	2	2	2	2
Acetylated BSA (1mg/ml)	2	2	2	2
Bam H1 (10U/ul)	1	1	0	0
Hind III (10U/ul)	1	0	1	0

0.1 - 0.5 µg of DNA was added to each reaction mixture and the reaction made up to 20µl with nuclease-free water. The digest was incubated at 37°C for 12 hours.

3.3.5 Restriction digestion of RT-PCR product

The RT-PCR product was digested using Bam H1 and Hind III to allow uni-directional cloning of the insert into the pIND vector. The reaction was assembled as shown in figure 3.7, column A. Bam H1 and Hind III digestion was performed simultaneously as the enzymes function optimally in the same buffer.

3.3.6 Restriction digestion of pIND plasmid sub-cloning vector

The pIND vector was digested with Bam H1 and Hind III. Several reactions were assembled as detailed in figure 3.7, columns A to D. After an incubation period of 2h, 100U of calf intestinal alkaline phosphatase (CIAP) was added to the reaction mixture in order to dephosphorylate the 5' sticky ends produced by restriction enzyme digestion and prevent re-ligation of the sticky ends.

3.3.7 Phenol: chloroform extraction of digested plasmid DNA

The restriction digest was then phenol chloroform extracted in order to remove restriction digest enzymes and calf intestinal alkaline phosphatase.

Two times the sample volume of phenol: chloroform (1:1 v/v) was added to the sample. The mixture was vortexed and then microcentrifuged for 5 minutes at 5000rpm. The upper aqueous phase was collected, leaving denatured proteins at the interface between the organic and aqueous phases. A volume of sodium acetate (3M, pH 5.2) equal to 1/10 of the volume of DNA was added to the recovered supernatant. This was followed by the addition of a volume of absolute ethanol equal to 2 times the volume of DNA sample. The DNA was pelleted for 10 minutes at 13000g in a microcentrifuge tube. The supernatant was carefully decanted and discarded.

A volume of 75% ethanol equal to the DNA volume was added to the DNA pellet. After thorough mixing, the tube was microcentrifuged for 10 minutes at 13000g. The supernatant was removed and the 75% ethanol wash was repeated. 50µl of absolute ethanol was added to the pellet and the tube was centrifuged again for 10 minutes at 13000g. The DNA pellet was left to dry in a heating block at 40°C (with the microcentrifuge tube lid open). The pellet was then resuspended in nuclease-free water.

3.3.8 Ligation of insert and vector DNA

The ligation reaction was assembled using the Bam H1 and Hind III restriction digested, dephosphorylated pIND plasmid vector and the restriction digested RT-PCR product as shown in figure 3.8.

E. Coli cells were transformed with the ligation products and selected with carbenicillin (section 2.4.3). Transformed cells were grown and harvested for the preparation of plasmid DNA (section 2.4.4). The plasmid DNA was used to confirm that the TF was cloned in the appropriate position in the pIND vector. As an initial test, the plasmid was used as a template for PCR of TF (figure 3.9), to determine the presence of the sequence in the plasmid. To confirm the correct positioning of the TF sequence in the recombinant pIND(+TF*wt*) plasmid, samples were sent to the Babraham Institute, Cambridge, U.K., for automated sequencing.

Figure 3.8: Ligation of restriction digested TF RT-PCR product and pIND plasmid

Reaction component	**Volume (µl)**
Vector; pIND plasmid DNA (12.5ng/µl)	1.5
Insert; PCR product (12.5ng/µl)	15.5
T4 DNA ligase (3U/µl)	1
Ligase buffer (10X)	2

Nuclease-free sterile water was added to bring the final volume to 20µl and the reaction mixture was incubated at 22°C for 3.5 hours.

Figure 3.9: PCR of plasmid templates

Reaction component	**Volume (µl)**
Buffer (10X)*	10
Forward primer (4.7 pmol/µl)	4
Reverse primer (9.8 pmol/µl)	4
Plasmid (0.5ng/µl)	2
$MgSO_4$ (25mM)	2
dNTP (10mM each)	1
Thermus *flavus* DNA polymerase (5U/µl)	1
Nuclease-free water	26
Total reaction volume	50

3.3.9 Site directed mutagenesis of pIND(+TF*wt*)

3.3.9a Design of mutagenic primers;

Both the coding and non-coding strands were designed to anneal to the same sequence on opposite strands of the template DNA. The primers were designed to encode the mutation in the middle of the sequence, flanked on both sides by approximately 10-15 bases. In addition the primers had a minimum G:C content of 40% and terminated in one or more G or C residues, particularly at the 3' terminus. The primers were designed to have a melting temperature approximately 10°C above the extension temperature of 68°C (figure 3.10). The melting temperature (T_m) was calculated using the following formula;

$T_m = 81.5 + 0.41(\%G:C) - (675/N) - \text{mismatched bases (\%)}$

where N = total number of bases and %G:C = the percentage of the sequence that is either G or C.

Primers were purchased to order from Genosys. The 3 O.D. scale synthesis oligomers were of sufficient purity to achieve successful mutations.

3.3.9b Reaction conditions for site-directed mutagenesis PCR of pIND(+TF*wt*)

The reaction components for site-directed mutagenesis of the pIND plasmid containing wild-type TF, pIND(+TF*wt*), were assembled in PCR tubes as shown in figure 3.11. The thermal cycling protocol for the PCR reaction is tabulated in figure 3.12. The PCR reaction was carried out using the 'hot-start' method to minimise the occurrence of false priming. The DNA polymerase was added only after the reactions reached the denaturation temperature.

The PCR reaction products were subsequently incubated with Dpn1 restriction enzyme for 3 hours at 37°C. Dpn1 digests the methylated wild-type parent plasmid but has no activity towards the non-methylated PCR product containing the mutated sequence. Subsequent to Dpn1 digestion, 10µl of the PCR reaction mix was used to transform JM109 as described in section 2.4.3. The transformed bacteria were plated onto LB agar containing 75µg/ml carbenicillin (section 2.4.2) and grown overnight. Colonies were picked using a sterile pipette tip and were expanded in a liquid culture of LB media. Plasmid was prepared for sequencing and transfection of mammalian cells (section 2.4.4). The plasmids were sent for automated sequencing (Babraham Institute, Cambridge, U.K.).

Figure 3.10: Primer sequences for site-directed mutagenesis

Cytoplasmic deletion mutant (coding strand)

WILD-TYPE **C ATC CTG GCT ATA TCT CTA CAC AAG TGT AG**

241-263del **C ATC CTG GCT ATA TAA CTA CAC AAG TGT AG**

Codon change; TCT to stop codon TAA

Ser253Ala mutagenic primer (coding strand)

WILD-TYPE **CA GGA GTG GGG CAG AGC TGG AAG GAG AAC**

ALA 253 MUTANT **CA GGA GTG GGG CAG GCC TGG AAG GAG AAC**

Codon change; AGC to GCC

Ser258Ala mutagenic primer (coding strand)

WILD-TYPE **GC TGG AAG GAG AAC TCC CCA CTG AAT G**

ALA 258 MUTANT **GC TGG AAG GAG AAC GCC CCA CTG AAT G**

Codon change; TCC to GCC

Ser263Ala mutagenic primer (coding strand)

WILD-TYPE **CC CCA CTG AAT GTT TCA TAA AGG ATC CAC TAG**

ALA 263 MUTANT **CC CCA CTG AAT GTT GCA TAA AGG ATC CAC TAG**

Codon change; TCA to GCA

Figure 3.11: Site-directed mutagenesis PCR of cloned tissue factor

Reaction component	**Volume (µl)**
10X buffer	5
Plasmid template at 5ng/µl	1
Mutagenic primer (coding) at 0.9pmol/µl (125ng of each)	2.5
Mutagenic primer (non-coding) at 0.9pmol/µl	2.5
DNTPs (2.5mM each)	2
Volume made up to 49µl with water	
Plus 1µl Pfu turbo DNA polymerase	

Figure 3.12: Thermal cycling parameters for site-directed mutagenesis PCR

Temperature (°C)	**Time (minutes)**
95	2
55	1
68	16
Number of cycles: **16**	

3.3.10 Selection of an appropriate cell line to studying cellular signalling by TF

The COS1 cell line was selected as a host for transfected TF, as this cell line has been previously reported to lack endogenous TF expression and has been used successfully for Ca^{2+} signalling studies by other groups (Rottingen J., 1995). However, before proceeding with the transfection studies, the procoagulant assay (section 2.2.1) was used to confirm the inability of COS1 cells to express TF.

3.3.11 Establishment of a clonally-derived CHO K1 cell-line stably transfected with plasmid pVgRXR

The pIND inducible expression system consists of two separate plasmids. The pVgRXR plasmid drives the expression of the cloned gene from the pIND plasmid. For expression studies, both of the plasmid vectors may be co-transfected into the appropriate cell line. Alternatively, a stably transfected cell-line containing the pVgRXR plasmid integrated into the genome can be created. The pIND vector is then transiently transfected into the cell-line for expression studies. Although the latter methodology is more time-consuming, it was selected as the method of choice. If the co-transfection method is used, the efficiency of transfection of the pVgRXR plasmid will vary between different transfection samples. Differences in the uptake of the pVgRXR during transfection could lead to variation in the final level of TF expression between samples. Such variation may reduce the comparability of results obtained with different transfection samples. Establishment of a cell-line derived from a single parent cell stably transfected with the pVgRXR plasmid ensures that all the cells will contain equivalent levels of the pVgRXR plasmid. Interpretation of the results obtained will not be confounded by differences in the level of gene induction from the expression plasmid.

3.3.11a Determination of the sensitivity of CHO K1 cells to Zeocin™

CHO K1 cells were maintained in DMEM: Ham's F12 media (complete media) containing 10% filtered, heat-inactivated, γ-irradiated FBS (section 2.1.4). Cells were harvested during logarithmic phase and were counted using a haemacytometer. 0.1 x 10^6 CHO K1 cells were seeded in T25 culture flasks and the culture volume was made up to 8ml with complete media. Zeocin™ was added at final concentrations of 50, 100 and 150μg/ml. A control flask without antibiotic was also prepared. The cells were maintained in a humidified incubator at 37°C under 5% CO_2. The media was changed every 4 days and fresh antibiotic was added. The cell samples containing antibiotic were observed daily for 10 days and compared to the control sample to assess cell survival in the presence of antibiotic.

3.3.11b Linearisation of pVgRXR plasmid

The plasmid constructs were linearised prior to transfection into CHO K1 cells to increase the probability of DNA becoming incorporated into the host genome to produce stably transfected cells. The pVgRXR plasmid was prepared using a plasmid purification procedure (section 2.4.5). The purified pVgRXR plasmid was linearised with the restriction enzyme Mlu1 in order to increase the chance of heterologous recombination into the host chromosome. The restriction digest was assembled in a microcentrifuge tube on ice. The reactants were assembled in the order shown in figure 3.13.

Figure 3.13: Restriction endonuclease digestion of pVgRXR plasmid with Mlu1

Reaction component	Volume (µl)
Water	2
Restriction digest buffer (10X)	13
Acetylated BSA (1mg/ml)	13
DNA (70µg/ml)	100
Mlu 1 (10U/µl)	4

The plasmid sample was digested with the restriction endonuclease at 37°C for 24h. The sample was resolved using agarose gel electrophoresis (section 2.4.7). The agarose gel was visualised under *uv*-transillumination to confirm that the plasmid was linearised. Following restriction digestion, the endonuclease was removed using a PCR preparation kit (Promega) as described in section 2.4.8.

The purity of the purified plasmid was determined using spectroscopy (section 2.4.5). All plasmid DNA used for the transfection of mammalian cells had a 260: 280nm ratio of between 1.8 and 1.9.

3.3.11c Electroporation of CHO K1 cell line with plasmid pVgRXR

Plasmid pVgRXR was introduced into CHO K1 cells using an electroporation technique. CHO K1 cells were grown in DMEM/Ham's F12 Nut Mix media containing Glutamax™ for a period of 24 hours prior to electroporation. CHO K1 cells were harvested in logarithmic phase using Versene™. The cells were washed, counted and resuspended in DMEM/high glucose at a concentration of 3 x 10^6 cells/ml.

Electroporation was performed at room temperature 800µl of cells were dispensed into an electroporation cuvette with a gap width of 0.4cm. 1-6µg of pVgRXR plasmid in 100µl of 1X TE buffer was added to the cell suspension. The DNA was incubated with the cells for 20

minutes. The cells were then electroporated using a BioRad Gene Pulser using the following settings (0.245kV, 960μF, 0.098kV/cm).

3.3.11d Cloning of a CHO K1 cell line stably transfected with plasmid pVgRXR

Two rounds of cloning using a limiting dilution method were used to establish a cell-line derived from a single parent cell. Non-transfected CHO K1 cells were cultured to determine the plating density of cells required to facilitate the formation of cell colonies derived from a single parent cell. A limiting dilution methodology was used to establish the optimal plating density. CHO K1 cells grew as isolated colonies when plated at an equivalent of 0.07 cells per cm^2 culture dish.

Subsequent to electroporation the cells were resuspended in a complete media. Each electroporation sample was dispensed into T175 tissue culture flasks. The cells were permitted to double twice under non-selective conditions. The cells were then switched to selective conditions (100μg/ml Zeocin™) and were maintained in logarithmic phase by splitting the cells when they reached confluence. The selection procedure was applied for approximately 2 weeks.

Several aliquots of the cells were stored in liquid nitrogen. In addition some cells were taken for the first round of cloning. The cells were harvested using Versene™ and were washed in media. 3000 cells were seeded into 8cm diameter petri-dishes (0.07 cells/cm^2). The cells were subsequently fed with selective medium containing 75μg/ml Zeocin™ every 4 days. The growth of colonies in culture flasks was monitored using a phase-contrast microscope.

Colonies containing 500-1000 cells were picked for a subsequent second round of cloning (sub-cloning). One end of an autoclaved O-ring was coated with autoclaved silicon grease. The O-ring was placed to encompass the colony of interest. The colony was dislodged by pipeting and was placed into a 96-well plate. Several of the colonies were expanded in culture and aliquots of the cells were stored in liquid nitrogen.

One of the colonies was arbitrarily chosen for a further round of sub-cloning. The cells were again plated at an equivalent of 0.07 cells/cm^2 culture dish and were maintained under selective conditions. The cultures were observed until colonies containing 500-100 cells were evident. In total, 40 colonies were picked from the sub-clones in order to isolate a cell-line with the pVgRXR plasmid stably integrated into the host genome. These colonies were expanded to a number at least exceeding 10 x 10^6, to provide sufficient cells for long-term storage under liquid nitrogen.

3.3.12 Expression of TF from pIND plasmid constructs in the stably transfected pVgRXR-positive CHO K1 cell line

3.3.12a Transfection of the pVgRXR-positive CHO K1 cell line with pIND(+TF) plasmid constructs

The stably transfected pVgRXR-positive CHO K1 cells were transfected with the various pIND plasmids encoding either wild type or mutant TF. In all cases the transfection procedure was the same.

1mg of Transfectam^{TM} was resuspended in 400µl of 100% ethanol to give a 2mM stock solution. The stock was vortexed and stored in the fridge at least 24 hours prior to use to ensure optimal solubilisation and maximal transfection efficiency.

Cells were seeded onto coverslips as described in section 2.1.8. Cells were grown to 40-50% confluence in DMEM/Ham's F12 media containing 10% γ-irradiated FBS. Cells were washed in DMEM/Ham's F12 in the absence of serum, which would otherwise inhibit the transfection process.

Two separate DMEM/Ham's F12 solutions were prepared for each transfection. The first solution consisted of DMEM/Ham's F12 (1ml per cm^2 culture area) supplemented with the appropriate TF-containing pIND plasmid (3µg per cm^2 culture area). A second media solution containing an equivalent volume of DMEM/Ham's F12 was prepared and 1.4µl of Transfectam^{TM} per µg of plasmid DNA was added to the media. Both solutions were briefly vortexed and then mixed to enable the Transfectam^{TM} to bind to the plasmid DNA. The transfection mixture was then added drop-wise to the washed cells. Cells were maintained at 37°C under 5% CO_2 in a humidified atmosphere for 24 hours to enable uptake of the plasmid into the cells.

3.3.12b Induction of gene expression from TF-positive pIND plasmid constructs

Cells were washed free of any excess transfection mixture using DMEM/Ham's F12 supplemented with 10% γ–irradiated FBS, penicillin and streptomycin. The cells were then resuspended in fresh complete DMEM/Ham's F12 media (3ml per cm^2 culture area). Muristerone^{TM} was added to the cells at the desired final concentration and the cells were replaced into the incubator for the required time period.

3.3.12c Measurement of TF expression on transfected pVgRXR/CHO K1 cells using a flow cytometric technique

The media was removed from the culture vessel and a quantity of Versene™ sufficient to cover the base of the culture dish was added. The culture vessels were replaced in the incubator until the cells were detached. Cells were washed with PBS and an aliquot removed for counting. For flow cytometry, two aliquots from each sample, containing a minimum of 0.1m cells each, were dispensed into 1.5ml microcentrifuge tubes. The cells were pelleted at 13 000g for 1 minute in a microcentrifuge. The supernatant was removed and the cells were resuspended in 100µl of PBS. 5µl of a mouse IgG1 monoclonal antibody to TF (Calbiochem) at a concentration of 0.1mg/ml was added to one tube and 5µl of a control antibody directed toward Aspergillus *nidulans* glucose oxidase was added to the other tube. The cells were incubated with the antibodies for 30 minutes on ice. The cells were then washed with 1ml of cold PBS and resuspended to 100µl in PBS. The cells were incubated with 5µl of a FITC-conjugated goat anti-mouse antibody (Becton Dickinson) for a further 30 minutes on ice in the dark prior to flow cytometric analysis.

TF expression on CHO K1 cells was examined using a Coulter Epics-MCL flow cytometer. Cells stained with negative control antibody were transferred to flow cytometry tubes and the tube was positioned into the machine. The voltage and gain of the forward scatter (FSC) and side scatter (SSC) photomultiplier tubes were adjusted so that the cell population was positioned in the centre of the FSC vs SSC dot plot. The threshold on the FSC signal was set in order to exclude machine noise from the FSC vs SSC dot plot. An amorphous gate was drawn around the region of interest to include cells and exclude cell debris. In addition, an amorphous region was also drawn around the cell debris/shed vesicles. The FL1 channel of the cytometer was used to detect the fluorescence of the FITC-conjugated antibodies. The fluorescence of at least 26, 000 events were collected and separate fluorescence histograms for cells and vesicles were displayed. Each histogram represents a plot of cell number versus the logarithm of the FL1 fluorescence intensity. The voltage and gain of the FL1 channel was set so that the lowest levels of fluorescent emission from the cells or vesicles were positioned within the first log decade. Linear regions were drawn in both log FL1 histograms in order for the software to perform calculations of the mean fluorescence intensity for the cells and vesicles/debris.

For each separate sample the fluorescence of cells stained with negative control antibody was used as a measure of background fluorescence arising from non-specific staining. The fluorescence of the control was subtracted from the fluorescence of the sample stained using the anti tissue factor antibody to give the relative level of cellular tissue factor expression.

3.4 Results

3.4.1 Isolation of poly (A)+ mRNA from THP-1 cells

The isolation of mRNA from THP-1 cells was confirmed qualitatively using SYBRI (Flowgen). SYBR I is a fluorescent dye that emits green fluorescence when it is bound to RNA. The fluorescent emission is selective and does not occur in the presence of DNA.

A 2µl sample of the poly (A)+ mRNA isolate was mixed with a 1 in 1000 dilution of the stock SYBR I solution. A strong fluorescence was evident when the sample was observed under ultra violet light at a wavelength of 254nm. The concentration and purity of the RNA sample was determined using a spectrophotometer as described in section 2.4.6.

3.4.2 RT-PCR of tissue factor from THP-1 cells

A 10µl sample of the products resulting from RT-PCR amplification of the poly A mRNA sample was subject to agarose gel electrophoresis as described in section 2.4.7. A 100bp ladder was loaded in parallel with the RT-PCR products. The RT-PCR of poly (A)+ mRNA isolated from THP-1 cells using the TF primers lead to the amplification of a distinct band that resolved equivalent to 900bp in the DNA ladder (figure 3.14). The calculated length of the band resulting from amplification of the appropriate TF mRNA was 900bp. The band that migrated equivalent to the 900bp in the DNA ladder band was excised. The PCR product was extracted from the gel as described in section 3.3.4.

3.4.3 Restriction digestion of pIND plasmid

In order to perform uni-directional cloning, the pIND plasmid was digested with BamH1 and Hind III. BamH1 and Hind III each cut the pIND plasmid once within the multiple cloning site. Since the two enzymes are functional in the same buffer, both enzymes were added simultaneously. The reaction mixture was assembled as shown in figure 3.7. An aliquot of the digestion mixture was subject to agarose gel electrophoresis to determine the success of the digestion procedure (figure 3.15). The excised fragment is too small to be detected easily on agarose gel electrophoresis. An alternate means of detecting the success of the digestion was devised. When the plasmid is cut by a restriction endonuclease, it becomes linearised and its mobility on agarose is reduced. However, since the plasmid only needs to be cut by one enzyme to become linearised, it is not possible to determine whether a linearised plasmid results from digestion by one or both of the enzymes. Furthermore, it was not possible to determine whether each enzyme had digested all of the plasmid. In order to confirm that each enzyme was functional and that the reactions had proceeded to complete digestion of all of the

plasmid, two additional reactions were set up as controls. One reaction contained Bam H1 and not Hind III and the other reaction was vice versa. Thus if each of the control reactions resulted in linearisation of the plasmid it was likely that the two enzymes were both functioning when incubated simultaneously. In addition, the control reactions revealed whether the incubation period was sufficiently long to allow digestion of all of the plasmid.

The gel image of the digestion is shown in figure 3.15. The uncut plasmid is visible as a single band in lane a. The bands in lanes a-d that migrate more slowly, indicating that these bands represent digested plasmid. The reaction products of the single enzyme digestions resolve as a single band (lanes a and c) showing that the digestion proceeded to completion for both enzymes. Thus the single band in lane d, from the reaction containing both restriction endonucleases, is likely to be homogeneous, consisting only of plasmid digested with both enzymes. It seems unlikely that the band consists of a heterogeneous mix of plasmid cut with one or other or both of the enzymes.

3.4.4 DNA sequencing of recombinant plasmid containing mutated tissue factor

Plasmids were prepared for sequencing using the procedure described in section 2.4.4. The sequence of the recombinant pIND plasmid containing wild-type and mutated of TF were determined at the Babraham Institute, Cambridge, U.K. Sequencing confirmed that the correct wild-type TF sequence was cloned into the pIND plasmid in-frame and in the appropriate position. In addition, sequencing confirmed the appropriate introduction of point mutations by the site-directed mutagenesis procedure.

3.4.5 Selection of a TF-negative cell line for the study of Ca^{2+} signalling by TF

COS1 cells were harvested for measurement of expression of TF using the prothrombin time test (2.2.1). COS1 cells were tested and found to express 0.36 ± 0.17 units of TF activity per 10^6 cells. These results contradict the findings of Rottingen et al (1995), who did not find TF expression in this cell line. In order to confirm that the procoagulant activity detected in the COS1 cells was due to TF expression, a procoagulant assay was repeated on these cells in the presence of FVII-deficient plasma rather than normal plasma. COS1 cells assayed for procoagulant activity in FVII-deficient plasma did not form clots. These results confirm that COS1 cells are not suitable for investigation of TF signalling as they express endogenous wild type TF.

An alternative cell line, Chinese Hamster Ovary K1 cells (CHO K1), was then tested for TF expression using the prothrombin time test. Whole and lysed CHO K1 cells failed to exhibit

Figure 3.14 : Gel image of TF RT-PCR product

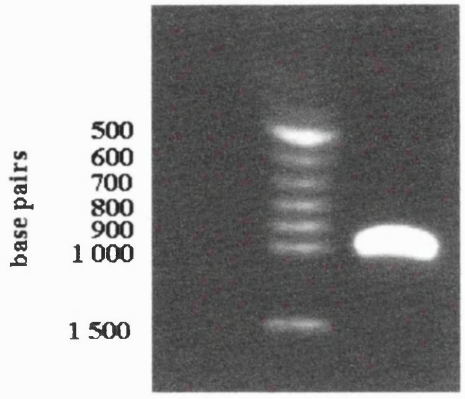

Poly(A)+ mRNA was extracted from THP-1 cells using an oligo d(T) latex methodology (R & D systems). Primers were designed for the amplification of TF mRNA (figure 3.4). RT-PCR of TF was perfomed using a single tube procedure (Access RT-PCR, Promega) as described in section 3.3.3. The reaction products were resolved using gel electrophoresis on a 1% agarose gel (2.4.7) and visualised under uv-transillumination.

Figure 3.15 : Gel image of restriction enzyme-digested pIND plasmid

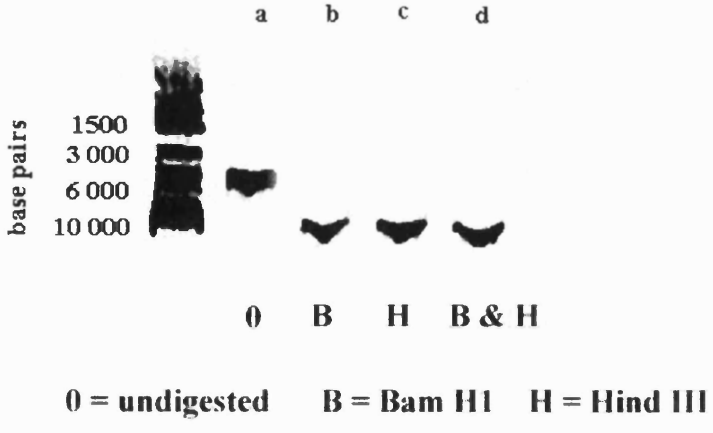

0.1-0.5mg of plasmid DNA was incubated with Bam H1 and Hind III as follows; a: control sample with no restriction enzymes, b: 1 unit of Bam H1, c: 1 unit of Hind III, d: 1 unit each of Bam H1 and Hind III (figure 3.7). The reactions were incubated for 12 hours at 37 C. The samples were then resolved by gel electrophoresis on a 1% agarose gel (2.4.7). The reaction products were visualised under uv-transillumination

TF activity in this assay, demonstrating that CHO K1 cells do not express endogenous TF. The CHO K1 cells were thus selected for transfection and expression of TF.

3.4.6 Cytotoxicity of CHO K1 cells to Zeocin™

The amount of Zeocin™ and length of treatment required to kill cells lacking resistance to Zeocin™ was determined in a cytotoxicity assay. The cytotoxic effect of antibiotics is most pronounced when added to cultures of cells that are actively dividing. CHO K1 cells were plated at 0.1 x 10^6 cells per 25cm^2 culture surface area. Zeocin™ was added at final concentrations of 50, 100 and 150 μg/ml. The cytotoxicity test at each concentration was performed in triplicate and the whole experiment was performed twice. The media was replaced with fresh media and re-supplemented with Zeocin™ every 4 days.

The results demonstrated that the minimum concentration of Zeocin™ required to efficiently kill CHO K1 cells is 100μg/ml for 10 days. This treatment regimen was used as the protocol employed to select for Zeocin™ resistant cells. This regimen should ensure that only cells transfected with the plasmid pVgRXR, which encodes proteins that detoxify Zeocin™, should survive the antibiotic selection procedure.

3.4.7 Identification of a pVgRXR-positive CHO K1 colony

pVgRXR plasmid was digested with the Mlu1 restriction endonuclease. Confirmation of the successful linearisation of the plasmid was determined by gel electrophoresis prior to transfection into CHO K1 cells. A cell line containing pVgRXR integrated into the host genome was established by prolonged selection in cytotoxic concentrations of Zeocin™, 100μg/ml for > 10 days, as described in section 3.3.10. The success of integration of the pVgRXR into the host genome was ascertained by testing whether the expression of wild-type TF could be attained in the isolated CHO K1 colonies, subsequent to transfection and induction of TF from the pIND(+TF*wt*) plasmid.

Cell colonies isolated after prolonged selection in Zeocin, which potentially contained the pVgRXR plasmid integrated into the host genome, were seeded on coverslips and transfected overnight with the pIND vector containing wild type TF (section 3.3.12). The induction of TF expression was initiated by the addition of 10μM Muristerone™. After 4.25 hours of incubation with 10μM Muristerone™, the levels of expression of wild type TF in transfected CHO K1 cells were determined using flow cytometry.

Cells were stained for TF expression using fluorescent antibodies as described in section 3.3.11c. The relative fluorescence intensity emitted from individual cells was determined using a Coulter Epic MCL flow cytometer. Machine noise was thresholded out on the FSC

channel. Cells were identified in a log FSC vs log SSC dot plot and a gate was constructed to exclude other events such as noise or vesicles. The fluorescence intensity of the gated cells was displayed in a log FL1H histogram. The mean and median fluorescence intensity of each sample was recorded. The mean and median values of the respective control sample were subtracted from the sample values, to give a relative fluorescence intensity value.

Cells transfected with wild-type TF expressed TF when induced with 10μM Muristerone^{TM} for 4.25h (figure 3.16). Cell surface TF fluorescence was 37-fold greater than the fluorescence emitted by the control sample. The data also demonstrates that the cell surface TF was not transferred to vesicles derived from the cell cultures up to 4.25h after induction of expression.

3.4.8 Determination of functionality of wild type TF expressed on CHO K1 cells

The absence of TF expression in non-transfected CHO K1 cells was confirmed using the prothrombin time assay as described. No procoagulant activity was detected in either whole or lysed CHO K1 cells however, cells transfected with wild type TF expressed 0.08 units of TF activity per 1 x 10^6 cells. The level of TF expression attained in the transfected cell line was compared to levels in cells that constitutively express TF. MDCK2, T24 and COS1 cells expressed TF at 0.72 ± 0.2, 1.81 ± 0.96 and 0.36 ± 0.17 respectively. Thus the CHO K1(+TF*wt*) cells expressed TF at 11.1%, 4.4% and 22.2% of the levels found in MDCK2, T24 and COS1 cells, respectively.

These results confirmed the successful isolation of a population of CHO K1 cells derived from a single ancestral cell that had undergone stable integration of the pVgRXR plasmid into the genome. This cell-line (CHO K1(pVgRXR)), was used for further studies to investigate TF in cellular signalling.

Figure 3.16a: Flow cytometric determination of cell surface tissue factor expression

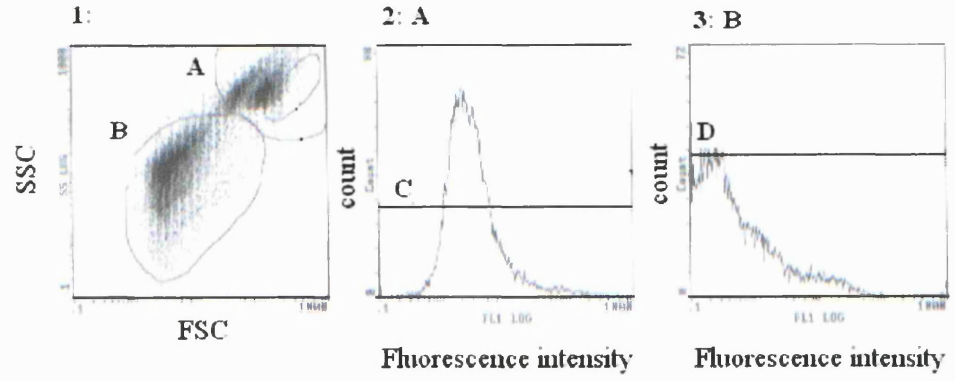

TF-transfected CHO K1 cells stained with fluorescent anti-TF antibodies were analysed using flow cytometry. The forward scatter (FSC) and side scatter (SSC) of cells, vesicles and debris passing through the laser were displayed as SSC vs FSC dot plots (window 1). Gate A was drawn around the cells and gate B was drawn around the vesicles and debris. The fluorescence histograms for each gate were displayed as separate windows (2 and 3, respectively), as the number of cells/vesicles versus their fluorescence intensity. A linear region was drawn in each of the fluorescent histograms (C and D) to calculate the mean fluorescence intensity of the cells or vesicles.

Figure 3.16b: Cell surface expression of TF in transfected CHO K1 cells

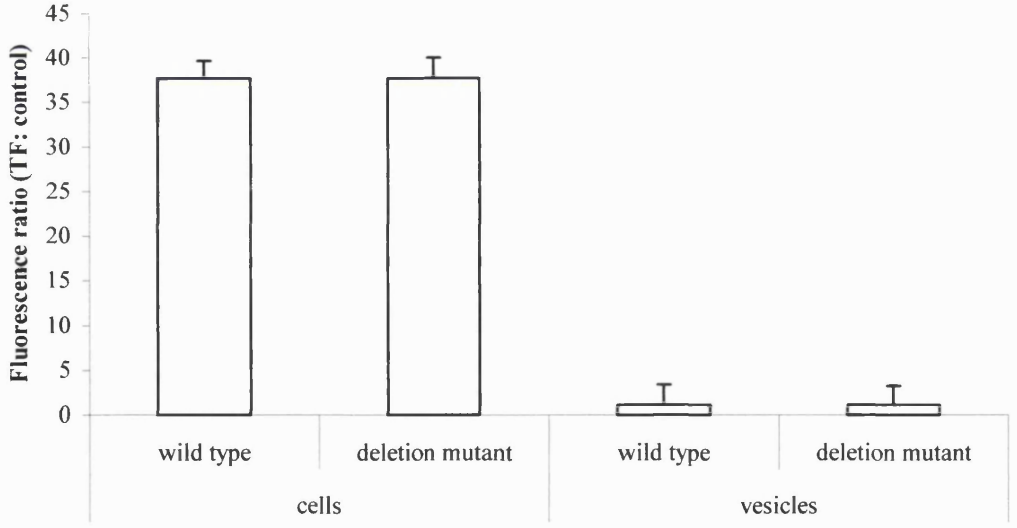

Cells were harvested and resuspended to 1m/100µl in PBS containing 1% BSA (pH 7.2). For each sample, two 100µl aliquots of cells were placed into 1.5ml microcentrifuge tubes. 5µl of FITC-conjugated antibody to tissue factor (0.1mg/ml, American Diagnostica) was added to one sample in order to determine tissue factor antigen. To the control tube, 5µl of an FITC-conjugated control antibody directed against Aspergillus *nidulans* glucose oxidase was added (0.1mg/ml, Dako). The antibodies were incubated with the samples on ice, in the dark for 30 minutes. 0.5ml of 1% BSA in PBS was added and the cells pelleted in a microcentrifuge for 0.5 minutes at 13000g. The supernatant was removed and the cell pellet was resuspended. 1ml of PBS was added to the cells prior to flow cytometric analysis. Results are shown as the mean ± S.E.M. of at least 10, 000 cells/vesicles.

3.4.9 Expression and activity of exogenous wild type and truncated TF in CHO K1 cells

Preliminary experiments were performed to determine the involvement of the entire cytoplasmic domain upon the induction of cytosolic Ca^{2+} transients by FVIIa, prior to embarking upon studies focussing upon any potential involvement of the three serine residues in the cytoplasmic domain of TF.

Cells transfected with recombinant plasmid vector containing either wild-type TF or mutant TF lacking the cytoplasmic domain, were plated onto glass coverslips as described in section 2.1.8. Cells were induced to express TF by the addition of 10μM Muristerone^{TM} to the cell cultures. Cells were incubated in the presence of Muristerone^{TM} for 4.25h.

Cell surface expression of wild type or truncated TF was determined using flow cytometry as described in section 3.3.12c. Cells transfected with pIND containing either wild type TF or truncated TF expressed TF at similar levels when expression was induced with 10μM Muristerone^{TM} for 4.25h (figure 3.16). In both cases, cell surface fluorescence was 37-fold greater than observed in cells incubated with fluorescent-labelled control antibody. These results demonstrated that the cytoplasmic domain of TF is not involved in the cell surface expression of TF.

The appropriate biological function of the exogenously expressed TF molecules was determined using the prothrombin time test. Cells expressing wild type and truncated TF expressed 0.08 and 0.07 units of TF activity per 10^6 cells. These levels of expression of TF activity in the transfected CHO K1 cells are between approximately 4 and 20% of levels seen in other cell types that express TF constitutively (section 3.4.8). The flow cytometry data demonstrates that a comparable number of TF molecules are expressed on cells transfected with wild type and truncated TF. Furthermore, since the procoagulant activities elicited by the cells transfected with wild type and truncated TF are similar, these results demonstrate that the activity of truncated TF is unaltered by deletion of the cytoplasmic domain.

3.4.10 Measurement of basal levels of cytosolic Ca^{2+} in CHO K1 cells expressing endogenous wild typeTF

TF-expressing CHO K1 cells were then loaded with the Ca^{2+}-sensitive fluorophore Fura2AM as described in section 2.3.2. Coverslips of Fura2-loaded cells were loaded into the chamber of a microscope integrated to a real-time fluorescent video imaging system. Levels of cytosolic Ca^{2+} were measured as described in section 2.3.

The basal levels of cytosolic Ca^{2+} were observed for at least 30 seconds prior to the addition of the FVIIa agonist. The mean and SEM of the basal level of cytosolic Ca^{2+} in CHO K1 (+TF*wt*) was 0.8 ± 0.1 (figure 3.17a).

3.4.11 Effect of FVIIa upon basal levels of cytosolic Ca^{2+} in CHO K1 transfected with wild type TF

The effect of the addition of 400nM FVIIa to the CHO K1 cells transfected with wild type TF is shown in figure 3.17a. The mean and S.E.M of cytosolic Ca^{2+} levels measured subsequent to the addition of the FVIIa is 0.77 ± 0.10. The levels of cytosolic Ca^{2+} measured after the addition of FVIIa were not significantly different from the basal cytosolic Ca^{2+} levels (Student's t-test $p = 0.25$).

3.4.12 Effect of transfection upon basal cytosolic Ca^{2+} levels in CHO K1 cells

The apparent failure of transfected CHO K1 cells to respond to the FVIIa stimulus was investigated. The possibility that the basal levels of Ca^{2+} in transfected CHO K1 cells were unstable was examined. The levels of cytosolic Ca^{2+} in CHO K1 cells that had not been transfected and were not exposed to transfection reagent were measured. The levels of cytosolic Ca^{2+} in control CHO K1 cells that were not exposed to the transfection reagent were 0.76 ± 0.01. In addition, the basal cytosolic Ca^{2+} levels in an alternative cell line (T24 cells) were measured and were found to be 0.74 ± 0.01 (figure 3.17b). The average S.E.M. of basal cytosolic Ca^{2+} levels in transfected CHO K1 cells was an order of magnitude greater than the basal levels in non-transfected CHO K1 cells and in T24 cells (0.10, 0.01 and 0.01 respectively). These data reveal that the basal cytosolic Ca^{2+} levels in TF-transfected CHO K1 cells were significantly more variable in comparison to basal levels of cytosolic Ca^{2+} in non-transfected CHO K1 cells and in T24 cells. Furthermore, the results show that the transfection procedure itself introduces the instability in cytosolic Ca^{2+} levels. Unfortunately, the instability in the cytosolic Ca^{2+} levels precludes the investigation of the role of the cytoplasmic domain of TF in the cell signalling responses of cells to FVIIa as the detection of any signal would be precluded by high levels of background noise. Further investigation of TF signalling using CHO K1 cells was not pursued since at this time Camerer E., et al (1999) observed a failure of CHO K1 cells expressing TF to respond to FVIIa. This suggests that CHO K1 cells are not a suitable cell type in which to study the mechanisms of TF: FVIIa signalling as they lack components involved in signal transduction and/or propagation.

Figure 3.17a: Cytosolic calcium levels in non-stimulated and FVIIa-treated CHO K1 cells expressing wild-type TF

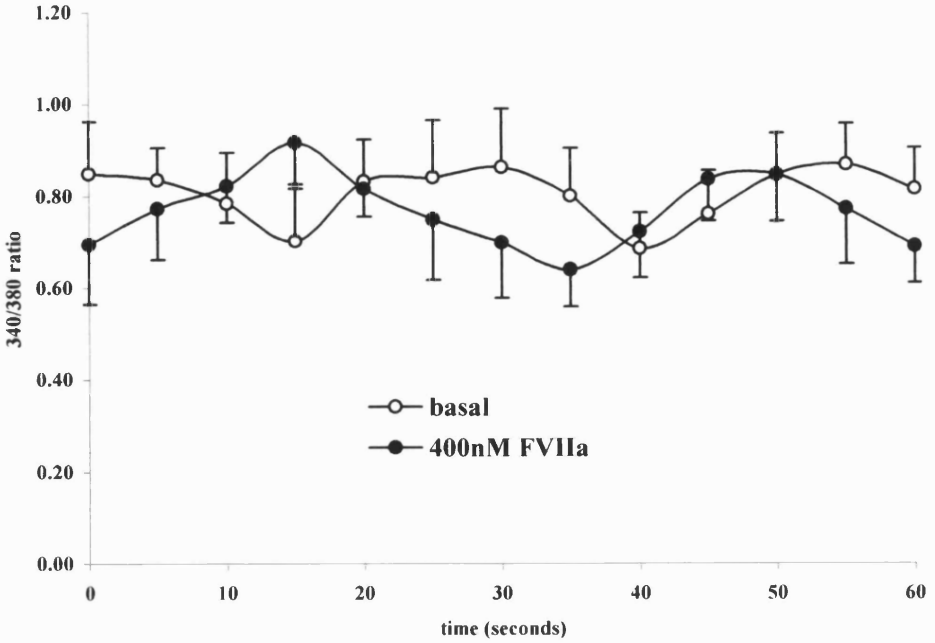

Figure 3.17b: Basal cytosolic Ca^{2+} levels in non-transfected CHO K1 and T24 cells

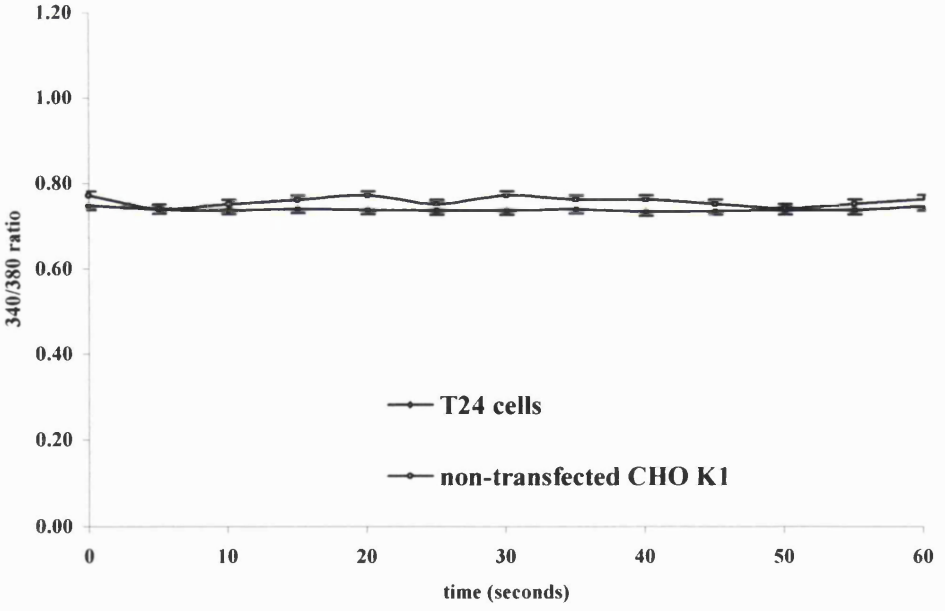

CHO K1 cells transfected with recombinant plasmid containing wild-type TF were induced to express TF (section 3.3.10). TF-expressing CHO K1 cells were loaded with the calcium-sensitive fluorophore Fura2AM as described in section 2.3.2. Cytosolic Ca^{2+} levels in non-stimulated and FVIIa-stimulated cells (400nM) were measured using a microscope integrated to a video fluorescence imaging system (figure 3.17a). Basal Ca^{2+} levels of non-stimulated cells were measured in non-transfected CHO K1 cells and in T24 cells (Figure 3.17b). Results are shown as the mean ± the SEM for at least 20 individual cells.

3.5 Conclusions

CHO K1 cells do not express endogenous TF. CHO K1 cells transfected with plasmid encoding wild type and TF lacking the cytoplasmic domain can be induced to express TF at the cell surface. The cell surface expressed TF retained functionality as determined by the prothrombin time assay. The level of expression of TF activity upon the transfected cells was found to be between approximately 0.05 and 0.2 times the amount of TF activity typically expressed on cell types that express TF endogenously. The results demonstrate that TF is expressed efficiently in CHO K1 cells using the dual vector pIND expression system (Invitrogen).

Kinetic imaging of CHO K1 cells expressing wild-type TF demonstrates that the basal cytosolic Ca^{2+} levels were highly unstable. The background noise in the basal Ca^{2+} levels was evident in 95% of the cells examined. Addition of FVIIa to these cells did not elicit significant increases in the cytosolic Ca^{2+}. Thus, the failure to detect induction of Ca^{2+} transients after the addition of FVIIa may be due the masking of a response due to a low signal to noise ratio. However, TF-transfected CHO K1 cells may lack the signal transduction machinery required for the induction of Ca^{2+} transients by FVIIa. Signal transduction by the TF: FVIIa complex has been found to be dependent upon the proteolytic activation of an additional receptor, recently identified as PAR2 (Camerer E., 2000b). The requirement for alternate or additional signalling proteins is implied since CHO K1 cells transfected with TF and PAR2 remain unresponsive to FVIIa. Investigation of the involvement of the cytoplasmic serine residues of TF in the induction of cytosolic Ca^{2+} transients was thus not feasible using the CHO K1 cell type. A more suitable cell line must be identified prior to further investigation of the involvement of the cytoplasmic domain of TF in Ca^{2+} signalling.

3.6 Discussion

The involvement of the cytoplasmic domain of TF in cellular signalling has been reported recently (Cunningham M.A., 1999). However, the involvement of the three intracellular serine residues in the induction of the Ca^{2+} signal remains unresolved. Hence, further investigation of the involvement of the intracellular serine residues in TF domain in TF signalling is warranted. In these studies, CHO K1 cells, lacking endogenous TF, were selected for expression of wild type and mutant TF, to investigate the involvement of the cytoplasmic domain of TF in the transduction of cytosolic Ca^{2+} signals.

CHO K1 cells were successfully transfected with wild type TF and TF lacking the cytoplasmic domain. However, the basal levels of cytosolic Ca^{2+} in TF-transfected CHO K1 cell line were unstable. The underlying cause of the cytosolic instability is derived from the

transfection procedure. It appears that the transfection reagent, which is engineered to traverse cell membranes, may interfere with the integrity of the membranes of intracellular Ca^{2+} stores. The instability of basal cytosolic Ca^{2+} may result from leakage of Ca^{2+} from intracellular stores into the cytoplasm. Subsequent removal of the cytosolic Ca^{2+} may explain the fluctuations in cytosolic Ca^{2+}. In addition, the persistence of the fluctuations may arise from cycles of leakage followed by re-sequestration of cytosolic Ca^{2+}. Further investigation of the involvement of the intracellular domain of TF in the induction of Ca^{2+} transients would be carried out using an alternative transfection protocol.

The involvement of the PAR-2 receptor in cellular signalling by the TF: FVIIa complex has been recently identified (Camerer E., 2000). The presence of expression of the PAR-2 receptor in CHO K1 cells should be established before further investigation of TF signalling in this cell line is pursued. Since PAR2 and TF are components of a common signalling pathway, PAR2 receptor expression may be linked to TF expression, it is thus possible that a cell line that expresses the PAR2 receptor in the absence of TF expression may be difficult to find. As an alternative, a cell line that constitutively expresses TF may be used for the investigation of TF signalling, for example, the human monocyte-derived cell line (U937) used in the study by Cunningham et al (1999) or KOLF lung fibroblasts as used by Camerer et al (2000). Investigation of cytosolic Ca^{2+} signals using a cell line known to express TF would be advantageous in that one could be sure that the required components of the signalling pathway are expressed in the chosen cell line. However, the investigation of the effect of mutation of TF in a cell line that expresses TF endogenously may be precluded due to the presence of wild type TF. Notwithstanding, expression of exogenous mutant TF in cells expressing endogenous TF may be a useful model provided that mutation of functional regions of TF involved in signalling were able to significantly modulate the overall response of the cells.

Unfortunately, constraints on access to imaging equipment prevented further pursuit of these investigations. However, useful observations were gained from these studies, which will aid further investigations. These data demonstrate that CHO K1 cells transfected with recombinant pIND containing either wild-type TF or TF lacking the cytoplasmic domain can be induced to express functional TF at the cell surface. This shows that the cytoplasmic domain of TF is not required for cell surface expression of TF. In addition, since cells expressing exogenous TF were capable of exhibiting procoagulant activity, these results confirm that the cytoplasmic domain is not required for the procoagulant activity of TF. In addition, the pIND/pVgRXR expression vector system is demonstrated to be suitable for expression of TF in mammalian cells. The levels of TF expression in attained in transfected

CHO K1 cells were between 5- and 20-fold lower that the levels of TF expression found in other cell lines that express TF endogenously. Importantly, the level of expression of TF in the CHO K1 cells could be enhanced, as the induction of recombinant genes in the pIND/pVgRXR is dependent upon the concentration of the inducer. Furthermore, since the inducer is related to the insect hormone ecdysone, increased expression of TF is attainable without the induction of expression of potentially undesirable endogenous proteins.

CHAPTER 4

INHIBITION OF TISSUE FACTOR: FVIIa-MEDIATED INDUCTION OF CYTOSOLIC Ca^{2+} TRANSIENTS BY AN APOLIPOPROTEIN B100-DERIVED PEPTIDE

4.1 Introduction

4.1.1 Modulation of TF activity by native and oxidized LDL

The activity of TF is differentially modulated by LDL depending upon its oxidation status. While oxidized LDL enhances TF activity, native LDL inhibits TF activity (Ettelaie C., 1995 and 1997). The ability of native LDL to inhibit TF activity results from direct protein: protein interactions between the apolipoprotein B-100 (apo B100) component of LDL and the TF molecule (Ettelaie C., 1996). The region of apo B100 responsible for this inhibitory capacity is located in residues 3147-3160 (KAQSKKNKHRHSTT) of the protein (Ettelaie C., 1998) and has been termed the KRAD14 peptide, (an acronym for lysine-rich apolipoprotein B100 domain 14-mer peptide). This region is within the LDL receptor-binding domain of apo B100 (Milne R., 1989, Lawn A., 1990, Chan L., 1992 and Olsson U., 1997). Furthermore, a region within TF (residues 58-66) is homologous to one of the repeated domains within the LDL-receptor protein (residues 283-291, Ettelaie C., 1996) responsible for the binding of apo B100 (Goldstein J.L., 1985) and a model of the interacting residues between the 58-66 region of TF and KRAD14 has been proposed. Mutational studies show that alanine substitution of the second and third lysine residues and the asparagine residue within KRAD14 markedly reduces its ability to inhibit the procoagulant activity of TF (Ettelaie C., 1998). Structural data regarding the interaction between TF and FVIIa demonstrate the importance of residues within the 58-66 region of TF in the activation of FVIIa (Pike A.C.W., 1999) and validates the potential for the binding of KRAD14 to this site to inhibit FVII activation.

4.1.2 The structure of tissue factor

TF was recognised as a member of the class II cytokine receptor superfamily (Bazan J.F., 1990) based upon its distinctive architecture within the extracellular region (figures 4.1 and 4.2). Each of the two compact fibronectin type domains in the extracellular region of TF consists of a three-stranded β-sheet and a four-stranded β-sheet. The three- and four-stranded sheets pack against each other to form a β-sandwich. Inter-strand loops from each module interdigitate in a manner similar to a dovetailed joint and form the module interface. Polymorphic sites have not been detected in TF (Mackman N., 1989) suggesting that variation in the structure is not tolerated. Despite its homology with the cytokine receptor superfamily, TF displays several idiosyncrasies that deviate from cytokine receptor topology (figures 4.3 and 4.4).

Figure 4.1: Arrangement of β-strands in the tissue factor molecule

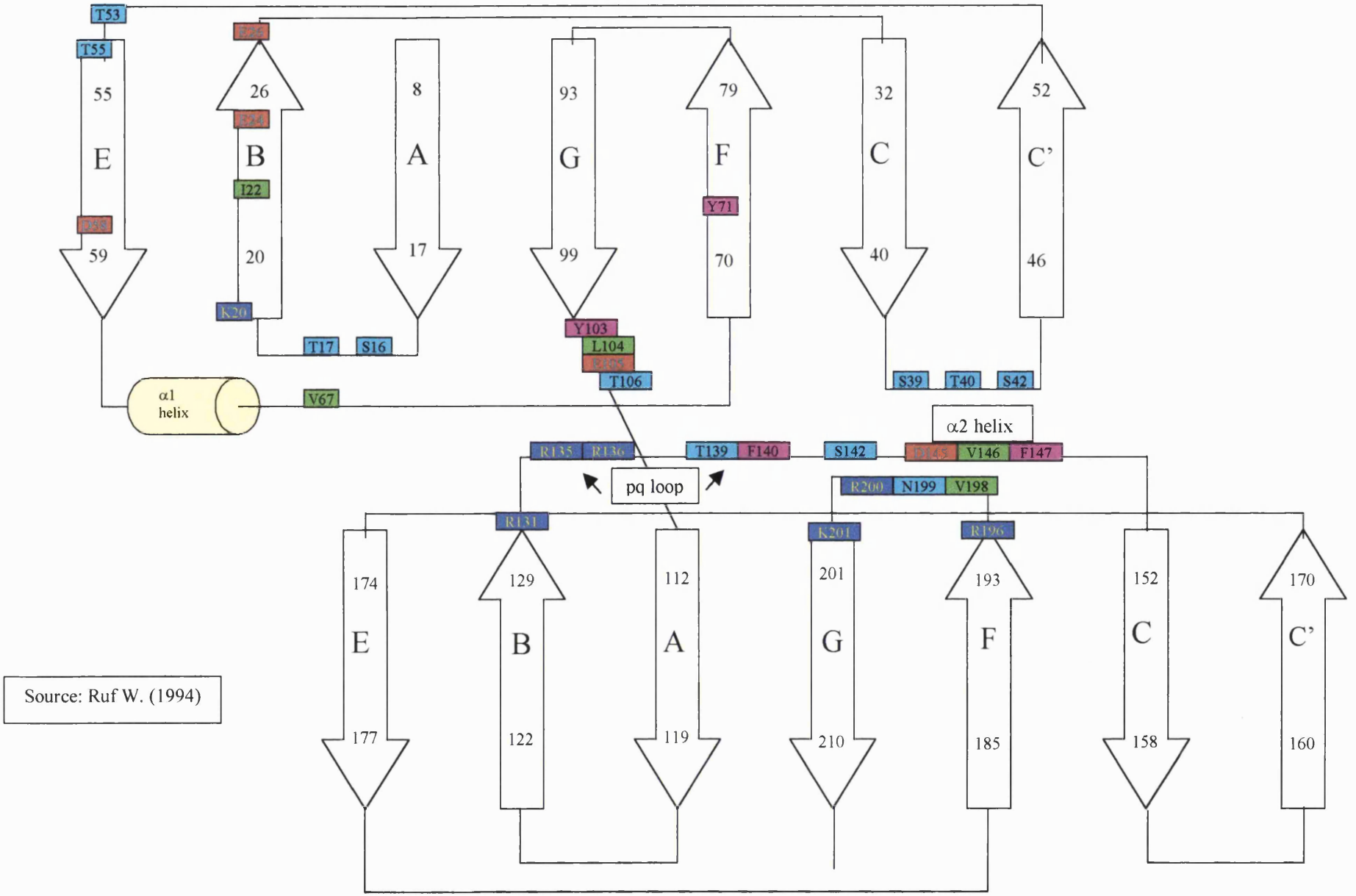

Source: Ruf W. (1994)

Figure 4.2: Structure of the extracellular domain of tissue factor

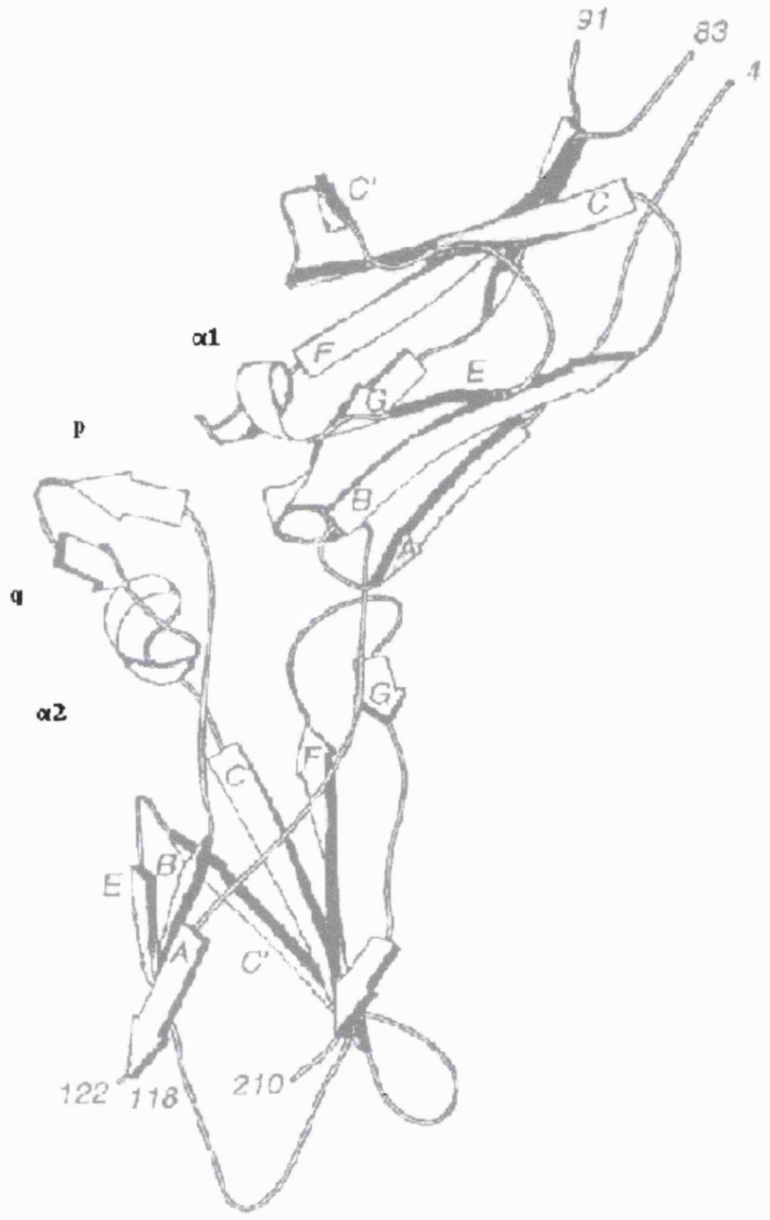

pq loop
α1 & α2 helices

Source: Muller Y.A. (1994)

Figure 4.3: Features of TF characteristic of the cytokine receptor II superfamily

- Single transmembrane domain
- β-strand modules homologous to the fibronectin III subclass of the immunoglobulin superfamily
- Disulphide bonding characteristic of the type II subclass of cytokine superfamily
- Ligand-binding site is topologically similar to cytokine superfamily
- WKS motifs

Figure 4.4: Features of TF that deviate from the cytokine receptor II superfamily

- Inter-domain hinge angle is 125°, 45° larger than growth hormone receptor (Harlos K., 1994)
- Ligand binding site extends to the concave side of the molecule
- Ligand binding residues are on β-strands rather than on inter-strand loops
- pq loop and α2 helix (extended binding finger) is 9 residues longer than in growth hormone receptor
- Disulphide bond between strands F and G of the C-terminal module is solvent accessible

4.1.3 The structure of coagulation factor VII

FVII possesses a modular organization with an N-terminal membrane binding γ-carboxyglutamic acid domain, two epidermal growth factor (EGF)-like domains and a C-terminal serine protease domain (Furie B., 1988). The active form of the enzyme comprises a light chain (152 residues) and a heavy chain (254 residues) liked by a disulphide bond. The active form is generated by the cleavage of the Arg152/Ile153 peptide bond, located between the second EGF domain (EGF2) and the protease domain (Khan A.R., 1998). The structure of Gla-domainless FVIIa (GD-FVIIa), bound to TF, is depicted as a ribbon representation in figure 4.5. The light chain forms a narrow stalk on which the protease domain sits. The EGF2 and protease domain associate into a compact structural unit in a similar manner to factors IXa, Xa and activated protein C. The EGF1 domain extends away from this compact core to yield a molecule 90Å in length. The EGF modules are stacked end on end and have a single stabilising bond between Asn93 and Lys 85.

4.1.4 The interaction of tissue factor and FVIIa

The relatively recent elucidation of the crystal structure of the complex of clotting factor FVIIa with the extracellular region of TF (sTF) to a resolution of 2Å (figure 4.5) provides a molecular analysis of complex formation (Banner D.W., 1996). The data tabulated in appendix 4 summarise studies where functionally important residues in TF have been identified. The results demonstrate that the majority of the binding energy arises from the light chain of FVIIa and both extracellular domains of TF. The membrane proximal region of TF binds the Gla domain of FVIIa. The front central region at the boundary between the two extracellular modules binds the EGF-1 domain of FVIIa. The top of the TF molecule binds the EGF-2 and catalytic domains of FVII.

The TF region 58-66, comprising the proposed binding site for the inhibitory KRAD14 peptide, contains residues that are important in FVIIa binding. Residues Glu56 and Asp58 form H-bonds with FVII (Banner D.W., 1996) Mutation of the Asp58 residue results in 5000-fold reduction in affinity for the FVII ligand (Martin D.M.A., 1995) and renders TF defective as a co-factor for FVIIa-dependent FX activation (Lee G.F., 1998). Interestingly, residues 58-66 in TF are highly conserved between species (Appendix 5, Andrews B.S., 1991)

4.1.5 Induction of cellular signalling by TF: FVIIa

TF was recognised as a member of the cytokine receptor superfamily in the early 1990s (Bazan J.F., 1990), however the ability of TF to induce cellular signals was not directly demonstrated until the mid-1990s (Rottingen J-A., 1995). FVIIa-induced increases in Ca^{2+} transients are observed in a number of cell types expressing TF including; human umbilical vein endothelial cells (HUVEC) induced to express TF by pre-treatment with IL-1β, human bladder carcinoma cells (J82); Madin-Darby canine kidney cells and COS-1 cells transfected with TF.

Active site-inhibited FVIIa (FVIIai) does not elicit Ca^{2+} transients demonstrating that ligand binding *per se* is not sufficient to induce cellular signalling and that the activation of FVII is required for the induction of Ca^{2+} transients. The identity of the substrate(s) of proteolytically active FVII involved in the induction of cytosolic Ca^{2+} signalling has been investigated and is discussed in detail in section 3.1.2.

ure 4.5: The crystal structure of the soluble tissue factor: Gla-domainless FVIIa complex

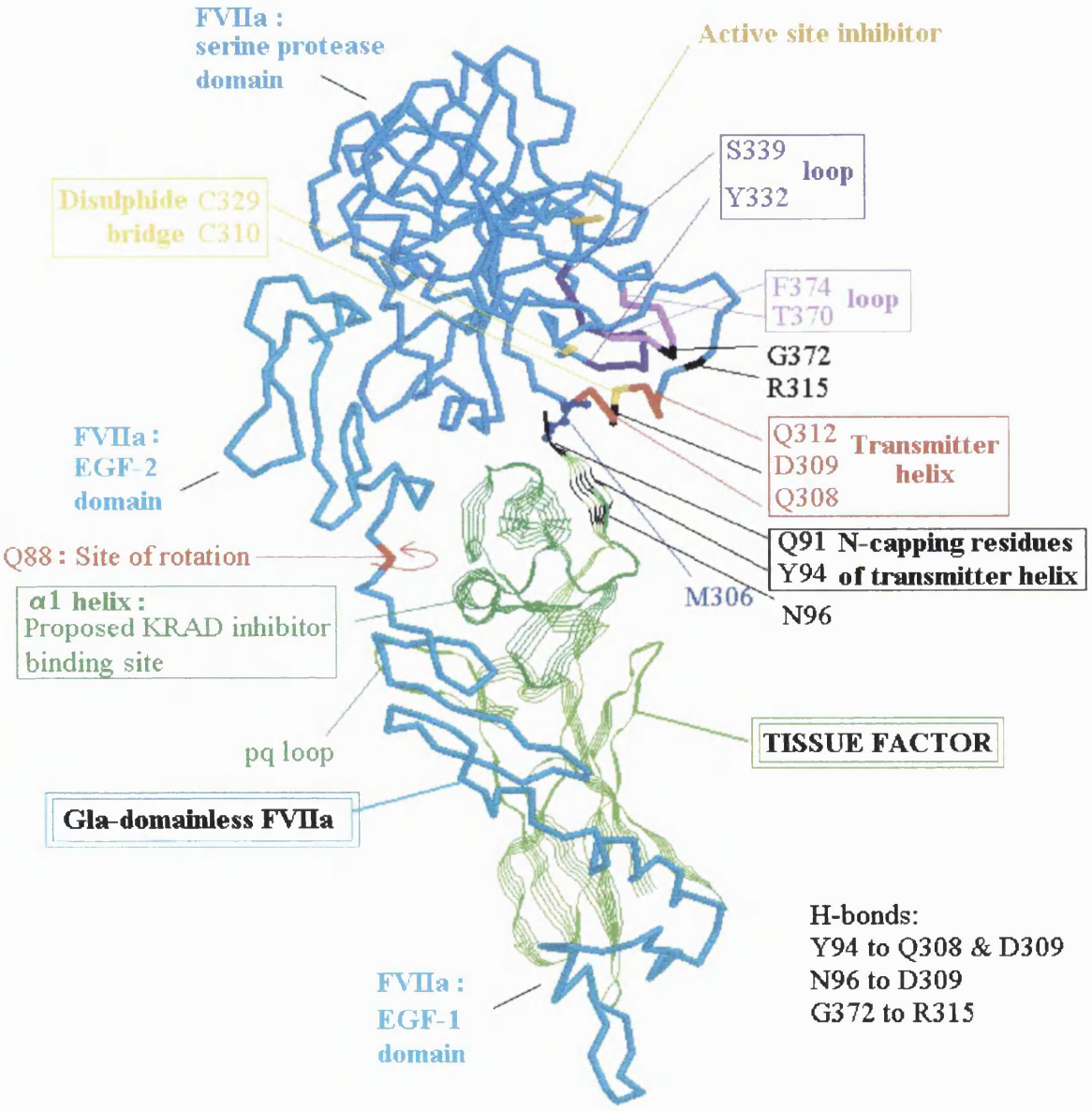

Source: Banner D.W., 1996

4.2 Aims

- To determine whether an inhibitor of the procoagulant activity of TF: FVIIa inhibits the cell signalling function of TF

- To re-evaluate the proposed mechanism of inhibition of FVII activation by the KRAD6 peptide, in respect of its compatibility with recent observations that reveal the mechanism of activation of FVII by TF

4.3 Methods

4.3.1 Cell preparation

MDCK2 cells were cultured, harvested and seeded onto glass coverslips as described in section 1.8. For experimentation coverslips of cells were loaded with the Ca^{2+}-sensitive fluorophore Fura2, as described in section 2.3.2. After the cells were loaded with Fura2, the coverslips were seated into the imaging equipment as detailed in section 2.3.4.

4.3.2 Assay for the inhibition of recombinant human TF by the KRAD6 peptide

The effect of the KRAD6 peptide upon inhibition of recombinant tissue factor activity *in vitro* was determined using the prothrombin time assay. Synthetic KRAD6 peptide was added to recombinant human TF (0.1 units) at a final concentration of 1μM. The sample was then assayed at 0, 4, 8, 11 and 16 minutes after addition of the peptide using the prothrombin time test as described in section 2.2.

4.3.3 Measurement of TF activity of intact MDCK2 cells

MDCK2 cells were harvested using trypsin as described in section 2.1.6. Cells were resuspended to 2m/100μl in PBS. The cell suspension was successively diluted 2-fold to a minimum concentration of 0.031 x 10^6 cells per 100μl. The TF activities of the intact cell suspensions were determined using the prothrombin time test as described in section 2.2. The clot times were recorded and were converted to TF units using the equation derived from the standard curve (section 2.2, figure 2.1); TF units = EXP{ [ln (prothrombin time / 27.059) / -0.2838] }. A plot of TF activity versus the number of MDCK2 cells is plotted in figure 4.6.

4.3.4 Measurement of cytosolic Ca^{2+} responses of MDCK2 cells

Cells were seeded onto sterile glass coverslips as described in section 2.1.8. The cells were loaded with the Ca^{2+}-sensitive Fura2AM as detailed in 2.3.2. Cytosolic Ca^{2+} transients within individual cells were recorded and analysed using a digital imaging system as described in section 2.3.

4.4 Results

4.4.1 Cell surface TF activity on MDCK2 cells

The quantity of TF activity expressed on MDCK2 cells is represented graphically in figure 4.6. A linear trendline was fitted to the curve, the gradient of the trendline is 0.13, thus 1 x 10^6 MDCK2 cells express 0.13 units of TF activity.

Prothrombin time assays performed on MDCK2 cells using FVII-deficient plasma failed to produce a clot (data not shown) and demonstrate that it is specifically the activity of TF that is responsible for the procoagulant activity manifested by MDCK2 cells.

4.4.2 Inhibition of recombinant human tissue factor by the KRAD6 peptide

The involvement of specific residues in the inhibition of TF by KRAD14 has been investigated by mutational analysis (Ettelaie C., 1998). Mutation of residues K and N in the KRAD14 sequence; KAQSK**KN**KHRHSIT, resulted in a significant reduction in the inhibitory capacity of the KRAD14 peptide. A 6-mer amino acid sequence from the KRAD14 peptide (KKNKHR) was synthesized and tested for its ability to inhibit TF activity (KRAD6). The results, presented in figure 4.7, indicate that the KRAD6 peptide at a concentration of 1μM inhibits TF activity by approximately 50% after 16 minutes.

4.4.3 Normality of the distribution of cytosolic Ca^{2+} responses to FVIIa

Examination of the Ca^{2+} responses of a population of cells exposed to a particular concentration of FVIIa (100-400nM) showed that the individual cells displayed great variation in the characteristics of the cytosolic Ca^{2+} responses (figure 4.8). These variations were evident in respect of; the manifestation of a response, the time taken for the cells to respond, the peak amplitude of the response and the decay time of the response. In addition, some cells responded to the FVIIa stimulus by exhibiting a series of Ca^{2+} spikes, the number of these oscillations also varied between cells in the population.

The magnitude of the response was measured by calculating the ratio of the average of the response of the cells to the average basal level (response: basal ratio, R: B ratio). The Shapiro-Wilke normality test was used to determine whether the R: B ratio of cells elicited in response to FVIIa was normally distributed (figure 4.9). The mean and median of the R: B ratios were 1.228 and 1.206 respectively, indicating that the distribution was not skewed. The *p* value for the Shapiro-Wilke test was 0.0006 showing that the data distribution can be considered to be normal with a high degree of confidence. Demonstration of the normality of the distribution indicated that ANOVA is appropriate for statistical analysis of the data.

Figure 4.6: Cell surface tissue factor activity on MDCK2 cells

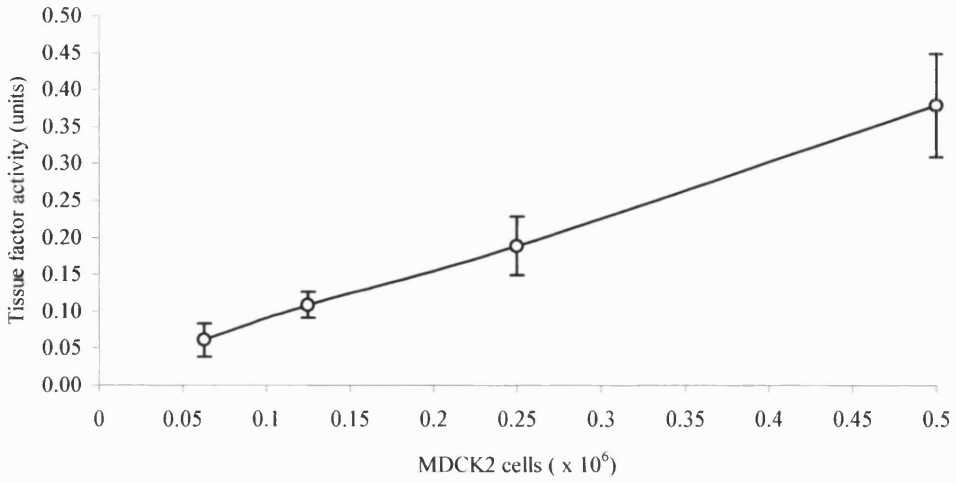

MDCK2 cells were harvested from culture and resuspended in PBS. Serial dilutions of MDCK2 cells in PBS were made and tested for procoagulant activity using the one stage prothrombin time test as described in section 2.2.1. Clotting times were converted to TF units using a standard curve (figure 2.1). The results are the means ± S.E.M. of four independent experiments.

Figure 4.7: The effect of the KRAD6 peptide upon procoagulant activity of TF

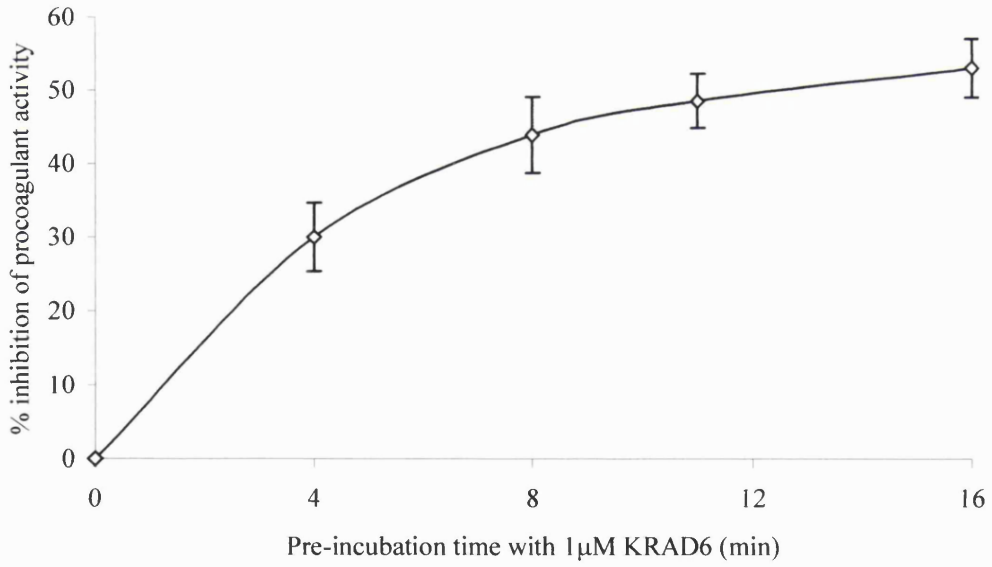

Recombinant human TF (100nM) was incubated with the KRAD6 peptide at a final concentration of 1μM. 100μl samples were removed at intervals and assayed for procoagulant activity using the one stage prothrombin time test (2.2.1). TF activity was calculated from the clotting time using a standard curve (figure 2.1). The results are the means ± S.E.M. for three independent experiments.

Figure 4.8: Variation in the response of MDCK2 cells to FVIIa

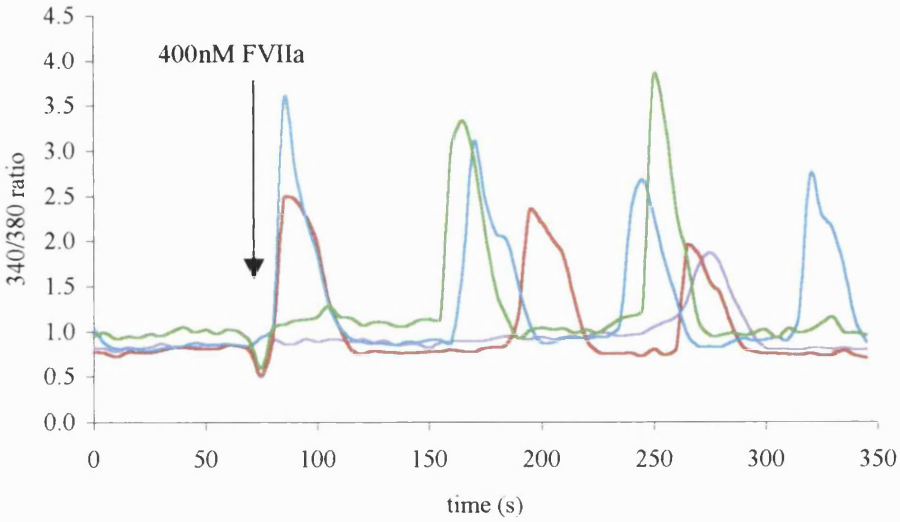

MDCK2 cells were grown on coverslips as described in section 2.1.8. For experiments cells were loaded with the Ca^{2+}-senstive fluorophore Fura2 (section 2.3.2). The effect of FVIIa upon the levels of cytosolic Ca^{2+} in individual cells was measured using kinetic fluorescence imaging. Results show the responses of 4 different cells to the FVIIa agonist.

Figure 4.9: Distribution of the cytosolic Ca^{2+} responses of MDCK2 to FVIIa

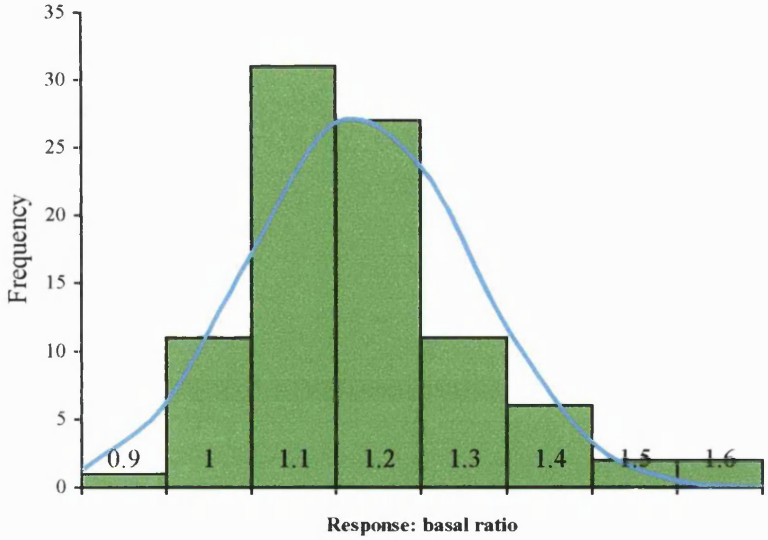

MDCK2 cells were grown on coverslips as described in section 2.1.8. For experiments cells were loaded with the Ca^{2+}-senstive fluorophore Fura2 (section 2.3.2). The effect of FVIIa upon the levels of cytosolic Ca^{2+} in individual cells was measured using kinetic fluorescence imaging. Results show the distribution of the responses of 91 individual cells to FVIIa, in terms of the response: basal ratio. The response: basal ratio was calculated by dividing the average of the 340/ 380 ratio after the addition of FVIIa by the average of the basal, pre-treatment 340/380 ratio.

4.4.4 Inter-experimental variation in the response of T24 cells to FVIIa

The Ca^{2+} response of MDCK2 cells seeded independently (on different days), was examined to determine the inter-experimental variation in the response of T24 cells to FVIIa. The response of the cells was analyzed in terms of the R: B ratios. Analysis of the data using an un-paired Student's t-test demonstrated that the response of cells to 400nM FVIIa varies between independent samples of T24 cells and that the degree of variation is highly significant (p=0.00027).

The data for the effect of the KRAD6 peptide upon Ca^{2+} transients induced by 400nM FVIIa (section 4.4.8) was derived from experiments performed with independently prepared samples of T24 cells. To enable the results to be pooled together the data were normalized against the response to 400nM FVIIa within each batch of experiments.

4.4.5 Dependence of cytosolic Ca^{2+} responses upon concentration of FVIIa

Linear regression analysis of normalized data was examined to determine whether the R:B ratio, the number of oscillatory peaks, the peak amplitude, the decay rate and the response integral were dependent upon the concentration of FVIIa (defined in section 2.3.7b, figure 4.10a). Linear regression analysis was performed on logarithmically transformed data, since the standard deviations of the transformed data were smaller than for the non-transformed data. In addition, since zero values cannot be logarithmically transformed, each data value was increased by a nominal value of 1. This value was subtracted again after regression analysis to maintain meaningful interpretation of the data.

The r^2 and p values for the linear regression analysis of logarithmically transformed data are shown in figure 4.10b. Significant positive correlations between the concentration of FVIIa and the cytosolic Ca^{2+} response were evident when the responses were analyzed in terms of; the response integral, the number of oscillatory peaks, the peak amplitude and the decay time.

The response integral is an index of the overall magnitude of the response. The data demonstrate that the significant increase in the overall magnitude of the response with larger doses of FVIIa, results from a combination of an increase in the peak amplitude, decay time and number of oscillations.

4.4.6 Synchronous oscillatory responses to FVIIa

Analysis of the data demonstrated that the Ca^{2+} transients seen in the cell population were synchronized. Examination of the video image files of the experiment showed that the initiation of the global Ca^{2+} wave emanated from a localized region of cells and was transmitted to adjoining cells in the monolayer.

Figure 4.10a: Linear regression analysis of the effect of FVIIa concentration upon the cytosolic Ca^{2+} response of MDCK2 cells

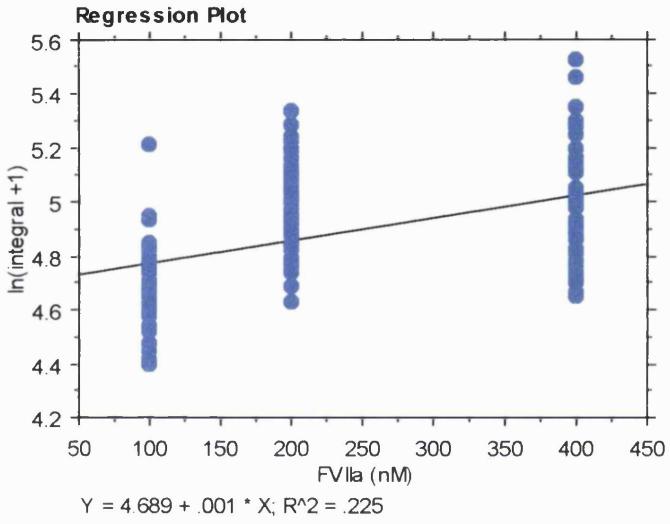

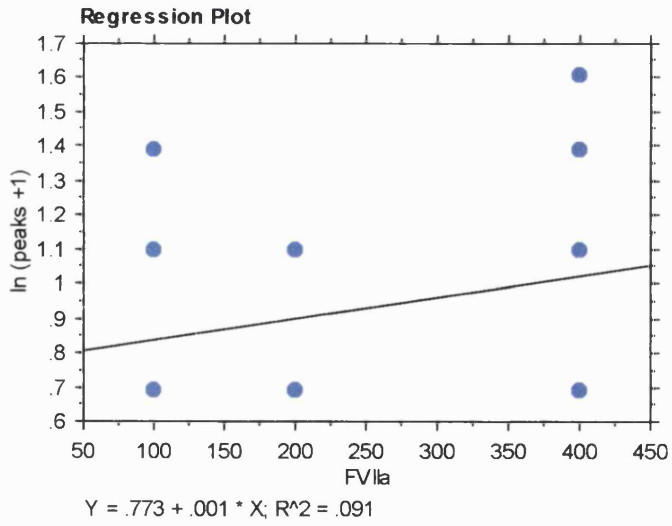

(continued)

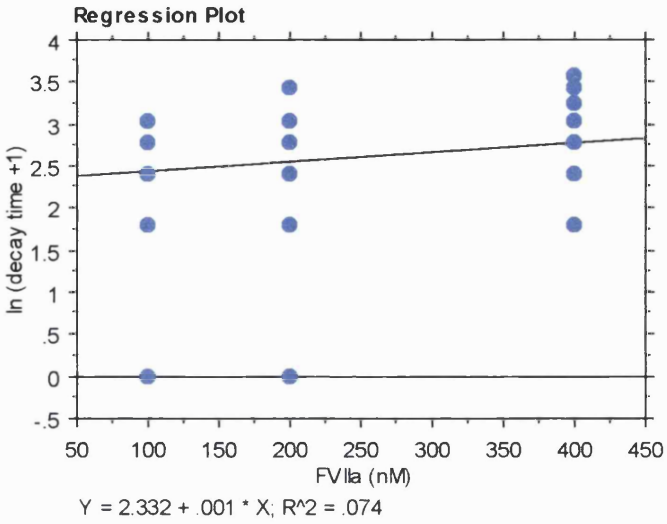

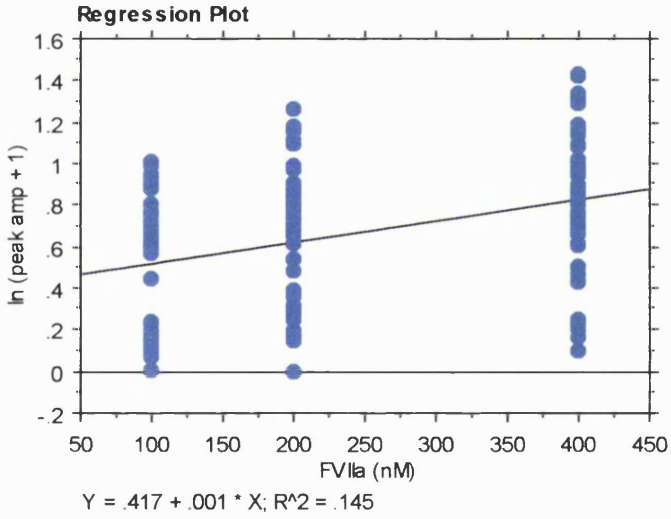

MDCK2 cells were grown on glass coverslips as described in section 2.1.8. Cells were loaded with the Ca^{2+}-sensitive fluorophore Fura2 (2.3.2). Cytosolic Ca^{2+} levels were measured in individual cells using kinetic fluorescence imaging. Cells were treated with 100, 200 and 400nM FVIIa. The effect of FVIIa concentration upon the induction of cytosolic Ca^{2+} transients was assessed in terms of the response to basal ratio (R: B ratio), the integral of the response, the number of peaks, the peak amplitude and the decay time of the cytosolic Ca^{2+} response using linear regression methodology.

Figure 4.10b: Linear regression co-efficients for the effect of FVIIa concentration upon the cytosolic Ca^{2+} response of MDCK2 cells

Index of Ca^{2+} response	r^2	*p*-value
ln (Response integral +1)	0.23	<0.0001
ln (Peak amplitude +1)	0.15	<0.0001
ln (Decay time +1)	0.07	0.0009
ln (Number of peaks +1)	0.09	0.004

Figure 4.11: The effect of KRAD6 upon cytosolic Ca^{2+} levels

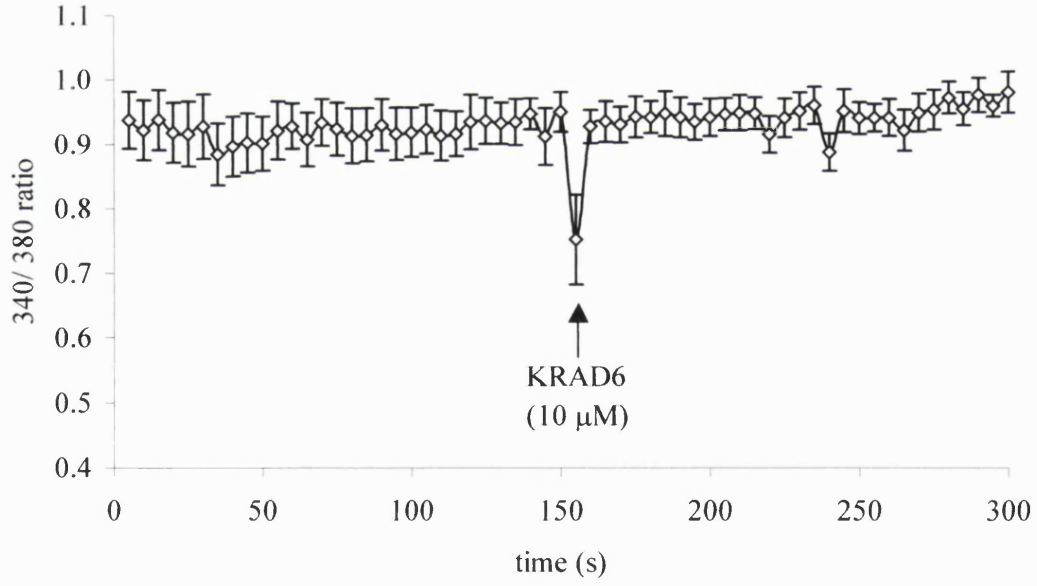

MDCK2 cells were grown on glass coverslips and loaded with the Ca^{2+}-sensitive fluorophore Fura2AM. Coverslips were placed in the chamber of a microscope linked to a video fluorescent imaging system. The basal levels of Ca^{2+} were observed for 150 seconds prior to the addition of the KRAD6 peptide (10μM). Cells were observed for a further 150 seconds to determine any effect of the KRAD6 peptide upon cytosolic Ca^{2+} levels. The results are expressed as the mean ± S.E.M. for five individual cells.

4.4.7 Effect of the KRAD6 peptide upon cytosolic Ca^{2+} levels

The 340: 380nm ratios of a population of cells were determined before and after the addition of 10μM KRAD6 peptide (figure 4.11). The results demonstrate that the cytosolic Ca^{2+} levels observed subsequent to the addition of the KRAD6 peptide were not significantly different from the basal, pre-treatment cytosolic Ca^{2+} levels. These results demonstrate that the KRAD6 peptide itself does not induce cytosolic Ca^{2+} transients.

4.4.8 Concentration dependence of the inhibition of FVIIa-induced Ca^{2+} responses by the KRAD6 peptide

Ratios of the average level of the response of the cells to the average basal level were calculated for each cell (R: B ratio). The R: B ratio reflects the magnitude of the response of each cell. The R: B ratios of cells treated with 400nM FVIIa subsequent to pre-treatment with various concentrations of KRAD6 peptide (10-0.1μM) were analyzed using linear regression analysis (figure 4.12a). Linear regression analysis demonstrated a significant negative correlation between the concentration of the KRAD6 peptide and the magnitude of the cytosolic Ca^{2+} response measured in terms of the natural log of the normalized R: B ratios ($p < 0.0001$).

The effect of pre-treatment of the cells with the KRAD6 peptide upon the response to FVIIa was also analyzed with respect to the percentage of the cell population eliciting a response. In this analysis the cells were categorized as either non-responsive or responsive using an arbitrary cut-off point (section 2.3.7d). The percentage inhibition was calculated relative to the percentage of responding cells in the controls. Consideration of the data in terms of the percentage of cells responding provides an analysis that is independent of the magnitude of the response. The data demonstrate that the percentage of cells responding to the FVIIa stimulus decreases as the amount of KRAD6 is increased (figure 4.12b).

Figure 4.12a: Linear regression analysis of the effect of the KRAD6 peptide upon FVIIa-induced Ca^{2+} responses

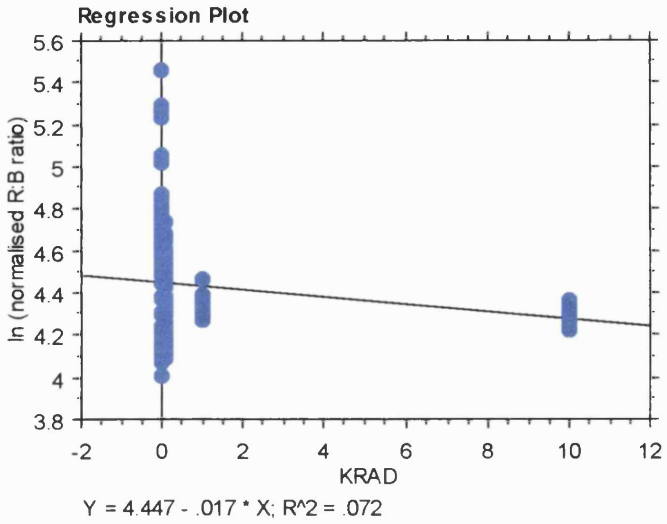

Figure 4.12b: Effect of KRAD6 peptide upon the percentage of cells eliciting cytosolic Ca^{2+} increases in response to FVIIa

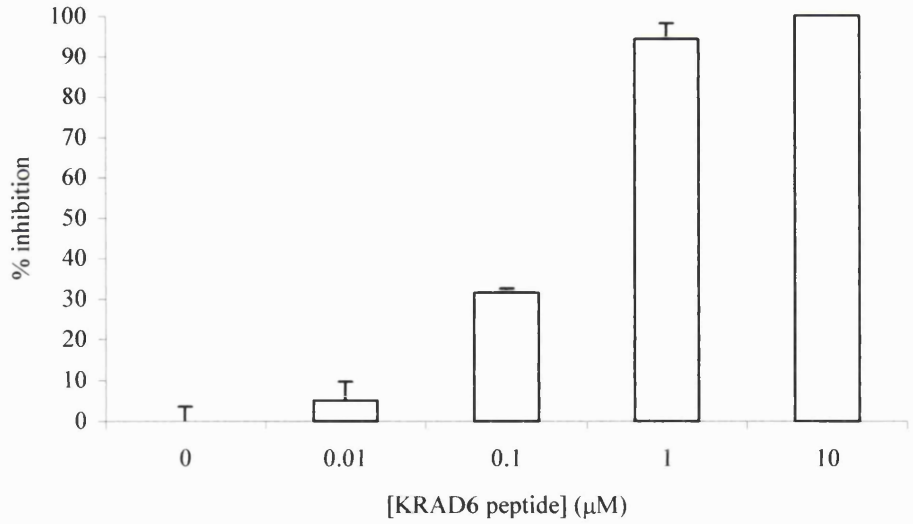

T24 cells were plated onto glass coverslips as described in section 2.1.8. Coverslips of cells were loaded with the Ca^{2+}-sensitive fluorophore Fura2 as described in section 2.3.2. Cytosolic Ca^{2+} levels in individual cells were observed using a microscope integrated to a fluorescent video imaging system. The effect of the KRAD6 peptide was calculated using the formula: 100 X [(% responding cells in control - % responding cells after KRAD6 treatment)/ % responding cells in control]. The results are expressed as the means ± S.E.M. for 3 independent experiments. At least 30 cells were observed within each experiment.

4.5 Conclusions

MDCK2 cells elicit Ca^{2+} transients in response to treatment with FVIIa. The kinetics of the induction of the cytosolic Ca^{2+} fluxes are distinctly variable amongst a population of treated cells. Many cells elicited an oscillatory series of Ca^{2+} spikes in response to treatment with FVIIa. The timing of these Ca^{2+} spikes was synchronized across the cell monolayer, and emanated from focal points in the cell population. This observation demonstrates the ability of a cell to transmit the response to adjoining cells. The cytosolic Ca^{2+} response of MDCK2 cells is dependent upon the concentration of FVIIa. Experimental analysis demonstrated that the magnitude of the Ca^{2+} response, measured in terms of the response integral, is positively and significantly correlated with the concentration of FVIIa used to treat the cells. Linear regression analysis of the Ca^{2+} response in terms of the peak amplitude, decay time and the number of oscillations was also positively correlated with the concentration of FVIIa.

The apo B100-derived KRAD14 sequence inhibits TF activity. At concentrations of 500nM the KRAD14 peptide completely abolishes TF activity after a pre-incubation period of approximately 7 minutes (Ettelaie C., 1998). Furthermore, the inhibition of TF by KRAD14 peptide is significantly attenuated by alanine substitution of K and N residues. A 6-mer sequence derived from the KRAD14 sequence (KRAD6; KKNKHR) was synthesized and was also found to inhibit the procoagulant activity of TF. At concentrations of 1μM, the KRAD6 peptide inhibits TF activity by approximately 50% after 16 minutes.

The effect of inhibition of TF activity by the KRAD6 peptide upon the induction of Ca^{2+} transients by FVIIa was determined. MDCK2 cells were incubated with KRAD6, prior to the addition of 400nM FVIIa. Addition of the KRAD6 peptide to the cell monolayer did not itself induce cytosolic Ca^{2+} signals in the MDCK2 since the basal level of Ca^{2+} remained constant after the addition of KRAD6 peptide. Linear regression analysis of the data showed that concentration-dependent inhibition of FVIIa-mediated Ca^{2+} transients was observed when the cells were pre-treated with the KRAD6 peptide. Maximal inhibition was obtained at a concentration of KRAD6 between 0.1 and 1μM. The KRAD6 peptide is an inhibitor of the TF: FVIIa complex, inhibition of the induction of Ca^{2+} transients by the KRAD6 peptide indicates that FVIIa-mediated Ca^{2+} transients are dependent upon the protease activity of TF: FVIIa.

4.6 Discussion

4.6.1 Responses of MDCK2 to FVIIa

The characteristics of the cytosolic Ca^{2+} response of individual MDCK2 cells within a population of cells were variable. The responses were variable in terms of; the overall magnitude, the frequency of Ca^{2+} spikes, the peak amplitude and the decay time. The Ca^{2+} transients induced in response to TF: FVIIa are dependent on a dual receptor mechanism, whereby FVIIa promotes activation of the PAR2 receptor (see section 3.1.2). The differences in the characteristics of the Ca^{2+} responses may arise from intercellular variation in TF expression or variation in PAR2 receptor expression.

Previous studies have demonstrated that MDCK2 cells treated with FVIIa elicit increases in cytosolic Ca^{2+} levels that are concentration-dependent with regard to the frequency, latency maximal amplitude and recruitment of responding cells (Rottingen J-A., 1995). The results reported here confirm that the overall magnitude of the response was positively correlated with the concentration of FVIIa. In addition, the data reported here shows that the increase in the magnitude of the response is mediated via an increase in peak amplitude, decay time and number of oscillations.

The induction of Ca^{2+} transients in MDCK2 was transmitted across the cell monolayer producing synchronised waves of increased cytosolic Ca^{2+}. These results confirm previous data (Camerer E., 1996) and demonstrate the existence of intercellular communication pathways in the response to FVIIa. Synchronous oscillations may depend upon intercellular gap junctions in a manner similar to the synchronous oscillations seen in response to bradykinin (Berridge M.J., 1998). Thus, the response of one cell to FVIIa results in a co-ordinated response of adjoining cells and the propagation of the signal away from the point of origin. The spatio-temporal regulation of responses seen in the MDCK2 monolayers may be a mechanism by which the response of any given cell is determined in terms of its proximity to the initial signal. Such a mechanism would facilitate a biochemical means of determining the response of a cell in terms of its spatial location in respect of the initial stimulus. In addition, since synchronous oscillations are dependent upon cell: cell contact, the signal is not transmitted to cells external to the monolayer. This affords regulation of biological responses where cell: cell contact is an important factor.

The frequency of oscillations is positively correlated with the concentration of FVIIa. Cells are able to determine the frequency of the Ca^{2+} signals and can vary the nature and/or the intensity of the physiological output accordingly (Nelson M.T., 1995, Porter V.A., 1998 and Dolmetsch R.E., 1998). Thus the induction of Ca^{2+} transients by different concentrations of FVIIa in MDCK2 cells may result in the activation of distinct phenotypic responses. This may be of importance *in vivo* allowing the cells to vary the response depending upon the

concentration of FVIIa, which in turn reflects the amount of TF exposed and thus the severity of the injury. In addition, the genetic response of cells may be modulated by their proximity to the source of the TF: FVIIa signal. Such a mechanism affords a spatially co-ordinated response within a tissue structure. These data show that differences in levels of FVIIa are sensed by the cells and are translated into a modulation of the nature of the cytosolic Ca^{2+} response. Variation in the cytosolic Ca^{2+} elevations may in turn translate into phenotypic variations in the response of individual cells (see section 7.6).

The concentration of FVIIa required to induce Ca^{2+} transients is significantly higher than the plasma concentration of FVIIa. However, *in vivo* the concentration of FVIIa produced local to an injured area is likely to be several orders of magnitude greater than the plasma concentration. The data thus support a physiological relevance of the *in vitro* findings to the *in vivo* scenario.

One author (Petersen L.C., 2000) has reported a failure of MDCK cells to respond specifically to FVIIa and suggest that the cytosolic Ca^{2+} responses to FVIIa, previously reported by Camerer E. et al 1996, are non-specific and result from a proposed ability of FVIIa to increase the rate of spontaneous firing. The inhibition of the Ca^{2+} response by pre-treatment of the cells with the KRAD6 peptide reported here, demonstrate that the responses to FVIIa are indeed specific and are mediated by TF-induced activation of FVIIa.

4.6.2 Inhibition of TF function by the KRAD6 peptide

The results presented here demonstrate that the KRAD6 peptide exhibits concentration-dependent inhibition of the induction of cytosolic Ca^{2+} transients by FVIIa. At concentrations of 1μM, the KRAD6 peptide almost completely abolishes the cell signalling activity of TF, measured in terms of the induction of cytosolic Ca^{2+} responses to FVIIa. The potency of KRAD6 in the inhibition of the procoagulant function of TF is approximately two-fold lower than its ability to inhibit signalling function of TF. The concentration of FVIIa used to stimulate Ca^{2+} transients is 400nM, which is 80 times the concentration of FVIIa expected in the procoagulant assay of TF activity (~5nM). The discrepancy in the potency of KRAD6 in the procoagulant and cell signalling assays of TF is not due to the presence of higher concentrations of FVIIa in the procoagulant assay. However, the discrepancy in the potency of KRAD6 between the two systems is relatively minimal. The KRAD6 peptide may be more effective in the assays of cytosolic Ca^{2+} as the buffer contains no macromolecules, whereas the procoagulant assay contains plasma proteins. The KRAD6 peptide may be subject to interactions with macromolecules in the plasma used in the procoagulant assay. Such interactions may reduce the rate at which KRAD6 binds to and inhibits TF activity.

Figure 4.13: Proposed model of the interaction of KRAD6 peptide with tissue factor

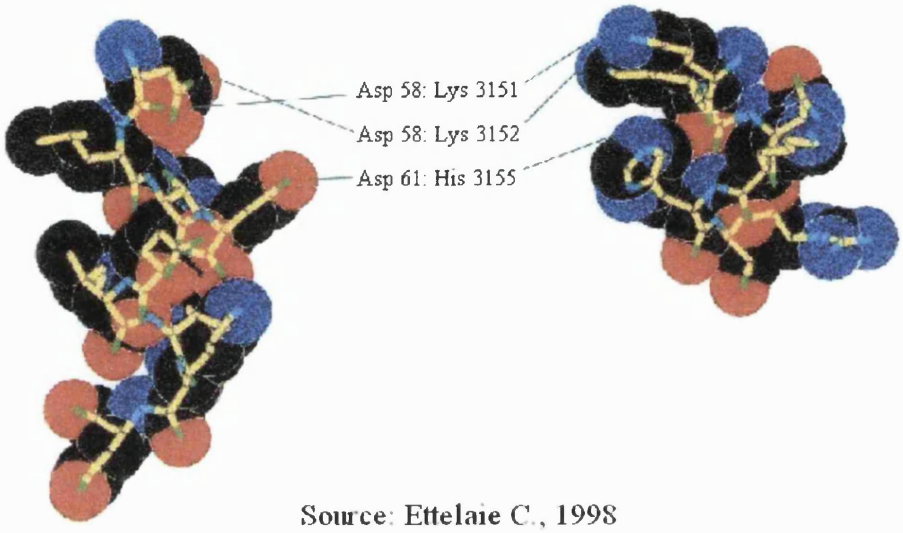

Source: Ettelaie C., 1998

4.6.3 Mechanism of inhibition of TF activity by the KRAD6 peptide

The reported data shows that the KRAD6 peptide prevents the maturation of the FVIIa active site. The conformational changes induced by binding of FVII to TF have been recently revealed (Pike A.C.W., 1999). Since the mechanism of the activation of FVIIa by its co-factor TF is now understood, the effect of KRAD6 binding, to its proposed binding site in TF (figure 4.13), can be evaluated in terms of its potential to interfere with the activation of FVII.

4.6.3a The mechanism of activation of FVII by TF

Superimposition of the peptide backbones of free Gla-domainless (GD-FVIIa, Pike A.C.W., 1999) and FVIIa bound to soluble TF (FVIIa sTF, Harlos K., 1994 and Muller Y.A., 1994) shows that the EGF1 domain in GD-FVIIa is rotated 180° about Gln88 in the linker hexapeptide (figure 4.5). Activation of the FVIIa: sTF complex is not mediated by a conformational change in TF upon FVII binding. Minor differences between GD-FVIIa and

FVIIa: sTF are primarily restricted to the loops that flank the active site cleft (figure 4.5; red, purple and mauve loops). A striking structural difference between GD-FVIIa and FVIIa: sTF, is observed for Leu305 to Glu325. In FVIIa: sTF this region consists of a short α-helix (307-312) next to a loop that defines the outermost face of the active site cleft. Stabilization of the 307-312 'transmitter helix' is a prerequisite for the appropriate formation of the activation domain and is the proposed allosteric control site.

The interface between the protease domain and TF is formed by the N-terminal part of this transmitter helix, which contains residues involved in proteolytic function as well as TF-binding (Dickinson C.D., 1996). In the FVIIa: sTF structure this helix is lengthened by three residues and is shifted 0.5-3Å away from the active site cleft. This shift leads to the movement of two neighbouring loops (Tyr332-Ser 339 and Thr370-Phe374) away from the active site.

Instability of the 307-312 transmitter helix in GD-FVII arises from the absence of an N-capping residue at position 306. Unlike serine proteases that exhibit co-factor independent activity, (Kamata K., 1998, Bode W, 1992 and Huber R., 1978), this position is occupied by a conserved Met residue in FVIIa. Residues in TF (Glu91, Tyr94 and Gln96) mediate stabilisation of the transmitter helix allowing C-capping of the transmitter helix (Banner D.W., 1996).

These observations show that the zymogen-to-enzyme transition of FVIIa is labile and its conformation and activity are co-factor dependent. The unstable transmitter helix is a disordered activation domain that prevents FVIIa activity in the absence of TF. The quiescence of the clotting cascade is maintained provided TF is sequestered from its ligand.

4.6.3b Mechanism of inhibition of FVII activation by the KRAD6 peptide

The binding site of the apo B100-derived KRAD6 peptide to TF is thought to occur at residues 58-62 in TF (figure 4.13, Ettelaie C., 1996). These residues form the C-terminal end of strand E and the N-terminal end of the α-helical domain α1 (figure 4.5). The α1 domain sits close to residue Glu88 in light chain of FVIIa, the pivot around which the FVII serine protease domain rotates upon TF-induced activation.

Activation of FVII is brought about by rotation of the serine protease domain about Glu88 in FVII. The structural data supports the hypothesis that the rotation of the protease head of FVII relative to the tail of FVII is dependent upon the immobilization of the tail of FVII immediately beneath Glu88. This interaction is mediated by H-bonds between FVII and TF, including Asp58 in TF that binds Gly78 in the light chain of FVII (Banner D.W., 1996). The involvement of Asp58 of TF in the activation of FVII has been reported previously in mutational studies (Banner D.W., 1996 and Muller Y.A., 1994). We propose that KRAD6

may interfere with FVII activation via its ability to bind to Asp58 in TF. This interaction may prevent the formation of H-bonds between TF and FVII required to enable rotation of the serine protease domain of FVII and maturation of the active site. In support of this hypothesis as a potential mechanism, point mutation of Asp58 residue results in 5000-fold reduction in affinity for the FVII ligand (Martin D.M.A., 1995) and renders TF defective as a co-factor for FVIIa-dependent FX activation (Lee G.F., 1998).

CHAPTER 5

THE ROLE OF TISSUE FACTOR IN THE FORMATION OF TUBULAR NETWORK STRUCTURES IN AN *IN VITRO* MODEL OF ANGIOGENESIS

5.1 Introduction

5.1.1 Tissue factor and angiogenesis

The involvement of TF in angiogenesis was first suggested indirectly by the results of studies on tumour genesis (section 3.1.1). A correlation between TF expression and metastatic capacity was established in the early 90's (Mueller B.M., 1992). A number of subsequent studies confirmed the association of TF with metastatic capacity in both humans (Contrino J., 1996, Vrana J.A, 1996, Pasqualini M.E. 1997, Koomagi R. 1998, Sawada M., 1999, Wojtukiewicz M.Z., 1999, Sawasda Y., 1999) and mice (Zhang Y., 1994 and Bromberg M.E., 1995) and also in cellular model systems (Kakkar A.K., 1999). The metastatic capacity of tumours is dependent upon the ability of the tumour to become vascularised due to neo-angiogenesis. These results therefore, suggest that TF mediates tumour angiogenesis permitting the metastasis that determines the aggressiveness of tumours. In addition, further studies show a direct relation between TF and the formation of new blood vessels (vasculogenesis). The role of TF in vasculogenesis in the chick embryo has recently been recognised (Carmeliet P., 1996). Angiogenesis is strictly regarded as being distinct from vasculogenesis, since it involves the sprouting of new capillaries from pre-existing ones. However, the processes are unlikely to be mutually exclusive and it is likely that TF may mediate angiogenesis in addition to its requirement in vasculogenesis.

5.1.2 Angiogenesis and the progression of atherosclerosis

The development of new capillaries is observed in advanced atherosclerotic plaques (figure 1.5). These capillaries, also called neoadventitia, are derived from blood vessels in the outer adventitial layer of the artery wall during a process referred to as angiogenesis. A full account of the role of angiogenesis in the progression of atherosclerosis and the manifestation of acute clinical symptoms is presented in section 1.2.4 and is summarised below.

The induction of wound healing in injured arteries can ultimately lead to intimal hyperplasia and the consequent reduction in the cross sectional size of the arterial lumen. Studies suggest that intimal hyperplasia is dependent upon angiogenesis (Kwon H.M., 1998). This hypothesis is supported by the fact that the formation of neoadventitia is first evident in type IV plaques and is more extensive in type V plaques (Stary H.C., 1995). Thus, the occurrence of angiogenesis in type IV plaques may facilitate the intimal hyperplasia that characterizes type V plaques.

Angiogenesis also promotes the progression of atherosclerosis in the acute stage of the disease. Myocardial or cerebral ischaemia commonly arises due to the rupture of unstable plaques. Angiogenic vessels at the periphery of plaques are fragile and prone to rupture. In

addition, T-lymphocytes and macrophages are more prevalent in areas of angiogenesis. These cells are associated with plaque instability probably due to their ability to secrete factors that degrade extracellular matrix proteins. The consequences of rupture may be the formation of haematoma within the plaque or the tearing of the plaque and exposure of the proatherogenic lipid core. Exposure of the proatherogenic lipid core initiates the coagulation cascade and may result in the formation of an obstructive thrombus and the precipitation of an ischaemic event. Alternatively, rupture of one side of the plaque may cause the fibrotic cap to lift into the lumen and obstruct the flow of blood. Rupture of the plaque may also result in complete detachment of all, or part of, the fibrous cap and its release into the circulation as an embolism. Emboli precipitate ischaemia by lodging in arteries with narrower bores.

Angiogenesis is thus a key determinant in the formation and rupture of atherosclerotic plaques and hence determines the progression of atherosclerosis and the ultimate precipitation of acute cardiovascular events.

5.1.3 Mechanisms of involvement of TF in angiogenesis

Angiogenesis is induced as part of the response that promotes wound healing. Wound healing is dependent upon cellular migration, proliferation and communication as well as degradation of existing extracellular matrix and the deposition of new matrix. Degradation of the extracellular matrix permits the infiltration of the neovascular capillaries. The mechanism(s) by which TF mediates angiogenesis are not fully understood. However, the ability of TF to induce a variety of cellular signals (figure 3.1) demonstrates the potential for TF to induce functional change in arterial cells. Moreover, the TF: FVIIa complex induces the expression of several genes that appear to fit different parts of a reparative response.

Like TF, plasminogen has been implicated in angiogenesis, tumour cell invasion, smooth muscle cell migration and angiogenesis (Dano K., 1985 and Odekon L.E., 1992). Plasminogen and TF co-localise in atherosclerotic plaques (Fan Z.Q., 1998). Activation of plasminogen in the fibrinolytic pathway induces various metalloproteinases that lyse the fibrin clot and are indispensable for wound healing (Romer J., 1996). Urokinase (uPA) plays an important role in pericellular proteolysis during cell migration and tissue remodelling by activation of plasminogen. The uPAR: uPA complex activates plasminogen and is involved in cellular adhesion to vitronectin (Chang A.W., 1998). uPA deficiency in mice prevents neointima formation and angiogenesis following arterial injury (Carmeliet P., 1999) and results in the formation of weak scars (conference communication). The involvement of TF in angiogenesis may be mediated via its ability to induce the uPAR (Camerer E., 2000). In addition, induction of the uPAR by TF: FVIIa may be the

mechanism by which TF regulates plasminogen activation on cell surfaces (Fan Z., 1998). Interestingly, the endogenous levels of uPAR gene expression are correlated with the expression of TF (Taniguchi T.,1998).

Inhibition of uPA is mediated by PAI-2 (Reinartz J., 1996). PAI-2 is strongly induced by the TF: FVIIa complex. Inhibition of uPA-mediated clot lysis may be necessary to inhibit degradation of fibrin in the early phase of wound healing prior to closure of the epithelial layer.

The TF: FVIIa complex leads to activation of phospholipase C and enhanced PDGF-BB stimulated chemotaxis in fibroblasts (Siegbahn A., 2000). In addition, FVIIa induces the expression of extracellular matrix signalling proteins, Cyr61 and CTGF (Pendurthi U., 2000). Exposure of fibroblasts to FVIIa results in the formation of filopodia, lamellipodia and membrane ruffles, which are indicative of cytoskeletal reorganisation mediated by cdc42 and Rac activation. The ability of the TF: FVIIa complex to induce the activation of the small GTPases, cdc42 and Rac via c-src and PI3K has been demonstrated (Versteeg H.H., 2000). In addition, induction of the GTPase Rho E, which induces cell spreading by the TF: FVIIa complex, has also been documented (Camerer E., 2000).

The involvement of TF in cellular organisation is also supported by the observation that the TF: FVIIa complex induces uPAR, collagenases 1 and 3 (Camerer E., 2000) and the extracellular matrix signalling proteins CTGF and cyr61 (Pendurthi U., 2000), PDGF-BB stimulated chemotaxis (Siegbahn A., 2000).

TF: FVIIa induces fra-1 (Camerer E., 2000), a protein implicated in the induction of cell motility and invasion *in vitro* (Kustikova O., 1998). Furthermore, formation of the TF: FVIIa complex leads to the up-regulation of collagenases 1 and 3 (Camerer E., 2000), which supports the migration of keratinocytes on type I collagen (Pilcher B.K., 1997).

Jagged1, a membrane-bound ligand acts in intercellular communication (Lindsell C.E., 1995) and is also induced by the TF: FVIIa complex. FVIIa: In addition, TF induces hbEGF and AR, which are members of the EGF family. Growth factors of the EGF family are implicated in the proliferation of keratinocytes at the wound edge (Martin P., 1997). hbEGF is found in wound exudates and is mitogenic and chemotactic for fibroblasts, smooth muscle cells and keratinocytes (Raab G., 1997).

5.1.4 T24 cells cultured on Matrigel™ as an *in vitro* model of angiogenesis

Tissue culture of human bladder carcinoma T24 cells on Matrigel™ results in the formation of networks of cells. The organisation of the T24 cells in this *in vitro* culture system has been previously reported to be as networks of tubules, thus the culture system is useful as a model for the study of capillary network formation. This system was used as a model to investigate the involvement of TF activity in the microanatomical organisation of the

tubular network structures. At the time these studies were undertaken, the cells provided by the ECACC were designated as endothelial ECV304 cells. Subsequent to phenotypic analysis the ECACC found that the cells supplied as ECV304 were in fact human bladder carcinoma T24 cells. Despite the fact that the cells are not in fact endothelial, the culture system remains useful as a system in which to determine the involvement of TF in the organisation of cells into a tubular network structures, analogous to capillaries.

5.2 Aims

- To determine the effect of inhibiting TF activity upon the formation of cellular network structures in an *in vitro* model of angiogenesis using;

  i: a 14-mer peptide derived from apo B100 (KRAD14)

  ii: an antibody with a neutralizing activity towards TF (TF85G9)

5.3 Methods

5.3.1 Tissue culture of T24 bladder carcinoma cells on Matrigel™

5.3.1a Coating of culture vessels with Matrigel™

Matrigel™ is a solubilised basement membrane matrix extracted from the Engelbreth-Holm-Swarm mouse sarcoma (Kleinman H. K., 1982). Its major component is laminin, followed by collagen IV, heparan sulphate proteoglycans, entactin and nidogen. It also contains growth factors, which occur naturally in the Engelbreth-Holm-Swarm mouse sarcoma.

Matrigel™ was purchased from Promega and was stored in at –20°C. Matrigel™ was thawed on ice overnight 24 hours prior to use. The base of each well (1.77cm^2) of a 24-well culture plate was coated with 40µl of Matrigel™. In order to aid spreading of the Matrigel™ matrix onto the base of the culture vessel, all equipment coming into contact with the matrix was cooled in the freezer for at least 30 minutes prior to the coating procedure. After the entire base of the each well had been coated with Matrigel™, the culture vessel was placed in at 37°C in an incubator to permit polymerization of the matrix. Cells were then plated directly onto the prepared matrix.

5.3.1b Plating of T24 cells onto Matrigel™

Cells were harvested from culture as described in section 2.1.2. Cells were washed and resuspended to 0.5 X 10^6/ml in DMEM containing Glutamax™ and 5% serum. 100µl aliquots of the cell suspension (0.05 x 10^6 T24 cells) were mixed with 0.4ml of DMEM containing Glutamax™ and 5% serum. The cells were then seeded onto the Matrigel™-coated 24-well plates. Cells were placed in an incubator at 37°C, 5% CO_2 for 24 hours prior to the determination of the density of network formation.

5.3.2 Determination of the density of network formation

The number of network structures was determined 24 hours subsequent to seeding of cells. The density of network formation was determined by counting the number of holes in the culture dish (figure 5.1). To aid counting, each culture vessel was scored on the underside of the vessel so that two parallel lines were seen through the microscope.

Figure 5.1: Schematic representation of network structures of T24 cells

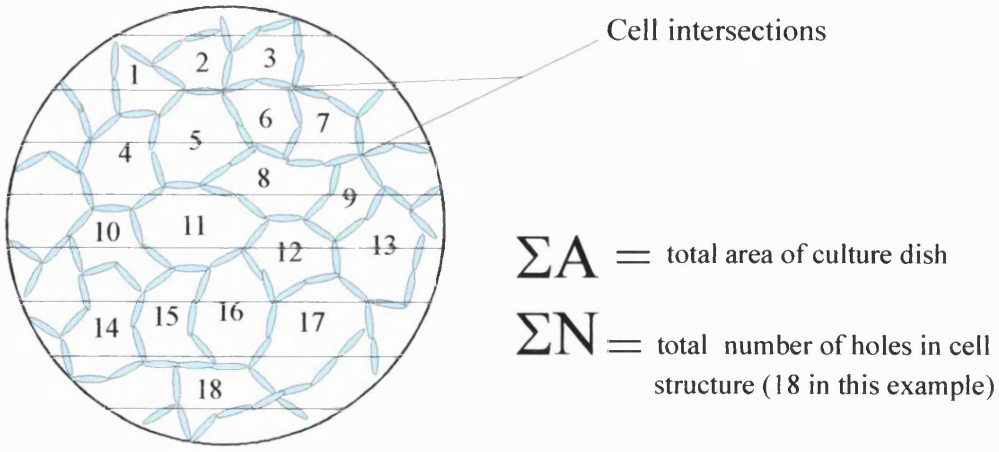

Validation that the number of holes represents the density of networks is proved below;

The typical area per hole (A_h) is given by;

$$\frac{\text{Total area of culture dish } (\Sigma A)}{\text{Total number of holes } (\Sigma N)}$$

Given that the cellular boundaries between the holes is small and the sample is sufficiently large. The number of cell intersections is proportional to the density of the networks Therefore the typical distance between two cell intersections (R) is of the order of;

$$\sqrt{\frac{\text{Total area of culture dish } (\Sigma A)}{\text{Total number of holes } (\Sigma N)}}$$

Therefore the number of cell intersections per unit area (density) is given by;

$$\frac{1}{R^2} = \frac{\Sigma N}{\Sigma A}$$

Since ΣA is constant, the number of holes (Σ N) in the culture dish is inversely proportional to the distance between cell intersections (R^2). Thus ΣN is an index of the density of cellular networks.

5.4 Results

5.4.1 Effect of serum concentration upon the formation of network structures

Cells were cultured as described in section 5.3.1 except for variation of the serum concentration. The culture media was supplemented with a range of serum concentrations from 2.5 to 10% and the formation of network structures was determined for 3 days (figure 5.2). The number of networks per well was reduced after day 1, and resulted from cell death. The lowest serum concentration at which tubular network formation is optimum is 5%.

5.4.2 Cell surface expression of tissue factor on T24 cells

Serial dilutions of T24 cells were prepared and the prothrombin time of the samples determined. The T24 cells were assayed independently 3 times. The prothrombin times were converted to units of tissue factor activity (figure 5.3) using the equation derived from the standard curve of recombinant TF activity versus prothrombin time (section 2.2).

The optimum seeding density for network formation in the 24-well culture plates is 0.05 x 10^6 cells/well. Using the standard curve the TF activity of 0.05 x 10^6 T24 cells was calculated and is equivalent to 0.1 units of recombinant human TF.

Figure 5.2: Effect of serum concentration upon the formation of tubular networks

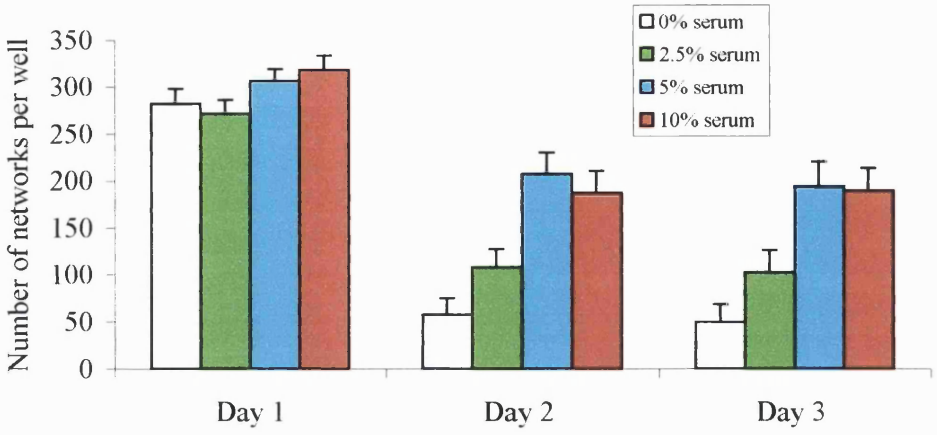

Individual wells in a 24-well culture plate were coated with specialised cell culture matrix, Matrigel™. The Matrigel™ was allowed to polymerise for 30 minutes at 37°C prior to the addition of cells. 0.05 x 10^6 T24 cells suspended in 0.5ml of DMEM containing a range of concentrations of serum (0-10%) were added to the culture wells. Cells were observed after 24h, 48h and 72h and the formation of network structures was scored (5.3.2). Networks were defined as cell-free areas bounded on all sides by cells (figure 5.1).

The results are the means ± S.E.M. of three independent experiments.

Figure 5.3: Cell surface expression of tissue factor activity on T24 cells

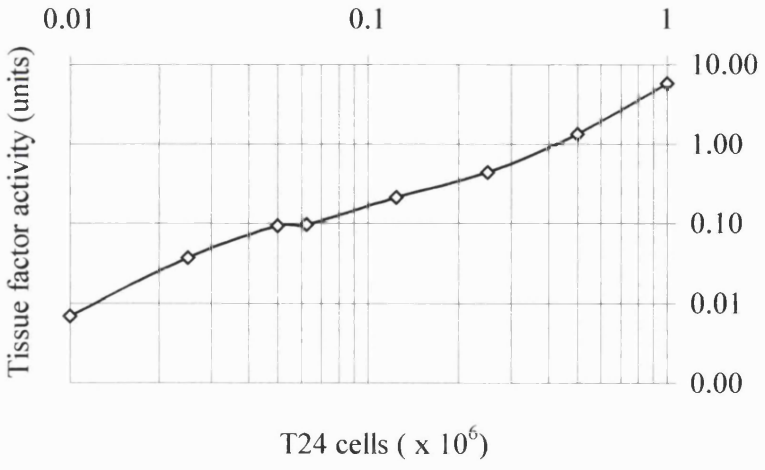

T24 cells were harvested from culture, washed and resuspended in PBS. Cell suspensions were prepared to contain a range of concentrations of T24 cells (10 x 10^6 to 0.1 x 10^6). The cell suspensions were tested for procoagulant activity using the one stage prothrombin time assay. 100µl aliquots of the cells were incubated with 100µl of control plasma at 37° C. Coagulation was initiated by the addition of 100µl of 25mM $CaCl_2$. The time taken for the clot to form was recorded and converted to TF units using a standard curve (figure 2.1)

5.4.3 Inhibition of the formation of network structures by the KRAD14 peptide

Culture plates were prepared with Matrigel™ and seeded with 0.05 x 10^6 T24 cells (section 5.3.1). KRAD14 peptide was added to the cultures at the desired final concentrations prior to the incubation of cells. Cells were scored for network formation as described in section 5.3.2. Inhibition of TF activity by the KRAD14 peptide resulted in a concentration-dependent inhibition of the formation of network structures (figure 5.4). 1μM KRAD14 peptide resulted in 86.5% inhibition of the formation of networks in the culture system. Reduction of the concentration of KRAD14 to 0.1μM resulted in an approximately 50% ± 3.4 reduction of inhibition to 46.5% ± 6.5.

5.4.4 Inhibition of the formation of network structures by TF85G9 antibody

The role of TF in the formation of cellular networks was also investigated using the TF85G9 antibody (Ruf W., 1991). TF85G9 is the Fab fragment of an IgG1 monoclonal antibody. TF85G9 interacts with the membrane proximal module of the TF molecule. Structural and mutagenesis data indicate that Tyr156, Lys 169, Arg200 and Lys201 are the most important residues in antibody binding (Huang M., 1998). The TF85G9 antibody binds rapidly to TF: FVIIa and acts as a competitive inhibitor for factor IX and factor X activation (Ruf W., 1991).

5.4.4a Comparison of the inhibition of recombinant human TF and TF expressed on T24 cells by the TF85G9 antibody

The amount of TF85G9 antibody required to inhibit 0.1 units of TF was calculated for both recombinant human TF and cellular T24 TF. The inhibition of cellular and recombinant TF by TF85G9 was compared in order to ascertain whether the antibody displays differential potency in the two systems. The resulting data was used to provide a guideline concentration of TF85G9 antibody to use in determining the effect of TF inhibition upon network in the cell culture assay.

The data displayed in figure 5.5 shows the inhibitory effect of concentrations of TF85G9 antibody ranging from 0.05μg/ml to 1.0μg/ml upon the prothrombin times elicited by 0.1 units of recombinant human TF or 0.1 units of cellular T24 TF.

The inhibition of recombinant TF activity or cellular TF activity by TF85G9 is similar and is maximal at around 0.5μg/ml. At low concentrations of TF85G9 (0.05-0.2μg/ml) inhibition of TF activity is slightly more efficient with cells than with recombinant TF.

5.4.4b Effect of TF85G9 upon the formation of network structures

In order to investigate the role of TF activity in the formation of network structures in T24 cells cultured on Matrigel™, formation of networks was determined in the presence of an

antibody that neutralises the activity of TF, TF85G9. A control antibody was tested in the culture system. The control antibody was an IgG1 Fab directed towards Aspergillus *nidulans* glucose oxidase, a protein not found in human cells.

Preincubation of T24 cells with the control antibody at a concentration of 0.1mg/ml had no effect upon the formation of cellular networks (figure 5.6). In contrast, addition of the TF85G9 antibody to the cell cultures lead to the inhibition of network formation. The data depicted in figure 5.6 demonstrates a concentration-dependent inhibition of capillary networks by the TF85G9 antibody. Network formation by T24 cells was significantly inhibited by 0.1mg/ml (~40μM) of TF85G9 antibody (Student's t-test, $p = 0.006$) and 0.2mg/ml TF85G9 (Student's t-test, $p = 0.0005$). Addition of TF85G9 to cultures at a concentration of 0.05mg/ml (~20μM) did not result in a significant inhibition of network formation compared to the controls (Student's t-test, $p=0.49$). The percentage inhibition of networks by the TF85G9 antibody at 0.1mg/ml and 0.2mg/ml was 56.1% and 66.7% respectively (figure 5.6b).

Figure 5.4: Effect of the KRAD14 peptide upon cellular network formation

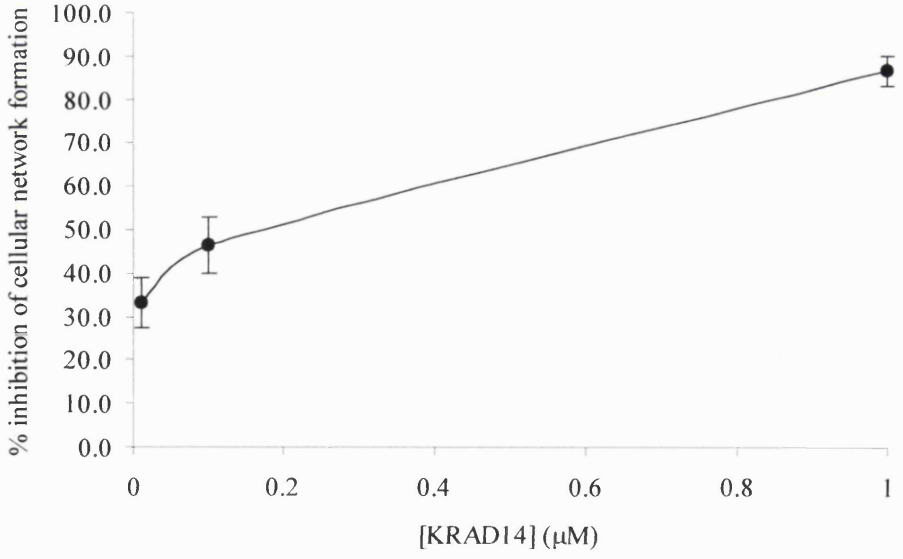

0.05 x 10^6 T24 cells were plated onto Matrigel™ as described in section 5.3.1. KRAD14 peptide was added to the cultures at final concentrations of 1μM, 0.1 μM and 0.01μM. The effect of inhibition of TF activity by the KRAD14 peptide was assessed after 24 hours. The results are the mean ± S.E.M. of three independent experiments.

Figure 5.5: Comparison of inhibition of recombinant TF and cellular TF by TF85G9

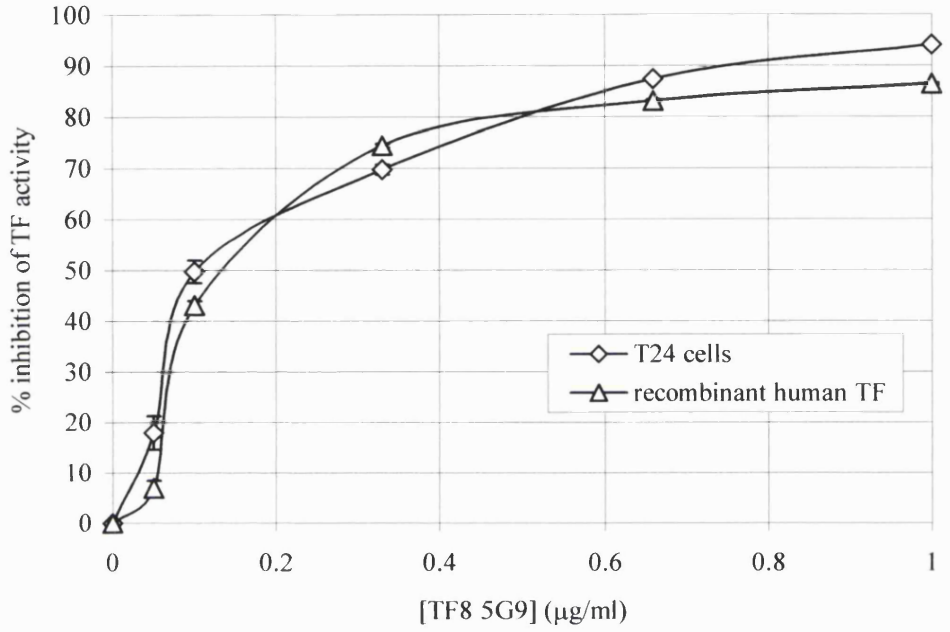

Inhibition of TF activity; (i) expressed on the surface of T24 cells and (ii) by recombinant human TF was compared. All samples were prepared to contain 0.1 units of TF activity. For T24 cells, 0.1 units of activity was expressed on approximately 0.05 x 10^6 cells. Samples of T24 cells and recombinant TF were incubated with TF85G9 antibody concentrations ranging from 0.05μg/ml to 1μg/ml for 2 minutes prior to assay. Samples were assayed for TF using the one stage prothrombin time test. All assays were performed at 37°C. 100μl samples were incubated with 100μl of control plasma. Coagulation was initiated by the addition of 100μl of 25mM $CaCl_2$. The time taken for the clot to form was recorded and converted to TF units using a standard curve (figure 2.1). The percentage inhibition was calculated from the formula; 100 x [(activity of control – activity of sample)/activity of control)]. Results are the means ± S.E.M. of four independent experiments.

Figure 5.6: Effect of TF85G9 upon the formation of T24 cellular networks

a.

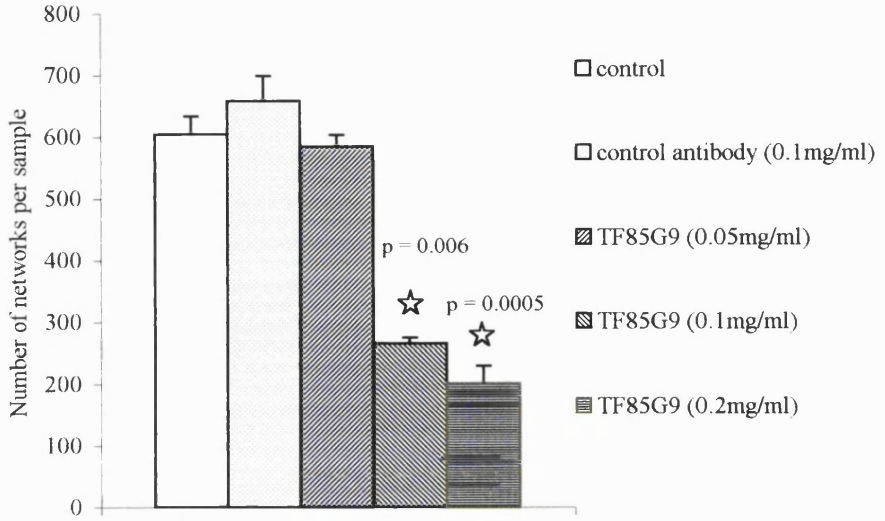

b.

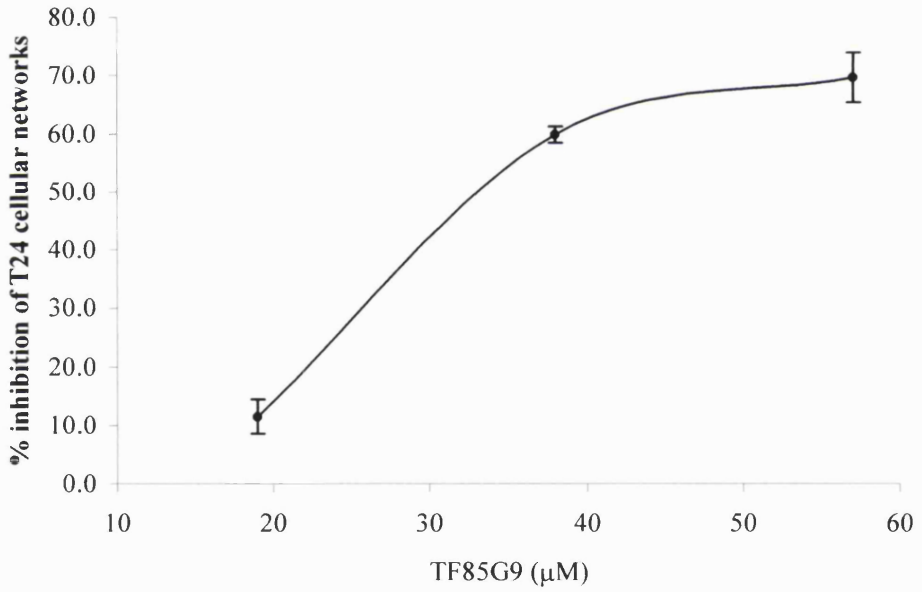

40μl of Matrigel was dispensed in the wells of a 24-well culture plate and allowed to polymerise at 37°C. T24 cells were harvested from culture and resuspended at 0.1 x 10^6/ml in DMEM containing Glutamax™ and 5% serum. 0.5ml aliquots of the cell suspension were added to the Matrigel™-coated wells. 10μl of control antibody, directed to Aspergillus *nidulans* glucose oxidase, was added at 0.1mg/ml to the control wells. 10μl aliquots of anti-TF antibody (TF85G9) were added to sample wells at concentrations of 0.05, 0.1 and 0.2mg/ml. Network structures were grown overnight at 37°C, 5% CO_2 in a humidified incubator. The density of network structures formed was determined following overnight incubation, as described in section 5.3.2. Results are shown as the mean ± SEM. The effect of inhibition of TF upon cellular network formation was determined by testing each test sample versus the control sample using the Student's t-test.

5.5 Conclusions

Human bladder carcinoma T24 cells form tubular networks when seeded onto a specialised matrix (Matrigel^{TM}). Inhibition of TF activity in the culture system by the KRAD14 peptide or the TF-neutralising antibody TF85G9, resulted in significant concentration-dependent attenuation of the formation of the network structures. Incubation of the cells with a control antibody did not result in modulation of the formation of tubular networks. This study demonstrates the involvement of TF in the biologic processes that determine the formation of networks of tubular structures and suggests that TF may be involved in angiogenesis *in vivo*. In addition, these results demonstrate that the KRAD14 peptide inhibits the angiogenic properties of TF in addition to its ability to inhibit the procoagulant properties of TF.

5.6 Discussion

The involvement of TF in both cancer and atherosclerosis has been demonstrated. TF expression correlates with the transformation of tumour cells to a malignant invasive phenotype (Mueller B.M., 1992, Contrino J., 1996, Mueller B.M., 1998 and Sawada M., 1999). In atherosclerosis, TF expression is increased in unstable angina (Misumi K., 1998) and is a predictor of susceptibility to repeated episodes of myocardial ischaemia (Suefuji H., 1997). The involvement of TF in the pathologies of both diseases may be linked to its ability to promote angiogenesis. Malignant transformation of tumours is associated with the vascularisation of primary tumours (Weidner N., 1991). In atherosclerosis, the rupture of neoangiogenic vessels that appear at the periphery of atheromatous plaques (Stary H.C., 1995), results in the precipitation of acute cardiovascular event such as myocardial infarction and cerebral ischaemia via embolism (Barger A.C., 1984). Macrophages, macrophage foam cells and lymphocytes are more densely concentrated in the lesion periphery (Stary H.C., 1995). Macrophage infiltration and is enhanced in unstable compared to stable angina, furthermore, TF expression on macrophages is more frequent in unstable angina (Kaikita K., 1997). Collectively these studies suggest that TF expression at the periphery of plaques may promote the development of angiogenic vessels and thus determine the propensity of plaque rupture. The function of TF in vasculogenesis has been previously recognized (Carmeliet P., 1996) and this also alludes to a role for TF function in angiogenesis.

We investigated the role of TF in angiogenesis using an *in vitro* model. T24 bladder carcinoma cells plated on a specialized matrix form networks of tubular structures that are structurally similar to the network of capillaries formed during angiogenesis. The effect of inhibition of TF activity in the T24 network culture system was assessed to ascertain the involvement of TF in the organisation of the tubular network structures. Attenuation of TF

activity in the culture system was achieved using two different inhibitors. An antibody with an inhibitory activity towards TF function (TF85G9) and the TF inhibitor peptide KRAD14 were used. Inhibition of TF by TF85G9 resulted in a significant concentration-dependent attenuation of the formation of the tubular network structures. Inhibition of network formation was evident at concentrations of TF85G9 as low as 0.1mg/ml (equivalent to ~20μM). In contrast, an equivalent concentration of a control antibody, directed towards a fungal protein not expressed in human cells, had no effect upon the formation of network structures (figure 5.6). The concentration of TF8G9 required to elicit inhibition of network formation was 1000-fold higher than the amount of TF85G9 to inhibit cellular TF procoagulant activity, on an equivalent number of cells in an *in vitro* assay (figure 5.5). The decreased antibody activity in the culture system compared to the *in vitro* assay may result from non-specific absorption of antibody to serum proteins present in the culture system.

Inhibition of TF activity by the KRAD14 peptide also resulted in a reduction in the number of tubular networks formed in the culture system. Concentrations of the KRAD14 peptide of 1μM resulted in almost complete abolition of network formation. A ten-fold reduction in the concentration of the KRAD14 inhibitor to 0.1μM maintained approximately 50% decrease in the formation of networks compared to the controls.

The concentrations of TF85G9 and KRAD14 required to elicit 50% inhibition of cellular network formations estimates from the data plotted in figures 5.6 and 5.4, were 0.2μM and 35μM respectively. These results demonstrate that the KRAD14 peptide is approximately 175 times more potent than TF85G9. The KRAD14 peptide is a much smaller molecule than the TF85G9 antibody. These facts suggest that use of the KRAD14 peptide, or a stable structural homologue, may be a more suitable means of inhibiting TF activity in the treatment of clinical disorders related to TF activation, which include tumour metastasis, disseminated intravascular coagulation and angiogenesis occurring in undesirable locations in atherosclerotic plaques. The small size of the KRAD14 inhibitor may be advantageous over TF85G9 Fab fragments in terms of drug delivery. For example KRAD14 would be small enough to be incorporated into liposomes that could be delivered to target tissues *in vivo*.

The involvement of TF in angiogenesis reported here has been subsequently confirmed in alternative models of angiogenesis. The ability of TF to support angiogenesis has been demonstrated in a diffusion chamber assay in rats, in an *in vitro* assay of bovine aortic endothelial cells in collagen gels (Watanabe T., 1999) and in tumours and wounds (Nakagawa K., 1998).

The mechanism of the involvement of TF activity in the formation of network cultures is unknown. However, the ability of the TF inhibitors TF85G9 and KRAD6 to attenuate the

formation of network structures suggests that TF may regulate the spatial organisation of networks of cellular tubules *in vitro*. TF may thus have an important role *in vivo* in determining the anatomical development of angiogenic capillaries. The formation of cellular network structures depends upon cell migration and cell proliferation. Inhibition of TF activity has been shown to attenuate the migration of tumour cells, smooth muscle cells and mononuclear phagocytes (Taniguchi T. 1998, Sato Y., 1997 and Randolph G.J., 1998). Furthermore, several of the genes induced by TF: FVIIa code for proteins related to cellular reorganisation and migration (figure 3.1 and section 5.1.3). These data confirm a role for TF in the regulation of cellular migration occurring during tissue remodeling and angiogenesis. The mechanism by which TF accomplishes this function may be discovered by an examination of the data available from other studies of TF function.

Neoangiogenesis is dependent upon the existence of cellular signals that define the orientation and 'spatial awareness' of cells within the cellular structure. Such signals are likely to determine the direction of growth and the frequency of branching of tubular structures. The regulation of cytoskeletal assembly in response to such signals is fundamental in cell migration. The ability of TF to associate with cytoskeletal structures, namely actin-binding protein 280, (ABP280, Ott I., 1998) implies a role for TF rearrangement of cellular cytoskeletal elements. ABP-280 is a ubiquitous, dimeric, actin cross-linking, phosphoprotein of peripheral cytoplasm that promotes the orthogonal branching of actin filaments (Gorlin J.B., 1990). The actin cytoskeleton of cells plays a pivotal role in cell motility, phagocytosis, cytokinesis and intracellular transport processes (Nobes C.D., 1995). Peripheral actin filaments can be arranged in different ways to allow non-muscle cells to achieve a variety of shapes. Actin stress fibres are organised into discrete types designed to fulfil specialised requirements during the life cycle of cells. In non-motile, non-dividing cells, actin stress fibres traverse the cell and are linked to the extracellular matrix through integrins and focal adhesion complexes. Moreover, it has been recently demonstrated that TF: FVIIa induces stimulation of the GTPases Rho (Camerer E., 2000), Rac and cdc42 (Versteeg H.H., 2000). Rho, rac and cdc42 GTPases regulate the assembly of the multi-molecular focal complexes associated with actin stress fibres, lamellipodia and filopodia (Nobes C.D., 1995). In addition, TF: FVIIa also activates other proteins involved with cellular migration, such as the src family members; c-src, lyn and yes, the phosphatidylinositol 3-kinase and c-akt/protein kinase B (Versteeg H.H, 2000). The TF: FVIIa complex is also able to induce factors that mediate extracellular matrix degradation (Camerer E., 2000 and Zucker S., 1998) a process essential for tissue remodeling.

TF associates with the γ-chain homodimer of the IgE receptor type I in human monocytes (Masuda M., 1996). The γ-chain is also a component of the Fcγ RI receptor, which has been studied in platelets. The absence of the γ-chain in platelets results in a loss of secretion and aggregation responses in platelets (Poole A., 1997). This data also suggests that TF may serve to regulate cytoskeletal changes.

TF may also control angiogenesis via its ability to regulate the proliferation of cells. Inhibition of TF activity by TFPI, results in the attenuation of proliferation in aortic smooth muscle cells (Kamikubo Y., 1997). Interestingly, inhibition of TF by TFPI has also been shown to induce apoptosis (Hamuro T., 1998). The cytoplasmic domain of TF contains the kinase substrate motifs for both PKC and cdc2. The cdc2 kinase is a member of a family of ubiquitous cell cycle regulators that are collectively responsible for the ordered transition of cells through the G1/G0, S, G2 and M phases of the cell cycle (Moreno S., 1990). The presence of the cdc2 kinase motif in the cytoplasmic domain of TF alludes to a role for TF in the process of transition through cell cycle checkpoints. For example if TF was a positive regulator of the G1 restriction point in the cell cycle, the point at which cells become committed to a round of mitosis, it would promote cell proliferation. It is conceivable that TF could control the cellular decision between proliferation, differentiation or death, via alterations in its conformation that in turn, may be determined by the phosphorylation status of its cytoplasmic domain.

The involvement of TF in angiogenesis is also linked to its ability to induce angiogenic growth factors including VEGF (Ollivier V., 1998), FGF-5 and CTGF (Camerer E., 2000). Interestingly, the cytoplasmic domain of TF is required for the induction of VEGF (Abe K., 1999). In addition, the metastasis of tumour cells (Bromberg M.E., 1995) depends upon the presence of the serine residues in the cytoplasmic domain of TF. The phosphorylation of the cytoplasmic domain and the procoagulant activity of the TF: FVIIa complex are required for the full metastatic effect of TF (Bromberg M.E., 1999). The dependence of metastasis upon the cytoplasmic domain may be due to a requirement for the production of VEGF that is necessary for the angiogenesis to permit metastasis.

However, the precise nature of the involvement of the intracellular domain in cellular signalling by the TF: FVIIa remains controversial. VEGF induction by TF: FVIIa is dependent upon egr-1 (Mechtcheriakova D., 1999) but a role for the cytoplasmic domain of TF in the activation of egr-1 has been refuted (Camerer E., 1999). This observation appears to contradict the finding of a requirement for the cytoplasmic domain in VEGF production and metastasis.

The progression of atherosclerosis may be attenuated via inhibition of TF and the consequent attenuation of neoangiogenesis. However, the spatial development of

neoangiogenesis in atherosclerotic plaques may lead to stabilisation or destabilisation of plaques; angiogenesis occurring at the boundary of plaques weakens the plaque structure and predisposes the plaque to rupture, the most common cause of myocardial infarction. In contrast, the development of collateral vessels stabilises plaques. The ability to inhibit neoangiogenesis at plaque boundaries and/or activate the formation of collateral vessels in patients with atherosclerosis may afford protection against plaque rupture and thus may provide a means of preventing myocardial infarction and stroke *in vivo*. However, the treatment of plaque instability in the clinical scenario would require targeted administration of TF inhibitors and/or activators to specific sites within atherosclerotic plaques. To achieve this, a more comprehensive understanding of the implications of the spatial organisation of neovascularisation in the development of atherosclerotic plaques is required.

CHAPTER 6

INVESTIGATION OF CELLULAR SIGNALLING INDUCED BY NATIVE AND OXIDATIVELY MODIFIED LOW DENSITY LIPOPROTEIN

6.1 Introduction

6.1.1 Chemistry of the oxidation of lipoproteins

Oxidation of LDL is a complex, free radical-driven lipid peroxidation process (Esterbauer H., 1995). Underlying the complexity of the oxidation of LDL is the fact that all the components of LDL; antioxidants, phospholipids, cholesteryl ester, triglycerides and apo B100 participate at certain stages leading to multiple secondary and tertiary reactions. The mechanism of lipid peroxidation is shown in figure 6.1.

The chronology of oxidation of LDL consists of three phases, namely a lag or induction phase, a propagation phase and a decomposition phase (figure 6.2). During the lag phase lipid peroxidation is low or absent due to the presence of antioxidants. Ubiquinol-10 is the first antioxidant to be depleted (Kontush A., 1994) and β-carotene is the last to remain. Following the exhaustion of the antioxidants in the LDL, lipid peroxidation enters a propagative phase and the rate of lipid peroxidation rapidly accelerates to a maximal rate. When polyunsaturated fatty acids (PUFA) become oxidized to lipid hydroperoxides, their isolated carbon-carbon double bonds are converted to conjugated double bonds called dienes. The maximum peroxide content coincides with the maximum diene content (Esterbauer H., 1990).

The decomposition phase begins when about 70-80% of the PUFAs have been oxidized. At this point, the rate of decomposition of lipid peroxides exceeds the rate of their formation. During the decomposition phase, the hydroperoxides are converted to reactive aldehydes. These secondary reactions are accelerated by transition metal ions that decompose lipid hydroperoxides to lipid alkoxyl radicals in a Fenton-type reaction (figure 6.3). The lipid alkoxyl radicals undergo β-cleavage reactions (homolytic scission) to yield aldehydes and carbon centred lipid radicals. It was hypothesised (Esterbauer H., 1997) that cleavage of carbon bonds in phospholipid and cholesteryl ester hydroperoxides would result in the formation of two classes of aldehydes namely, aliphatic aldehydes derived from the methyl terminus and aldehyde bound to the parent lipid (core aldehydes). The detection of cholesteryl oxoalkanoates and phospholipid oxoalkanoates confirmed this notion (Kamido H., 1992). Aldehydes form the predominant class of products identified in oxLDL. The lipid oxidation products demonstrated in Cu^{2+} oxidized LDL are tabulated in figure 6.4.

6.1.2 The source of the initiating radical in lipid peroxidation

The nature of the initiating radical remains elusive both in *in vitro* systems (e.g. copper-mediated oxidation) and *in vivo*. It is thought that lipid peroxidation by copper results in the binding of copper to discrete sites in apo B100 forming centres for repeated free radical

production (Chevion M., 1998). Once bound, Cu^{2+} must be reduced by the net transfer of one electron. The presence of Cu^{2+} appears to be essential to cell-mediated oxidation of LDL since oxidative changes *in vitro* only occur if the media contains trace amounts of metal ions. Furthermore, with respect to the scenario *in vivo*, copper and iron are present in atherosclerotic lesions (Smith C., 1992). A proposal suggesting the involvement of thiols in transition metal ion-dependent cell-mediated oxidation (Heinecke J.W, 1987) is supported by the observation that LDL oxidation by endothelial cells and macrophages is dependent on the appearance of thiol in medium containing transition metal ions (Sparrow C.P., 1993).

The ability of lipoxygenase to mediate oxidation of LDL was first demonstrated using soybean lipoxygenase (Sparrow C.P., 1988). However, the relevance of cell-derived lipoxygenases in LDL oxidation in the context of atherosclerosis is equivocal. 15-lipooxygenases occur in human and rabbit atheroma and co-localise with deposits of oxLDL (Yla-Herttuala S., 1990 and 1991). However, the non-specific production of positional and stereoisomers suggest that *in vivo* non-enzymatic peroxidation processes govern the production of cholesterol esterified keto- and hydroxyoctadecadienoic acids that have been found in atherosclerotic aortas from patients who died from myocardial infarction (Kuhn H., 1992). The pattern of products produced by oxidation of LDL with human umbilical vein endothelial cells in Ham's F10 medium for 20h is also characteristic of non-enymatic degradation (Wang T., 1992). The main products are the monohydroxy derivatives of linoleic acid (9-HODE and 13-HODE) and arachidonic acid (5-, 8-, 9-, 11-, 12- and 15- HETEs). Small amounts of hydroxlyated derivatives of oleic acid (8-, 10- and 11- hydroxy; 18:1) are also formed. In addition, the isomer distribution of LDL oxidized for 5h with Cu^{2+} is identical to that of endothelial cell-oxidized LDL. Although the pattern of products in the arterial wall suggests the involvement of non-enzymatic peroxidation mechanisms, monocyte and/or endothelial 15-lipoyxgenase may be instrumental in initiating non-enzymatic processes by providing the initial hydroperoxides. Formation of hydroperoxides would render the LDL susceptible to further transition metal catalysed non-enzymatic peroxidation.

6.1.3 Molecular nature of oxidative changes in LDL

Aldehydic modification of LDL increases its negative charge and leads to a decrease of the affinity of LDL for the LDL receptor. Conversely, its affinity for the scavenger receptor is increased. The molecular nature of the modification of LDL that renders it capable of binding the scavenger receptor has been investigated. Various lines of research indicate that the aldehydes present in oxidized LDL interact with positively charged ε-amino groups of lysine residues in the apo B100 moiety (Juergens G., 1987 and Esterbauer H., 1992). It has

been proposed that phospholipid hydroperoxides interacting with protein amino groups undergo a secondary oxidation to form protein-linked aldehydes (Freubis J., 1992). The precise chemical structure of the aldehyde apo B100 conjugates and their location on apo B100 remain to be determined.

Oxidation of LDL is extremely complex since the protein, lipid and antioxidant moieties can be attacked (Steinberg D., 1990 and Parthasarathy S., 1992). The extent of the changes depends upon the pro-oxidant conditions and the availability of antioxidants, which may vary considerably. Therefore there is a broad spectrum of oxidized LDLs and no discrete particle corresponding to oxidized LDL exists (Witzum J.L., 1991). The heterogeneity between the products of LDL oxidation is responsible for the distinct biological effects of different classes of oxidized LDL. Much work remains to be done to correlate the formation of particular active oxidation products of oxidized LDL with the induction of specific functional changes.

6.1.4 Lipid peroxidation products in atherosclerotic plaques

The physiological relevance of the biologically active species of lipoprotein oxidation (figure 6.4) is supported by studies revealing the presence of oxysterols and lipid hydroperoxides in atherosclerotic plaques (Carpenter K.L.H., 1993). Extraction of lipids from atheroma reveals the presence of 7-hydroxycholesterol and isometric HODES. A subsequent study by the same group characterised the appearance of oxidized lipids in relation to the stage of lesion progression (Carpenter K.L.H., 1995). 26-hydroxycholesterol and 7β-hydroxycholesterol were significantly elevated in lesions compared to normal artery. The highest 7β-hydroxycholesterol: cholesterol ratio was found in fatty streaks, suggesting that this type of lesion exhibits the greatest level of free radical activity. Some lesions were devoid of 26-hydroxycholesterol and 7β-hydroxycholesterol, which supports the proposition that lesion progression is intermittent. Furthermore, 26-hydroxycholesterol levels were higher in macrophage-rich lesions than their fibrous counterparts and this distinction was evident for most other lipid components. Since macrophage-rich lesions are more prone to rupture, the presence of 26-hydroxycholesterol may be indicative of the risk of an acute cardiovascular event.

Figure 6.1: The oxidation of lipoproteins

Reaction 1; initiation

$LH + X^{\circ} \longrightarrow L^{\circ} + XH$

Reaction 2; oxygen addition

$L^{\circ} + O_2 \longrightarrow LOO^{\circ}$

Reaction 3; propagation

$LOO^{\circ} + LH \longrightarrow LOOH + L^{\circ}$

Reaction 4; scavenging by antioxidants

$LH + X^{\circ} \longrightarrow L^{\circ} + XH$

Reaction 5; termination

$LOO^{\circ} + LOO^{\circ} \longrightarrow$ non-radical product + O_2

Legend; LH, lipid; LOO°, lipid peroxyl radical; LOOH, lipid hydroperoxide; L°, lipid radical; AOH, antioxidant

Figure 6.2: Phases of lipid peroxidation

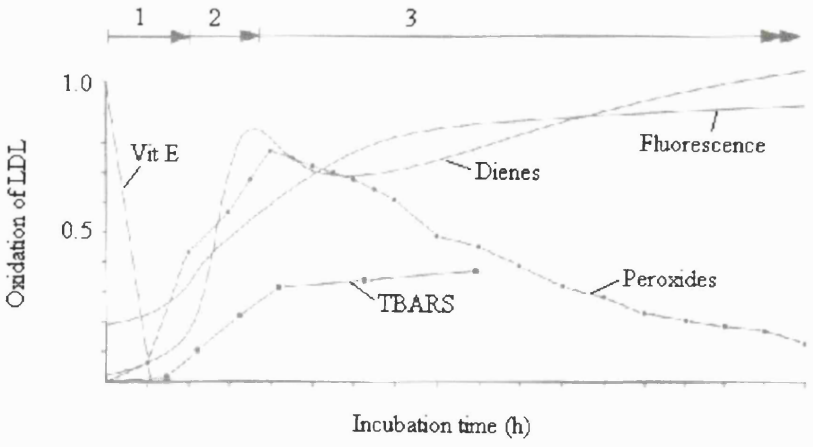

Source: Esterbauer H. in Oxidative stress, lipoproteins and cardiovascular dysfunction, Eds; Rice-Evans C. and Bruckdorfer K.R., Portland Press Ltd, London, 1995.

Figure 6.3: Decomposition of lipid hydroperoxides

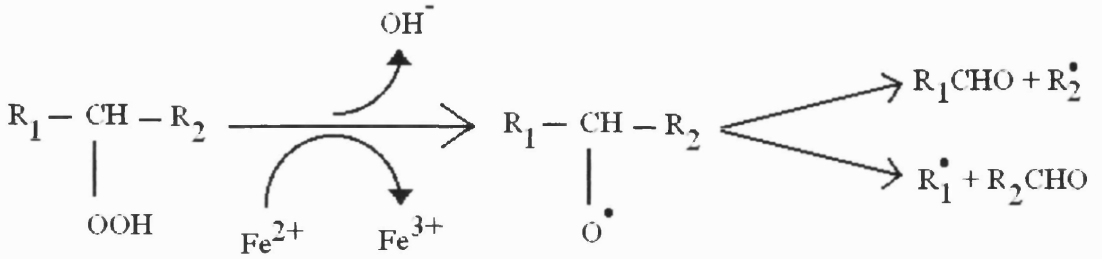

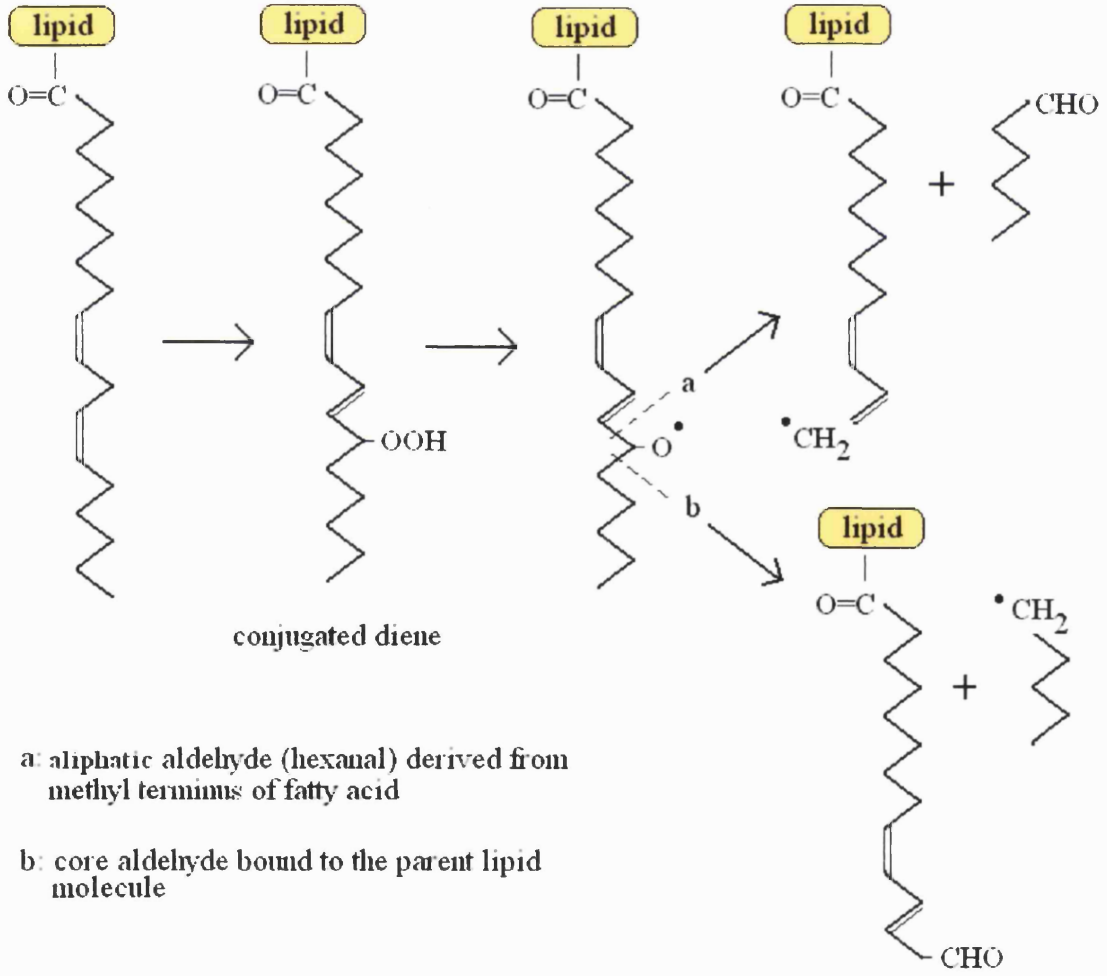

a: aliphatic aldehyde (hexanal) derived from methyl terminus of fatty acid

b: core aldehyde bound to the parent lipid molecule

Figure 6.4: Lipid peroxidation products detected in Cu^{2+}-oxidized LDL

Oxidation product	Source	Lipid oxidation products (nmol/mg protein)		
		4-5h	20-24h	Cita-tion
Total peroxides		1000	227	1
Phospholipid hydroperoxides	Phospholipid	60	-	2
Cholesteryl ester hydroperoxides	Cholesterol	180	-	2
Conjugated dienes	PUFAS	240	-	2
TBARS		85	114	1
Total aldehydes and TBARS		210	540	1
Hydroxyoctadecenoic acid*	Oleic	7	50	3
Hydroxyoctadecadienioc acid†	18:2 (linoleate)	110	30	3
Hydroxyeicosatetraenoic acid‡	20:4 (arachidonate)	17	0	3
7-hydroxy & 7-hydroperoxy cholesterol	Cholesterol	60	120	4, 5
7-ketocholesterol	Cholesterol	ND	ND	4, 5, 6
Cholesteroloxoalkanoylester	Cholesterol	ND	30	7
7-ketocholesterolalkanoylester	Cholesterol	ND	30	7
5,6-epoxycholesterol	Cholesterol	ND	Trace	5, 6
25, hydroxycholesterol	Cholesterol	ND	Trace	6
Cholest-3,5-dien-7-one	Cholesterol	ND	ND	4, 6

PUFA, polyunsaturated fatty acid

* Sum of 8-, 10- and 11-hydroxy-derivatives of oleic acid

† Sum of 9-HODE and 13-HODE

‡ Sum of 5-HETE, 8-HETE, 9-HETE, 11-HETE, 12-HETE and 15-HETE

ND not determined

1. Esterbauer H. (1992) 0.1μM LDL, 1.66μM Cu^{2+}, PBS, 22 °C
2. Noguchi N. (1993) 0.5μM LDL, 2μM Cu^{2+}, PBS, 37 °C
3. Wang T. (1992) 0.4μM LDL, 20μM Cu^{2+}, Ham's F10, 37°C
4. Malavasi B. (1992) 0.4μM LDL, 20μM Cu^{2+}, PBS, 37 °C
5. Zhang H. (1990) 0.4μM LDL, 5μM Cu^{2+}, PBS, 37 °C
6. Bhadra S. (1991) 0.2–0.4μM LDL, ?μM Cu^{2+}, M199
7. Tamasawa N. (1992) 30μM LDL, 5μM Cu^{2+}, 22 °C

6.1.5 The induction of Ca^{2+} transients by native and oxidatively modified LDL

The induction of cytosolic Ca^{2+} transients has been observed in response to treatment of cells with both native and oxidized LDL. In porcine vascular endothelial cells nLDL triggers intracellular Ca^{2+} transients that act as a second messenger to induce the expression of VCAM-1 and E-selectin expression (Allen S., 1998).

Exposure of bovine aortic endothelial cells to mmLDL leads to a delayed, sustained peak of intracellular Ca^{2+} (Negre-Salvaryre A.G., 1992). Enhanced increases intracellular free Ca^{2+} concentration, resulting in pronounced hypertrophy and enhanced cell migration, are observed in vascular smooth muscle cells in response to oxidative modification of LDL (Weisser B., (1992). OxLDL has been reported to stimulate (Chautan M., 1993) or inhibit (Hirata K., 1991) phosphoinositide turnover in endothelial cells and to increase it in smooth muscle cells (Resink T.J., 1992).

The binding of LDL to a number of cell types including platelets (Block L.H., 1988), vascular smooth muscle cells (Scott-Burden T., 1989), fibroblasts (Sachindis A., 1990) and endothelial cells (Smirnov V.N., 1990) is known to trigger cellular events which lead to activation of phospholipase C and the subsequent production of inositol 1,4,5-trisphosphate and diacylglycerol. These factors cause the release of intracellular Ca^{2+} and PKC activation respectively.

6.1.6 Calcium and atherosclerosis.

Several lines of evidence suggest that lipid-mediated intracellular Ca^{2+} increases are involved in atherogenesis. The amount of Ca^{2+} within atherosclerotic lesions correlates with the patient's dyslipoproteinaemia (Barbir M.F., 1997). Endothelial cell injury is causally related to an increase of Ca^{2+} in atheromatous regions (Phair R.D., 1988). In addition, a five-fold increase in intracellular Ca^{2+} in endothelial cells of cholesterol-fed rabbits has been observed compared with normal rabbits (Strickberger S.A., 1988). Furthermore, Ca^{2+} antagonists have an anti-atherogenic effect in cholesterol-fed animals (Henry P.D., 1981). The inhibitory effects of Ca^{2+} antagonists on smooth muscle cell migration may explain their inhibitory effect on the progression of atherosclerotic lesions (Lichtlen P.R., 1990).

6.1.7 Modulation of TF activity by native and oxidized lipoproteins

The procoagulant activity of TF is modulated by LDL and the effect of LDL upon TF activity depends upon its oxidation status. While native LDL (nLDL) exhibits an inhibitory activity towards TF activity, oxidized LDL (oxLDL) mediates enhancement of TF activity (Ettelaie C., 1995). The inhibition of TF activity by nLDL is mediated via direct interaction with the apo B100 moiety (Ettelaie C., 1996). Residues in the apo B100 molecule mediating the inhibitory effect have been located to a short peptide domain in apo B100 (KRAD14)

(Ettelaie C., 1998). This region of apo B100 forms part of the LDL receptor-binding domain (Milne R., 1989, Lawn A., 1990, Chan L., 1992 and Olsson U., 1997). Furthermore, the proposed site in TF (Ettelaie C., 1998), to which the inhibitory KRAD14 peptide binds, is homologous to the ligand-binding region of the LDL receptor (Goldstein J.L., 1985). The nature of the molecular interaction between TF and the KRAD14 peptide and the mechanism by which the peptide inhibits the procoagulant activity of TF are discussed in section 4.6.3.

Oxidation of LDL results in the loss of inhibitory activity towards TF, moreover oxidation renders LDL capable of enhancing the activity of TF. Oxidation of LDL results in the modification of the lipoprotein-associated tissue factor pathway inhibitor (TFPI), (Lesnik P., 1995). TFPI is a physiological inhibitor of TF activity. Copper and cell-mediated oxidation of LDL results in the loss of the inhibitory activity of TFPI towards TF (Lesnik P., 1995). In addition, hydrogen peroxide enhances the latent activity of TF on the surface of vascular smooth muscle cells (Penn M.S., 1999). It is thought that hydrogen peroxide may enhance TF activity by causing dissociation of TF from TFPI. The dissociation of TF from TFPI may result in increased cell surface expression of TF, since TFPI regulates the cell surface activity of TF by mediating internalization of cell surface TF into caveolae (Sevinsky J.R., 1996, Le D.T., 1992 and Iakhiaev A., 1999). Endogenous TFPI expression has been observed on human macrophages and smooth muscle cells (Petit L., 1999 and Kamikubo Y., 1997).

Native and oxidatively modified LDL are also capable of enhancing TF expression in various cell types The expression of TF in human endothelial cells is induced by mmLDL and oxLDL (Drake T.A., 1991). In addition, oxLDL enhances the induction of TF by LPS in human adherent monocytes (Brand K., 1994). Both nLDL and oxLDL induce TF mRNA in smooth muscle cells, however, nLDL does not markedly increase TF activity (Penn M.S., 2000). Increases in TF activity induced by oxLDL are mediated via an oxidant dependent mechanism, which may involve the inactivation of TFPI (Lesnik P., 1995).

6.2 Aims

- To determine the effect of concentration of native and oxidatively modified LDL upon the induction of cytosolic Ca^{2+} transients
- To determine the effect of oxidation of LDL upon the induction of cytosolic Ca^{2+} transients
- To investigate the involvement of TF activity in the induction of cytosolic Ca^{2+} transients by oxLDL
- To investigate the effect of nLDL upon the induction of cytosolic Ca^{2+} transients by FVIIa

6.3 Methods

6.3.1 Preparation of low density lipoprotein

6.3.1a An overview of methods of preparation of low density lipoprotein

Various methods have been developed for the isolation of LDL from plasma. Density gradient centrifugation using sodium or potassium bromide generated gradient is a popular methodology, however it has drawbacks. Preparation of the LDL requires two ultracentrifugation steps requiring 18 hours. The quality of LDL prepared using salt gradients may be compromised due to the modification of proteins by the high salt concentrations required to form the density gradients. Relatively recently a commercial reagent, OptiPrep™ (Nycomed) has become available, that has several advantages. LDL can be prepared in a single five-hour centrifugation step, (smaller samples within 2 hours). This minimises the loss of lipid/lipoprotein from LDL caused by physical shear forces resulting from ultracentrifugation. In addition, the opportunity for LDL oxidation during preparation is minimised. Furthermore, Optiprep™ acts as an antioxidant during the isolation and can be removed from the sample by dialysis.

6.3.1b Preparation of human blood serum

Blood was collected from human volunteers by venepuncture into a syringe. Serum was recovered from the supernatant subsequent to centrifugation of the blood sample at 1500g for 10 minutes at room temperature.

6.3.1c Preparation of LDL using density gradient ultracentrifugation

Serum was mixed with 60% Iodixanol (OptiPrep™) solution at a 4:1 ratio. 0.67ml of basic density solution (d=1.006g/ml) was dispensed into 13 x 32mm (3.5ml) Quick Seal ultracentrifuge tubes (Beckman) using a syringe fitted with a hypodermic needle. 2.4ml aliquots of the OptiPrep™ /serum mixture was then layered beneath the basic density solution in the ultracentrifuge tubes (3.6:1 ratio) using a hypodermic needle. The ultracentrifuge tubes were balanced to an accuracy of 0.01g. The tubes were heat-sealed and the samples loaded into a fixed angle rotor TL-100 (Beckman). The rotor was situated in a Beckman ultracentrifuge and the samples were centrifuged at 100 000rpm for 2.5h at 10°C.

After centrifugation the tubes were removed from the centrifuge and the caps were cut. The LDL band resolved as a bright orange band. The VLDL at the top of the tube was removed and discarded. A syringe fitted with a hypodermic needle was then inserted into the tube to collect the LDL fraction.

6.3.1d Dialysis of LDL

LDL collected from density gradient ultracentrifugation of human serum was dispensed into dialysis tubing, which was sealed at one end. The dialysis tubing was sealed at the other end and the tubing placed in 5L of Hank's buffer. The sample was protected from light and was agitated using a magnetic stirrer bar overnight.

The following day the dialyzed LDL was removed from the dialysis tubing and the protein concentration was determined using the Bradford reagent (section 2.4.8). The LDL sample was diluted to 1mg of LDL apo B/ml with Hank's buffer.

The purity and integrity of LDL was established on the basis of criteria described by Chapman et al (1988). Electrophoresis was used to exclude contamination by VLDL, HDL or serum albumins or globulins (6.3.2b). The lipid peroxide content of the isolated LDL was determined (see section 6.3.2) to ensure that the samples contained native, non-oxidized LDL (El-Saadani M., 1989).

6.3.1e Oxidation of LDL

The oxidation of LDL samples (1mg of LDL apo B/ml) prepared as described in section 6.3.1d was induced by the addition of $CuS0_4$ to a final concentration of 2μM. Oxidation of the samples was monitored as described in section 6.3.2.

6.3.2 Measurement of lipid peroxidation

6.3.2a Measurement of LDL oxidation using fluorescence

A fluorescence methodology was selected to determine the progression of LDL oxidation. Oxidized LDL emits strong fluorescence emission around 430-450nm when excited at 360nm. This methodology was selected for several reasons. The fluorescence is almost entirely associated with the modification of the apo B100 moiety of the LDL. As the LDL is progressively modified aldehydes attack ε-amino groups of lysine. The fluorescence technique was chosen since the ability of nLDL to inhibit TF depends upon the extent of modification of lysine residues in apo B100. In addition, extensive modification of the lysine residues renders LDL amenable to interaction with the scavenger receptor and the ability to interact with the classic LDL receptor is lost (Berliner J.A., 1990). Since the change in fluorescence is linked to the modification of lysine residues this method is appropriate for the study as it links the chemical and biological changes of LDL. In addition, the graph in figure 6.2 shows the progression of the oxidation of LDL measured in a variety of ways including the determination of thiobarbituric acid reactive substances, conjugated dienes and peroxides. These data show that the fluorescence of LDL increases almost uniformly as LDL oxidation progresses, unlike the alternate methodologies. Measurement of LDL oxidation using fluorescence is also rapid, in addition the LDL sample can be retrieved for use in experiments.

0.2ml samples of LDL at 1mg of LDL apo B100 /ml were dispensed into the wells of a microtitre plate. The plate was then loaded into a fluorimeter and the fluorescent emissions of the samples were read at 440nm. The progression of oxidation was monitored using a plot of the fluorescent emission of the sample against time.

6.3.2b Electrophoretic determination of the degree of LDL oxidation

During oxidation the negative surface charge of LDL increases. The increase in the negative charge arises from the binding of aldehydic lipid peroxidation products to the ε-amino groups of lysine residues. This binding neutralises positive charges and results in a net increase in negative charge. In addition, reactive oxygen species attack histidine and proline converting these residues to negatively charged aspartic acid and glutamic acid respectively. The relative increase in charge can readily be determined by electrophoretic separation of LDL on agarose gels.

Electrophoretic separation of plasma lipoproteins was detected using the Sebia Hydragel lipo and lp(a) system. Lipoprotein samples were loaded at the origin of the gel. The gel was placed in the running buffer in accordance with manufacturer's instructions. The gel was run at 50V for 90 minutes. Subsequent to electrophoresis, the gel was dried and submersed

in a solution consisting of 9 volumes of Fat Red 7B (0.023% w/v in methanol) and 1 volume of water. To reveal the locations of the lipoprotein fractions, the gel was destained using a 2:1 mixture of methanol in water.

6.3.2c Measurement of lipid peroxides

Lipid peroxides were determined as described previously (El-Saadani M., 1989). The assay is performed using a commercially available reagent, CHODE-Iodide (Sigma), consisting of 0.2M potassium phosphate (pH 6.2), 0.12M potassium iodide, 0.15mM sodium azide, 2g/l polyethyleneglycol mono [p-(1,1',3,3'-tetramethyl-butyl)-phenyl] ether, 0.1g/l alkylbenzyldimethylammonium chloride and 10mM ammonium molybdate. The assay is based on the oxidative ability of lipid peroxides to convert iodide to iodine, the absorption of which can be determined at 365nm. The concentration of iodine produced is directly proportional to the amount of organic peroxide present. The concentration of lipid peroxide may be accurately determined using the molar extinction co-efficient ($2.46 \pm 0.25 \times 10^4$).

A standard curve was obtained by preparing 100µl aliquots of H_2O_2 ranging from 0 to 100µM. 1ml aliquots of CHODE-Iodide reagent were added to the H_2O_2 solutions. The solutions were incubated for 30 minutes in the dark at ambient temperature prior to determination of the absorption at 365nm in a cuvette with 1cm path length. The results were plotted, (minus the reagent blank) and a line of best fit was applied to the plotted data. The correlation equation was;

$$\text{Log}_{10}\,[H_2O_2]\ (\mu M) = 0.94 \times \log_{10}(A_{365}) - 0.47$$

6.3.2d Measurement of thiobarbituric acid reactive substances

Incubation of peroxidised lipids with thiobarbituric acid under acidic conditions produces a red pigment with absorption maximum at 532nm. This pigment is a product of TBA-MDA interacting at a 1:2 ratio. The change in concentration of MDA is proportional to the amount of lipid undergoing peroxidation.

A range of solutions from 0-20µM was prepared by adding 1M HCl to 100µM malondialdehyde *bis*-dimethylacetate (Sigma). The solutions were incubated at 50°C for 1 hour and the absorption at 535nm was determined against a distilled water blank. The results were plotted and the correlation equation was found to be;

$$[\text{MDA}]\ (\mu M) + 4.76 \times (A_{535})$$

Thiobarbituric acid solution (TBA, 0.67% w/v) was prepared by dissolving 0.67g of 2-thiobarbituric acid (Sigma) in 1M sodium hydroxide, which was then made up to 100ml with distilled water. The concentration of MDA in 1ml of test sample was measured by the

addition of 1ml of 20% w/v trichloroacetic acid and 2ml TBA. The mixture was incubated at 100C for 10 minutes. The sample was centrifuged at 400g for 5minutes and the absorption measured at 535nm against a distilled water blank.

6.4 Results

6.4.1 Determination of the degree of LDL modification

In order to establish whether LDL was native (nLDL), minimally-modified (mmLDL) or extensively oxidised (oxLDL), the following criteria were used. Native LDL was designated as LDL samples containing <29nmol lipid peroxide/mg LDL as determined using the CHODE-Iodide reagent (see 6.3.2c). mmLDL was designated as LDL containing 2-5nmol TBARS (see 6.3.2d) per mg cholesterol with no change in electrophoretic mobility (see 6.3.2b). The cut-off point indicating the onset of formation of extensively oxidised LDL was defined as LDL with electrophoretic mobility and apo B100 fluorescence increased 10% or more above native non-oxidised LDL.

6.4.2a Measurement of endogenous fluorescence emission from native and oxidized LDL

The presence of fluorescence emission at 540nm resulting from excitation of native and oxidatively modified LDL at 340nm and 380nm was determined to ascertain whether the LDL species themselves lead to alteration of the 340:380nm ratio. These background fluorescence values were derived from regions in the cell-free areas of the coverslip and were calculated for 4 independent samples of native, minimally modified and fully oxidized LDL. The 340:380nm ratios obtained before and after the addition of the various LDL samples were determined (figure 6.5).

The background 340:380nm ratio was unaltered for concentrations of nLDL as high as 0.5mg of LDL apo B/ml (figure 6.5a) demonstrating that excitation of nLDL at 340nm and 380nm does not produce fluorescence emission at 540nm. Slight decreases in the background ratio were evident with concentrations of mmLDL at 0.5mg of LDL apo B/ml, however at concentrations of 0.05mg of LDL apo B/ml and below, mmLDL had no significant effect on the 340:380nm ratio (figure 6.5b). In contrast, oxLDL produced a pronounced decrease in the 340:380nm ratio at 0.5mg of LDL apo B/ml (figure 6.5c). Addition of 0.05mg of LDL apo B/ml of oxLDL also resulted in decreases in the 340:380nm ratio although the reduction was much less pronounced. Concentrations of 0.005mg of LDL apo B/ml oxLDL did not significantly alter the background fluorescence.

The origin of the decrease in background fluorescence by mmLDL and oxLDL was determined. The emissions from the 340nm and 380nm excitation wavelengths were plotted

separately and it was found that the increased 340:380nm ratios resulted from a decrease in the emission derived from the 340nm excitation wavelength rather than from an increase in the 380nm ratio. These results demonstrate that the oxidation of LDL results in the dampening of fluorescence intensity emitted at 540nm when the excitation wavelength is 340nm.

Figure 6.5: Background fluorescence emitted by nLDL, mmLDL and oxLDL

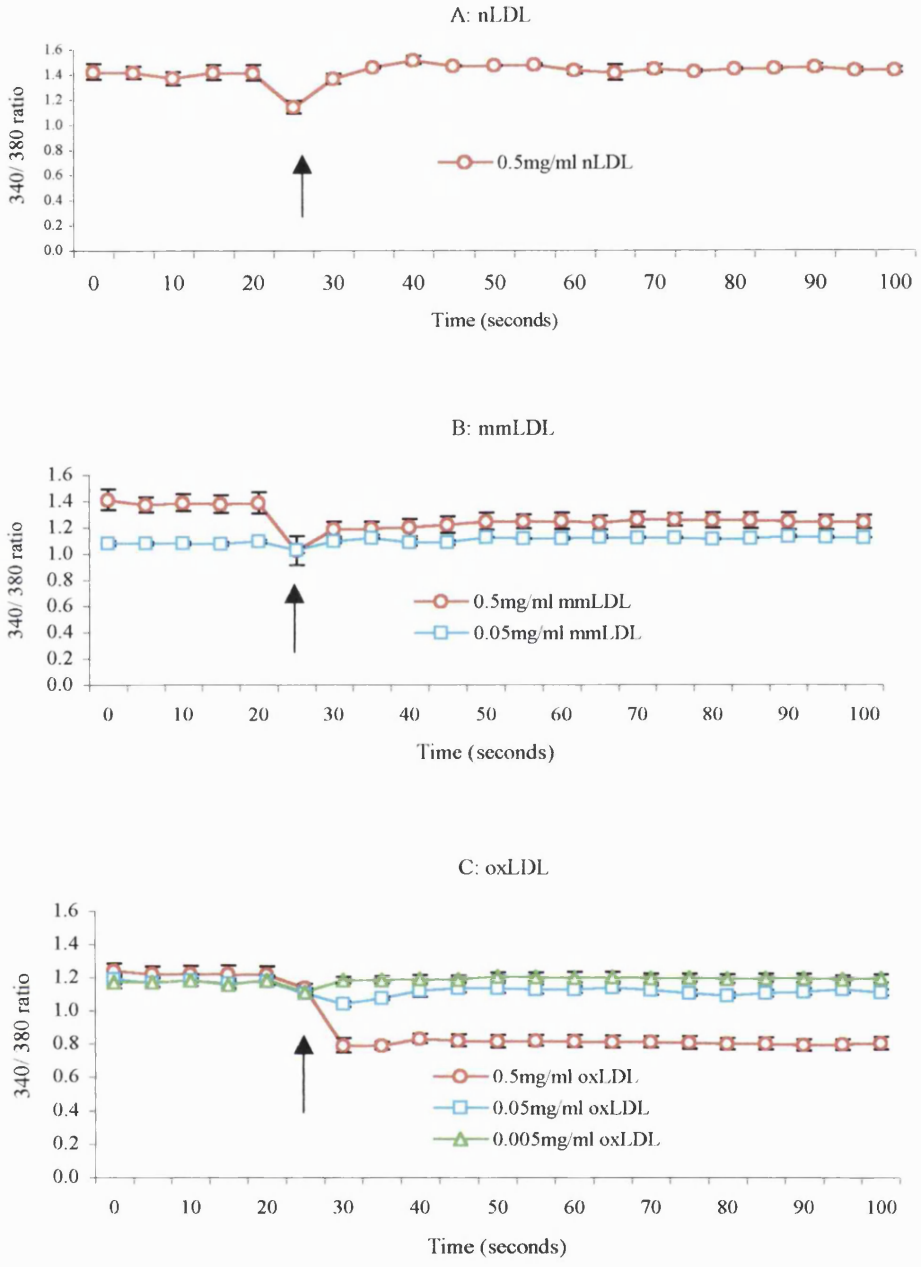

⟶ Indicates time of addition of LDL to the sample chamber. Fluorescence measurements at this time point are ignored since the pipeting procedure usually introduces an artefactual error.

A: nLDL, concentrations as high as 0.5mg nLDL/ml have no effect upon the fluorescence.

B: mmLDL, 0.5mg mmLDL/ ml exhibits endogenous fluorescence, 0.05mg mmLDL/ml does not

C: oxLDL; 0.5mg oxLDL/ml exhibits endogenous fluorescence

Samples of nLDL, mmLDL and oxLDL were placed in the chamber of a microscope integrated to a fluorescence video imaging system. To determine the emission of endogenous fluorescence by the LDL, the samples were illuminated with light at 340nm and 380nm and the fluorescent emission at 540nm was collected. Fluorescence of the samples was examined for an extended period of time to determine whether the exposure of the LDL to the *u-v* light resulted in time dependent changes in fluorescent emission.

6.4.2b Experimental analysis of samples with high background fluorescence

Since changes in background fluorescence were produced by 0.5mg of LDL apo B/ml mmLDL and 0.5mg of LDL apo B/ml and 0.05mg of LDL apo B/ml oxLDL, adjustment to the method of analysis of the data was necessary at these concentrations of oxidized LDL. The background fluorescence emitted by these concentrations of mmLDL and oxLDL introduces an error into the data since the time point prior to the addition of LDL does not reflect the true basal value. An accurate basal value was obtained by subtracting the value for the change in 340:380nm ratio due to the intrinsic fluorescence of oxidised LDL from the basal values.

6.4.3 Effect of concentration of native and oxidatively modified LDL upon the induction of Ca^{2+} transients

The concentration dependence of the induction of cytosolic Ca^{2+} transients by native and oxidized lipoproteins was determined using several parameters that define the kinetics/characteristics of cytosolic Ca^{2+} responses (section 2.3.7b);

- The percentage of the cell population eliciting a response
- The magnitude of the response in terms of the response integral
- The peak amplitude
- The decay time

The inductions of cytosolic Ca^{2+} transients by native, minimally modified and oxidized LDL are shown in figures 6.6a and 6.6b. The graphs in figure 6.6a show the mean responses to varying concentrations of native, minimally modified and oxidized LDL using data from all cells within the field of view, irrespective of whether or not a response was elicited by the LDL sample in question. The graphs in figure 6.6b show the mean responses of only the cells in the field of view that responded to the LDL treatment i.e. non-responding cells were excluded from the analysis.

Figure 6.6a: Effect of concentration and oxidative modification of LDL upon the induction of cytosolic Ca^{2+} transients in T24 cells (all cells, responding and non-responding)

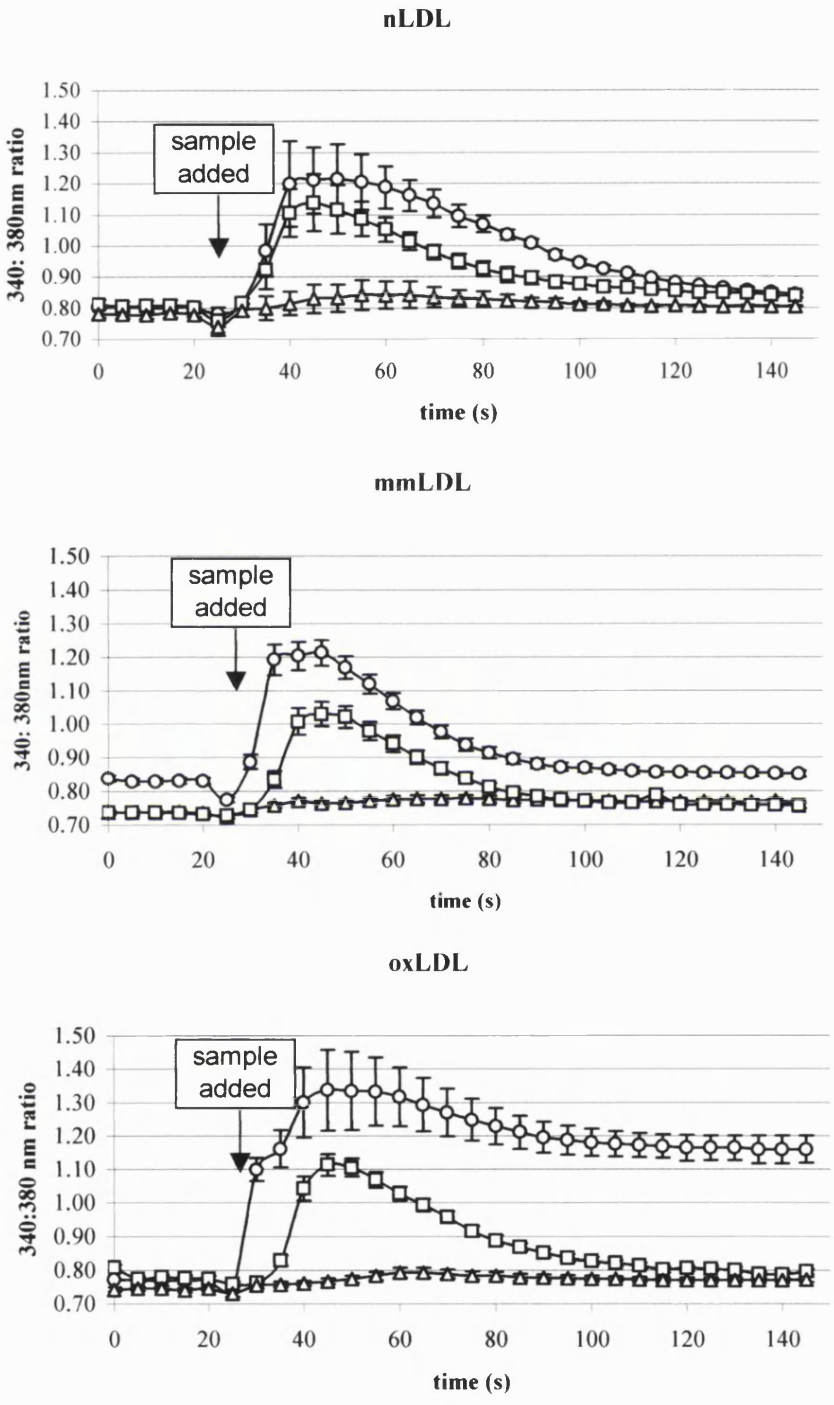

T24 cells were grown on glass coverslips as described in section 2.1.8. The effect of varying the concentration and degree of oxidative modification of LDL upon the induction of Ca^{2+} transients was measured in single cells as described in section 2.3. LDL was added at 25 seconds. Results are expressed as the mean ± SEM of all cells within the field of view (responding and non-responding cells, n > 100). Circles, 0.5mg/ml; squares, 0.05mg/ml and triangles, 0.005mg/ml

Figure 6.6b: Effect of concentration and oxidative modification of LDL upon the induction of cytosolic Ca^{2+} transients in T24 cells (excluding non-responsive cells)

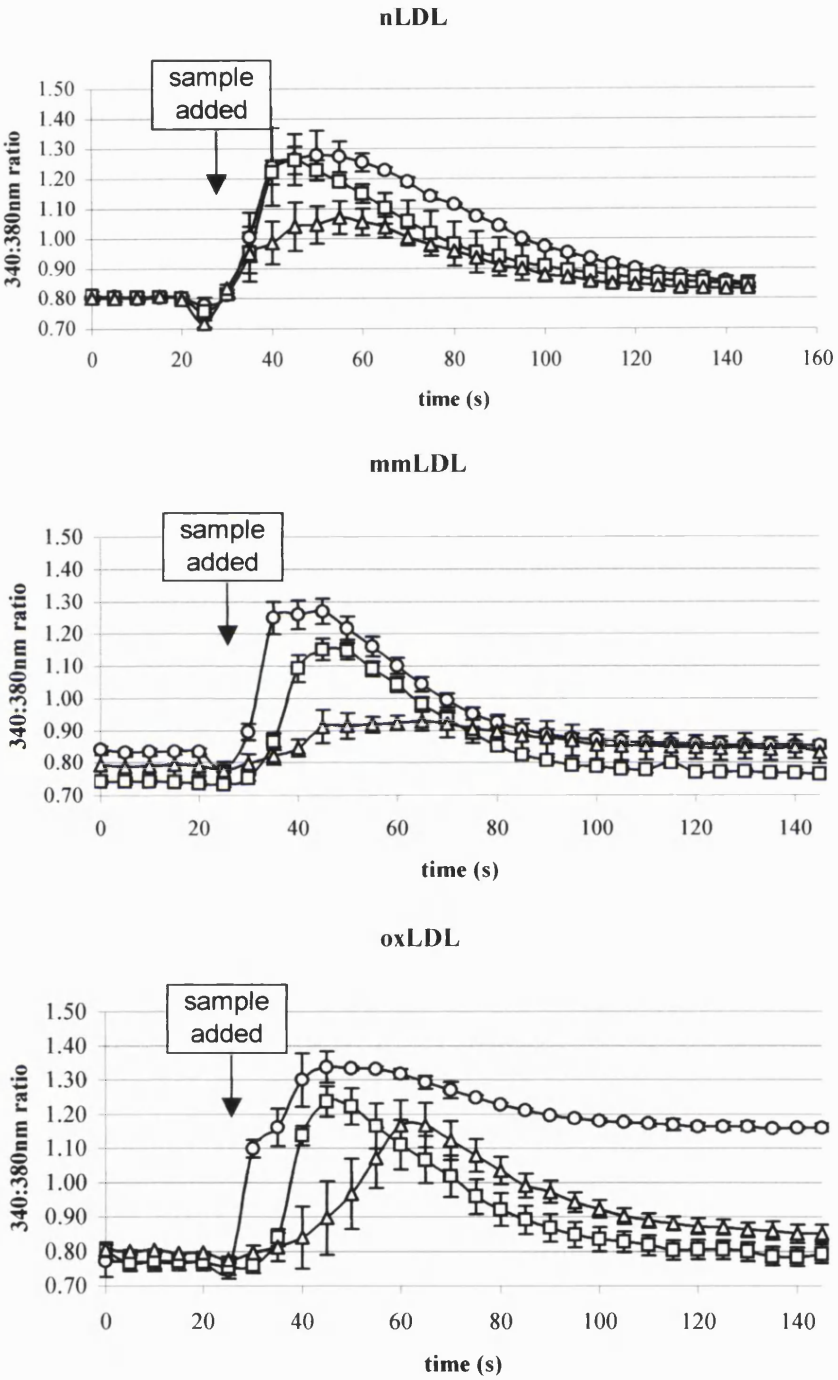

T24 cells were grown on glass coverslips as described in section 2.1.8. The effect of varying the concentration and degree of oxidative modification of LDL upon the induction of Ca^{2+} transients was measured in single cells as described in section 2.3. LDL was added at 25 seconds. Results are expressed as the mean ± SEM of cells within the field of view that elicited a response and exclude non-responding cells, n > 100). Circles, 0.5mg/ml; squares, 0.05mg/ml and triangles, 0.005mg/ml.

6.4.3a Effect of LDL concentration on the percentage of the cell population eliciting a cytosolic Ca^{2+} response

The percentage of the population of T24 cells that elicit a cytosolic Ca^{2+} response subsequent to treatment with LDL is positively correlated with the concentration of native, minimally modified or fully oxidized LDL (figure 6.7). The graphs show that the sensitivity of T24 cells to nLDL, mmLDL and oxLDL is maximal between concentrations of 0.005 and 0.05 mg of LDL apo B/ml. nLDL, mmLDL and oxLDL at 0.005mg of LDL apo B/ml elicit responses in 18.1 ± 5.5, 6.6 ± 5.2 and 6.5 ± 4.6% of the cell population respectively. A ten-fold increase of nLDL, mmLDL or oxLDL to 0.05mg of LDL apo B/ml leads to the induction of cytosolic Ca^{2+} responses in a far greater proportion of the cell population, 67.5± 10.7, 69.1 ± 9.6 and 91.5 ± 6.1 respectively. At 0.5mg of LDL apo B/ml of LDL, a further increase in the percentage of T24 cells eliciting a cytosolic Ca^{2+} response is evident; 80.0 ± 9.9, 92.0 ± 11.3 and 100.0 ± 0.0 %, respectively.

The effect of oxidation status upon the percentage of cells eliciting a response for various concentrations of LDL (0.005, 0.05 and 0.5 mg of LDL apo B/ml), was determined to ascertain whether the percentage of cells responding was significantly different for native and minimally modified LDL in comparison to oxLDL. Statistical analysis showed that at 0.005mg of LDL apo B/ml the percentage of cells responding to native or minimally modified LDL was not significantly different from the proportion of cells responding to oxLDL (Student's t-test, $p = 0.99$ and 0.07 respectively). For concentrations of LDL of 0.05mg of LDL apo B/ml, no significant difference was observed between oxidized LDL and minimally modified LDL ($p = 0.10$). However, the proportion of cells responding to native LDL was significantly less than the proportion responding to oxidized LDL at 0.05mg of LDL apo B/ml ($p = 0.04$). No significant effects of oxidation upon the percentage of cells responding to 0.5mg of LDL apo B/ml were evident when the responses to oxLDL were compared with native or minimally modified LDL ($p = 0.15$ and 0.13 respectively).

The data was analyzed within each oxidation class to determine the effect of concentration upon the percentage of cells exhibiting cytosolic Ca^{2+} increases. Statistical analysis demonstrated that the proportion of cells eliciting a response was significantly lower at 0.005mg/ml compared to 0.5mg of LDL apo B/ml for native, minimally modified and oxidized LDL ($p = 0.002$, 0.001 and 0.002 respectively). In addition, significant differences in the proportion of responding cells was evident at 0.05mg of LDL apo B/ml lipoprotein compared to 0.5mg of LDL apo B/ml for minimally modified LDL ($p = 0.04$). However, in the case of native and fully oxidized LDL, no significant differences in the proportion of responding cells was observed between 0.05mg of LDL apo B/ml and 0.5mg of LDL apo B/ml ($p = 0.61$ and 0.22 respectively). These results demonstrate that the proportion of the

cell population eliciting a cytosolic Ca^{2+} response increases as the LDL concentration increases between 0.005 and 0.05mg LDL apo B/ml for all classes of LDL; native, minimally modified and fully oxidized LDL.

6.4.3b Effect of LDL concentration upon the magnitude of cytosolic Ca^{2+} transients

The response integral was used as an index of the magnitude of the response (section 2.3.7b). Analysis of the response integral was determined using only the responsive cells (see section 2.3.7d for definition).

The data was statistically analyzed using a linear regression methodology. Linear regression analysis was performed on logarithmically transformed data, (a nominal value of 1 was added), since the non-transformed response integral values in each LDL class formed positively-skewed normal distributions. Regression analysis demonstrated that the integral of the cytosolic Ca^{2+} response was positively correlated with the lipoprotein concentration for nLDL, mmLDL and oxLDL (figures 6.8 and 6.9a, $p<0.0001$ in all cases).

6.4.3c Effect of LDL concentration upon the peak amplitude of cytosolic Ca^{2+} transients

The linear regression analyses for the effect of concentration of native and oxidatively modified LDL upon the peak amplitude of the Ca^{2+} responses are shown in figure 6.9b. A positive correlation between concentration and peak amplitude was seen for nLDL, mmLDL and oxLDL ($p = 0.05$, 0.03 and <0.0001 respectively).

The data is consistent with the interpretation that the peak amplitudes of the cytosolic Ca^{2+} increases are dependent upon the concentration of native, minimally modified and fully oxidized LDL at physiological plasma concentrations.

6.4.3d Effect of LDL concentration upon the decay time of cytosolic Ca^{2+} transients

The effect of concentration upon the decay time of cytosolic Ca^{2+} peaks for native, minimally and fully oxidized LDL was subject to linear regression analysis (figure 6.9c). The data were logarithmically transformed prior to analysis. The statistical analysis showed that the decay time was positively correlated with the concentration of the lipoprotein for both native and oxidatively modified LDL. The data were significant for native, minimally modified and fully oxidized LDL ($p<0.0001$, 0.03 and <0.0001 respectively).

Figure 6.7: The effect of concentration upon the percentage of cells eliciting Ca^{2+} transients in response to nLDL, mmLDL and oxLDL

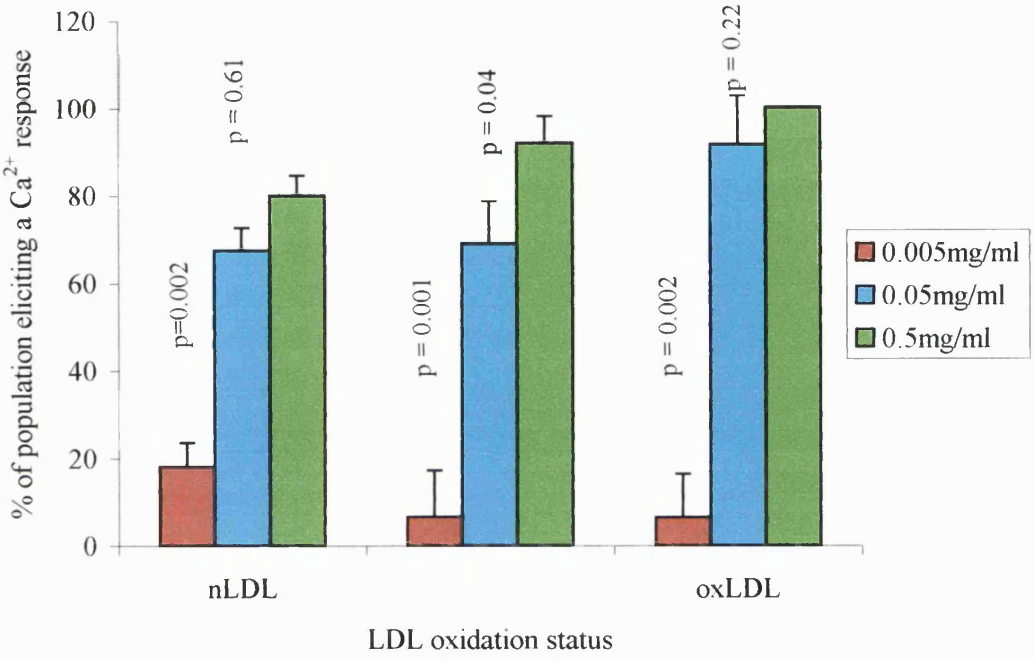

T24 cells were grown on glass coverslips as described in section 2.1.8. For experiments cells were loaded with the Ca^{2+}-sensitive fluorophore Fura2 (section 2.3.2). The effect of concentration of nLDL, mmLDL and oxLDL upon the induction of cytosolic Ca^{2+} transients in individual cells was determined using a fluorescence video imaging system. Cells were treated with 0.005, 0.05 and 0.5 mg LDL apo B/ml concentrations of nLDL, mmLDL and oxLDL. Results are shown as the mean ± S.E.M. of 3 independent experiments. For statistical analyses the percentage of cells responding to 0.005mg/ml and 0.05mg/ml of lipoprotein were analyzed versus the responses to 0.5mg/ml using the Student's t-test.

Figure 6.8: Tabulation of regression analyses for the effect of LDL concentration upon cytosolic Ca^{2+} transients

Response parameter	nLDL		mmLDL		oxLDL	
	r^2	p	r^2	p	r^2	p
ln (integral +1) [2]	0.15	**<.0001**	0.24	**<.0001**	0.93	**<.0001**
ln (peak amplitude+1) [2]	0.04	**0.05**	0.06	**0.03**	0.20	**<.0001**
ln (decay time +1) [2]	0.26	**<.0001**	0.06	**0.03**	0.40	**<.0001**

[1]Entire cell population used for linear regression analysis

[2]Only responding cells used for linear regression analysis

Figure 6.9a **Regression analysis of the effect of concentration of nLDL, mmLDL and oxLDL upon the magnitude of Ca^{2+} responses**

Integral of the Ca^{2+} response versus concentration of nLDL, responding cells only

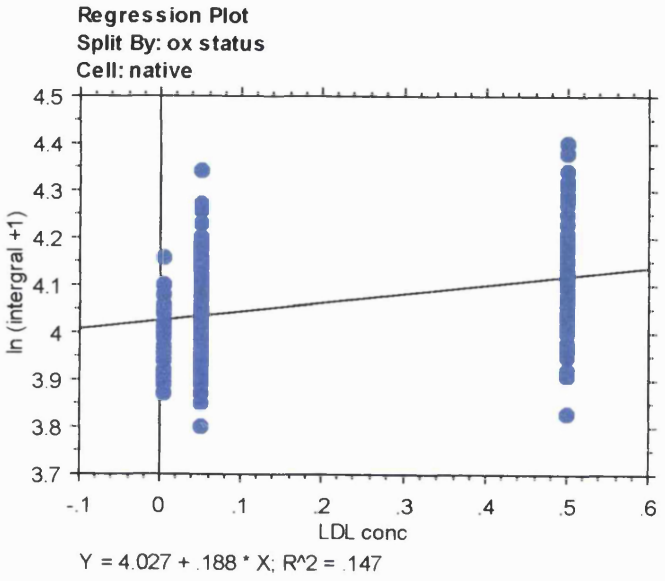

Integral of the Ca^{2+} response versus concentration of mmLDL, responding cells only

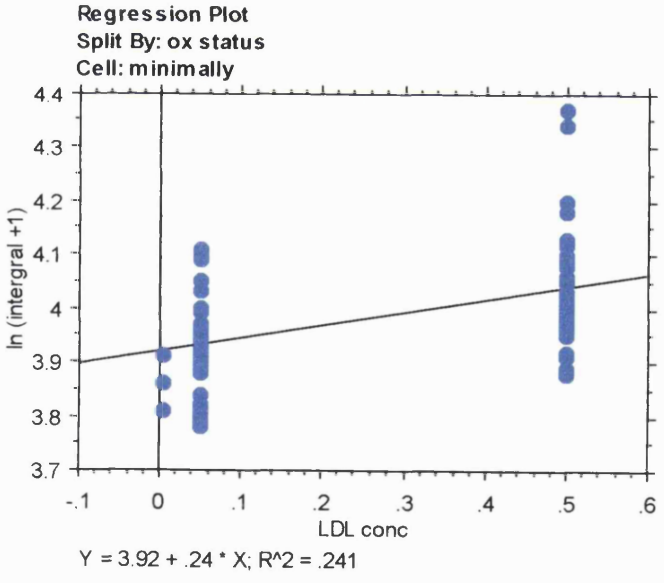

(continued)

Integral of the Ca^{2+} response versus concentration of oxLDL, responding cells only

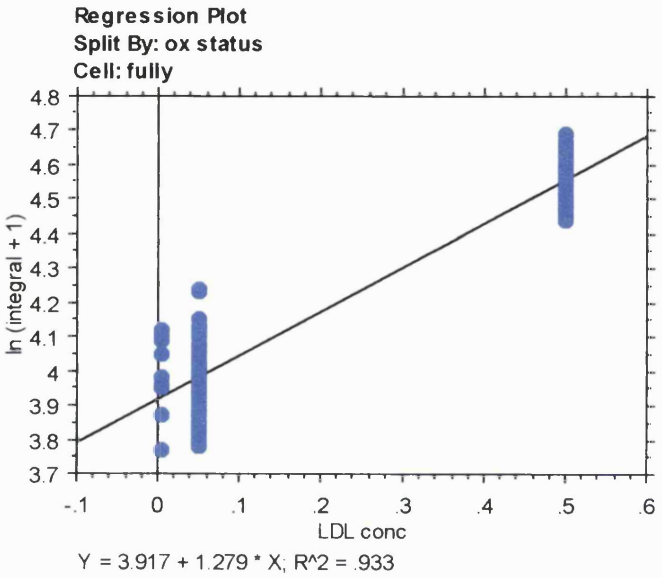

T24 cells were grown on glass coverslips as described in section 2.1.8. For experiments cells were loaded with the Ca^{2+}-sensitive fluorophore Fura2 (section 2.3.2). The effect of concentration of nLDL, mmLDL and oxLDL upon the induction of cytosolic Ca^{2+} transients in individual cells was determined using a fluorescence video imaging system. Cells were treated with 0.005, 0.05 and 0.5 mg/ml concentrations of nLDL, mmLDL and oxLDL.

The effect of increasing concentrations of nLDL, mmLDL and oxLDL upon the magnitude of the cytosolic Ca^{2+} transients was analyzed in terms of the integral of the response i.e. the area under the response curve. The response integral is a measure of the increase in cytosolic Ca^{2+} above the basal level. Linear regression analysis was used to determine the effect of lipoprotein concentration upon the integral of the response. Cells that failed to respond to the stimulus were excluded from the linear regression analysis. i.e. only data from the responding cells was analyzed..

Figure 6.9b Regression analysis of the effect of concentration of nLDL, mmLDL and oxLDL upon the peak amplitude of Ca^{2+} responses

Peak amplitude of cytosolic Ca^{2+} response versus concentration of nLDL, responding cells only

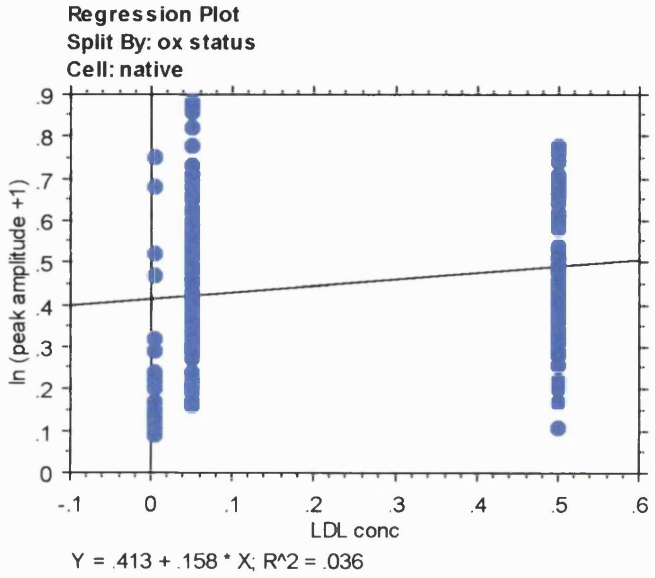

Peak amplitude of cytosolic Ca^{2+} response versus concentration of mmLDL, responding cells only

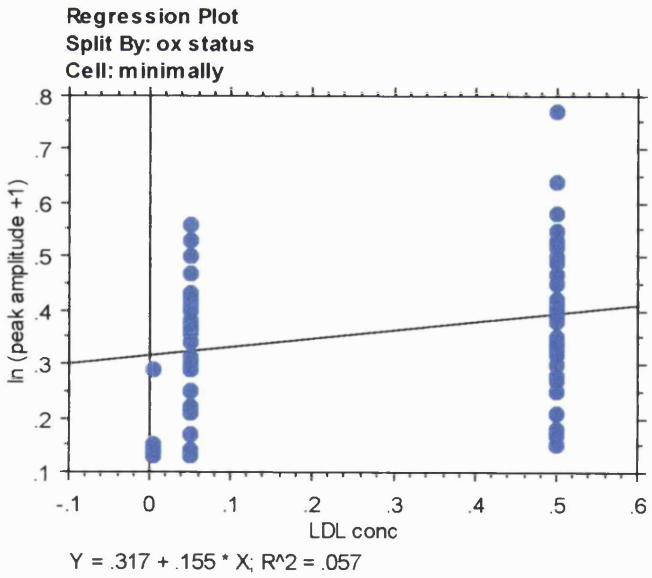

(continued)

Peak amplitude of cytosolic Ca^{2+} response versus concentration of oxLDL, responding cells only

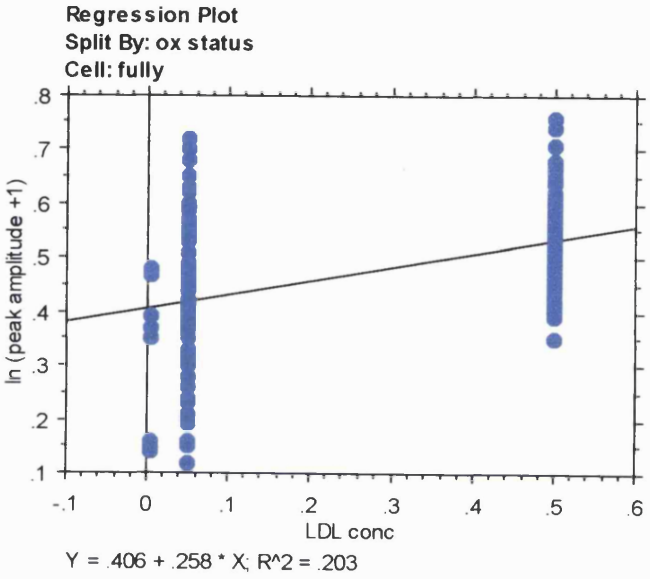

T24 cells were grown on glass coverslips as described in section 2.1.8. For experiments cells were loaded with the Ca^{2+}-sensitive fluorophore Fura2 (section 2.3.2). The effect of concentration of nLDL, mmLDL and oxLDL upon the induction of cytosolic Ca^{2+} transients in individual cells was determined using a fluorescence video imaging system. Cells were treated with 0.005, 0.05 and 0.5 mg/ml concentrations of nLDL, mmLDL and oxLDL.

The effect of increasing concentrations of nLDL, mmLDL and oxLDL upon the magnitude of the cytosolic Ca^{2+} transients was analyzed in terms of the peak amplitude the response i.e. the maximal level of cytosolic Ca^{2+} observed for each cell. Linear regression analysis was used to determine the effect of lipoprotein concentration upon the peak amplitude. Cells that failed to respond to the stimulus were excluded from the linear regression analysis. i.e. only data from the responding cells was analyzed..

Figure 6.9c **Regression analysis of the effect of concentration of nLDL, mmLDL and oxLDL upon the decay time of Ca^{2+} responses**

Decay time of cytosolic Ca^{2+} response versus concentration of nLDL, responding cells only

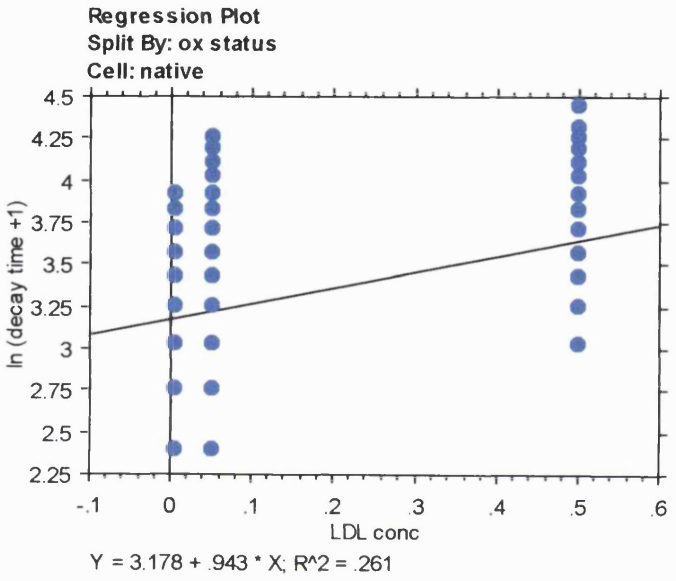

Decay time of cytosolic Ca^{2+} response versus concentration of mmLDL, responding cells only

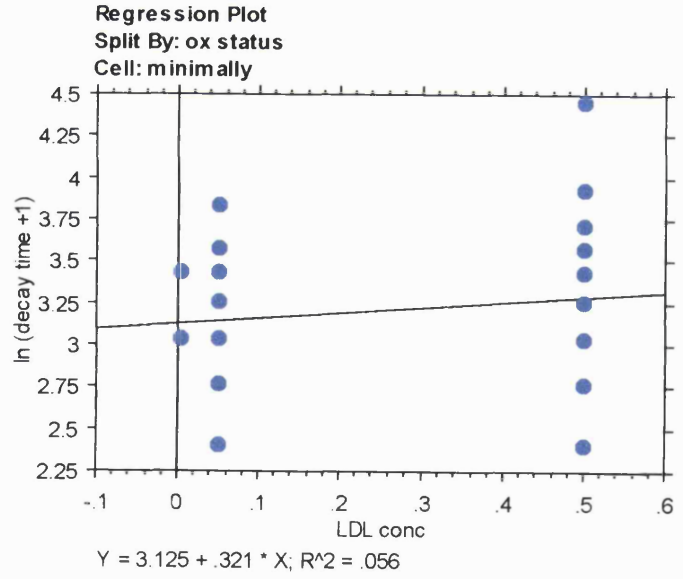

(continued)

Decay time of cytosolic Ca^{2+} response versus concentration of oxLDL, responding cells only

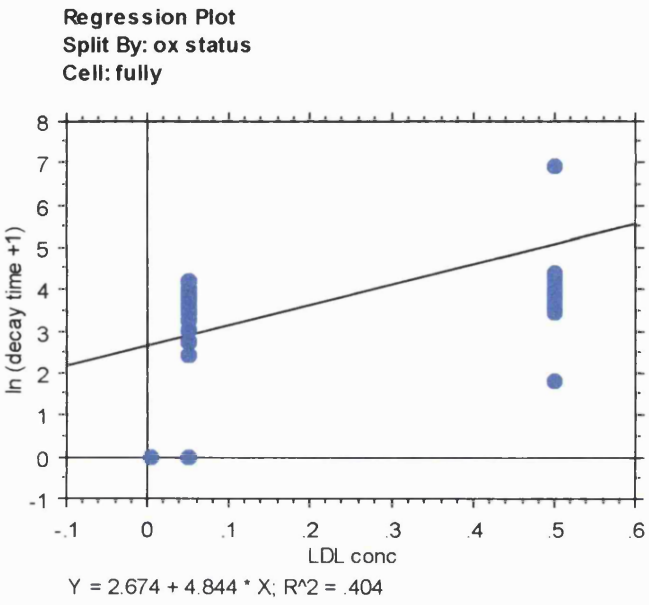

T24 cells were grown on glass coverslips as described in section 2.1.8. For experiments cells were loaded with the Ca^{2+}-sensitive fluorophore Fura2 (section 2.3.2). The effect of concentration of nLDL, mmLDL and oxLDL upon the induction of cytosolic Ca^{2+} transients in individual cells was determined using a fluorescence video imaging system. Cells were treated with 0.005, 0.05 and 0.5 mg/ml concentrations of nLDL, mmLDL and oxLDL.

The effect of increasing concentrations of nLDL, mmLDL and oxLDL upon the magnitude of the cytosolic Ca^{2+} transients was analyzed in terms of the decay time of the response i.e. the time taken for the peak response value to decay to half. Linear regression analysis was used to determine the effect of lipoprotein concentration upon the decay time. Cells that failed to respond to the stimulus were excluded from the linear regression analysis. i.e. only data from the responding cells was analyzed..

6.4.4 The effect of oxidation status upon the induction of Ca^{2+} transients

The cytosolic Ca^{2+} responses of T24 cells to 0.05mg of LDL apo B/ml of native, minimally modified or fully oxidized LDL were examined to determine the effect of oxidation upon the induction of Ca^{2+} transients. A concentration of 0.05mg of LDL apo B/ml was chosen since this concentration of LDL elicits responses in the majority of the cells (figure 6.7). Linear regression analyses of the data were achieved by expressing the nominal data groups (native, minimally or fully oxidized LDL) in the form of a continuous variable, namely the LDL fluorescence value (section 6.3.2a), an index of the degree of oxidative modification. The effect of oxidation status upon the induction of Ca^{2+} transients was compared in terms of the logarithmically transformed data for the integral, peak amplitude and the decay time of the cytosolic Ca^{2+} responses (figure 2.4). A nominal value of 1 was added to each value prior to logarithmic transformation. Graphical representation of the linear regression analysis is shown in figure 6.10.

Linear regression analysis of the data demonstrated that the integrals, peak amplitudes and decay times of the cytosolic Ca^{2+} responses were positively and significantly correlated with the degree of oxidation of the LDL ($p < 0.0001$ in each case). Collectively, these data indicate that the overall magnitude of the cytosolic Ca^{2+} response is positively correlated with the degree of oxidative modification of LDL. The increase in the overall magnitude of the response is mediated by an increase in the peak amplitudes and the decay times of the cytosolic Ca^{2+} responses of the T24 cells. The peak of the absolute change in concentration of cytosolic Ca^{2+} was estimated from the peak amplitude, using the instrument calibration curve (section 2.3.8). The peak changes in cytosolic Ca^{2+} were 158.5nM, 122.0nM and 173.2nM for native, minimally modified and fully oxidized LDL respectively.

T24 cells elicit greater and more prolonged elevations of cytosolic Ca^{2+} in response to progressively oxidized LDL. Further experiments were undertaken to determine the duration of the sustained cytosolic Ca^{2+} responses seen in response to oxidatively modified LDL.

Figure 6.10: Linear regression analysis of the effect of oxidative modification of LDL upon the induction of Ca^{2+} transients

$p < 0.0001$

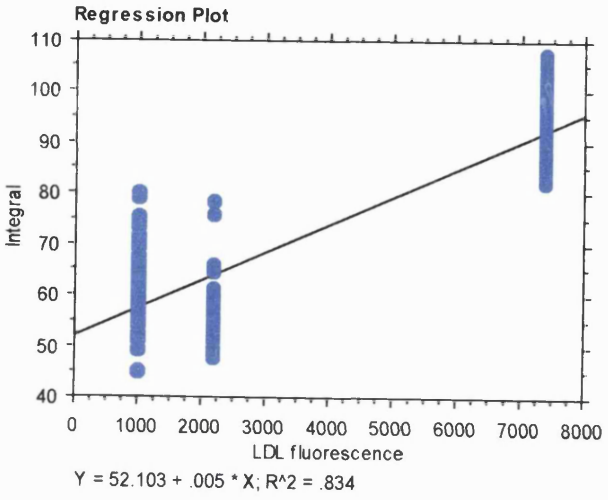

$p < 0.0001$

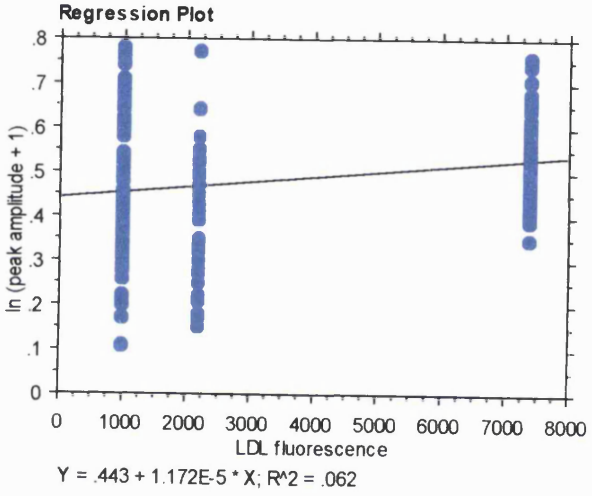

$p < 0.0001$

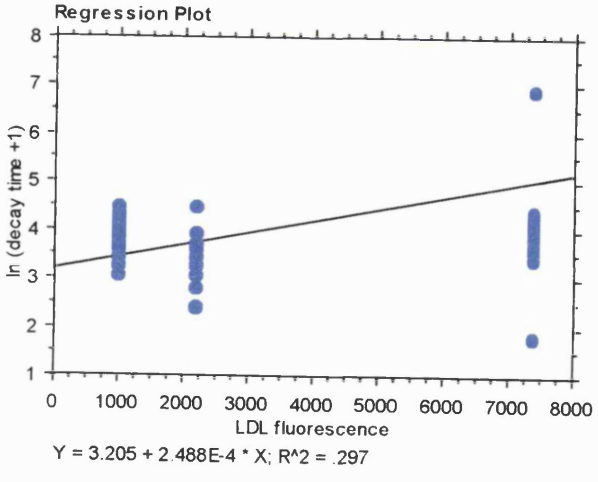

The effect of oxidative modification of nLDL (0.05 mg/ml) upon the induction of cytosolic Ca^{2+} transients in individual cells was determined using a fluorescence video imaging system. Cu^{2+}-mediated LDL oxidation was determined using a fluorimeter (section 6.3.2). The induction of Ca^{2+} transients by native and oxidatively modified LDL was assessed in terms of the average increase in cytosolic Ca^{2+} above basal (response: basal ratio, R: B ratio), the peak amplitude of the response and the decay time of the response (figure 2.4) using linear regression.

6.4.5 Sustained elevations of cytosolic Ca^{2+} elicited by fully oxidized LDL

In order to determine the duration of cytosolic Ca^{2+} elevations elicited by T24 cells in response to oxidatively modified LDL, cells were observed for extended periods of time. Cells treated with native or oxidatively modified LDL were observed intermittently over a period of 10 minutes. The levels of cytosolic Ca^{2+} 520-565 seconds after the addition of native or fully oxidized LDL were determined. The Student's t-test was used to determine whether the levels of cytosolic Ca^{2+} observed after 520-565 seconds exposure to either native or oxidized LDL returned to basal levels. The results show that there is no significant difference between the basal Ca^{2+} level and the level of Ca^{2+} after 520 seconds following treatment of T24 cell with native LDL ($p= 0.47$). This shows that the cytosolic Ca^{2+} increase in cells treated with nLDL is transient and that the basal, pre-treatment levels of cytosolic Ca^{2+} are rapidly restored. The re-establishment of the basal level of Ca^{2+} was observed in the entire cell population. In contrast, cells treated with mmLDL exhibited sustained elevations of cytosolic Ca^{2+} levels after 520 seconds (figure 6.11b, $p = 1.03 \times 10^{-24}$). Similarly, a highly significant difference between the basal Ca^{2+} levels and the levels of Ca^{2+} 520 seconds after treatment with fully oxidized LDL was evident (figure 6.11c, $p = 3.18 \times 10^{-24}$).

Comparison of the data for each LDL class demonstrates that the rate of increase in cytosolic Ca^{2+} for nLDL is rapid in comparison to mmLDL and oxLDL (figures 6.11a-c). Interestingly, the rate of increase is slower for mmLDL than oxLDL. Furthermore, the maximal amplitude is greater in the case of mmLDL compared to oxLDL. These results for mmLDL and oxLDL are in contrast to the results of the independent experiments represented in figure 6.6b, where the peak amplitude and onset of cytosolic Ca^{2+} transients are larger and longer for oxLDL compared to mmLDL. In addition, the rate of increase in cytosolic Ca^{2+} is slower for mmLDL than oxLDL in one experiment (figure 6.11a-c) and is vice versa in the other (figure 6.6b). It is likely that this variation between experiments probably results from variation in the LDL compositions of samples from different donors. The heterogeneity of LDL results in variation in the oxidation products between different donor samples (see section 6.1.3).

Figure 6.11a: Induction of cytosolic Ca^{2+} transients by nLDL in T24 cells

Cytosolic Ca^{2+} levels 0-145 seconds after the addition of nLDL

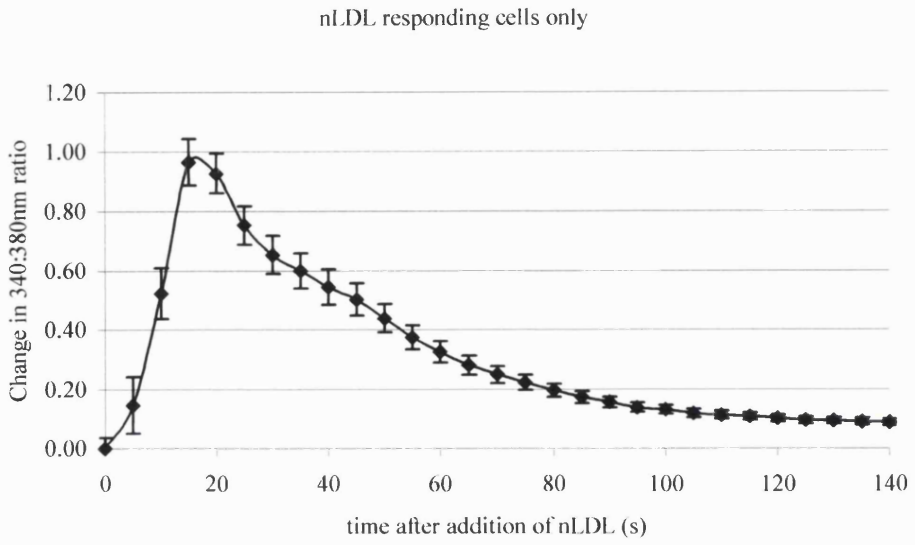

Cytosolic Ca^{2+} levels 520-565 seconds after the addition of nLDL

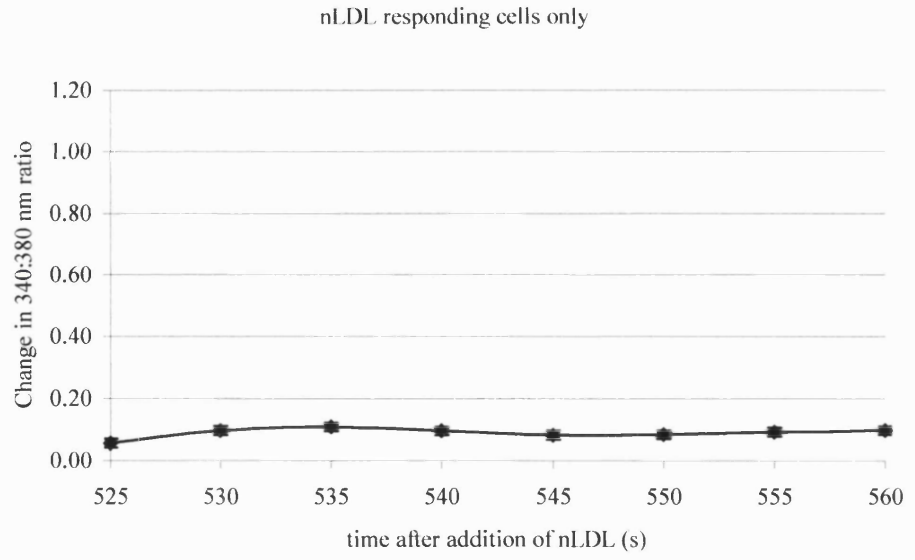

The effect of LDL oxidation upon the induction of cytosolic Ca^{2+} transients in T24 cells was determined in individual cells using a video fluorescence imaging system. Cells were observed immediately following the addition of nLDL (0.05mg/ml) and again after 520 seconds to determine whether the elevation of cytosolic Ca^{2+} levels were sustained for extended periods in comparison to mmLDL and oxLDL (figure 6.11b and 6.11c). Results are the mean ± S.E.M. for 15 individual cells.

Figure 6.11b: Induction of cytosolic Ca^{2+} transients by mmLDL in T24 cells

Cytosolic Ca^{2+} levels 0-145 seconds after the addition of mmLDL

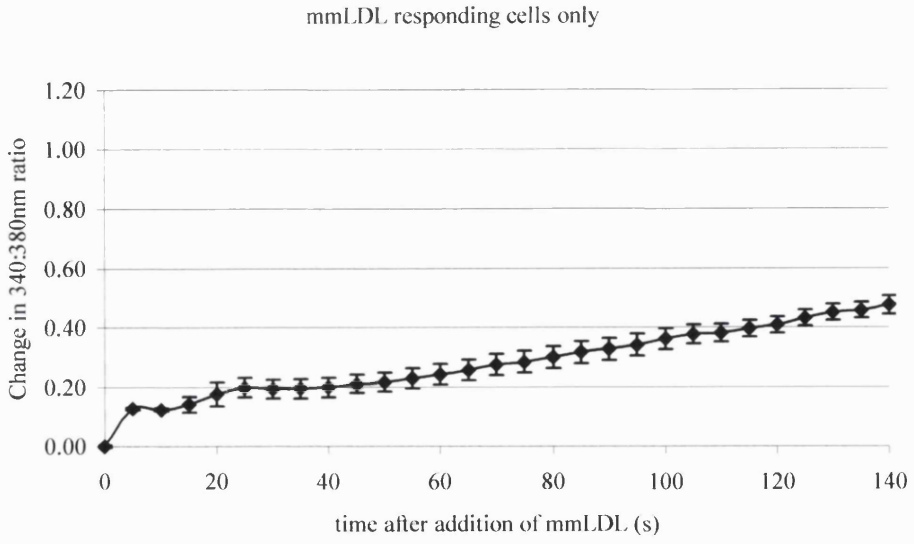

Cytosolic Ca^{2+} levels 520-565 seconds after the addition of mmLDL

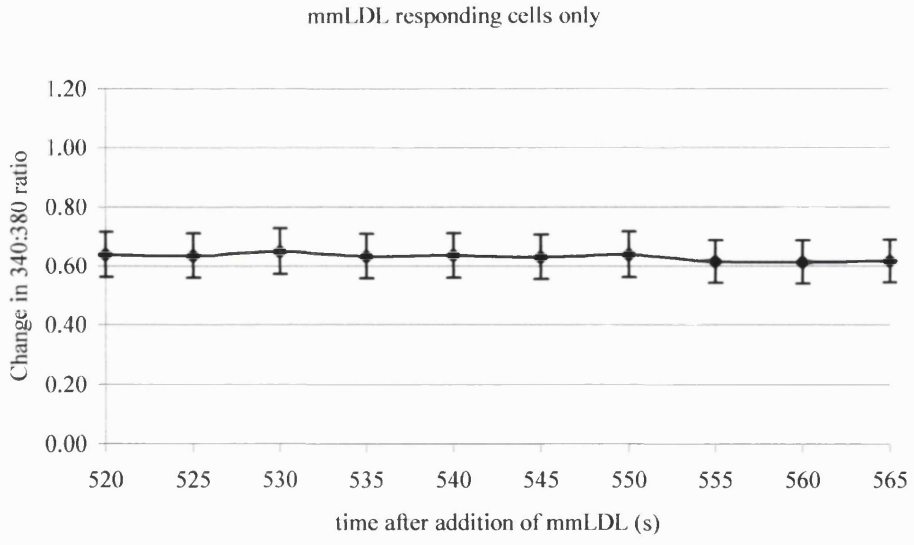

The effect of LDL oxidation upon the induction of cytosolic Ca^{2+} transients in T24 cells was determined in individual cells using a video fluorescence imaging system. Cells were observed immediately following the addition of mmLDL (0.05mg/ml) and again after 520 seconds to determine whether the elevation of cytosolic Ca^{2+} levels were sustained for extended periods in comparison to nLDL and oxLDL (figure 6.11a and 6.11c). Results are the mean ± S.E.M. for 15 individual cells.

Figure 6.11c: Induction of cytosolic Ca^{2+} transients by oxLDL in T24 cells

Cytosolic Ca^{2+} levels 0-145 seconds after the addition of oxLDL

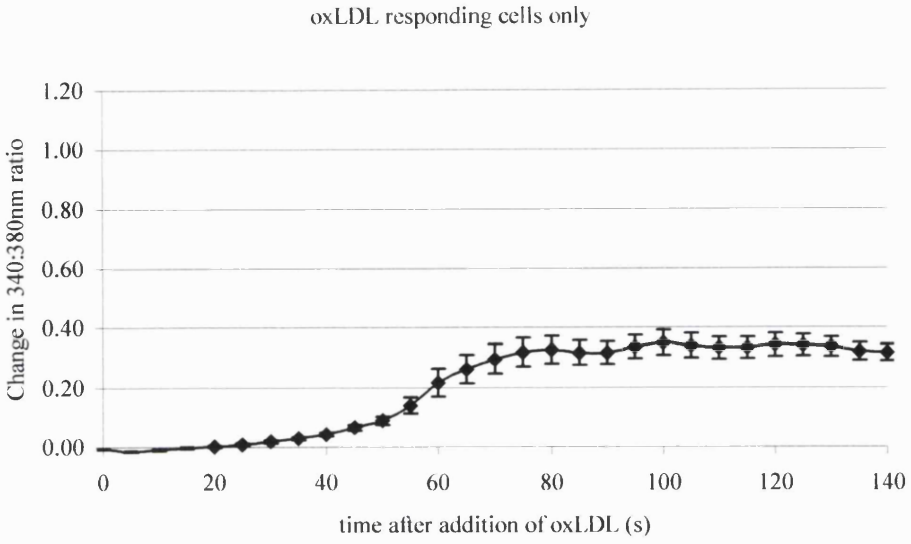

Cytosolic Ca^{2+} levels 520-565 seconds after the addition of oxLDL

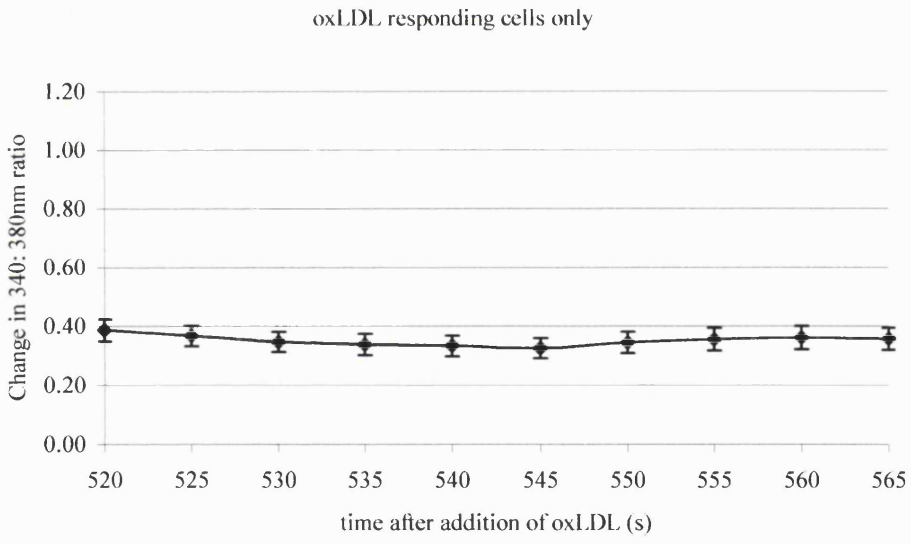

The effect of LDL oxidation upon the induction of cytosolic Ca^{2+} transients in T24 cells was determined in individual cells using a video fluorescence imaging system. Cells were observed immediately following the addition of oxLDL (0.05mg/ml) and again after 520 seconds to determine whether the elevation of cytosolic Ca^{2+} levels were sustained for extended periods in comparison to nLDL or mmLDL. Results are the mean ± S.E.M. for 15 individual cells.

6.4.6 Effect of inhibition of TF activity upon the induction of Ca^{2+} transients by nLDL and oxLDL

The involvement of TF in the induction of Ca^{2+} transients by nLDL and oxLDL was examined using an inhibitory antibody towards TF activity (TF8 5G9). T24 cells were pre-incubated with TF8 5G9 at a final concentration of 0.01mg/ml for 2 minutes prior to the addition of either native, minimally modified or oxidized LDL. The basal level of cytosolic Ca^{2+} in T24 cells was unaffected by the addition of the TF8 5G9 antibody (figure 6.12).

Treatment of T24 cells with nLDL resulted in an average increase of 0.09 ± 0.01 in the 340:380nm ratio above basal levels. The average increase in the 340:380nm ratio of cells exposed to nLDL after pre-treatment of cells with 0.01 mg/ml TF8 5G9 was 0.12 ± 0.01 above the basal levels. Statistical analysis of these data showed no that the response of cells to nLDL was unaltered by pre-exposure of the cells to TF8 5G9 (Student's t-test, p = 0.09, figure 6.13a). Similarly, the TF8 5G9 antibody had no effect upon the induction of cytosolic Ca^{2+} transients induced by oxidatively modified LDL (figure 6.13b). Treatment of cells with oxLDL resulted in an increase of 0.12 ± 0.01 in the 340:380nm ratio above basal levels. Cells pre-treated with TF8 5G9 elicited increases of 0.14 ± 0.01 in the 340:380nm ratio above basal levels. Statistical comparison of the two treatment groups demonstrated that the data were not statistically different (Student's t-test, p = 0.37). However, although inhibition of TF activity had no effect upon the induction of cytosolic Ca^{2+} signals seen in response to this particular sample of oxLDL it is not possible to conclude that TF is not involved in the induction of cytosolic Ca^{2+} signals by oxLDL. This is because the oxLDL used in this experiment did not elicit sustained elevations of cytosolic Ca^{2+} as seen with other samples. Differences between responses to oxLDL are not unexpected since nLDL is heterogeneous in terms of its composition and resistance to oxidative attack. Due to constraints upon equipment access time we were unable to determine whether inhibition of TF activity would affect the induction of sustained cytosolic Ca^{2+} transients by oxLDL.

Collectively, these results demonstrate that the induction of Ca^{2+} transients in response to nLDL is not mediated via TF. In addition, a role for TF in the maintenance of elevated cytosolic Ca^{2+} levels seen in response to some samples of oxLDL has not been excluded.

Figure 6.12: Effect of TF8 5G9 antibody upon basal cytosolic Ca^{2+} levels in T24 cells

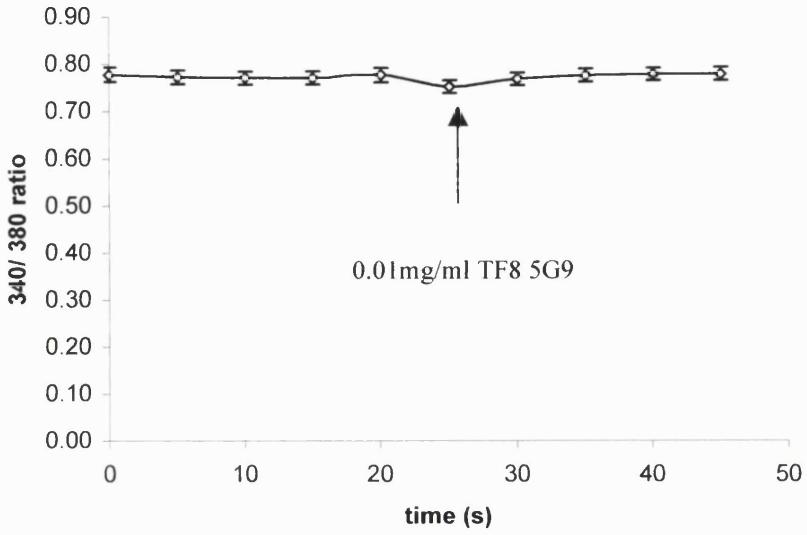

⟶ Indicates the time of addition of the TF-neutralizing TF8 5G9 antibody.

T24 cells were seeded onto glass coverslips and grown overnight as described in section 2.1.8. For experimentation, cells were loaded with the Ca^{2+}-sensitive fluorophore Fura2. The effect of the TF8 5G9 antibody upon cytosolic Ca^{2+} levels in individual cells was examined using a microscope integrated to a fluorescence video imaging system. Basal cytosolic Ca^{2+} levels were measured for 20 seconds prior to the addition of TF8 5G9 antibody at a final concentration of 0.1mg/ml. Cells were observed for a further 20 seconds after the addition of the antibody. Results are the mean ± S.E.M. of ten individual cells.

Figure 6.13a: The effect of inhibition of TF activity upon the induction of Ca^{2+} transients by nLDL

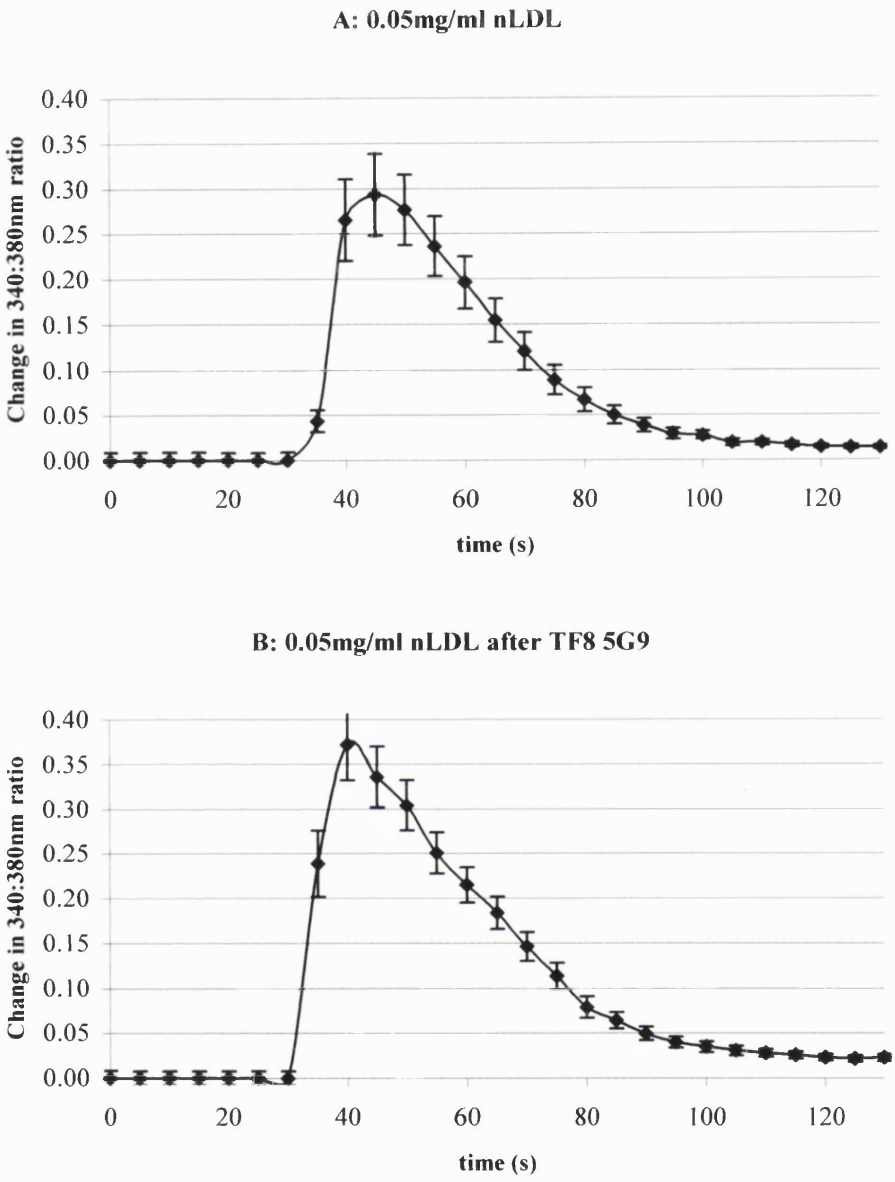

A: Basal cytosolic Ca^{2+} levels were observed for 20 seconds prior to the addition of 0.05mg/ml nLDL. The cytosolic Ca^{2+} response of the cells was measured for 120 seconds after the addition of the nLDL. The change in cytosolic Ca^{2+} levels were calculated from the 340:380nm fluorescence ratios. The mean ± S.E.M. of the change in cytosolic Ca^{2+} of at least 40 cells is shown.

B: Cells were incubated with the TF8 5G9 antibody for 2 minutes. Cells were observed for 20 seconds prior to the addition of 0.05mg/ml nLDL. The mean ± S.E.M. of the change in cytosolic Ca^{2+} of at least 40 cells is shown.

The effect of inhibition of TF8 5G9 upon the induction of Ca^{2+} transients by 0.05mg/ml nLDL was determined using the un-paired Student's t-test. No significant differences were observed between cells treated with TF8 5G9 prior to nLDL and cells treated with nLDL only ($p = 0.09$).

Figure 6.13b: The effect of inhibition of TF activity upon the induction of cytosolic Ca^{2+} transients by oxLDL

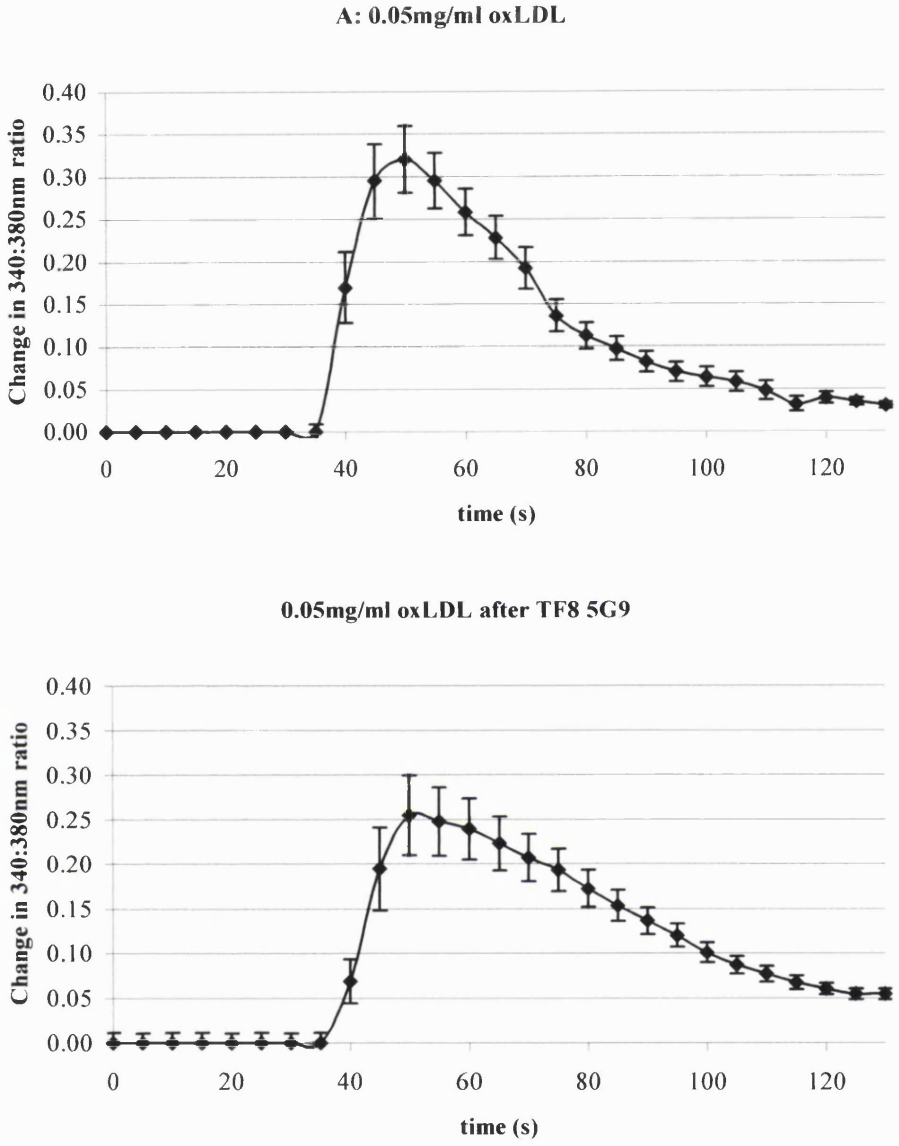

A: Basal cytosolic Ca^{2+} levels were observed for 20 seconds prior to the addition of 0.05mg/ml oxLDL. The cytosolic Ca^{2+} response of the cells was measured for 120 seconds after the addition of the oxLDL. The change in cytosolic Ca^{2+} levels were calculated from the 340:380nm fluorescence ratios. The mean ± S.E.M. of the change in cytosolic Ca^{2+} of at least 40 cells is shown.

B: Cells were incubated with the TF8 5G9 antibody for 2 minutes. Cells were observed for 20 seconds prior to the addition of 0.05mg/ml oxLDL. The mean ± S.E.M. of the change in cytosolic Ca^{2+} of at least 40 cells is shown.

The effect of inhibition of TF8 5G9 upon the induction of Ca^{2+} transients by 0.05mg/ml oxLDL was determined using the un-paired Student's t-test. No significant differences were observed between cells treated with TF8 5G9 prior to oxLDL and cells treated with oxLDL only ($p= 0.37$).

6.5 Conclusions

Exposure of T24 cells to native, minimally modified or fully oxidized LDL results in the induction of increases in cytosolic Ca^{2+} levels. The effect of the concentration of native, minimally modified and fully oxidized LDL upon cytosolic Ca^{2+} transients was determined over the range of 0.005 to 0.5mg of LDL apo B/ml. The overall magnitude of the responses was positively correlated with the concentration of native, minimally modified or fully oxidized LDL. The increases in the magnitude of the cytosolic Ca^{2+} transients for each class of LDL were due to increases in the peak amplitudes of the responses and lengthening of the decay times.

Differences in the characteristics of the cytosolic Ca^{2+} increases were compared between identical concentrations of native, minimally modified and fully oxidized LDL (0.5mg of LDL apo B/ml) to determine the effect of oxidative modification of LDL. Linear regression analysis demonstrated a significant positive correlation between the overall magnitude of the response, measured in terms of the area under the response curve, and the degree of oxidative modification of the LDL. The increase in the magnitude of the cytosolic Ca^{2+} response resulted from increases in the peak amplitudes and decay times of the Ca^{2+} responses in cells treated with oxLDL.

Progressive oxidation of LDL results in the prolongation of elevated cytosolic Ca^{2+} levels. Exposure of T24 cells to native LDL results in the immediate induction of short-lived increases in cytosolic Ca^{2+}. In contrast, exposure of T24 cells to fully oxidized LDL results in prolonged elevations of the cytosolic Ca^{2+} levels, which are of slow onset and are sustained for at least 10 minutes. Cytosolic Ca^{2+} levels were sustained for prolonged periods upon treatment with some mmLDL samples but not with others. The rate of increase of the cytosolic Ca^{2+} response to mmLDL was slower than that seen in response to nLDL. However, when compared to fully oxidised LDL, the onset of the response could be faster or slower. These variations may result from the heterogeneity in composition between donor LDL samples. This heterogeneity leads to variation in the chemical composition of the oxidation intermediates produced in different LDL samples.

Inhibition of TF activity had no effect upon the induction of cytosolic Ca^{2+} increases by nLDL demonstrating that TF: FVIIa activity is not involved in mediating the Ca^{2+} responses elicited nLDL. It remains to be seen whether inhibition of TF activity affects the persistence of increased cytosolic Ca^{2+} when the Ca^{2+} elevation is sustained in response to oxLDL. However, in the case of oxLDL samples that elicit transient cytosolic Ca^{2+}, the increases in cytosolic Ca^{2+} were not dependent upon TF.

6.6 Discussion

6.6.1 Differential responses of cells to native and oxidatively modified LDL

Oxidative modification of LDL is a progressive process and LDL can be minimally or fully oxidized. Native, minimally modified and fully oxidized LDL elicit the induction of a variety of proatherogenic responses in arterial cells (figure 1.8). The studies tabulated in figure 1.8 demonstrate the effect of progressive oxidation of LDL upon the induction of proatherogenic responses. Unfortunately, in many studies the effect of LDL species of differing oxidation statuses upon the factor in question was not determined. However, differential effects between native and oxidized LDL were identified in several studies.

Unlike nLDL, oxidized LDL leads to; increased permeability in endothelial cells (Siess W., 1999), secretion of the chemotactic factor MCP-1 in endothelium and smooth muscle cells (Cushing S.D., 1990), induction of the adhesion molecule ELAM-1 in endothelial cells (Berliner J.A., 1990, Lehr H.A., 1992), enhancement of G-CSF and GM-CSF production by endothelium (Rajavashisth T.B., 1990), scavenger receptor A expression on smooth muscle cells (Meitus-Snyder M., 2000), PDGF expression in macrophages (Malden L.T., 1991), cytotoxicity in fibroblasts (Morel D.W., 1983) and vasoconstriction via endothelin induction and inactivation of nitric oxide (Boulanger C.M., 1993, Galle J., 1991 and Chin J.H., 1992).

Some investigations have demonstrated the absence of differential effects of native and oxidized LDL upon cellular responses. Both nLDL and oxLDL may directly increase the expression of the scavenger receptor B (CD36) on macrophages (Han J., 1997 and Feng J., 2000), E-selectin on endothelium (Allen S., 1998) and TF on smooth muscle cells (Cui M.Z., 1999). However in each of these studies, oxLDL is a more potent agonist than nLDL.

Both native and oxidized LDL induce enhanced expression of the scavenger A receptor (Han J., 1997), PDGF-AA and the PDGF receptor (Stiko-Rahm A., 1992), IGF-1, the IGF-1 receptor and IGF binding proteins 2 and 4 (Scheidegger K.J., 2000). No differential effect of the different LDL classes was found in these studies.

6.6.2 Characteristics of cytosolic Ca^{2+} signals induced by native and oxidized LDL

The observed differences in the biological responses of arterial cells to minimally and oxidized LDL suggests that each class of LDL induces the activation of distinct signalling pathways. Since, the involvement of cytosolic Ca^{2+} fluxes in cellular responses to extracellular signals is a ubiquitous feature of cellular signalling mechanisms, studies were undertaken to investigate whether native and progressively modified LDL induce discrete patterns of cytosolic Ca^{2+} fluxes.

The data presented here, demonstrate that nLDL, mmLDL and oxLDL elicit cytosolic Ca^{2+} fluxes in bladder carcinoma T24 cells. The kinetics of the cytosolic Ca^{2+} fluxes were determined by the degree of oxidative modification of the LDL. Progressive oxidation of LDL promoted increases in the overall magnitude of the cytosolic Ca^{2+} response via increases in the peak amplitude and prolongation of elevated cytosolic Ca^{2+} levels. Cytosolic Ca^{2+} levels in cells exposed to nLDL were transiently increased, but returned to basal levels rapidly. Exposure of cells to fully oxidized LDL resulted in extension of elevated cytosolic Ca^{2+} such that the cytosolic Ca^{2+} levels did not return to basal levels. Increased cytosolic Ca^{2+} levels were sustained for more than 10 minutes. Sustained elevations of cytosolic Ca^{2+} are associated with the induction of apoptosis (Trump B.F., 1995) and the link the ability of oxLDL to induce apoptosis with its ability to promote sustained elevation of cytosolic Ca^{2+}.

These data demonstrate that the characteristics of cytosolic Ca^{2+} flux are discrete for nLDL, mmLDL and oxLDL. As the LDL is progressively oxidized, the cellular response is altered resulting in increases in the peak amplitudes and the decay times. These data suggest that oxidation of LDL causes larger amounts of Ca^{2+} to be released and leads to suppression of the activity of pathways involved in the removal of cytosolic Ca^{2+}.

The results of studies of intracellular Ca^{2+} rises in other cell types demonstrate similar kinetics of cytosolic Ca^{2+} transients as reported here. Exposure of endothelial cells to nLDL (0.5mg of LDL apo B/ml) results in increases in cytosolic Ca^{2+} transients that are maximal after approximately 16 seconds and decay to basal within 160 seconds (Allen S., 1998). In contrast to the findings reported here, these authors did not detect cytosolic Ca^{2+} transients in response to mmLDL (0.1mg of LDL apo B/ml). The absence of a Ca^{2+} response to mmLDL (0.1mg of LDL apo B/ml) has also been reported by Essler et al (1999). In our system, these concentrations of mmLDL were sufficient to elicit cytosolic Ca^{2+} transients, indeed, we observed Ca^{2+} responses to mmLDL at concentrations as low 0.005mg of LDL apo B/ml. Furthermore, the results of Mietus-Snyder et al (2000), demonstrate that induction of the scavenger A receptor in smooth muscle cells by mmLDL is dependent upon Ca^{2+} flux.

In addition to the investigation of differential responses to native and minimally modified LDL, the effect of LDL concentration upon the kinetics of Ca^{2+} transients within each class of LDL; native, minimally or fully oxidized LDL was studied. The normal plasma LDL apo B concentration is around 0.5mg/ml, which is equivalent to ~1μM LDL. Cells were exposed to native and oxidatively modified LDL at concentrations in the range of 0.005 to 0.5 mg of LDL apo B/ml. The characteristics of the induction of Ca^{2+} transients were compared between different concentrations of native, minimally modified and fully oxidized LDL to

determine whether varying the concentration of each class of LDL elicits discrete cytosolic Ca^{2+} responses in T24 cells. The results demonstrate that for each class of LDL; native, minimally modified or fully oxidized, the magnitude of the response is correlated with the concentration of the LDL stimulus. Further analysis of the data revealed that the increased magnitude of the response resulted from increases in the peak amplitudes and decay times. Thus increasing the concentration of LDL results in an increase in Ca^{2+} release and an attenuated rate of removal of Ca^{2+} from the cytosol. A concentration-dependent effect of LDL upon Ca^{2+} transients has been observed previously. Allen et al (1998) demonstrated a concentration-dependent effect of nLDL upon the magnitude of Ca^{2+} transients in endothelial cells. Furthermore, a positive correlation between the nLDL concentration and the peak amplitude of the Ca^{2+} response was identified as a mechanism for the increased magnitude of the response. Similarly, the results reported here demonstrate concentration-dependent increases in the peak amplitude. Our data shows that attenuation of the rate of removal of cytosolic Ca^{2+}, detected as an increase in the decay time, in concert with an elevation of the peak amplitude are responsible for increasing the magnitude of the responses as the LDL concentration is increased.

The data presented here and elsewhere demonstrate that each class and concentration of LDL elicits a unique characteristic pattern of cytosolic Ca^{2+} flux. This suggests the existence of a mechanism by which the concentration of LDL and the degree of oxidation can be 'sensed' by the cells. The sensor mechanism translates the extracellular signals into a unique characteristic pattern of Ca^{2+} flux. The distinct pattern of Ca^{2+} flux in turn, encodes a set of phenotypic instructions appropriate to the nature of the extracellular stimulus. In this way cells can elicit differential responses to native, minimally modified and fully oxidized LDL. Our data alludes to the possibility that the extent of oxidative modification of LDL is 'sensed' by the cell and is encoded into the decay time of the cytosolic Ca^{2+} elevation. An appropriate analogy is that each LDL species invokes a 'signature response', which results in the induction of the appropriate cellular response.

The existence of 'signature responses' to distinct agonists and varying concentrations of agonist has been documented previously. Ca^{2+} is an intracellular messenger that relays information within cells to regulate their activity. However, almost all cellular processes are regulated by calcium (figure 6.14) and in order to co-ordinate all its different functions, Ca^{2+} signals need to be flexible and precisely regulated. This versatility arises through the ability of Ca^{2+} ions to act in the contexts of space, time and amplitude.

The data demonstrate that the induction of cytosolic Ca^{2+} transients by nLDL samples from different donors is variable in terms of the rate of onset and decay. These differences may arise from differences in the LDL profile between donor samples. The

LDL isolated in these studies consists of a mixture of light, intermediate and small dense LDL subspecies. The proportion of each subspecies varies between individuals such that each donor has a unique LDL profile. The distinct physicochemical and biological properties of each subclass (see section 1.2.5) are a likely determinant of the variation in cytosolic Ca^{2+} responses seen upon treatment with nLDL from different donor samples. Furthermore, the unique profiles of different donor LDL may lead to variation in the repertoire of peroxidation products formed after oxidation. The variation in peroxidation products may be responsible for the differences in the characteristics of cytosolic Ca^{2+} responses of cells seen with different donor oxidised LDL.

Figure 6.14: Versatility of calcium signalling in cell life and death

Elementary events	Global Ca^{2+} waves (intracellular)	Global Ca^{2+} wave (intercellular)
Growth cone migration	Fertilisation	Wound healing
Membrane excitability	Smooth muscle contraction	Ciliary beating
Mitochondrial metabolism	Skeletal muscle contraction	Glial cell function
Vesicle secretion	Cardiac muscle contraction	Bile flow
Smooth muscle relaxation	Apoptosis	Insulin secretion
Mitosis	Gene transcription	Endothelial NO synthesis
Synaptic plasticity	Cell proliferation	

Adapted from Berridge M.J., 1998

6.6.3 Involvement of TF in the induction of Ca^{2+} transients by native and oxidised LDL

Oxidised LDL activates the procoagulant activity of TF (Ettelaie C., 1995). Since both oxidised LDL and FVIIa induce increases in cytosolic Ca^{2+}, the potential involvement of TF in the induction of Ca^{2+} transients by oxLDL was investigated. Inhibition of TF activity using the TF-neutralising TF8 5G9 antibody did not alter Ca^{2+} transients induced by oxLDL in cases where the oxLDL sample in question resulted in transient cytosolic Ca^{2+} elevations. Thus activation of TF by oxLDL does not contribute to transient increases in cytosolic Ca^{2+}. While this sample of oxLDL resulted in transient induction of cytosolic Ca^{2+} elevation, other oxLDL samples resulted in the induction of sustained elevations of cytosolic Ca^{2+}. The effect of TF inhibition upon the maintenance of elevated cytosolic Ca^{2+} transients by

oxLDL could not be determined due to time constraints on access to equipment. We cannot therefore exclude the possibility that TF is involved in the maintenance of sustained elevations of cytosolic Ca^{2+} induced by oxLDL.

The induction of cytosolic Ca^{2+} transients by nLDL was also unaltered by preincubation of cells with the TF8 5G9 antibody demonstrating that TF is not involved in mediating the induction of cytosolic Ca^{2+} increases by nLDL. However, this result does not exclude the possibility that nLDL exhibits some binding to cell surface TF. Moreover, since native LDL inhibits the procoagulant activity of TF, it would be of interest to determine whether pre-treatment of cells with nLDL would result in the inhibition of cytosolic Ca^{2+} transients induced by FVIIa. Unfortunately, due to technical problems this question could not be addressed.

6.6.4 Mechanisms of cytosolic Ca^{2+} increases induced by native and oxidised LDL

The source of the increase in cytosolic Ca^{2+} elicited in response to native, minimally modified and oxidised LDL could be determined to ascertain whether it is derived from extracellular milieu and/or intracellular Ca^{2+} stores. Addition of native or oxidised LDL in the absence of extracellular Ca^{2+} could be performed to determine whether the rise in cytosolic Ca^{2+} is derived from extracellular sources. In addition, intracellular Ca^{2+} stores may be emptied of Ca^{2+} using thapsigargin prior to the addition of native or oxidised LDL, to determine whether the cytosolic Ca^{2+} elevations are store dependent.

6.6.5 Biologically active components of native and minimally modified LDL

The induction of unique signature responses by native and oxidatively modified species must arise from differences in the nature of the biologically active component(s) between the LDL species. Identification of such species is technically difficult. Some of the active species responsible for the induction of various proatherogenic responses have been identified and are presented below. These data provide a means by which the underlying molecular basis of differential responses to native and oxidized LDL can be rationalized. The mechanism underlying the induction of differential patterns of cytosolic Ca^{2+} transients by LDL of differing concentration and oxidation statuses in T24 cells presented in this chapter may be due to the activity of some of these previously encountered biologically active species.

Oxidation of the phospholipid component of LDL results in the production of lysophosphatidylcholine (LPC) and lysophosphatidic acid (LPA). The induction of PAI-1 in human smooth muscle cells is invoked by oxLDL and not by nLDL (Dichtl W., 1999). The authors found that lysophosphatidylcholine (LPC), a phospholipid oxidation product, could also elicit PAI-1 induction and propose that LPC is the active component of oxLDL. LPC

also induces VCAM-1 in human endothelial cells (Kume N., 1992), while native LDL does not. In another study, oxLDL and not mmLDL induces VCAM-1 expression. Consolidation of these observations suggests that LPC is present in extensively and not minimally oxidized LDL. LPC also induces P-selectin in endothelium and platelets (Murohara M., 1996), VEGF in macrophages (Ramos M.A., 1998) and synthesis of the vasoconstrictor endothelin-1 (Boulanger C.M., 1992). In addition, the LPC component of oxLDL is directly chemotactic for monocytes (Quinn M.T., 1988) and smooth muscle cells (Autio I., 1990). The phospholipid hydroperoxide LPA may be responsible for the increased permeability of endothelial cells that is induced by mmLDL (Essler M., 1999, Siess W., 1999).

The potential for oxidized phosphatidylcholine to promote atherosclerosis *in vivo* is demonstrated by the observation that antibodies to oxidized phosphatidylcholine detect elevated levels of circulating oxLDL (Toshima S., 2000). The antibody also cross-reacts with phosphatidylcholine hydroperoxides. 7β-hydroperoxycholest-5-en-3-β-ol is found in atherosclerotic lesions and is the primary cytotoxin of oxidized LDL (Chisholm G.M., 1994).

Oxidation of cholesterol results in the formation of oxysterols that inhibit gap junctional communications between cells, which may in turn induce smooth muscle cell proliferation (Zwijsen R.M.L., 1992). In addition, cholestanetriols and 25-hydroxycholesterol may cause further injury to endothelial cells and smooth muscle cells (Peng S., 1991).

Both phospholipid and cholesterol ester hydroperoxides may oxidise to produce hydroxyoctadecadienoic acids (HODES). 9-hydroxyoctadecadienoic acid may be the active oxidized lipid species in oxLDL that mediates inhibition of the production of IL-12 in macrophages (Chung S.W., 2000).

The heterogeneity of native and oxidized LDL complicates the interpretation of data derived from studies of LDL. Firstly, nLDL itself is a heterogeneous mixture of molecular species. Furthermore, the products of oxidation of LDL obtained from different donors may vary markedly due to considerable differences in properties that can influence oxidation (e.g., antioxidant content, PUFA content, endogenous apo B100 modification). In addition, it is not known whether all of the molecules within LDL are oxidized at the same rate and to the same extent. It is possible that oxidation of different LDL samples results in the production of variable molecular species, such that some oxidation products may be present in some samples but absent in others. Further investigations are required to correlate the differential effects of native and oxidized LDL with the nature of the active component(s).

6.6.6 Mechanisms of induction of proatherogenic responses by lipoproteins

Various intermediates of signalling pathways involved in the induction of proatherogenic responses to LDL have been previously identified and are described below. Cytosolic Ca^{2+} levels modulate the activities of many of these intermediates. The mechanistic basis for the ability of oxLDL to increase vascular permeability may arise from the ability of mmLDL to activate Rho/Rho kinase and myosin light chain phosphatase in human endothelial cells (Essler M., 1999). Activation of these proteins results in the formation of actin stress fibres and the formation of intercellular gaps that lead to an increase in vascular permeability.

The involvement of the protein kinase C pathway in the induction of proatherogenic responses has been demonstrated by a number of observations. The induction of CD36 on monocytes by oxLDL is dependent upon protein kinase C (Feng J., 2000). Phosphatidylinositol turnover (Block L.H., 1988) and IP_3 receptor density (Massaeli H.M.J., 1999) are involved in the cellular responses to lipoproteins. OxLDL has also been observed to induce lesions in ryanodine channels (Massaeli H.M.J., 2000). In addition, G protein-coupled receptor pathways and protein kinase A pathways are both implicated in cellular signalling elicited in response to mmLDL (Parhami F., 1993 and Parhami F., 1995).

Several transcription factors that mediate responses to lipoproteins have been identified. The induction of TF in response to native and oxidized LDL is mediated by the transcription factors egr-1 and sp-1 (Cui M.Z., 1999). The transcription factor NFkB is involved in the inhibition of IL-12 by oxLDL in mouse macrophages (Chung S.W., 2000). Furthermore, the suppression of IL-12 depends upon physical interactions between NFkB and the peroxisome proliferator-activated receptor-γ (PPARγ). The involvement of PPARγ in lipoprotein-induced cellular signalling has been reported elsewhere. OxLDL attenuates chemokine CCR2 expression and induces CD36 expression in macrophages via signalling pathways involving PPARγ (Han J., 2000 and Feng J., 2000). Transcription factors may be activated by MAP kinases and the stimulation of MAP kinase in response to oxLDL has also been observed (Kusuhara M., 1997).

The redox-sensitive transcription factors c-jun and CCAAT enhancer-binding protein (CEBP) correlate with the induction of the scavenger A receptor by oxidized LDL in smooth muscle cells (Mietus-Snyder M., 2000). These observations demonstrate that oxidatively modified lipoproteins are a source of intracellular oxidative stress. The increase in SRA expression is associated with increased cyclooxygenase 2 activity (COX-2). Cellular oxidative stress generated by oxLDL is associated with a rise in intracellular free calcium (Negre-Salvayre A., 1992). Inhibition of Ca^{2+} flux suppresses induction of the SRA by oxLDL while calcium ionophore enhanced the induction. Calcium ionophore may, in part, mediate the enhancement of SRA expression via increasing the activity of

phospholipase A2 and the release of arachidonic acid (AA). The AA may provide the substrate for COX-2 that facilitates induction of the SRA.

Various investigations have identified differential cellular responses to native and oxidized LDL. The mechanism underlying these differential responses may be derived from unique patterns of Ca^{2+} signalling induced by distinct classes of LDL; native, minimally modified or fully oxidized. The existence of discrete patterns of Ca^{2+} flux in response to distinct agonists (signature responses) has been previously explored. These investigations demonstrate that cells can sense the frequency, amplitude and decay time of Ca^{2+} transients. The characteristics of the Ca^{2+} signals are biologically decoded by Ca^{2+}-sensitive proteins and result in the induction of distinct phenotypic responses.

The data presented here shows that cells elicit distinct patterns of release and removal of cytosolic Ca^{2+} in response to LDL species of differing oxidation statuses. The ability of cells to couple discrete stimuli with the induction of distinct patterns of Ca^{2+} signals enables separate stimuli to elicit 'signature' responses. These distinct Ca^{2+} responses act like a fingerprint and enable gene regulatory pathways to interpret the identity of the agonist allowing cells to respond with phenotypic changes appropriate to their environment. In order to unravel the mechanisms by which agonist-specific phenotypic responses are manifest, several questions should be addressed. The identity of the biological species in LDL responsible for the discrete Ca^{2+} signalling responses should be determined. These studies could focus upon the patterns of Ca^{2+} signalling induced by oxidation intermediates that have previously been encountered for their signalling properties (section 6.6.4). In this way, the component(s) of native or oxidatively modified LDL that is/are directly responsible for the distinct patterns of Ca^{2+} signalling may be identified. In addition, it would be of interest to investigate whether Ca^{2+}-sensitive proteins, such as calmodulin dependent protein kinases, are involved in translating the Ca^{2+} signals elicited by native or oxidised LDL into changes in the activities of pathways regulating gene transcription or mRNA translation/processing.

CHAPTER 7

GENERAL DISCUSSION

7.1 TF in coagulation

TF is a transmembrane glycoprotein that is responsible for the initiation of the extrinsic pathway of coagulation (figure 1.2). TF exposed upon injury to endothelium and acts as a co-factor for trace levels of activated FVII (FVIIa) in the circulation. The majority (99%) of FVII exists in the inactive form. The TF: FVIIa complex can either be formed through direct capture of FVIIa or through capture of FVII bound to TF followed by conversion of bound FVII to FVIIa. TF: FVIIa complexes can catalyze the activation of FVII bound to TF via an autoactivation reaction which proceeds via the interaction of distinct protease: co-factor and zymogen: co-factor complexes. Furthermore, the autoactivation is dependent upon the membrane-anchoring transmembrane region of TF (Neuenschwander P.F., 1992 and Morrissey J.H., 2001). In addition, it is possible that the membrane-proximal cysteine residue in the cytoplasmic domain of TF is involved in the formation of TF dimers, given that cysteine-linked TF homodimers have been observed (Bach R., 1988). Thus, it appears that trace levels of activated FVIIa in the circulation prime the clotting cascade. The TF: FVIIa complex triggers a proteolytic cascade that culminates in the formation of thrombin. Activated thrombin cleaves circulating fibrinogen and results in the formation of a fibrin clot on the injured surface.

Down regulation of the coagulation cascade in vivo occurs due to inhibition of the TF: FVIIa complex. The TF: FVIIa complex is susceptible to inhibition by tissue factor pathway inhibitor (TFPI) and antithrombin III. In addition to direct inhibition of TF: FVIIa, TFPI promotes the internalization and degradation of TF: FVIIa complexes and the translocation of TF: FVIIa complexes to glycosphingolipid rich domains (Sevinsky J.R., 1996).

7.2 Non-haemostatic functions of TF

The procoagulant function of TF has been known for some time. More recently however, alternative functions of TF have emerged. TF has emerged as a receptor molecule, a function not unexpected given its homology to members of the cytokine receptor II superfamily. These non-haemostatic activities are diverse (figure 3.1) and include roles for TF in proliferation (Kamikubo Y., 1997), apoptosis (Hamuro T., 1998 and Greeno E.W., 1996), chemotaxis (Sato Y., 1997 and Siegbahn A., 2000), adhesion (Randolph G.J, 1998), angiogenesis (Watanabe T., 1999), tumour metastasis (Mueller B.M., 1992 and 1998). A recent study shows the ability of TF: FVIIa to induce genes involved in wound healing including growth factors, proinflammatory mediators, transcription factors and mediators of cellular reorganization (chemotactic factors and extracellular matrix proteases),(Camerer E., 2000 and Pendurthi U.R., 2000).

TF is associated with the progression of atherosclerosis. The mechanism of involvement of TF in atherosclerosis results from its non-haemostatic as well as its prothrombotic

functions. Furthermore TF appears to be involved in both the early and late stages of this chronic disease (figure 1.13).

Thickening of the intima observed in the early stages of the disease (figure 1.5) may be brought about by the ability of TF to induce chemotaxis of fibroblasts (Siegbahn A., 2000) and smooth muscle cells (Sato Y., 1997). The deposition of extracellular lipid in stage III may result from TF-mediated apoptosis of foam cells (Hamuro T., 1998). Deposition of extracellular lipid may promote plaque rupture since plaque instability is promoted by a low collagen: lipid ratio (Stary H.C., 1995). Plaque instability is also advanced due to the incorporation of large thrombi (Stary H.C., 1995). Interestingly, high plasma FVIIa levels have been suggested to augment the size of thrombi formed following plaque rupture (Ruddock V., 1994).

Angiogenesis occurring at the periphery of plaques may also render plaques unstable (Barger A.C., 1990). A requirement for TF in angiogenesis was first reported in relation to studies of tumour metastasis some time ago (Weidener N., 1991, Mueller B.M., 1992, Nawroth P.P. 1994 and Zhang Y., 1994). The involvement of TF in angiogenesis alludes to the possibility that TF may contribute to plaque instability. It should be noted however, that the formation of collateral vessels in atherosclerotic regions might serve to stabilize plaques. Thus the spatial pattern of development of angiogenic vessels and its relation to plaque morphology may determine whether angiogenesis promotes or impedes disease progression.

It has been demonstrated that inhibition of TF activity reduces the density of cellular networks in an *in vitro* model of angiogenesis. In addition, a direct effect of TF on angiogenesis *in vivo* and *in vitro* has been reported recently elsewhere (Watanabe T., 1999 and Kakkar A.K., 1999). These results support a role for TF in mediating angiogenesis. It is speculated that TF may influence the spatial development of angiogenic capillaries in plaques *in vivo*. The microanatomical pattern of TF expression may influence whether the plaque stabilizes via collateral vessel formation, or destabilizes via formation of neoangiogenic capillaries at the plaque peripheries.

7.3 Inhibition of TF in the treatment of disease

TF has a central role in several diseases where secondary hypercoagulability is a feature of disease pathogenesis. Such conditions include cancer (Shoji M., 1998), diabetic retinopathy (Zumbach M., 1997 and Tschoepe D., 1997), thrombotic thrombocytopenic purpura (Morrissey J.H. 2001), anti-phospholipid syndrome (Dabado-Berrios P.M., 1999), deep vein thrombosis (Smith A., 1999). Similarly, the role of TF in angiogenesis makes it a central factor in the pathology of diseases where angiogenesis is a feature including tumour metastasis, atherosclerosis and diabetic microangiopathy.

TF is thus an obvious target for clinical intervention of these pathologies. A number of artificial inhibitors of TF: FVIIa have been developed. Antibodies against TF and FVII have been successfully used in animal models of sepsis and thrombosis to reduce coagulopathy (Morrissey J.H., 2001). In addition, inhibition of TF activity inhibits the progression of atherosclerosis in animal models of atherosclerosis. TFPI inhibits intimal hyperplasia following repeated balloon injury of rabbit aorta (Asada Y., 1998 and Brown D.M., 1996). In addition, blockade of TF inhibits restenosis in a rabbit atherosclerotic femoral artery injury model (Jang Y., 1995). Inhibition of restenosis may arise indirectly from inhibition of angiogenesis since intimal hyperplasia appears to be dependent upon the prior induction of angiogenesis (Moulton K.S., 2000).

Malignant transformation of tumours is dependent upon angiogenesis (Gullino P.M., 1978). The ability of TF to promote angiogenesis (Abdulkadir S.A., 2000 and Koomagi R., 1998) may be involved in the transformation of tumours to a metastatic phenotype. In many tumours, TF expression correlates with the transformation of tumours to a malignant phenotype (Contrino J., 1996, Kakkar A.K., 1999, Abdulkadir S.A., 2000). Since a variety of different angiogenesis inhibitors have been effective in the treatment of cancer (Carmeliet P., 2000), inhibition of TF function also offers a therapeutic target for the development of inhibitors of tumour metastasis.

We have previously found that an apolipoprotein B100-derived 14-mer peptide (KRAD14) potently inhibits the procoagulant activity of TF: FVIIa (Ettelaie C., 1998). The studies reported here extend these results and show that this peptide is effective in inhibiting non-haemostatic functions of TF. The ability of the core sequence of this peptide, KRAD6, to inhibit cytosolic Ca^{2+} transients induced by the TF: FVIIa complex has been demonstrated. In addition, the KRAD14 peptide was found to attenuate cellular network formation in an in vitro model of angiogenesis. A mechanism by which KRAD6 inhibits the activation of FVIIa by TF is proposed (section 4.6.3). Since the TF: FVIIa complex is a desirable target for the development of antithrombotic drugs, the KRAD peptide, or a stable analogue may be useful in the treatment of diseases in which thrombosis and/or angiogenesis is a key feature of the pathogenesis. Moreover, in some model systems, inhibition of TF is effective in decreasing thrombosis without causing the bleeding side effects associated with some antithrombotic agents (Morrissey J.H., 2001).

7.4 Pathways involved in signal transduction induced by TF: FVIIa

The mechanisms involved in the induction of cellular signals by TF: FVIIa (figure 3.1) are the subject of intense investigation. Figure 7.1 is a schematic diagram of the current understanding of TF: FVIIa signalling mechanisms. An understanding of the TF: FVIIa signalling mechanisms are important in the development of therapeutic drugs.

Figure 7.1: TF: FVIIa signal transduction mechanisms

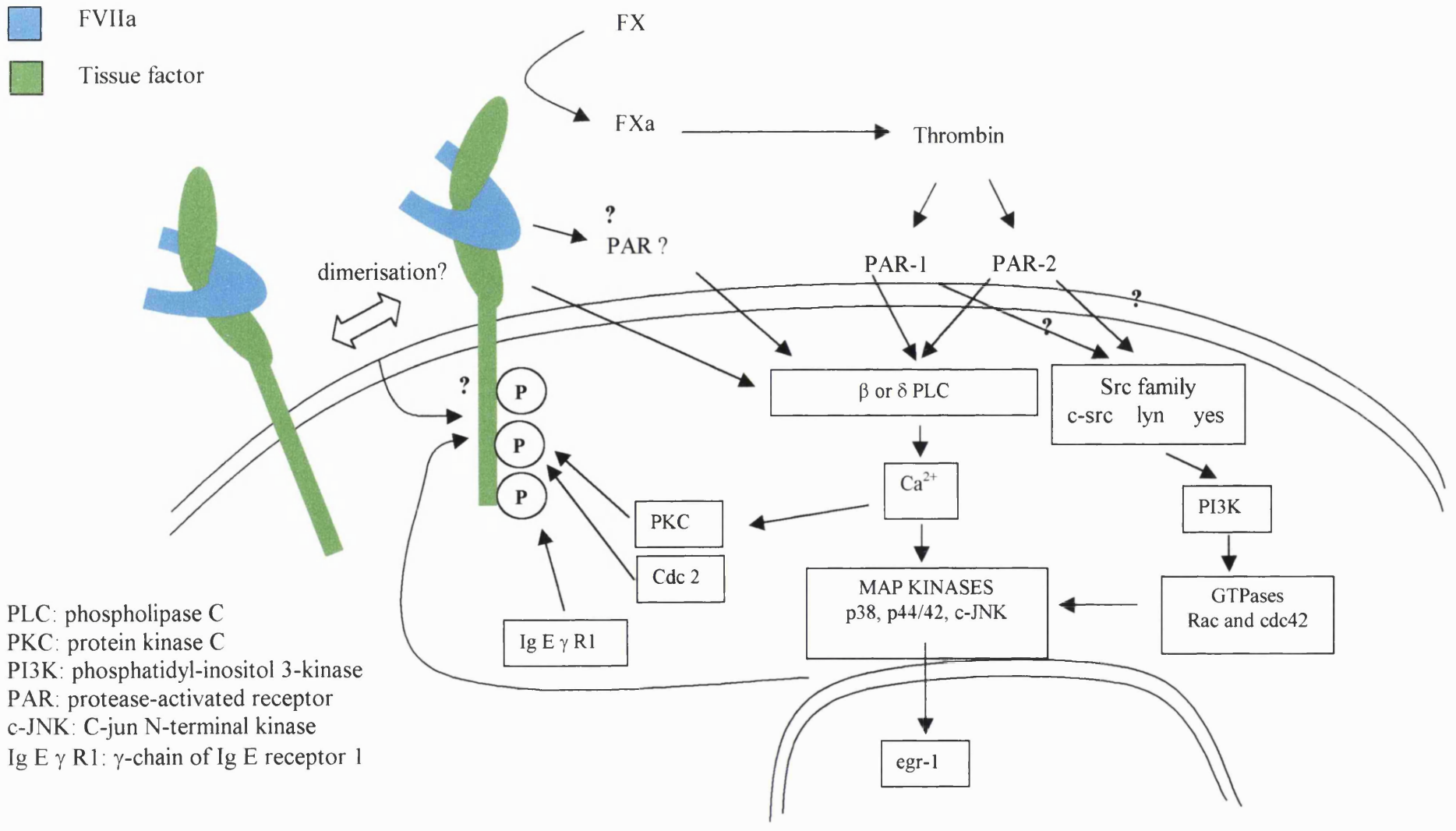

PLC: phospholipase C
PKC: protein kinase C
PI3K: phosphatidyl-inositol 3-kinase
PAR: protease-activated receptor
c-JNK: C-jun N-terminal kinase
Ig E γ R1: γ-chain of Ig E receptor 1

Formation of the TF: FVIIa complex results in the production of intracellular signals via changes in cytosolic Ca^{2+} (Rottingen J.A., 1995), transient tyrosine phosphorylation (Masuda M., 1996), MAP kinase activation (Sorensen B.B., 1999 and Poulsen L.K., 1998) and gene transcription (Camerer E., 2000, Pendurthi U., 1997 and Pendurthi U., 2000). The diversity of pathways illustrates the complexity of TF signalling, which itself is dependent upon cell type.

The mechanism by which TF transduces signals across the cell membrane is unknown. The proteolytic activity of TF: FVIIa is required to induce intracellular activity (Camerer E., 1996, Mueller B.M., 1998 and Sorensen B., 1999). Camerer et al (2000) reported that TF: FVIIa activates the PAR2 receptor, however, this observation has been contradicted by the work of Petersen et al (2000).

Conflicting data exists regarding the involvement of the cytoplasmic domain of TF in cellular signalling. Rottingen J.A. et al (1996) report that the cytoplasmic domain of TF is not involved in the generation of cytoplasmic Ca^{2+} transients. In contrast, Cunningham et al (1999) have shown that PLC-dependent Ca^{2+} signalling requires the cytoplasmic domain of TF. This question was addressed. Wild type and mutant TF were successfully expressed in CHO K1 cells. The effect of mutation upon the induction of cytosolic Ca^{2+} transients was examined using real-time video fluorescence imaging. The baseline cytosolic Ca^{2+} levels in the transfected cells were highly unstable and this precluded determination of the involvement of the cytoplasmic domain of TF in the generation of cytosolic Ca^{2+} signals by the TF: FVIIa complex.

Several studies unequivocally demonstrate the importance of the cytoplasmic domain of TF in certain aspects of signalling by TF: FVIIa. The induction of angiogenesis is dependent upon the cytoplasmic domain of TF (Abe K., 1999). This dependence may relate to the requirement of VEGF in angiogenesis, since the cytoplasmic domain of TF is also required in the induction of VEGF (Abe K., 1999). Interestingly, since the upregulation of the transcriptional factor egr-1 by FVIIa and FXa occurs independently of the cytoplasmic domain of TF (Camerer E., 1999), either egr-1 activity is not required for VEGF induction and angiogenesis or, if egr-1 is involved, loss of its function can be compensated via other transcription factors that do not require the cytoplasmic domain of TF. Similarly the independence of p44/42 MAP kinase activation from the cytoplasmic domain of TF (Sorensen B.B., 1999), suggests that VEGF induction and angiogenesis are either not dependent upon p44/42 MAP kinase activation or MAP kinase activation can be compensated for by alternate signalling pathway(s) that are independent of the cytoplasmic domain of TF.

The involvement of the cytoplasmic domain of TF in angiogenesis, metastasis and cell migration may relate to the interaction of the cytoplasmic domain of TF with ABP-280 (Ott I., 1998) since ABP-280 is a cytoskeletal protein involved in the migration of cells.

Phosphorylation of the cytoplasmic domain is required for the full metastatic effect of TF (Bromberg M.E., 1999), thus the interaction of TF with ABP-280 may be influenced by the phosphorylation status of the cytoplasmic domain. Indeed, the cytoplasmic domain of TF is phosphorylated by PKC (Zioncheck T.F., 1992). In addition it is possible the activation of Rac, cdc42 (Versteeg H.H., 2000), IgE R1 γ-chain (Masuda M., 1996) by the TF: FVIIa complex may be involved either directly or indirectly, in regulating the phosphorylation of the cytoplasmic domain. Interestingly, Rac promotes cytoskeletal reorganisation via modulation of p38 MAP kinase and both have been implicated in tumourigenesis (Versteeg H.H., 2000). In addition, the IgE R1 γ-chain is involved in secretion and aggregation in platelets (Poole A., 1997).

The cytoplasmic domain of TF contains a putative p34cdc2 motif, preliminary data has been obtained that demonstrates the ability of p34cdc2 kinase to phosphorylate the cytoplasmic domain of TF. TF is an immediate early gene (Almendral J.M., 1988) and p34cdc2 kinase is a cell cycle control protein. It is possible that phosphorylation of TF by p34cdc2 (and other kinases) may be involved in the decision of cells to commit to proliferation, apoptosis and differentiation.

The TF mutants that were engineered for studies of Ca^{2+} signalling (figure 3.2) could be employed to determine the involvement of the three serine residues in the induction of VEGF by TF: FVIIa and the interaction of TF with ABP-280.

7.5 The relationship between TF and oxLDL in atherosclerosis

The activity of TF is modulated by LDL and this modulation is dependent upon the oxidation status of the LDL. While nLDL inhibits the activity of TF, oxidised LDL enhances its activity (Ettelaie C., 1995). Both oxLDL and TF are markers of risk of cardiovascular disease; oxLDL correlates closely with the risk of cardiovascular disease (Khoo J.C., 1990) and inhibition of TF: FVIIa reduced restenosis and intimal hyperplasia in a rabbit atherosclerotic femoral artery model (Jang Y., 1995). Furthermore, plasma TF levels are associated with disease activity in unstable angina (Misumi K., 1998, Kaikita K., 1997 and Suefuji H.).

Since oxLDL activates TF, and both are risk factors in atherosclerosis, it is speculated that the proatherogenic properties of oxLDL may be associated with its ability to enhance TF activity.

The research presented here compares the cellular signalling responses invoked by native, minimally modified and oxidized LDL in terms of the characteristics of the patterns of cytosolic Ca^{2+} flux (figure 2.4). In addition, the effect of the concentration of nLDL, mmLDL and oxLDL upon the characteristics of cytosolic Ca^{2+} increases was determined. IT has been demonstrated that native, minimally modified and oxidized LDL elicit distinct patterns of cytosolic Ca^{2+} flux in T24 cells. The overall magnitude of the cytosolic Ca^{2+} response is positively correlated with the extent of oxidative modification of the LDL. This increase in the magnitude of the response was due to lengthening of the decay phase of the Ca^{2+} transient and an increase in the peak amplitude.

nLDL elicits rapid induction of short-lived Ca^{2+} transients. As LDL is progressively oxidized, a parallel increase in the duration of elevated cytosolic Ca^{2+} levels is evident. The sustained elevation of cytosolic Ca^{2+} levels in cells treated with oxLDL lasts for at least 8 minutes. In contrast, the cytosolic Ca^{2+} increases in response to nLDL tends to return to basal after 10-20 seconds. A link between sustained elevated Ca^{2+} and apoptosis has been reported (Trump B.F., 1995). The cytotoxic effect of oxLDL has been documented previously (Morel D.W., 1983). The results presented here suggest that oxLDL-induced apoptosis is executed via sustained elevations of cytosolic Ca^{2+}.

The effect of varying the concentration of each species of LDL (native, minimally modified or fully oxidized) upon the induction of Ca^{2+} transients was also examined. The results demonstrate that for each species of LDL, the magnitude of the response is positively correlated with the concentration of the LDL. Investigation of the basis for the increase in the overall magnitude of the response revealed that increases in the concentration of LDL lead to a lengthening of the decay time and an increase in the peak amplitude of the cytosolic Ca^{2+} increase. Increases in the overall magnitude of the Ca^{2+} responses due to lengthening of the decay time and increases in the peak amplitude must occur via the modulation of signalling pathways that control removal of cytosolic Ca^{2+}.

We investigated whether cytosolic Ca^{2+} transients induced by treatment oxLDL were altered by inhibition of TF activity. Pre-incubation of cells with an inhibitory antibody to TF (TF85G9) had no effect upon the induction of Ca^{2+} transients by oxLDL. However, the response to oxLDL in these experiments was not typical in that sustained elevations of cytosolic Ca^{2+} were not manifest. Due to constraints on equipment access time repetition of the experiment with an oxLDL sample capable of eliciting sustained Ca^{2+} elevations was not possible. The involvement of TF in the cytosolic Ca^{2+} response to oxLDL thus remains unresolved. The effect of TF inhibition upon the induction of cytosolic Ca^{2+} transients by nLDL was also investigated. The induction of cytosolic Ca^{2+} transients by nLDL was found to be independent of TF activity. It can be surmised that the cytosolic Ca^{2+} response to nLDL is not dependent upon the LDL-R binding domain of TF, since the apo B100-derived

KRAD6 peptide did not induce cytosolic Ca^{2+} elevations. Since nLDL inhibits the procoagulant activity of TF, investigation of the effect of pre-incubation of cells with nLDL upon Ca^{2+} signalling induced by the TF: FVIIa complex is also warranted.

7.6 Cytosolic Ca^{2+} and the regulation of cellular responses

The data presented here demonstrates that LDL of discrete concentrations and oxidation status elicit the induction of cytosolic Ca^{2+} increases with distinct kinetic characteristics. The unique kinetics of the Ca^{2+} transients can thus act as a biological fingerprint of the agonist and probably enables the cell to respond appropriately to the agonist type and its concentration. The pathways involved in the induction of the appropriate responses must be regulated by the activity of proteins whose activities are Ca^{2+}-sensitive. The involvement of Ca^{2+}-sensitive proteins in the regulation of biological responses in cells has previously been demonstrated.

It has been observed that frequency modulation is used to vary the intensity and nature of the physiological output (Nelson M.T., 1995, Porter V.A., 1998 and Dolmetsch R.E., 1998). Calmodulin dependent protein kinase II is the best-known example of a decoder that responds to the frequency and longevity of the Ca^{2+} signals. The enzyme is composed of identical subunits that are activated to varying degrees, depending on the frequency of the signal, enabling the kinase to 'count' Ca^{2+} transients. Thus the enzyme activity is coupled to the agonist concentration.

Information is also encoded in the amplitude of Ca^{2+} signals. Cells can interpret modest changes in the concentration of Ca^{2+} and variation of the amplitude of Ca^{2+} signals leads to the activation of different genes (Dolmetsch R.E., 1997).

Cytosolic elevations in Ca^{2+} permit it to act as a signalling messenger, however, sustained elevations can be lethal (Berridge M.J., 1998). The observation that oxLDL elicits sustained elevated Ca^{2+} transients, reported here and elsewhere (Allen S., 1998), is consistent with the cytotoxicity of oxLDL (Negre-Salvayre A., 1992). Sustained elevations of cytosolic Ca^{2+} are associated with apoptosis (Berridges M.J., 1998) indicating that oxLDL induces apoptosis. Since apoptosis determines plaque thrombogenicity upon plaque rupture (Mallat Z., 1997), and plaque instability is determined by the size of the thrombus formed, the induction of apoptosis by oxLDL probably represents one mechanism by which the proatherogenic properties of oxLDL are manifest *in vivo*. Furthermore, the enhancement of plaque thrombogenicity by oxLDL-induced apoptosis may be compounded by the ability of oxLDL to enhance the procoagulant activity of TF, directly and indirectly via phosphatidylserine exposure arising concomitant to cellular apoptosis.

In addition, oxLDL may also promote the progression of atherosclerosis via the promotion of neointimal hyperplasia, since thapsigargin, an inhibitor of cytosolic Ca^{2+} release, inhibits the proliferation of smooth muscle cells in human saphenous vein (George S.J., 1996).

Cells may avoid death by using low amplitude, transient Ca^{2+} signals. When information has to be transmitted over a long period of time, cells use repetitive oscillatory signals (Berridges M.J., 1998). The induction of oscillatory cytosolic Ca^{2+} transients in MDCK2 cells treated with FVIIa was observed. This suggests that the Ca^{2+}-activated signalling pathways that mediate phenotypic responses to FVIIa must be transmitted for extended periods. The reasons for this are unclear however, the sustained Ca^{2+} oscillations may an integral part in the maintenance of a cascade of responses, where Ca^{2+} regulates the early as well as late events.

Cellular Ca^{2+} is derived from two sources, external and internal. Ca^{2+} can enter cells through membrane-spanning channels in the plasma membrane or it may be released internally from endoplasmic or sarcoplasmic reticulum (Berridge M.J., 1993 and Clapham D.E., 1995). When a Ca^{2+} channel opens, a plume of Ca^{2+} forms and then dissipates. The spatio-temporal properties of these plumes differ depending on the nature and location of the channels. These elementary signals either activate localized processes or recruit additional channels to elicit a global cellular response. Furthermore, recruitment of channels in adjacent cells can lead to a coordinated cellular response within a tissue.

7.7 A protective role for nLDL in atherogenesis?

Although high LDL levels were generally indicative of risk of cardiovascular disease, a significant proportion of hypercholesterolaemic subjects do not manifest clinical signs of cardiovascular disease. It appears to be the oxidation status of LDL that is the principle factor determining the risk of cardiovascular disease progression. The ability of antioxidants to attenuate atherosclerosis in human and animal studies (Stephens N.G., 1996 and Hodis H.N., 1992) demonstrates the importance of the oxidation of LDL in atherogenesis. Moreover it has been shown that the rate of progression of atherosclerosis is associated with the titre of antibodies to oxLDL (Khoo J.C., 1990). It would be of interest to determine whether the treatment of cells with nLDL renders the cells refractory to the induction of Ca^{2+} elevations by oxLDL. If this proves to be the case, the presence of nLDL may check the induction of the proatherogenic effects of oxLDL. The presence of nLDL *in vivo* may determine to what extent oxLDL is able to elicit its proatherogenic effects.

7.8 Identification of the biologically active components of LDL

The identification of the active lipoprotein components responsible for the discrete functions of native and oxidized LDL is essential to understanding the proatherogenic

effects of native and oxidized lipoprotein species. Some proatherogenic properties of oxLDL reside in the oxidized lipid fraction (MCP-1 release) while others appear to reside in the modified protein moiety (recognition by the acetyl-LDL receptor).

The work presented here demonstrates that discrete Ca^{2+} transients are elicited by nLDL, mmLDL and oxLDL. The specific lipid peroxidation products that are responsible for these distinct responses are unknown. Identification of the active species in oxLDL is complicated by the fact that the lipid, protein and antioxidant moieties can be attacked. The oxidation products derived from each moiety can undergo multiple secondary and tertiary reactions. Since the extent of the changes varies considerably depending on the pro-oxidant conditions and the availability of antioxidants there is a broad spectrum of oxLDL and no discrete particle corresponding to oxLDL exists (Witzum J.L., 1991).

Some of the products of lipid peroxidation (figure 6.4) have been shown to be capable of eliciting biological responses. The induction of PAI-1, VCAM-1, VEGF, endothelin-1 and P-selectin by oxLDL is mediated by the presence of the phospholipid hydroperoxide, lysophosphatidylcholine (LPC), (Dichtl W., 1999, Kume N., 1992, Ramos M.A., 1998, Boulanger C.M., 1992 and Murohara M., 1996). 7β-hydroperoxycholest-5-en-3β-ol has been identified as the primary cytotoxin of oxLDL (Chisholm G.M., 1994). 9-hydroxyoctadecadienoic acid, derived from either phospholipid or cholesterol ester hydroperoxides, may mediate production of IL-12 by oxLDL in macrophages (Chung S.W., 2000). Oxysterols, derived from cholesterol oxidation, may induce proliferation of smooth muscle cells via the inhibition of gap junctional communication (Zwijsen R.M.L., 1992). Cholestanetriols and 25-hydroxycholesterol may cause injury to endothelial and smooth muscle cells (Peng S., 1991). The presence of 7-hydroxycholesterol and isometric HODES in atheroma has been detected (Carpenter K.L.H., 1993) and attests to the physiological relevance of these oxidation products in atherosclerosis. These previously identified biologically active products of lipoprotein oxidation could be tested to determine if any are responsible for the prolonged elevations of cytosolic Ca^{2+} seen in response to the treatment of cells with oxLDL.

7.9 Therapeutic applications of TF: FVIIa inhibition

TF activity is a key mediator of the progression of atherosclerosis in the early as well as the late stages of the disease. It is suggested that the proatherogenic effects of oxLDL (figure 1.8) may be mediated, at least in part, by its ability to enhance TF activity. Finally, a hypothetical pathway (figure 7.2), in which known cardiovascular risk factors are evaluated in terms of their ability to alter either the activity of TF either directly or via the promotion of LDL oxidation, is presented.

Given that TF activation appears to be a common mechanism underlying the promotion of atherosclerosis arsing from the biological effects of the various cardiovascular risk factors, inhibition of TF activity *in vivo* is a valuable approach to the treatment of atherosclerosis. In addition, inhibition of TF activity is an appropriate target for the treatment of metastatic transformation of tumour cells. A stable homologue of the KRAD6 peptide may facilitate the development of a pharmaceutical reagent for use in the treatment of atherosclerosis and in the prevention of tumour metastasis.

Figure 7.2: Relationship between risk factors for cardiovascular disease and tissue factor activity

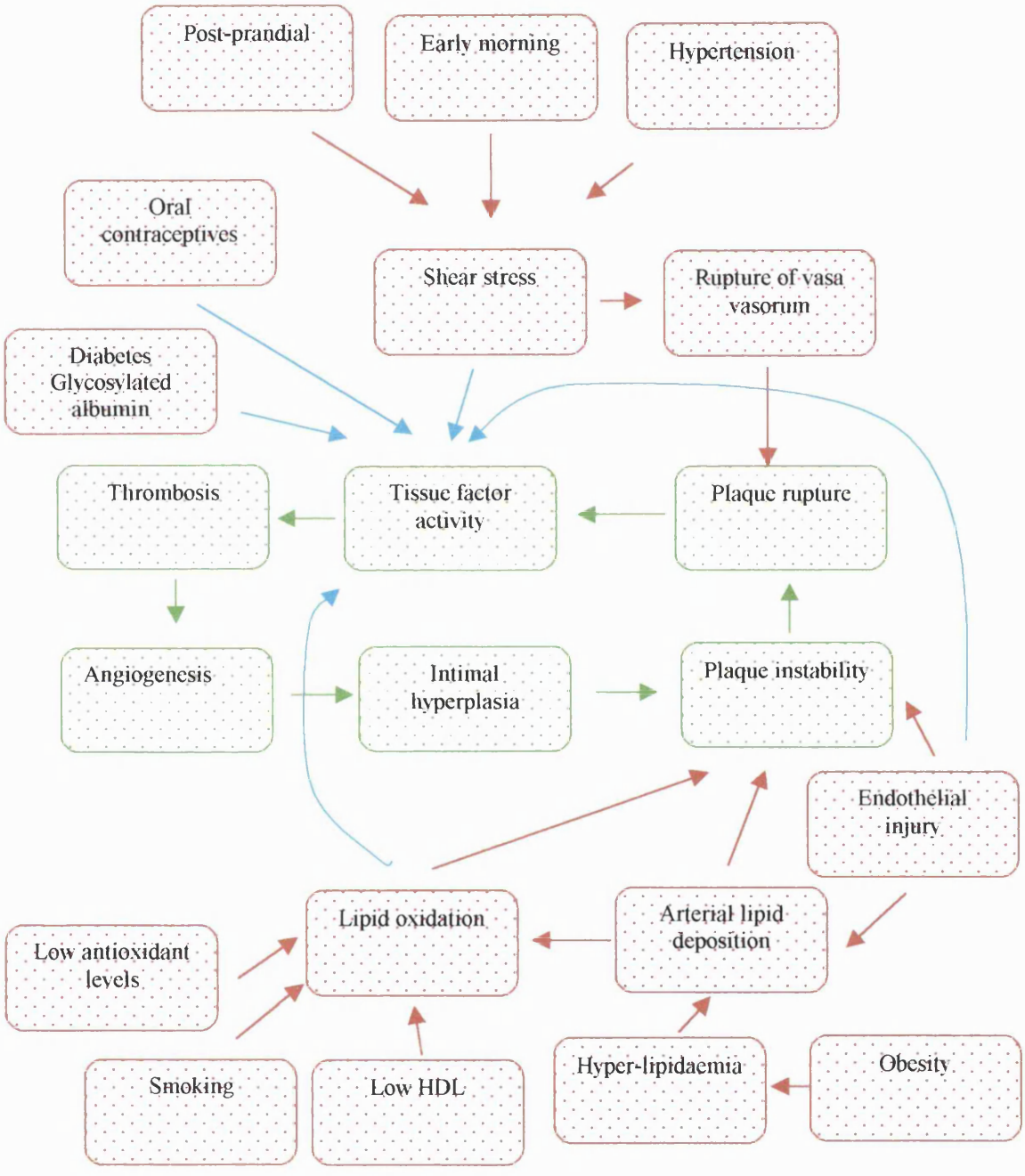

Green boxes: Repeated cycles of injury/rupture and repair results in the progression of plaques.
Red boxes: Risk factors for cardiovascular disease progression.

APPENDICES

APPENDIX 1: Tabulated review of agents that induce or inhibit tissue factor

REFERENCE	CELL TYPE	Inducers of TF	Inhibitors of TF
ALM (1999)	ENDOTHELIUM	PAR-2	
AMIRKHOSRAVI, (1998)		HYPOXIA	
BANKA (1991)	THP-1, macrophages	nLDL, mmLDL, activated platelets	
BIERHAUS (1995)	BOVINE AORTIC ENDOTHELIAL CELLS	TNFα	
BRAND (1994)	ADHERENT MONOCYTES	OxLDL, LPS-free	
CALMUS (1992)	PERIPHERAL BLOOD MONONUCLEAR CELLS	LIVER CIRRHOTICS	
CAMERER (2000)		bFGF	
CAMERER (1999)		TNFα	
CELI (1994)	HUMAN PBMs	CHO CELLS EXPRESSING P-SELECTIN AND	
COLLINS (1995)	HUVEC AND MONOCYTES	CO-CULTURE	
CROSSMAN 1990	HUVEC	PMA	
CROSSMAN 1990	HUVEC	LPS	
CRUTCHLEY (1992)	THP-1		PROSTACYCLIN ANALOGS
CRUTCHLEY (1995)	THP-1	COPPER	ANTIOXIDANTS
CRUTCHLEY (1992)	THP-1	LPS	
CRUTCHLEY (1992)	THP-1	IL1β	
CRUTCHLEY (1992)	THP-1	TNFα	
CRUTCHLEY (1995)	THP-1	LPS	K^+ CHANNEL INHIBITORS
CUI (1994)	EPITHELIAL CELLS	SERUM AND PMA	
DRAKE (1991)	HUMAN AORTIC ENDOTHELIAL CELLS	mmLDL, nLDL	
ERNOFSSON (1996)	HUMAN MONOCYTES	MCP-1	IL4, IL10
ERNOFSSON (1996)	HUMAN MONOCYTES	CRP	IL4, IL10
ERNOFSSON (1996)	HUMAN MONOCYTES	LPS	IL4, IL10
FAN (1995)	HUMAN PBMs	α4 OR β1 INTEGRIN ENGAGEMENT WITH	AP-1 AND NFkB MUTATION IN TF PROMOTER
FROSTEGARD (1990)	MONOCYTES, U937	oxLDL	
FRYER (1993)	ENDOTHELIAL CELLS	HOMOCYSTEINE	
GREGORY (1989)	MONOCYTES	LPS	
GREGORY (1990)	MONOCYTES	CYCLOHEXIMIDE	
HERBERT (1996)	HUMAN MONOCYTES AND ENDOTHELIAL CELLS	LPS	
HERBERT (1993)	ENDOTHELIAL CELLS	LPS, IL1β AND TNFα	CHELERYTHRINE
HERBERT (193)	ENDOTHELIAL CELLS AND MONOCYTES	PYROGEN	IL-4 AND IL-13
HOLSCHERMAN (1997)	MONOCYTES		CYCLOSPORIN A
JUNGI (1994)	HUMAN MACROPHAGES		TGFβ AMD IL-10

JUNGI (1996)	MONOCYTE	CD40 ENGAGEMENT	
KANEKO (1994)	U937	MERCURY COMPOUNDS	
KORNBERG (1994)	MONOCYTES	ANTI CARDIOLIPIN ANTIBODIES	
LANGER (1999)	ENDOTHELIAL CELLS	PAR-2	
LAWSON (1995)		HYPOXIA	
LESNIK (1992)	MONOCYTES	EXOGENOUS FREE CHOLESTEROL	
LESNIK (1992)	ENDOTHELIUM	mmLDL	
LESNIK (1992)	ENDOTHELIUM	oxLDL	
LIN (1994)	HUMAN PBMs	LIGATION OF β1 INTEGRINS	HERBIMYCIN, GENISTEIN
LIN (1997)	HUVEC	LAMINAR SHEAR STRESS	
LO (1995)	HUVEC, THP-1, U937, MM6	ADHESION TO ENDOTHELIUM	anti e-selectin, anti vcam-1, anti icam-1, anti CD11/CD18
LYBERG (1981)	HUMAN MONOCYTES	PHORBOL ESTERS	
MACKMAN (1994)	HUMAN MONOCYTES	LPS	PROTEASE INHIBITORS
MACKMAN (1991)	THP-1	LPS	
MARCHANT (1995)	HUMAN MONOCYTES	oxLDL	α-TOCOPHEROL (200uM), PROBUCOL (50uM)
MARTIN (1993)	HUVEC	TNFα	IL4
MESZAROS (1994)	MONOCYTES	LPS	RECOMBINANT FRAGMENT OF BACTERICIDAL PERMEABILITY-INCREASING PROTEIN
MULDER (1994)	ENDOTHELIUM	TNFα	
NAPOLEONE (1997)	ENDOTHELIAL CELLS	MONOCYTES	
NISHIMURA	MONOCYTES	IL-2 AND VARIOUS CYTOKINES	
NOGUCHI (1989)	HUMAN ENDOTHELIAL CELLS	A NOVEL TUMOUR-DERIVED PROTEIN	
OETH (1997)	HUMAN MONOCYTES	LPS	
OLLIVIER (1993)	HUMAN MONOCYTES	ENDOTOXIN	PENTOXYFYLLINE
OSNOS (1996)	MONOCYTES	IL-1	IL-4, IL-10 AND IL-13
PARK (1997)	HUMAN PBMs	LPS	TFPI
QUIRK (1996)		OESTROGEN	
RANGANATHAN, (1991)		TGFβ	
SATTA (1994)	HUMAN MONOCYTES	LPS	
STEPHENS (1994)	BONE MARROW MONOCYTE PROGENITORS	PROMYELOCYTIC LEUKAEMIA	
TEDESCO (1997)	HUVEC	INACTIVE TERMINAL COMPLEMENT	
VAN DER LOGT 1992	Hu PBM	LPS	
XUEREB, (1997)		PDGF-ββ	
ZUCKER (1998)	ENDOTHELIAL CELLS	VEGF	

Appendix 2

Visual Basic Macros for automated digital image processing

Plot XY; plots and print graphs of cytosolic calcium levels versus time
MeanStDev ; calculates the means and standard deviations of cytosolic calcium levels
PeakAmpDecay; calculates the peak amplitude and decay times of cytosolic calcium levels

Sub PlotXY()

```
'PlotXY Macro
'Macro recorded 14/10/98 by Nickie James

Dim Counter As Integer
Dim Offset As Integer
Dim n As Integer, i As Integer, J As Integer, Startpos As Integer
Dim Wide As Integer, High As Integer, Wide1 As Integer, Callit As String

'Set Wide1 flag to 0 outside of for next loop j
Wide1 = 0

'Activate ImagingMacro and set the number of files to analyse as the value in cell A15
Windows("ImagingMacro.XLS").Activate
n = Range("A15").Value

'Open files from a: drive listed in ImagingMacro from cell A2 to cell A14
For J = 1 To n
   Windows("ImagingMacro.XLS").Activate
   Callit = Cells(J + 1, 1)
   Workbooks.OpenText Filename:="a:\" & Callit & ".plt"
   Sheets(Callit).Select

   'Find "ND Index Time (msec)"(MUST BE IN COLUMN 1) and set counter as row
number
   For i = 1 To 100
      If Cells(i, 1) = "ND Index Time (msec)" Then Counter = i: GoTo 1
   Next i
1
   'Measure width (wide = no of columns) of datablock
   For i = 1 To 26
      If Cells(Counter, i) = "" Then Wide = i - 1: GoTo 5
   Next
5
   'Measure height of data block (must be <200) including ND index time cell
   For i = 1 To 199
      If Cells((Counter + i - 1), 1) = "" Then High = i - 1: GoTo 10
   Next
10
   'Format number cells to 2dp
   Range(Cells((Counter + 1), 2), Cells((Counter + High - 1), Wide)).Select
   Selection.NumberFormat = "0.00"
```

```
'Format time to 0dp
Range(Cells((Counter + 1), 1), Cells((Counter + High - 1), 1)).Select
Selection.NumberFormat = "0"

'Divide time column by 1000 to give seconds
For i = 1 To High - 1
   Cells(Counter + i, 1) = Cells(Counter + i, 1) / 1000
Next

'Number the incoming cells individually
For i = 1 To Wide - 1
  Cells(Counter, i + 1) = i
Next

'Plot xyscatter graph, send to printer and save file in .xls format
Range(Cells(Counter, 1), Cells((High + Counter - 1), Wide)).Select
Charts.Add
ActiveChart.ChartType = xlXYScatterSmooth
Dim R As String, AA As Integer, B As Integer
AA = Asc("A")
B = Asc("B")
R = Chr(AA) & (Counter + 1) & ":" & Chr(AA + Wide - 1) & (Counter + High - 1)
ActiveChart.SetSourceData Source:=Sheets(Callit).Range(R), PlotBy:=xlColumns
ActiveChart.Location Where:=xlLocationAsNewSheet
 Sheets("Chart1").Select
With ActiveChart
   .HasTitle = True
   .ChartTitle.Characters.Text = (Callit)
   .Axes(xlCategory, xlPrimary).HasTitle = True
   .Axes(xlCategory, xlPrimary).AxisTitle.Characters.Text = "Time (seconds)"
   .Axes(xlValue, xlPrimary).HasTitle = True
   .Axes(xlValue, xlPrimary).AxisTitle.Characters.Text = _
   "Ca2+ -bound Fura2 : Ca2+ -free Fura2"
End With

With ActiveChart.Axes(xlCategory)
   .HasMajorGridlines = False
   .HasMinorGridlines = False
End With

With ActiveChart.Axes(xlValue)
   .HasMajorGridlines = False
   .HasMinorGridlines = False
End With

ActiveChart.PlotArea.Select

With Selection.Border
   .Weight = xlThin
   .LineStyle = xlNone
End With

Selection.Interior.ColorIndex = xlNone
ActiveWindow.SelectedSheets.PrintOut Copies:=1, Collate:=True
Windows(Callit & ".plt").Activate
```

```
   ActiveWorkbook.SaveAs Filename:="C:\My Documents\" & Callit & ".xls"
   ActiveWorkbook.Close
Next J

   Stop
   End Sub
```

Sub MeanStDev()

```
'Calcium1.xls must be opened and ImagingMacro.xls

Dim firstblank As Integer, Wide As Integer, BeginNumberBasal As Integer,
StopNumberBasal As Integer
Dim BeginRowBasal As Integer, EndRowBasal As Integer, Relativerow As Integer, AA As
Integer, _
   TransferMean As Single, FileNo As Integer, J As Integer, K As Integer, _
   Counter As Integer, TransferStDev As Single, CellNo As Integer

Dim Callit As String, R As String

'Loop as many times as files to analyse (equal to number in A15 in ImagingMacro.xls)
Windows("ImagingMacro.XLS").Activate
FileNo = Cells(15, 1)
For J = 1 To FileNo

   'Open and activate files (loopwise) listed from cell A2 downwards (Max = 13)
   Windows("ImagingMacro.XLS").Activate
   Callit = Cells(J + 1, 1)

   Workbooks.Open Filename:="I:\" & Callit & ".xls"
   Windows(Callit & ".xls").Activate
   Sheets(Callit).Select
   ' Find ND Index Time (msec) cell and set counter as row number
   For i = 1 To 100
      If Cells(i, 1) = "ND Index Time (msec)" Then Counter = i: GoTo 1
   Next i
1

   ' measure width (no of columns) of datablock
   For i = 1 To 26
      If Cells(Counter, i) = "" Then Wide = i - 1: GoTo 5
   Next

5  'loop as many times as cells to analyse
   For K = 1 To Wide - 1

      'Obtain frame number from ImagingMacro.xls cell A16 for beginning of basal block
      Windows("ImagingMacro.xls").Activate
      BeginNumberBasal = Cells(16, 1)
      BeginNumberBasal = BeginNumberBasal + Counter
      'Obtain frame number from ImagingMacro.xls cell A17 for end of basal block
      StopNumberBasal = Cells(17, 1).Value
      StopNumberBasal = StopNumberBasal + Counter

     'Obtain frame number from ImagingMacro.xls cell A18 for beginning of respone block
```

```
    Windows("ImagingMacro.xls").Activate
    BeginNumberResponse = Cells(18, 1)
    BeginNumberResponse = BeginNumberResponse + Counter
    'Obtain frame number from ImagingMacro.xls cell A19 for end of response block
    StopNumberResponse = Cells(19, 1).Value
    StopNumberResponse = StopNumberResponse + Counter

    'Goto file containing data to analyse
    Windows(Callit & ".xls").Activate

    'Define range of cells to determine mean and standard deviation of basal
    ' N.B. range is defined relative to the location of the cell
    ' containing the formula, with syntax e.g. (R[-3]C[-1]:R[-20]C)
    BeginRowBasal = BeginNumberBasal - 200
    EndRowBasal = StopNumberBasal - 200

    'Define range of cells to determine mean and standard deviation of response
    ' N.B. range is defined relative to the location of the cell
    ' containing the formula, with syntax e.g. (R[-3]C[-1]:R[-20]C)
    BeginRowResponse = BeginNumberResponse - 200
    EndRowResponse = StopNumberResponse - 200

    'Select cell in row 200 of the current column
    AA = Asc("A")
    R = Chr(AA + K) & 200
    Range(R).Select

    'Make the output of the selected cell be the average of the pre-treatment Ca2+ level
    ActiveCell.FormulaR1C1 = "=AVERAGE(R[" & BeginRowBasal & "]C:R[" &
EndRowBasal & "]C)"
    Selection.NumberFormat = "0.00"
    TransferMean = ActiveCell.Value

    'Find first blank row in third column of Calcium1.xls
    Windows("Calcium1.xls").Activate
    For i = 1 To 5000
      If Cells(i, 3) = "" Then Cells(i, 3) = TransferMean: Selection.NumberFormat =
"0.00": GoTo 10
      'SelectCell = (i, 3): GoTo 10
    Next i
10
    'Select cell in row 201 of the current column
    Windows(Callit & ".xls").Activate
    RR = Chr(AA + K) & 201
    Range(RR).Select

    'Make the output of the selected cell be the average of the pre-treatment Ca2+ level
    ActiveCell.FormulaR1C1 = "=STDEV(R[" & BeginRowBasal - 1 & "]C:R[" &
EndRowBasal - 1 & "]C)"
    Selection.NumberFormat = "0.00"
    TransferStDev = ActiveCell.Value

    'Find first blank row in sixth column of Calcium1.xls
    Windows("Calcium1.xls").Activate
    For i = 1 To 5000
```

```
        If Cells(i, 6) = "" Then Cells(i, 6) = TransferStDev: Selection.NumberFormat =
"0.00": GoTo 15
    Next i
15
    'Select cell in row 202 of the current column
    Windows(Callit & ".xls").Activate
    RR = Chr(AA + K) & 202
    Range(RR).Select

    'Make the output of the selected cell be the average of the pre-treatment Ca2+ level
    ActiveCell.FormulaR1C1 = "=AVERAGE(R[" & BeginRowResponse - 2 & "]C:R["
& EndRowResponse - 2 & "]C)"
    Selection.NumberFormat = "0.00"
    TransferStDev = ActiveCell.Value

    'Find first blank row in fourth column of Calcium1.xls
    Windows("Calcium1.xls").Activate
    For i = 1 To 5000
        If Cells(i, 4) = "" Then Cells(i, 4) = TransferStDev: Selection.NumberFormat =
"0.00": GoTo 20
    Next i
20
    'Select cell in row 203 of the current column
    Windows(Callit & ".xls").Activate
    RR = Chr(AA + K) & 203
    Range(RR).Select

    'Make the output of the selected cell be the average of the pre-treatment Ca2+ level
    ActiveCell.FormulaR1C1 = "=STDEV(R[" & BeginRowResponse - 3 & "]C:R[" &
EndRowResponse - 3 & "]C)"
    Selection.NumberFormat = "0.00"
    TransferStDev = ActiveCell.Value

    'Find first blank row in seventh column of Calcium1.xls
    Windows("Calcium1.xls").Activate
    For i = 1 To 5000
        If Cells(i, 7) = "" Then Cells(i, 7) = TransferStDev: Selection.NumberFormat =
"0.00": GoTo 25
    Next i
25
    'Write filename to first column of Calcium1.xls
    For i = 1 To 5000
        If Cells(i, 1) = "" Then Cells(i, 1) = Callit: GoTo 30
    Next i
30
    'Write cell number to second column of Calcium1.xls
    Windows(Callit & ".xls").Activate
    CellNo = Cells(Counter, K + 1)
    Windows("Calcium1.xls").Activate
    For i = 1 To 5000
        If Cells(i, 2) = "" Then Cells(i, 2) = CellNo: GoTo 35
    Next i
35
  Next K
```

```
Windows(Callit & ".xls").Activate
'ActiveWorkbook.SaveAs Filename:="c:" & Callit & ".xls"
ActiveWorkbook.Close

Next J
   'Save Calcium1.xls
   Windows("Calcium1.xls").Activate
   ActiveWorkbook.SaveAs Filename:="c:Calcium1.xls"

Stop
End Sub
```

Sub PeakAmpDecay()

```
'Calcium1.xls and ImagingMacro.xls must be open

Dim ResponseFrames As Integer, Peak As Integer, Frame(1 To 200) As Single
Dim firstblank As Integer, Wide As Integer, BeginNumberBasal As Integer,
StopNumberBasal As Integer
Dim BeginRowBasal As Integer, EndRowBasal As Integer, Relativerow As Integer, AA As
Integer, _
   TransferMean As Single, FileNo As Integer, J As Integer, K As Integer, _
   Counter As Integer, TransferStDev As Single, CellNo As Integer, DecayTime As Single,
_
   HalfPeak As Single, UnderHalfPeak As Single
Dim Callit As String, R As String

'Loop as many times as files to analyse (equal to number in A15 in ImagingMacro.xls)
Windows("ImagingMacro.XLS").Activate
FileNo = Cells(15, 1)
For J = 1 To FileNo

   'Open and activate files (loopwise) listed from cell A2 downwards (Max = 13)
   Windows("ImagingMacro.XLS").Activate
   Callit = Cells(J + 1, 1)
   Workbooks.Open Filename:="I:\" & Callit & ".xls"
   Windows(Callit & ".xls").Activate
   Sheets(Callit).Select

   ' Find ND Index Time (msec) cell and set counter as row number
   For i = 1 To 100
      If Cells(i, 1) = "ND Index Time (msec)" Then Counter = i: GoTo 1
   Next i
1
   ' measure width (no of columns) of datablock
   For i = 1 To 26
      If Cells(Counter, i) = "" Then Wide = i - 1: GoTo 5
   Next

5  'loop as many times as cells to analyse
   For K = 1 To Wide - 1

      'Obtain frame number from ImagingMacro.xls cell A16 for beginning of basal block
      Windows("ImagingMacro.xls").Activate
      BeginNumberBasal = Cells(16, 1)
      BeginNumberBasal = BeginNumberBasal + Counter
```

```
    'Obtain frame number from ImagingMacro.xls cell A17 for end of basal block
    StopNumberBasal = Cells(17, 1).Value
    StopNumberBasal = StopNumberBasal + Counter

    'Find average of basal to set baseline value
    'Define range of cells to determine mean and standard deviation of basal
    ' N.B. range is defined relative to the location of the cell
    ' containing the formula, with syntax e.g. (R[-3]C[-1]:R[-20]C)
    BeginRowBasal = BeginNumberBasal - 200
    EndRowBasal = StopNumberBasal - 200
    basalframes = StopNumberBasal - BeginNumberBasal + 1

    'Obtain frame number from ImagingMacro.xls cell A18 for beginning of response
block
    Windows("ImagingMacro.xls").Activate
    BeginNumberResponse = Cells(18, 1)
    BeginNumberResponse = BeginNumberResponse + Counter
    'Obtain frame number from ImagingMacro.xls cell A19 for end of response block
    StopNumberResponse = Cells(19, 1).Value
    StopNumberResponse = StopNumberResponse + Counter

    'calculate number of frames in response block to analyse
    ResponseFrames = StopNumberResponse - BeginNumberResponse + 1

    'Goto file containing data to analyse
    Windows(Callit & ".xls").Activate

    'Select cell in row 200 of the current column
    AA = Asc("A")
    R = Chr(AA + K) & 200
    Range(R).Select

    'Make the output of the selected cell be the average of the pre-treatment Ca2+ level
    ActiveCell.FormulaR1C1 = "=AVERAGE(R[" & BeginRowBasal & "]C:R[" &
EndRowBasal & "]C)"
    Selection.NumberFormat = "0.00"
    TransferMean = ActiveCell.Value * 0.68

    'Find first blank row in third column of Calcium1.xls
    Windows("Calcium1.xls").Activate
    For i = 1 To 5000
      If Cells(i, 3) = "" Then Cells(i, 3) = TransferMean: Selection.NumberFormat =
"0.00": GoTo 10
    Next i
10
    'Goto file containing data to analyse
    Windows(Callit & ".xls").Activate

    'Calculate peak amplitude using basal average as starting value
    PeakValue = TransferMean
    For Peak = (1 + basalframes) To (ResponseFrames + basalframes)
    If Cells(Peak + Counter, K + 1) > PeakValue _
      Then PeakValue = Cells(Peak + Counter, K + 1): PeakFrame = Peak
    Next Peak
    PeakValue = PeakValue - TransferMean
```

```
    'Output peak amplitude value to Calcium1.xls
    'Find first blank row in fourth column of Calcium1.xls
    Windows("Calcium1.xls").Activate
    For i = 1 To 5000
      If Cells(i, 4) = "" Then Cells(i, 4) = PeakValue: Selection.NumberFormat = "0.00":
GoTo 20
    Next i
20
     'Goto file containing data to analyse
    Windows(Callit & ".xls").Activate

    'Calculate time (number of frames x 5) for response to return halfway back to basal
    DecayTime = 0
    HalfPeak = (TransferMean + (PeakValue / 2))
    'For FindDecay = (1 + PeakFrame) To (36)
    For FindDecay = (1 + PeakFrame) To (ResponseFrames + basalframes)
    UnderHalfPeak = Cells(Counter + FindDecay, K + 1).Value
    If UnderHalfPeak < HalfPeak Then DecayTime = ((FindDecay - PeakFrame) * 5):
GoTo 21
    Next FindDecay
21
    'If response does not decay below half basal within experimental
    ' time course, output a value of 1000
    If UnderHalfPeak > HalfPeak Then DecayTime = 1000

   'Output DecayTime value to fifth column of Calcium1.xls
   Windows("Calcium1.xls").Activate
   For i = 1 To 5000
   If Cells(i, 5) = "" Then Cells(i, 5) = DecayTime: Selection.NumberFormat = "0.00":
GoTo 22
   Next i
22
    'Calculate area under response curve using average of basal as baseline
    'Read values into an array (make sure value higher than baseline)
    For i = 1 To ResponseFrames
      Windows(Callit & ".xls").Activate
      If Cells(Counter + i + basalframes, K + 1) > TransferMean _
      Then Frame(i) = Cells(Counter + i + basalframes, K + 1) _
      Else Frame(i) = TransferMean
    Next i

    'Read back array values and apply the trapezium rule to integrate area under curve
    Trapezium = 0
    For i = 2 To ResponseFrames - 1
      CurrentValue = Frame(i)
      Trapezium = CurrentValue + Trapezium
    Next i
    Trapezium = Trapezium + Frame(1) + Frame(ResponseFrames)
    Trapezium = 2.5 * Trapezium

    'Output Trapezium Value to Calcium1.xls
    'Find first blank row in sixth column of Calcium1.xls
    Windows("Calcium1.xls").Activate
    For i = 1 To 5000
```

```
        If Cells(i, 6) = "" Then Cells(i, 6) = Trapezium: Selection.NumberFormat = "0.00":
GoTo 25
      Next i
25
     'Write filename to first column of Calcium1.xls
      For i = 1 To 5000
        If Cells(i, 1) = "" Then Cells(i, 1) = Callit: GoTo 30
      Next i
30
      'Write cell number to second column of Calcium1.xls
      Windows(Callit & ".xls").Activate
      CellNo = Cells(Counter, K + 1)
      Windows("Calcium1.xls").Activate
      For i = 1 To 5000
        If Cells(i, 2) = "" Then Cells(i, 2) = CellNo: GoTo 35
      Next i
35
   Next K

Windows(Callit & ".xls").Activate
ActiveWorkbook.SaveAs Filename:="c:" & Callit & ".xls"
ActiveWorkbook.Close

Next J
   'Save Calcium1.xls
   Windows("Calcium1.xls").Activate
   ActiveWorkbook.SaveAs Filename:="c:Calcium1.xls"

Stop
End Sub
```

Appendix 5: Sequences of the pIND and pVgRXR plasmids

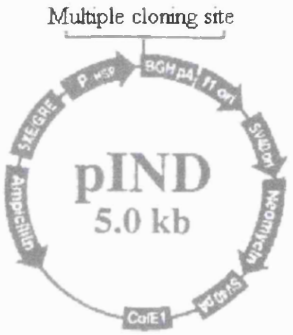

pA: polyadenylation sequence
E/GRE: ecdysone/ glucocorticoid response elements
ColE1: pUC-derived high copy number replication origin
P-HSP: Heat shock promoter
f1 ori: f1 origin for single strand rescue
BGH: bovine growth hormone
Ampicillin: ampicillin resistance gene
Neomycin: neomycin resistance gene

ColE1: pUC-derived high copy number replication origin
pA: polyadenylation sequence
f1 ori: f1 origin for single strand rescue
BGH: bovine growth hormone
Zeocin: Zeocin resistance gene
P CMV: cytomegaloviral promoter
P RSV: rous sarcoma virus promoter

Appendix 4:
Functionally important residues identified in TF

A; FVII activation, B; FVII binding, I; interface domain, H; hydrogen bonding

Residue	Function	Observations	Citations
N-module fibronectin repeat			
Loop A-B; 15-20			
K15		Solvent exposed face of 3 stranded sheet	Muller Y.A. (1994)
S16A	I	30-98% loss of function	Ruf W. (1994)
T17A	I	30-98% loss of function	Ruf W. (1994)
F19	I	Hydrophobic core of domain interface, 30-98% loss of function	Harlos K. (1994), Ruf W. (1994)
K20	**A** B H	Solvent exposed face of 3 stranded sheet, H-bonds to C70L and G78L, 30-98% loss of function	Muller Y.A. (1994), Banner D. W. (1996), Ruf W. (1994) Schullek J.R. (1994), Kelley R.F. (1995), Lee G.F. (1998), Martin D.M. (1995), Gibbs C.S. (1994)
K20A/D58W		Mutant is defective for X activation	Lee G.F. (1998)
Strand B; 21-26			
I22	B	R79L, 30-98% loss of function, binds FVII but is not involved in catalysis	Banner (1996), Ruf W. (1994), Schullek J.R. (1994), Martin D.M. (1995)
E24	B, H	H-bond to R79L, solvent exposed face of 3 stranded sheet	Banner D.W. (1996), Muller Y.A. (1994)
E24A/E26A		30-98% loss of function	Ruf W. (1994)
W25		Strictly conserved in cytokine receptor family	Muller Y.A. (1994)
E26		Solvent exposed face of 3 stranded sheet	Muller Y.A. (1994)
K28		Solvent exposed face of 3 stranded sheet	Muller Y.A. (1994)
Strand C; 32-40			
V33		Exposed hydrophobic residue	Harlos K. (1994)
Q37	B, H	H-bond to R74T, S47T and F275H, convex binding surface	Banner D.W. (1996), Martin D.M. (1995)
S39	B, H	H-bond to W45T and R277H	Banner D.W. (1996)

S39/T40/S42		43% decrease in function	Ruf W. (1994)
G43	B, H	H-bond to W45T and R277H	Banner D.W. (1996)
D44	A	Induces conformational change in FVII, convex binding surface	Gibbs C.S. (1994), Martin D.M. (1995)
W45	B A H	Induces conformational change in FVII, binds to R277H, H-bonds to S39T, G43T and F275H, H-bond to H_2O, solvent exposed side of 4 stranded sheet convex binding surface	Martin D.M. (1995), Banner D.W. (1996), Kelley R.F. (1995), Muller Y.A. (1994), Gibbs C.S. (1994)
Strand C'; 46-52			
K46	B	FVIIa binding, convex binding surface	Gibbs C.S. (1994), Martin D.M. (1995)
S47	H	H-bond to Q37T	Banner D.W. (1996)
K48	B, H	H-bond to E77L, convex binding surface	Banner D.W. (1996), Martin D.M. (1995)
C49		Disulphide bridge to C57 in strand E	
F50	B	Exposed hydrophobic residue, buried by Q88L to N93L	Muller Y.A. (1994), Banner D.W. (1996)
Y51		Exposed hydrophobic residue	Muller Y.A. (1994)
Strand E; 55-59			
T53A/T55A		40% loss of function	Ruf W. (1994)
D54		Solvent exposed side of 3stranded sheet	Muller Y.A. (1994)
E56	B, H	H-bond to R79L, solvent exposed side of 4stranded sheet	Banner D.W. (1996), Muller Y.A. (1994)
D58	B, H	H-bond to G78L, but not involved in catalysis, solvent exposed side of 3 stranded sheet	Banner D.W. (1996), Martin D.M. (1995), Schullek J.R. (1994), Kelley R.F. (1995), Lee G.F. (1998), Muller Y.A. (1994)
α1; 60-64			
D61		Solvent exposed side of 3 stranded sheet	Muller Y.A. (1994)
V64		Hydrophobic core of domain interface	Harlos K. (1994)
V67		Hydrophobic core of domain interface, 53% decrease in function	Harlos K. (1994), Ruf W. (1994)
Strand F; 70-79			
Y71		98% decrease in function	Ruf W. (1994)

R74	B, H	Binds to M306H, H-bond to Q37T, 3 H-bonds to H_2O	Banner D.W. (1996),
F76	B	Exposed hydrophobic residue, binds to M306H	Muller Y.A. (1994)
Y78		Exposed hydrophobic residue	Muller Y.A. (1994)
Strand G; 93-99			
P92	B	Exposed hydrophobic residue, binds to M306H	Harlos K. (1994), Banner D.W. (1996)
Y94	B H	Exposed hydrophobic residue, binds to M306H, H-bonds to Q308H and D309H	Muller Y.A. (1994), Banner D.W. (1996), Kelley R.F. (1995)
N96	B	H-bond to D309H	Banner D.W. (1996)
Linker sequence P102-N107			
Y103-T106		Mutation affects function and not major structure	Martin D.M. (1995)
P102	I	Hydrophobic core of domain interface	Martin D.M. (1995)
Y103	I	Hydrophobic core of domain interface	Harlos K. (1994)
L108	I	Hydrophobic core of domain interface	Harlos K. (1994)
Q110	B, H	H-bond to Q64L and S43L	Banner D.W. (1996), Martin D.M. (1995), Gibbs C.S. (1994)
C-module fibronectin repeat			
R131	B	binds F71L, 30-50% decrease in function	Banner D.W. (1996), Ruf W. (1994)
Loop P; L133-136			
L133	B	Hydrophobic core of domain interface, binds to F71L	Harlos K. (1994), Banner D.W. (1996)
V134	I	Hydrophobic core of domain interface	Harlos K. (1994)
R135	B	FVIIa binding, but not involved in catalysis	Schullek J.R. (1994), Gibbs C.S. (1994), Martin D.M. (1995)
Loop Q; 138-141			
T139A/S142A		30-50% decrease in function	Ruf W. (1994)
F140	B	Binds to F71L, Cα atom 13.1A from Cα of K20, but is not involved in catalysis	Banner D.W. (1996), Schullek J.R. (1994), Kelley R.F. (1995), Gibbs C.S. (1994), Martin D.M. (1995)
α2; 143-D150			
L143	I	Hydrophobic core of domain interface	Harlos K. (1994)

D145A		30-50% decrease in function	Ruf W. (1994)
V146	I	Hydrophobic core of domain interface, 30-50% decrease in function	Harlos K. (1994), Ruf W. (1994)
F147		Hydrophobic core of domain interface, 30-50% decrease in function	Harlos K. (1994), Ruf W. (1994)
K149-D150		Helical turn	Harlos K. (1994)
Strand C; 152-158			
Y157		Buried beneath K165/K166, confers stability	Martin D.M. (1995)
W158		Binds to V207T, buried beneath K165/K166, confers stability	Banner D.W. (1996), Martin D.M. (1995)
Loop; 159-166			
K159	A	FVII activation	Martin D.M. (1995)
S163	A	FVII activation	Martin D.M. (1995)
Strand C'; 166-170			
K165/K166		Most significant contributors to FX activation	Roy S. (1991)
Strand F; 185-193			
C186	S	Disulphide bridge to C209 in strand G, S atoms are solvent-exposed	
C186-C209	B	Binds to F31L	Banner D.W. (1996)
Strand G; 196-210			
V198	I	Hydrophobic core of domain interface, 30-80% decrease in function	Harlos K. (1994), Ruf W. (1994)
N199A		30-80% decrease in function	Ruf W. (1994)
R200A/K201A		30-80% decrease in function	Ruf W. (1994)
V207	B	Binds to W158T and F40L	Banner D.W. (1996), Martin D.M. (1995), Gibbs C.S. (1994)

Appendix 5:
Conservation of primary amino acid sequence of tissue factor sequences in human, rabbit, mouse and guinea pig.

Row 1: exon boundaries; Row 2: β-strand letter code; Row 3: Residue number; Rows 4-7: human, rabbit and mouse and guinea pig sequences respectively.
☺ Residue identical to corresponding residue in human TF sequence.
Colour coding of amino acids: positive, hydrophobic, uncharged, hydrophilic, negative, aromatic

1	2.						A	A	A	A	A	A	A	A
1	2	3	4	5	6	7	8	9	10	11	12	13	14	15
S	G	T	T	N	T	V	A	A	Y	N	L	T	W	K
		A	D	T	☺	G	R	☺	☺	☺	☺	☺	☺	☺
		A	G	I	P	E	K	☺	F	☺	☺	☺	☺	I
		E	G	I	P	☺	K	P	☺	☺	☺	☺	☺	☺

A	A			B	B	B	B	B	B	B				
16	17	18	19	20	21	22	23	24	25	26	27	28	29	30
S	T	N	F	K	T	I	L	E	W	E	P	K	P	V
☺	☺	☺	☺	☺	☺	☺	☺	☺	☺	☺	☺	☺	S	I
☺	☺	D	☺	☺	☺	☺	☺	☺	☺	☺	Q	☺	☺	T
☺	☺	☺	☺	☺	☺	☺	☺	☺	☺	☺	☺	☺	☺	I

								2	3					
	C	C	C	C	C	C	C	C	C					
31	32	33	34	35	36	37	38	39	40	41	42	43	44	45
N	Q	V	Y	T	V	Q	I	S	T	K	S	G	D	W
D	H	☺	☺	☺	☺	☺	☺	☺	☺	R	L	E	N	☺
☺	Y	T	☺	☺	☺	☺	☺	☺	D	R	☺	R	N	☺
☺	N	☺	☺	☺	☺	☺	☺	☺	☺	A	L	E	☺	☺

C'	C'	C'	C'	C'	C'	C'			E	E	E	E	E	a
46	47	48	49	50	51	52	53	54	55	56	57	58	59	60
K	S	K	C	F	Y	T	T	D	T	E	C	D	L	T
☺	☺	☺	☺	☺	L	☺	A	E	☺	☺	☺	☺	☺	☺
☺	N	☺	☺	☺	S	☺	☺	☺	☺	☺	☺	☺	☺	☺
☺	☺	I	☺	☺	S	I	☺	A	☺	☺	☺	☺	☺	☺

a	a	a	a	a	a				F	F	F	F	F	F
61	62	63	64	65	66	67	68	69	70	71	72	73	74	75
D	E	I	V	K	D	V	K	Q	T	Y	L	A	R	V
☺	☺	V	☺	☺	☺	☺	G	☺	☺	☺	M	☺	☺	☺
☺	☺	☺	☺	☺	☺	☺	T	W	A	☺	E	☺	K	☺
S	☺	M	A	P	N	☺	Q	☺	☺	☺	☺	☺	☺	☺

F	F	F	F											
76	77	78	79	80		81	82	83	84	85	86	87	88	89
F	S	Y	P	A	0	G	N	V	E	S	T	G	S	A
L	☺	☺	☺	☺	0	R	☺	G	N	T	☺	☺	F	P
L	☺	V	☺	R	R	N	S	☺	H	G	D	☺	D	Q
I	☺	0	0	L	L	P	☺	☺	☺	☺	☺	☺	☺	☺

								G	G	G	G	G	G	G
				90	91		92	93	94	95	96	97	98	99
0	0	0	0	G	E	0	P	L	Y	E	N	S	P	E
				0	☺	E	☺	P	F	R	☺	☺	☺	☺
L	V	I	H	☺	☺	E	☺	P	F	T	☺	A	☺	K
			F	L	☺	D	A	V	☺	S	☺	☺	☺	☺

					3	4						A	A	A
			a	a	a									
100	101	102	103	104	105	106	107	108	109	110	111	112	113	114
F	T	P	Y	L	E	T	N	L	G	Q	P	T	I	Q
G	☺	☺	☺	☺	D	☺	☺	☺	☺	☺	☺	☺	☺	☺
☺	L	☺	☺	R	D	☺	☺	☺	☺	☺	☺	V	☺	☺
☺	☺	☺	☺	Q	☺	☺	☺	☺	☺	☺	☺	K	☺	☺

A	A	A	A	A			B	B	B	B	B	B	B	B
115	116	117	118	119	120	121	122	123	124	125	126	127	128	129
S	F	E	Q	V	G	T	K	V	N	V	T	V	E	D
☺	☺	☺	☺	☺	☺	☺	☺	L	☺	☺	☺	☺	Q	☺
Q	☺	☺	☺	D	☺	R	☺	L	☺	☺	V	☺	K	☺
☺	☺	K	L	☺	☺	☺	☺	L	☺	☺	☺	☺	R	☺

													a	a
130	131	132	133	134	135	136	137	138	139	140	141	142	143	144
E	R	T	L	V	R	R	N	N	T	F	L	S	L	R
A	☺	☺	☺	☺	☺	☺	☺	G	☺	☺	☺	☺	☺	☺
S	L	☺	☺	☺	☺	K	☺	G	☺	☺	☺	T	☺	☺
T	Q	☺	☺	A	☺	S	☺	G	☺	☺	☺	☺	☺	☺

a	a	a	a	a	a		C	C	C	C	C	C	C	
145	146	147	148	149	150	151	152	153	154	155	156	157	158	159
D	V	F	G	K	D	L	I	Y	T	L	Y	Y	W	K
A	☺	☺	☺	☺	☺	☺	N	☺	☺	☺	☺	☺	☺	R
Q	☺	☺	☺	☺	☺	☺	G	☺	I	I	T	☺	R	☺
☺	I	☺	☺	☺	N	☺	Q	☺	M	☺	☺	☺	☺	R

					4	5								
						C'	C'	C'	C'	C'				E
160	161	162	163	164	165	166	167	168	169	170	171	172	173	174
S	S	S	S	G	K	K	T	A	K	T	N	T	N	E
A	☺	☺	T	☺	☺	☺	☺	☺	☺	T	☺	☺	☺	☺
G	☺	☺	T	☺	☺	☺	☺	N	I	☺	☺	☺	☺	☺
☺	☺	T	T	☺	☺	☺	☺	☺	M	☺	☺	☺	☺	☺

E	E	E								F	F	F	F	F
175	176	177	178	179	180	181	182	183	184	185	186	187	188	189
F	L	I	D	V	D	K	G	E	N	Y	C	F	S	V
☺	☺	☺	☺	☺	☺	☺	☺	☺	☺	☺	☺	☺	☺	☺
☺	S	☺	☺	☺	E	E	☺	V	S	☺	☺	☺	F	☺
☺	☺	☺	☺	☺	☺	☺	☺	Q	D	☺	☺	☺	F	☺

F	F	F	F			G	G	G	G	G	G	G	G	G
190	191	192	193	194	195	196	197	198	199	200	201	202	203	204
Q	A	V	I	P	S	R	T	V	N	R	K	S	T	D
☺	☺	☺	☺	☺	☺	☺	K	R	K	Q	R	☺	P	E
☺	☺	M	☺	F	☺	☺	K	T	☺	Q	N	☺	P	G
☺	☺	☺	☺	☺	☺	☺	K	T	☺	Q	N	☺	P	E

													5	6
G	G	G	G	G	G									
205	206	207	208	209	210	211	212	213	214	215	216	217	218	219
S	P	V	E	C	M	G	Q	E	K	G	E	F	R	E
☺	L	T	☺	☺	T	S	R	I	Q	☺	R	A	☺	☺
☺	S	T	V	☺	T	E	☺	W	☺	S	F	L	G	☺
☺	I	T	V	☺	T	R	L	☺	☺	☺	K	☺	☺	☺

220	221	222	223	224	225	226	227	228	229	230	231	232	233	234
I	F	Y	I	I	G	A	V	V	F	V	V	I	I	L
M	☺	F	☺	☺	☺	☺	☺	☺	0	☺	☺	A	L	☺
T	L	I	☺	V	☺	☺	☺	☺	L	L	A	T	☺	F
M	S	F	I	V	V	P	☺	I	L	☺	I	☺	V	V

235	236	237	238	239	240	241	242	243	244	245	246	247	248	249
V	I	I	L	A	I	S	L	H	K	C	R	K	A	G
I	☺	V	☺	S	V	T	V	Y	☺	☺	☺	☺	☺	R
I	☺	L	☺	☺	☺	☺	☺	C	☺	R	☺	☺	N	R
I	A	L	F	L	L	V	0	C	☺	☺	☺	☺	☺	K

250	251	252	253	254	255	256	257	258	259	260	261	262	263
V	G	Q	S	W	K	E	N	S	P	L	N	V	S
A	☺	P	☺	G	☺	☺	S	☺	☺	☺	☺	I	A
A	☺	☺	K	G	☺	N	T	P	S	R	L	I	0
A	R	☺	☺	G	☺	☺	G	☺	☺	☺	☺	☺	A

Appendix 6

List of suppliers

American Diagnostica Inc.	Greenwich, Connecticut, USA
Baxter Diagnostics Inc.,	Deerfield, Illinois, USA
BioRad	Hemel Hempstead, England
Digital Pixel	Brighton, England
Gibco BRL	Paisley, Scotland
Helena Biosciences	Sunderland, England
Gamidor	Abingdon, England
Invitrogen	9704, CH Groningen, Netherlands
Kinetic Imaging	Liverpool, England
Lab Tech International	Horsham, England
Molecular Probes	Eugene, Oregon, U.S.A.
NovoNordisk Pharmaceuticals Ltd	Crawley, England
R&D systems	Oxon, England
Raymond Lamb Supplies	Sussex, England
Sebia	Issy-les-moulineaux, France
Sigma Aldrich Co. Ltd	Poole, Dorset, England

REFERENCES

- Abdulkadir S.A. Carvalhal G.F., Kaleem Z., Kiesel W., Humphrey P.A. and Catalona W.J. et al (2000) Tissue factor expression and angiogenesis in human prostate carcinoma Hum Pathol 31; 443
- Abe K., Shoji J., Chen A., Bierhaus I., Danave C., Micko C., Casper D.L., Dillehay D.L., Nawroth P.P. and Rickles F.R. (1999) Regulation of vascular endothelial growth factor production and angiogenesis by the cytoplasmic tail of tissue factor PNAS USA 96; 8663
- Allen S., Khan, S., Al-Mohanna, F., Batten, P., Yacoub, M. (1998) Native low density lipoprotein-induced calcium transients trigger VCAM-1 and E-selectin expression in cultured human vascular endothelial cells JCI 101: 1064-1075
- Alm A-K., Norstrom E., Sundelin J. and Nystedt S. (1999) Stimulation of proteinase activated receptor-2 causes endothelial cells to promote coagulation in vitro Thromb Haemost 81; 984
- Alpern-Elran H., Morog N., Robert F., Hoover G., Kalant N. and Brem S. (1989) Angiogenic activity of the atherosclerotic carotid artery plaque J Neurosurg 70; 942
- Ambrose J.A., Hjemdahl-Monsen C.E., Borrico S., Gorlin R. and Fuster V. (1988a) Angiographic demonstration of a common link between angina pectoris and non-Q wave acute myocardial infarction Am J Cardiol 61; 244
- Ambrose J.A., Tannenbaum M.A., Alexopoulos D. et al (1988b) Angiographic progression of coronary artery disease and the development of myocardial infarction J Am Coll Cardiol 12; 56
- Ambrose J.A., Winters S.L., Arora R.R. (1986) Angiographic evolution of coronary artery morphology in unstable angina J Am Coll Cardiol 7; 472
- Ambrose J.A., Winters S.L., Stern A., et al (1985) Angiographic morphology and the pathogenesis of unstable angina pectoris J Am Coll Cardiol 5; 609
- Amirkhosravi A., Meyer T., Warnes G., Amaya M., Malik Z., Biggerstaff J.P., Siddiqui F.A., Sherman P. and Francis J.L. (1998) Pentoxyfylline inhibits hypoxia-induced upregulation of tumour cell tissue factor and vascular endothelial growth factor Thromb Haem 80; 598-602
- Ananyeva N.M., Tjurmin A.V., Berliner J.A., Chisholm G.M., Liau G., Winkles J.A. and Haudenschild C.C. (1997) Oxidised LDL mediates the release of fibroblast growth factor 1 Arterio Thromb Vasc Biol 17; 445

- Anber V., Millar J.S., McConnel M., Shepherd J. and Packard C.J. (1997) Interaction of very low density, intermediate density and low density lipoproteins with human arterial wall proteoglycans Arterioscler Thromb Vasc Biol 17; 2507
- Andrews B.S., Rehemtulla A., Fowler B.J., Edgington T.S. and Mackman N. (1991) Conservation of tissue factor primary sequence among three mammalian species Gene 98; 265-
- Annex B.H., Denning S.M., Channon K.M., Sketch M.H., Stack R.S., Morrissey J.H. and Peters K.G. (1995) Differential expression of tissue factor protein in directional atherectomy specimens from patients with stable and unstable coronary syndromes Circulation 91; 619
- Annex B.H., Denning S.M., Channon K.M., Sketch M.H., Stack R.S., Morrissey J.H. and Peters K.G. (1995) Differential expression of tissue factor protein in directional atherectomy specimens from patients with stable and unstable coronary syndromes Circulation 91; 619
- Anon (1994) Alpha-tocopherol and beta-carotene Cancer Prevention Study Group. The effect of vitamin E and beta-carotene on the incidence of lung cancer and other cancers in male smokers N Eng J Med 330; 1029
- Aqel N., Ball R., Waldmann H. and Mitchison M. (1984) Monocytic origin of foam cells human atherosclerotic plaques Atherosclerosis 53; 265
- Ardissino D., Merlini P.A., Ariens R., Coppola R., Bramucci E. and Mannucci P.M. (1997) Tissue factor antigen and activity in human coronary atherosclerotic plaques Lancet; 349; 769
- Armstrong D.A. (1992) Oxidised LDL ceroid and prostaglandin metabolism in human atherosclerosis Med Hypotheses 38; 244
- Asakara H., Kamikubo Y., Goto A., Shiratori Y., Yamazaki M., Jokaji H., et al (1995) Role of tissue factor in disseminated intravascular coagulation Thromb Res 80; 217
- Austin M.A., Breslow J.L., Hennekens C.H., Buring J.E., Willet W.C. and Krauss R.M. (1988) Low density lipoprotein subclass patterns and risk of myocardial infarction JAMA 260; 1917
- Autio I., Jaakkola O., Solakivi T. and Nikkari T. (1990) Oxidized low-density lipoprotein is chemotactic for arterial smooth muscle cells in culture FEBS Letts 277; 247
- Aviram M. and Brook J.G. (1987) Platelet activation by plasma lipoproteins. Prog Cardiovasc Dis 30; 61

- B.F. Trump and Berezesky (1995) Ca^{2+} mediated injury and cell death FASEB J 9;219
- Bach R. et al (1988) Cysteine-linked homodimers of TF Biochemistry 27; 4227
- Bach R., Gentry R. and Nemerson Y. (1986) FVII binding to tissue factor in reconstituted lipid vesicles: induction of cooperativity by phosphatidylserine Biochemistry 25; 4007
- Bachman F. and Kruithof E.K.O. (1984) Tissue plasminogen activator chemical and physiological aspects Semin Thromb Haemost 10; 6
- Bachman F. and Kruithof E.K.O. (1984) Tissue plasminogen activator chemical and physiological aspects Semin Thromb Haemost 10; 6
- Badimon L., Badimon J.J., Galvez A., Chesebro J. and Fuster V. (1986) Influence of arterial damage and wall shear rate on platelet deposition Arteriosclerosis 6; 312
- Badimon L., Badimon J.J., Turrito V.T., Vallabhajosula S. and Fuster V. (1988) Platelet thrombus formation on collagen type I Circ 78; 1431
- Bake J.B., Low D.A. and Simmer R.L. (1980) Protease nexin: a cellular component that links thrombin and plasminogen activator and mediates their binding to cells Cell 21; 37
- Baker J.B., Low D.A. and Simmer R.L. (1980) Protease nexin: a cellular component that links thrombin and plasminogen activator and mediates their binding to cells Cell 21; 37
- Ball R.Y., Stowers E.C., Burton J.H., Cary N.R.B., Skepper J.N. and Mitchison M.J. (1995) Evidence that h the death of macrophage foam cells contributes to the lipid core of atheroma Atherosclerosis 114; 45
- Banner D.W., D'Arcy A., Chene C., Winkler F.K., Guha A., konigsberg W.H., Nemerson Y. and Kirchofer D. (1996) The crystal structure of blood coagulation factor VIIa with soluble tissue factor Nature 380; 41
- Barenghi L., Bradamante S., Giudici G.A. and Vergani C. (1990) NMR analysis of low-density lipoprotein oxidatively-modified in vitro Free Rad Res Comm 8; 175
- Barger A.C. and Beeuwkes R. (1990); Rupture of coronary vasa vasorum as a trigger of acute myocardial infarction Am J Cardiol 66; 41G
- Barger A.C., Beeuwkes R. III., Lainey L.L. and Silverman K.J. (1984) Hypothesis: vasa vasorum and neovascularisation of human coronary arteries- a possible role in the pathophysiology of atherosclerosis N Engl J Med 310; 175
- Baron J.A., Gridley G., Weiderpass E., Nyren O. and Linet M. (1998) Venous thromboembolism and cancer Lancet 351; 1077

- Bauer K.A., Kass B.L., ten Cate H., Hawiger J.J. and Rosenberg R.D. (1990) Factor IX is activated *in vivo* by the tissue factor mechanism Blood 76; 731
- Bazan J.F. (1990) Structural design and molecular evolution of a cytokine receptor superfamily PNAS USA 87;6934-6938
- Beeuwkes R. III., Barger A.C., Silverman K.J. and Lainey L.L. (1990) Cinematographic studies of the vasa vasorum of human coronary arteries in Glagov S., Newman W.P., Schaffer S.A. eds. Pathobiology of the human atherosclerotic plaque. New York, NY; Springer-Verlag; 425
- Bell W.R. (1996) The fibrinolytic system in neoplasia Semin Thormb Haemost 22; 459
- Bennett M.R., Evan G.I. and Schwatrz S.M. (1995) Apoptosis of human vascular smooth muscle cells derived from normal vessels and coronary atherosclerotic plaques J Clin Invest 95; 2266
- Berliner J.A., Territo M.C., Sevanian A., Ramin S., Kim J.A., Bamshad B., Esterson M. and Fogelman A.M. (1990) Minimally modified low density lipoprotein stimulated monocyte endothelial interactions J Clin Invest 85; 1260
- Berridge M.J., Bootman M.D. and Lipp P. (1998) Calcium – a life and death signal Nature 395; 645-648
- Berridge M.J. (1993) Nature 361; 315
- Berridge M.J. (1997) J Physiol., Lond 499, 291
- Bhadra S., Arshad M.A.Q., Rymaszewski Z., Norman E., Wherley R. and Subbiah M.T.R. (1991) Oxidation of cholesterol moiety of low density lipoprotein in the presence of human endothelial cells or Cu^{2+} ions: identification of major products and their effects Biochem Biophys Res Comm 176; 431
- Bhatnagar D., Durrington P.N., Channon K.M., Prais H. and Mackness M.I. (1992) Atherosclerosis 98; 25
- Blomback B. and Blomback M. (1972) The molecular structure of fibrinogen Ann N Y Acad Sci 202; 77-97
- Bode W., Turk D. and Karshikov A. (1992) The refined 1.9-A X-ray crystal structure of D-Phe-Pro-Arg chloromethylketone-inhibited human alpha-thrombin: structure analysis, overall structure, electrostatic properties, detailed active-site geometry, and structure-function relationships Protein Sci 1; 426
- Boulanger C.M., Tanner F.C., Bea M.L., Hahn A.W., Werner A. and Luscher T.F. (1992) Oxidised low density lipoproteins induce mRNA expression and release of endothelin from human and porcine endothelium Circ Res 70; 1191

- Boulanger C.M., Tanner F.C., Bea M.L., Hahn A.W., Werner A. and Lusher T.F. (1992) Oxidised lipoproteins induce mRNA expression and release of endothelin from human and porcine endothelium Circ Res 70; 1191
- Bouma B.N. and Griffin J.H. (1977) Human blood coagulation factor XI. Purification, properties, and mechanism of activation by activated factor XII J Biol Chem 252; 6432-6437
- Bromberg M.E., Koninsberg W.H., Madison J.F., Pawashe A. and Garen A. (1995) Tissue factor promotes melanoma metastasis by a pathway independent of blood coagulation PNAS USA 92; 8205
- Bromberg M.E., Sundaram R., Homer R.J., Garen A. and Konigsberg W.H. (1999) Role of tissue factor in metastasis: functions of the cytoplasmic and extracellular domains of the molecule Thromb Haem 82; 88
- Brown B.G., Zhao X.Q., Sacco D.E. and Albers J.J. (1993) Lipid lowering and plaque regression: new insights into prevention of plaque disruption and clinical events in coronary disease Circulation 87; 1781
- Brown D.M., Kania N., Choi E.T., Lantieri L.A., Pasia E.N., Wun T. and Khouri R.K. (1996) Local irrigation with tissue factor pathway inhibitor inhibits intimal hyperplasia induced by arterial interventions Arch Surg 131; 1086
- Brown G., Albers J. and Fisher L. (1990) Regression of coronary artery disease as a result of intensive lipid lowering therapy in men with high levels of apolipoprotein B New Eng J Med 323; 1289
- Brown M.S. and Goldstein J.L. (1983) Lipoprotein metabolism in the macrophage: implications for cholesterol deposition in atherosclerosis Annu Rev Biochem 52;223
- Broze G.J. Jr, Girard T.J. and Novotny W.F. (1990) Biochemistry 29; 7539
- Broze G.J. Jr., Girard G.J. and Novotny W.F. (1990) Regulation of coagulation by a multivalent Kunitz-type inhibitor Biochemistry 29; 7539
- Bui M.N., Sack M.N., Moutsatsos G., Lu D.Y., Katz P., McCown R., Breall J.A. and Rackley C.E. (1996) Autoantibody titres to oxidised low density lipoproteins in patients with coronary atherosclerosis Am Heart J 131; 6633
- Byington R.P., Jukema J.W., Salonen J.T., Pitt B., Bruschke A.V., Hoen H., Furberg C.D. and Mancini G.B. (1995) Reduction in cardiovascular events during pravastatin therapy: pooled analysis of clinical events of the Pravastatin Atherosclerosis Intervention Program Circulation 92; 2419
- Cameliet P. and Jain R. (2000) Angiogenesis in cancer and other diseases Nature 407; 249

- Camera M., Giesen P.L.A., Fallon J., Aufiero B.M., Taubman M., Tremoli E. and Nemerson Y. (1999) Cooperation between VEGF and TNFα is necessary for exposure of active tissue factor on the surface of human endothelial cells Arterio Thromb Vasc Biol 19; 531
- Camerer E. And Prydz H. (1996) Notes on cell biology of tissue factor Haemostasis 26(supppl 1); 25-30
- Camerer E., Gjernes E., Wiiger M., Pringle S. and Prydz H. (2000a) Binding of factor VIIa to tissue factor on keratinocytes induces gene expression J Biol Chem 275(9); 6580
- Camerer E., Huang W. and Coughlin S.R. (2000b) Tissue factor- and factor X-dependent activation of protease-activated receptor 2 by factor VIIa Proc Natl Acad Sci USA 97(10); 5255
- Camerer E., Rottingen J.A., Iversen J.G. and Prydz H. (1996) Coagulation factors VII and X induce Ca^{2+} oscillations in MDCK cells only when proteolytically active JBC 271; 29034
- Camerer E., Rottingen J-A., Gjernes E., Larsen K., Skartlien A.H., Iversen J.-G. and Prydz H. (1999) Coagulation factors VIIa and Xa induce cell signaling leading to up-regulation of the egr-1 gene J Biol Chem 274(45); 32225
- Campos H., Blijlevens E., McNamara J.R., Ordovas J.M., Posner B.M., Wilson P.W., Castelli W.P. and Schaefer F.J. (1992) Low density lipoprotein particle size and coronary artery disease Arteriosclerosis Thrombosis 12; 1410
- Caplice N.M., Mueske C.S., Kleppe L.S. and Simari R.D. (1998) Presence of tissue factor pathway inhibitor in human atherosclerotic plaques is associated with reduced tissue factor activity Circulation 98; 1051-1057
- Carew T.E., Schwerke D.C. and Steinberg D. (1987) Anti-atherogenic effect of probucol unrelated to its hypocholesterolemic effect: evidence that antioxidants *in vivo* can selectively inhibit low density lipoprotein degradation in macrophage-rich fatty streaks and slow the progression of atherosclerosis in the Watanabe heritable hyperlipidemic rabbit PNAS USA 84; 7725
- Carlos T.M. and Harlan J.M. (1990) Membrane proteins involved in phagocyte adherence to endothelium Immunol Rev 114; 5
- Carmeliet P. et al (1999) Insights in vessel development and vascular disorders using targeted inactivation and transfer of VEGF, tissue factor and the plasminogen system Annal NY Acad Sci
- Carmeliet P., Mackman N., Moons L., Luther T., Gressens P., Van Vlanderen I., Demunck H., kasper M., Breier G., Evrard P., Muller M., Rissau W., Edgington T.

and Collen D. (1996) Role of tissue factor in embryonic blood vessel development Nature 383; 73

- Carpenter K.L.H., Ballantine J.A., Fussell B., Enright J.H. and Mitchison M.J. (1993) Biochim Biophys Acta 1167, 121
- Carpenter K.L.H., Taylor S., van der Veen C., Williamson B.K., Ballantine J.A. and Mitchison M.J. (1995) Lipids and oxidised lipids in human atherosclerotic lesions at different stages of development BBA 1256;141
- Casciola-Rosen L.A., Rosen A., Petri M. and Schlissel M. (1996) Surface blebs on apoptotic cells are sites of enhanced procoagulant activity: implications for coagulation events and antigenic spread in systemic lupus erythematosus PNAS USA 93; 1624
- Cathcart M.K., Morel D.W. and Chisholm G.M. (1985) Monocytes and neutrophils oxidise low density lipoprotein making it cytotoxic J Leuk Biol 38; 341
- Chait A., Brazg R.L., Tribble D.L. and Krauss R.M. (1993) Susceptibility of small, dense, low density lipoproteins to oxidative modification in subjects with the atherogenic lipoprotein phenotype, pattern B Am J Med 94; 350
- Chan L. (1992) J. Biol. Chem. 267, 25621-25624
- Chang A.W., Kuo A., Barnathan E.S. and Okada S. (1998) Urokinase receptor-dependent upregulation of smooth muscle cell adhesion to vitronectin by urokinase Arterioscler Thromb Vasc Biol 18; 1855
- Chapman I. (1965) Morphogenesis of occluding coronary artery thrombosis Arch Pathol 80; 256
- Chapman M.J., Laplaud P.M., Luc G., Forgez P., Bruckert E., Goulinet S. and Lagrange D. (1988) Further resolution of the low density lipoprotein spectrum in normal human plasma: physicochemical characteristics of discrete subspecies separated by density gradient ultracentrifugation J Lip Res 29; 442
- Chapman M.J., Guerin M. and Bruckert E. (1998) Atherogenic, dense low density lipoproteins: pathophysiology and new therapeutic approaches Eur Heart J 19; A24-A30
- Chautan M., latron M., Anfosso F., Alessi M.C., Lafont H., Juhan-Vague I. And Nalbone G. (1993) J Lipid Res 34; 101
- Chen J., Bierhaus A., Scheiekofer S., Andrassy M., Boasheng C., Stern D.M. and Nawroth P.P. (2001) Tissue factor- a receptor involved in the control of cellular properties including angiogenesis Thromb Haem 86; 334
- Chevion M. (1998) Free Rad Biol Med 5; 27

- Chin J.H., Azhar S. and Hoffman B.B. (1992) Inactivation of endothelial derived relaxing factor by oxidised lipoproteins J Clin Invest 89; 10
- Chisholm G.M., Ma G., Irwin K.C. et al (1994) 7 beta-hydroperoxycholest-5-en-3 beta-ol, a component of human atherosclerotic lesions, is the primary cytotoxin of oxidised human low density lipoprotein PNAS USA 91, 11452
- Chung S.W., Kang B.Y., Kim S.H., Pak Y.K., Cho D., Trinchieri G. and Kim T.S. (2000) Oxidized low density lipoprotein inhibits interleukin 12 production in lipopolysaccharide activated mouse macrophages via direct interactions between peroxisome proliferator-activated receptor γand NFκB JBC 275; 32681
- Clapham D.E. (1995) Calcium signaling Cell 80; 259
- Clauss M., Grell M., Fangmann C., Fiers W., Scheurich P. and Risau W. (1996) Synergistic induction of endothelial tissue factor by TNF and VEGF: functional analysis of the TNF receptors FEBS Letts 390(3); 334
- Coetzee G.A. and van de Westhuyzen D.R. (1992) Curr Opin Lipidol 3; 60
- Cohen M., Sherman W., Rentrop K.P. and Gorlin R. (1989) Determinants of collateral filling observed during sudden controlled artery occlusion in human subjects J Am Coll Cardiol 13; 297
- Connolly D.T., Heurelman D.M., Nelson R., Olander J.V., Eppley B.L., Delfino J.J., Siegel N.R., Leimgruber R.M. and Feder J. (1989) Tumour vascular permeability factor stimulates endothelial cell growth and angiogenesis J Clin Invest 84; 1470
- Constantinides P. (1966) Plaque fissures in human coronary thrombosis J Atheroscle Res 6;1
- Constantinides P.(1990) Plaque hemorrhages: their genesis and their role in supra-plaque thrombosis and atherogenesis: In Glagov S., Newman W.P., Schaffer S.A. eds. Pathobiology of the human atherosclerotic plaque, New York, NY: Springer – Verlag; 394
- Contrino J., Hair G., Kreutzer D.L. and Rickles F.R. (1996) In situ detection of tissue factor in vascular endothelial cells: correlation with the malignant phenotype of human breast disease Nature Medicine 2(2); 209
- Crawley J., Lupu F., Westmuckett A.D., Severs N.J., Kakkar V.V. and Lupu C. (2000) Expression, localisation and activity of TF pathway inhibitor in normal and atherosclerotic human vessels Arterioscler Thromb Vasc Biol 20; 1362-1373

- Cui M.Z., Penn M.S. and Chisholm G.M. (1999) Native and oxidised low density lipoprotein induction of tissue factor gene expression in smooth muscle cells is mediated by both egr-1 and sp-1 JBC; 274(46); 32975
- Cunningham M.A., Romas P., Hutchinson P., Holdsworth S.R. and Tipping P.G. (1999) Tissue factor and factor VIIa receptor/ligand interactions induce proinflammatory effects in macrophages Blood 94(10): 3413
- Curtis C.G., Brown K.L., Credo R.B., Domanik R.A., Gray A., Stenberg P. and Lorand L. (1974) Calcium-dependent unmasking of active centre cysteine during activation of fibrin stabilizing factor Biochemistry 13; 3774-3780
- Cushing S.D., Berliner J.A., Valente A.J., Territo M.C., Navab M., Parhami F., Gerrity R., Schwartz C.J. and Fogelman A.M. (1990) Minimally modified low density lipoprotein induces monocyte chemotactic protein 1 in human endothelial cells and smooth muscle cells Proc Natl Acad Sci USA 87; 5134
- Dano K., Andreasen P.A., Grondahl-Hansen J., Kristensen P., Neilsen L.S. and Skrivers L. (1985) Plasminogen activator, tissue degradation and cancer Adv Canc Res 44; 139
- Davie E.W. and Ratnoff O.D. (1964) The coagulation cascade: initiation, maintenance, and regulation Science 145; 1310
- Davie E.W., Fujikawa K. and Kiesel W. (1991) Biochemistry 30; 10363
- Davies M., Richardson P.D., Woolf N., Katz D.R. and Mann J. (1993) Risk of thrombosis in human atherosclerotic plaques: role of extracellular lipid, macrophage and smooth muscle cell content Br H J 69; 377
- Davies M.J. (1992) Anatomic features in victims of sudden coronary death: coronary artery pathology Circulation 85SI; I-19
- Davies M.J. and Thomas A.C. (1985) Plaque fissuring causes acute myocardial infarction, sudden ischaemic death and crescendo angina Br Heart J 53; 363
- Davies M.J., Bland M.J., Hangartner W.R., Angelini A. and Thomas A.C. (1989) Factors influencing the presence or absence of acute coronary thrombi in sudden ischaemic death Eur Heart J 10; 203
- Davies M.J., Woolf N., Rowles P.M. and Pepper J. (1988) Morphology of the endothelium over atherosclerotic plaques in human coronary arteries Br Heart J 60; 459
- Davies P.F. (1986) Lab Invest 55; 5
- De Graaf J., Hak-Lemmers H.L.M., Hectors M.P.C., DeMacker P.N.M., Mendricks J.C.M. and Stalenhoef A.F.M. (1991) Enhanced susceptibility to in vitro oxidation

of the low density lipoprotein subfraction in healthy men Arteriosclerosis Thrombosis 11; 298

- Dejager S., Bruckert E. and Chapman M.J. (1993) Dense low density lipoprotein subspecies with diminished oxidative resistance predominate in combined hyperlipidemia J Lipid Res 34; 295
- Dichtl, W., Stiko, A., Eriksson, P., Goncalves, I., Calara, F., Banfi, C., Ares, M. P. S., Hamsten, A., Nilsson, J. (1999). Oxidized LDL and lysophosphatidylcholine stimulate plasminogen activator inhibitor-1 expression in vascular smooth muscle cells Arterioscler Thromb Vasc Biol 19: 3025-3032
- Dickinson C.D. and Ruf W. (1997) Active site modification of FVIIa affects interactions of the protease domain with tissue factor JBC 272(32); 19875
- Dickinson C.D., Kelly C.R. and Ruf W. (1996) Identification of surface residues mediating tissue factor binding and catalytic function of serine protease factor VIIa PNAS USA 93; 14379
- DiCorleto P.E. and Bowen-Pope D.F. (1983) Cultured endothelial cells produce a platelet-derived growth factor-like protein PNAS USA 80; 1919
- DiScipio R.G., Hermodson M.A. and Davie E.W. (1977) Biochemistry 16; 5253-5260
- DiScipio R.G., Kurachi K. and Davie E.W. (1978) J Clin Invest 61; 1528
- Dolmetsch R.E., Lewis R.S., Goodnow C.C. and Helay J. (1997) Differential activation of transcription factors induced by Ca^{2+} response amplitude and duration Nature 386; 855
- Dolmetsch R.E., Xu K. and Lewis R.S. (1998) Calcium oscillations increase the efficiency and specificity of gene expression Nature 392; 933
- Drake T.A., Hannani K., Fei H., Lavi S. and Berliner J.A. (1991) Minimally oxidised LDL induces tissue factor expression in cultured human endothelial cells Am J Path 138(3); 601
- Drake T.A., Morrissey J.H. and Edgington T.S. (1989) Selective expression of tissue factor in human tissues Am J Path 134(5); 1087
- Duguid J.B. (1946) Thrombosis as a factor in the pathogenesis of coronary atherosclerosis J Pathol Bacteriol 58; 207
- Duguid J.B. (1946) Thrombosis as a factor in the pathogenesis of coronary atherosclerosis J Pathol Bacteriol 58; 207
- Durrington P.N. (1994) Hyperlipidaemia: diagnosis and management, 2nd edition, Butterworth Heinemann, Oxford

- Dvorak H.F., Dickersin G.R., Dvorak A.M., Mabseau J.E. and Pyne K. (1981) Human breast carcinoma: fibrin deposits and desmoplasia J Natl Canc Inst 67; 335
- Eaton D., Rodriguez H. and Vehar G.A. (1986) Proteolytic processing of human factor VIII. Correlation of specific cleavages by thrombin, factor Xa, and activated protein C with activation and inactivation of factor VIII coagulant activity Biochemistry 25; 505-512
- Edgington T.S., Mackman N., Brand K. and Ruf W. (1991) The structural biology of expression and function of tissue factor Thromb Haem 66;67-79
- Ellis S., Alderman E.L., Cain K., Wright A., Bourassa M. and Fisher L. (1989) Morphology of left anterior descending coronary territory lesions as a predictor of anterior myocardial infarction; a CASS Registry Study J Am Coll Cardiol 13; 1481
- El-Saadani M., Esterbauer H., El-Sayed M., Goher M., Nasser A.Y. and Juergens G. (1989) A spectrophotometric assay for lipid peroxides in serum lipoproteins using a commercially available reagent J Lipid Res 30; 627-630
- Esmon C.T. (1979) The subunit structure of thrombin-activated factor V. Isolation of activated factor V, separation of subunits, and reconstitution of biological activity J Biol Chem 254; 964-973
- Esmon C.T. (1987) The regulation of natural anticoagulant pathways Science 235; 1348
- Esmon C.T., Ding W., Yasuhiro K., et al (1997) The protein C pathway: new insights. Thromb Haemost 78; 70
- Essler M. et al (1999) Mildly oxidised LDL induces contraction of human endothelial cells through activation of Rho/Rho kinase and inhibition of myosin light chain phosphatase J Biol Chem 274(43); 30361
- Esterbauer H. The chemistry of oxidation of lipoproteins in Oxidative stress, lipoproteins and cardiovascular dysfunction, Eds; Rice-Evans C. and Bruckdorfer K.R., Portland Press Ltd, London, 1995
- Esterbauer H., Dieber-Rotheneder M., Waeg G., G. Striegl and Jurgens G. (1990) Biochemical, structural and functional properties of oxidised low density lipoprotein Chem Res Toxicol 3(2); 77-91
- Esterbauer H., Gebicki J., Puhl H. and Jeurgens G. (1992) Free Rad Biol Med 13; 341
- Esterbauer H., Juergens G., Quehenberger O. and Koller E. (1987) Autoxidation of human low density lipoprotein: loss of polyunsaturated fatty acids and vitamin E and generation of aldehydes J Lipid Res 28; 495

- Ettelaie C., Howell R.M. (1992) The inhibition of thromboplastin by apolipoprotein B and the effect of various lipids Thromb Res 68;175-184
- Ettelaie C., Howell R.M. and Bruckdorfer K.R. (1995) The effect of lipid peroxidation and lipolysis on the ability of lipoproteins to influence thromboplastin activity Biochim Biophys Acta 1257; 25-30
- Ettelaie C., James N.J., Adam J.M., Nicola K.P., Wilbourn B.R. and Bruckdorfer K.R. (1998) Identification of a domain in apolipoprotein B-100 that inhibits the procoagulant activity of tissue factor Biochem J 333; 433-438
- Ettelaie C., James N.J., Wilbourn B., Adam J.M., Naseem K.M. and Bruckdorfer K.R. (1996) The mechanism of inhibition of factor III (thromboplastin) activity by apolipoprotein B-100: protein: protein interactions Arterio Thromb Vasc Biol 16;639-647
- Exner M., Susani M., Witzum J.L., Hovorka A., Curtiss L.K., Spitzauer S. and Kerjaschki D. (1996) Lipoproteins accumulate in immune deposits and are modified by lipid peroxidation in passive Heymann nephritis Am J Pathol 149; 1313
- Falciani M., Gori A.M., Fedi S., Chiarugi L., Simonetti I., Dabizzi R.P., Prisco D., Pepe G., Abbate R., Gensini G.F. and Serneri G.G. (1998) Elevated tissue factor and tissue factor pathway inhibitor circulating levels in ischaemic heart disease patients Thromb Haem 79; 495
- Falk E. (1985) Unstable angina with fatal outcome: dynamic coronary thrombosis leading to infarction and/or sudden death: autopsy evidence of recurrent mural thrombosis with peripheral embolization culminating in total vascular occlusion Circ 71; 699
- Falk E. (1985) Unstable angina with fatal outcome: dynamic coronary thrombosis leading to infarction and/or sudden death: autopsy evidence of recurrent mural thrombosis with peripheral embolization culminating in total vascular occlusion Circ 71; 699
- Falk E. (1989) Morphologic features if unstable atherothrombotic plaques underlying acute coronary syndromes Am J Cardiol 63; 114E
- Falk E. (1992) Why do plaques rupture? Circulation 86 (suppl III):30-42
- Fan Z.Q., Larson P.J., Bognacki J., Raghunath P.N., Tomaszewski J.E., Kuo A., Canzini G., Chaiken I., Cines D.B. and Higazi A.A. (1998) Tissue factor regulates plasminogen binding and activation Blood 91; 1987
- Feng J., Han J., Pearce S.F.A., Silverstein R.T., Gotto A.M. Jr., Hajjar D.P. and Nicholson A.C. (2000) Induction of CD36 expression by oxLDL and IL-4 by a

common signaling pathway dependent on protein kinase C and PPAR-γ J Lip Res 41; 688

- Ferrara N. and Davis-Smyth T. (1997) The biology of vascular endothelial growth factor Endocrine Rev 18;4
- Fischer E.G., Ruf W. and Mueller B.M. (1995) Tissue factor initiated thrombin generation activates the signaling thrombin receptor on malignant melanoma cells Canc Res 55; 1629
- Fogelman A.M., Haberland M.E., Seager J., Hokom M. and Edwards P.A. (1981) Factors regulating the activities of the LDL receptor and the scavenger receptor on human monocyte-macrophages J Lipid Res 22; 1131
- Folk J.E. and Finlayson J.S. (1977) The epsilon-(gamma-glutamyl)lysine crosslink and the catalytic role of transglutaminases Adv Protein Chem 31; 1-133
- Folkman J. (1995) Angiogenesis in cancer, vascular, rheumatoid and other diseases Nature Medicine 1(1); 27
- Fox P.L., Chisolm G.M. and DiCorleto P.E. (1987) Lipoprotein-mediated inhibition of endothelial cell production of platelet-derived growth factor-like protein depends on free radical lipid peroxidation JBC 262 (13); 6046
- Freubis J., Parasarathy S. and Steinberg D. (1992) Proc Natl Acad Sci USA 89; 6876
- Friedman M., van den Bovencamp G.J. (1966) The pathogenesis of coronary thrombosis Am J Pathol 48; 19
- Frostegard J., Wu R., Giscombe R., Holm G., Lefvert A.K. and Nilsson J. (1992) Induction of T cell activation by oxidised low density lipoprotein Arterioscler Thromb 12; 461
- Fulton W.F.M. (1965) The coronary arteries: arteriography, microanatomy and pathogenesis of obliterative coronary disease. Springfield, III: Charles C. Thomas 230
- Furie B. and Furie B.C. (1988) Cell 53; 505
- Fuster V., Badimon L., Badimon J.and Cheesebro J. (1992a) The pathogenesis of coronary artery disease and the acute coronary syndromes I New Eng J Med 326; 242
- Fuster V., Badimon L., Badimon J.and Cheesebro J. (1992b) The pathogenesis of coronary artery disease and the acute coronary syndromes part II New Eng J Med 326; 310

- Fuster V., Badimon L., Cohen M., Ambrose J.A., Badimon J.J. and Cheesbro J. (1988) Insights into the pathogenesis of acute ischaemic syndromes Circulation 77; 1213
- Fuster V., Frye R.L., Kennedy M.A., Connolly D.C. and Mankin H.T. (1979) The role of collateral circulation in the various coronary syndromes Circulation 59; 1137
- Fuster V., Stein B., Ambrose J.A., Badimon L. and Badimon J.J. (1990) Atherosclerotic plaque rupture and thrombosis: evolving concepts Circ 82(S2); 47-59
- Gailani D. and Broze G.J. Jr (1991) Factor XI activation of coagulation in a revisited model of blood coagulation Science 253; 909
- Galle J., Mulsch A., Busse R. and Bassenge E. (1991) Effects of native and oxidized low density lipoproteins on formation and inactivation of endothelium-derived relaxing factor Arterioscler Thromb Vasc Biol 11; 198.
- Geng Y.J. and Libby P. (1995) Evidence for apoptosis in advanced human atheroma. co-localisation of IL-1β converting enzyme Am J Path 147(2); 251-66
- Gerrity R.G., Goss J.A. and Soby L. (1985) Arteriosclerosis 5; 55
- Ghosh S., Basu M.K. and Schweppe J.S. (1993) Charge heterogeneity of human low density lipoprotein Proc Soc Exp Biol Med 142; 1322-1325
- Gillett M.P.T. and Owen J.S. (1992) in Lipoprotein Analysis – A practical approach (Converse C.A. and Skinner E.R., eds), pp187-202, Oxford University Press, Oxford
- Girard T.J., Warren L.A., Novotny W.F., Likert K.M., Brown S.G., Miletich J.P. and Broze G.J. (1989) Nature 338; 518
- Girma J.P., Meyer D., Verweij C.L., Pannekoek H. and Sixma J.J. (1987) Structure-function relationship of human von Willebrand factor Blood 70; 605-611
- Glagov S., Weisenber E., Zarins C.K., Stankunavicius R. and Kolettis G.J. (1987) Compensatory enlargement of human atherosclerotic coronary arteries 316; 1371
- Glagov S., Zarins C., Giddens D.P. and Ku D.N. (1988) Hemodynamics and atherosclerosis; insights and perspectives gained from studies of human arteries Arch Pathol Lab Med 112; 1018
- Goldstein J.L. and Brown M.S. (1985) Receptor-mediated endocytosis: concepts emerging from the LDL receptor system Ann Rev Cell Biol 1;1
- Goldstein J.L., Ho Y.K., Basu S.K., Brown M.S. (1979) Binding site on macrophages that mediates uptake and degradation af acetylated low density lipoprotein, producing massive cholesterol deposition Proc Natl Acad Sci USA 76; 333

- Gorlin J.B., Yamin R., Egan S., Stewart M., Stossel T.P., Kwaiatkowski D.J. and Hartwig J.H. (1990) Human endothelial actin-binding protein (ABP-280), non-muscle filamin): a molecular leaf spring J Cell Biol 111; 1089
- Goulinet S. and Chapman M.J. (1997) Plasma LDL and HDL subspecies are heterogeneous in particle content of tocopherols and oxygenated and hydrocarbon carotenoids Arterioscler Thromb Vasc Biol 17; 786
- Greeno E.W., Bach R.R. and Moldow C.F. (1996) Apoptosis is associated with increased surface tissue factor procoagulant activity Lab Invest 75; 281
- Griffith R.L., Virella G.T., Stevenson H.C., Lopes-0Virella M.F. (1988) Low density lipoprotein metabolism by human macrophages activated with low density lipoprotein immune complexes: a possible mechanism of foam cell formation J Exp Med 168; 1041
- Guinto E.R., and Esmon C.T. (1982) Formation of a calcium-binding site on bovine activated factor V following recombination of the isolated subunits J Biol Chem 257; 10038-10043
- Gullino P.M. (1978) Angiogenesis and oncogenesis J Natl Cancer Inst 61; 639
- Habib G.B., Heibig J., Forman S.A. et al (1991) Influence of coronary collateral vessels on myocardial infarct size in humans Circulation 83; 739
- Hackman A.Y., Abe W., Insull W. Jr., Pownall H., Smith L., Dunn K., Gotto A.M. Jr. and Ballantyne C.M. (1996) Levels of soluble adhesion molecules in patients with dyslipidaemia Circ 93; 1334
- Hagen F.S., Gray C.L., O'Hara P., Grant F.J., Saari G.C., Woodbury R.G., Hart C.E., Insley M., Kiesel W., Kurachi K. and Davie E.W. (1986) Characterization of a cDNA coding for human factor VII PNAS USA 83; 299-302
- Haller H.D., Schaper W., Ziegler W., Philipp S., Kuhlmann M., Distler A. and Luft F.C. (1995) Low density lipoprotein induces vascular adhesion molecule expression on human endothelial cells Hypertension 25; 511
- Hamuro T., Kamikubo Y., Nakahara Y., Miyamoto S. and Funatsu A. (1998) Human recombinant tissue factor pathway inhibitor induces apoptosis in cultured human endothelial cells FEBS Lett 421;197
- Han J., Hajjar D.P., Febbraio M. and Nicholson A.C. (1997) Native and modified low density lipoproteins increase the functional expression of the macrophage class B scavenger receptor 272 (34); 21654
- Han K.H., Chang M.K., Bouiller A., Green S.R., Li A., Glass C.K., Quehenberger O. (2000) Oxidised LDL reduces monocyte CCR2 expression through pathways involving peroxisome proliferator-activated receptor JCI 106; 793

- Harlos K., Martin D.M.A., O'Brien D.P., Jones E.Y., Stuart D.I., Polikarpov I., Miller A., Tuddenham E.G.D. and Boys C.W.G. (1994) Crystal structure of the extracellular region of human tissue factor Nature 370;662-.
- Hatakeyama K., Asada Y., Marutsuka K., Sato Y., Kamikubo Y. and Sumiyoshi A. (1997) Localisation and activity of tissue factor in human atherosclerotic lesions Atherosclerosis 133; 213-219
- Hedner U. and Davie E.W. (1987) in Hemostasis and Thrombosis (Colman R.W., Hirsh J., Marder V.J. and Salzman E.W., Eds.) pp 39-47, J.B. Lippincott Co., Philadelphia, PA.
- Heeb M.J., Espana F. and Geiger M. (1987) Immunological identity of heparin-dependent plasma and urinary protein C inhibitor and plasminogen activator 3 J Biol Chem 262; 15813
- Heinecke J.W., Rosen H., Suzuki L.A., and Chait A. (1987) J Biol Chem 262; 10098
- Henney A.M., Wakeley P.R., Davies M.J., Foster K., Hembury R., Murphy G. and Humphries S. (1991) Localisation of stromelysin gene expression in atherosclerotic plaques by in situ hybridisation Proc Natl Acad Sci USA 88; 8154
- Henriksen T., Mahoney E.M. and Steinberg D. (1981) Enhanced macrophage degradation of low density lipoprotein incubated with cultured endothelial cells: recognition by receptors for acetylated low density lipoprotein Proc Natl Acad Sci USA 78; 6499
- Henriksen T., Mahoney E.M. and Steinberg D. (1982) Interactions of plasma lipoproteins with endothelial cells Ann N Y Acad Sci 401; 102
- Henriksen T., Mahoney E.M. and Steinberg D. (1983) Enhanced macrophage degradation of biologically modified low density lipoprotein Arteriosclerosis 3; 149
- Henry, P.D., and K.I. Bentley (1981) Suppression of atherogenesis in cholesterol-fed rabbits treated with nifedipine. J. Clin. Invest. 68: 1366-1369
- Higashi S., Matsumoto N. and Iwanaga S. (1996) Molecular mechanism of tissue factor mediated acceleration of factor VIIa activity JBC 271(43); 26569
- Hirata K., Akita H. and Yokoyama M. (1991) FEBS Lett 287; 181
- Hodis H.N., Chauhan A., Hashimoto S., Crawford D.W. and Sevanian A. (1992) Atherosclerosis 96; 125
- Hoffman M., Monroe D.M., Oliver J.A. and Roberts H.R. (1995) Factors IXa and Xa play distinct roles in tissue factor dependent initiation of coagulation Blood 86; 1784

- Holland J.A., Pritchard K.A., Rogers N.J. and Stemerman M.B. (1992) Atherogenic levels of low density lipoprotein increase endocytotic activity in cultured human endothelial cells Am J Pathol 140; 551
- Holvoet P. and Collen D. (1994) Oxidised lipoproteins in atherosclerosis and thrombosis FASEB 8; 1279
- Hornyak T.J. and Shafer J.A. (1991) Role of calcium ion in the generation of factor XIII activity Biochemistry 30; 6175-6182
- Huang M., Syed R., Stura E.A., Stone M.J., Stefanko R.S., Ruf W., Edgington T.S. and Wilson I.A. (1998) The mechanism of an inhibitory antibody on TF-initiated blood coagulation revealed by the crystal structures of human tissue factor, Fab 5G9 and TF 5G9 complex J Mol Biol 275; 873-894
- Huber R. and Bode W. (1978) Acc Chem Res 11; 114
- Hurt E. and Camejo G. (1987) Effect of arterial proteoglycans in the interaction of LDL with human monocyte-derived macrophages Atherosclerosis 67; 115
- Iakhiaev A., Pendurthi U.R., Voigt J., Ezban M. and Rao V.M. (1999) Catabolism of factor VIIa bound to tissue factor in fibroblasts in the presence and absence of tissue factor pathway inhibitor J Biol Chem 274(52); 36995
- Ichinose A., Hendrikson L.E., Fujikawa K. and Davie E.W., (1986) Amino acid sequence of the a subunit of human factor XIII Biochemistry 25; 6900-6906
- Jang Y., Guzman L.A., Lincoff A.M., Guttsauner-Wolf M., Forudi F., Hart C.E., Courtman D.W., Ezban M., Ellis S.G. and Topol E.J. (1995) Influence of blockade at specific levels of the coagulation cascade on restenosis in rabbit atherosclerotic femoral artery injury model Circ 92; 3041
- Jessup W., Rankin S. M., De Whalley C.V., Hoult J.R.S. ,Scott J. and Leake D.S. (1990) Alpha-tocopherol consumption during low-density-lipoprotein oxidation Biochem J 265, 399
- Johnson J.M., Kennelly M.M., Decesare D., Morgan S. and Sparrow A. (1985) Natural history of asymptomatic carotid plaque Arch Surg 120; 1010
- Jougasaki M., Kugiyama K., Saito Y., Nakao K., Imura H. and Yasue H. (1992) Biochem Biophys Res Comm 186; 1410
- Juergens G., Hoff H.F., Chisholm G.M. and Esterbauer H. (1987) Chem Phys Lipids 45; 315
- Kahlon R., Shapiro J. and Gotlier A. (1992) Angiogenesis in atherosclerosis Can J Cardiol 8(1); 60
- Kaikita K., Ogawa H., Yasue H., Takeya M., Takahashi K., Saito T., Hayasaki K., Horiuchi K., Takizawa A., Kamikubo Y. and Nakamura S. (1997) Tissue factor

expression on macrophages in coronary plaques in patients with unstable angina Arterio Thromb Vasc Biol 17(10); 2232

- Kaikita K., Takeya M., Ogawa H., Suefuji H., Yasue H. and Takahashi K. (1999) Co-localisation of tissue factor and tissue factor pathway inhibitor in coronary atherosclerosis J Pathol 188; 180-188
- Kakkar A. K., DeRuvo N., Chinswangwatanakul V., Tebbutt S. and Williamson R.C. (1995) Extrinsic pathway activation in cancer with high FVIIa and tissue factor 346; 1004
- Kakkar A.K., Chinswangwatanakul V., Lemoine N.R., Tebbutt S. and Williamson R.C.N. (1999) Role of tissue factor expression on tumour cell invasion and growth of experimental pancreatic adenocarcinoma Br J Surg 86; 890
- Kamat B.R., Galli S.J., Barger A.C., Lainey L.L. and Silverman K.J. (1987) Neovascularisation and coronary atherosclerotic plaque: cinematographic localization and quantitative histologic analysis Hum Pathol 18; 1036
- Kamata K., Kawamoto H., Honma T., Iwama T. and Kim S-H (1998) Structural basis for chemical inhibition of human blood coagulation factor Xa PNAS USA 95; 6630
- Kamido H., Kuksis A., Marai L. and Myher J,J, (1992) Identification of cholesterol-bound aldehydes in copper-oxidized low density lipoprotein FEBS Lett 304, 269
- Kamikubo Y., Nakahara Y., Takemoto S., Hamuro T., Miyamoto S., Funatsu A. (1997) Human recombinant tissue factor pathway inhibitor prevents the proliferation of cultured human neonatal aortic smooth muscle cells FEBS Letts 407; 116
- Karino T., Goldsmith H.L., Motomiya M. et al (1987) Flow patterns in vessels of simple and complex geometries Ann N Y Acad Sci 516; 422
- Kelley R.F., Costas K., O'Connell M.P. and Lazarus R.A. (1995) Analysis of the factor VIIa binding site on human tissue factor: effects of tissue factor mutations on the kinetics and thermodynamics of binding Biochemistry 34; 10383
- Khan A.R. and James M.N.G. (1998) Protein Sci 7; 815
- Khoo J.C., Miller E., McLoughlin P. and Steinberg D. (1990) Prevention of low density lipoprotein aggregation by high density lipoprotein or apolipoprotein A-I J Lipid Res 31; 645
- Khoo J.C., Miller E., Pio F. Steinberg D. and Witzum J.L. (1992) Monoclonal antibodies against LDL further enhance macrophage uptake of LDL aggregates Arterioscler Thromb 12; 1258

- Kita T., Nagano Y, Yokode M, Ishii K, Kume N, Ooshima A, Yoshida H and Kawai C (1987) Probucol prevents the progression of atherosclerosis in Watanabe heritable hyperlipidemic rabbit, an animal model for familial hypercholesterolaemia PNAS USA 84; 5928
- Kleinman H.K., McGarvey M.L., Liotta L.A., Robey P.G., Tryggvason K. and Martin G.R. (1982) biochemistry 21; 6188
- Klepfish A, Greco MA, Karpatkin S (1993) Thrombin stimulates melanoma tumor-cell binding to endothelial cells and subendothelial matrix Int J Cancer 53; 978
- Klimov A.N., Denisenko A.D., Popov A.V., Nagornev V.A., Pleskov V.M., Vinogradov A.G., Denisenko T.V. and Magracheva E.Y. (1985) Lipoprotein-antibody immune complexes: their catabolism and role in foam cell formation Atherosclerosis 58; 1
- Kontush A., Hubner C., Finckh B., Kohlschutter A. and Beisiegel U., (1994) Low density lipoprotein oxidizability by copper correlates to its initial ubiquinol-10 and polyunsaturated fatty acid content FEBS Letters 341; 69-73
- Koomagi R. and Volm M. (1998) Tissue factor expression in human non-small-cell lung carcinoma measured immunohistochemistry: correlation between tissue factor and angiogenesis Int J Canc 79; 19
- Kotze J.F. et al (1997) Transient interruption of arterial thrombosis by inhibition of FXa results in long term anti-thrombotic effects in baboons Thromb Haem 77; 1137
- Kragel A., Gertz S.D. and Roberts W.C. (1991) Morphologic comparison of frequency and types of acute lesions in the major epicardial coronary arteries in unstable angina pectoris, sudden coronary death and acute myocardial infarction J Am Coll Cardiol 18; 801
- Krauss R.M. and Burke D.J. (1982) Identification of multiple subclasses of plasma low density lipoproteins in normal humans J Lipid Res 23; 97-104
- Krauss R.M. (1991) Curr Opin Lipidol 2; 248
- Ku D.N., Giddens D.P., Zarins C.K. and Glagov S. (1985) Pulsatile flow and atherosclerosis in the human carotid bifurcation: positive correlation between plaque location and low oscillating shear stress Arteriosclerosis 5; 293
- Ku D.N., Giddens D.P., Zarins C.K. and Glagov S. (1985) Pulsatile flow and atherosclerosis in the human carotid bifurcation: positive correlation between plaque location and low oscillating shear stress Arteriosclerosis 5; 293
- Kugiyama K., Kerns S.A., Morrissett J.D., Roberts R. and Henry P.D. (1990) Impairment of endothelium-dependent arterial relaxation by lysolecithin in modified low density lipoproteins Nature 344; 160

- Kugiyama K., Sakamoto T., Misumi I., Sugiyama S., Ohgushi M., Ogawa H., Horiguchi M. and Yasue H. (1993) Transferable lipids in oxidised low density lipoprotein stimulate plasminogen activator inhibitor-1 and inhibit tissue type plasminogen activator release from endothelial cells Circ Res 73; 335
- Kuhn H., Belkner J., Wiesner R., Schewe T., Lankin V.Z. and Tikhaze A.K. (1992) Eicosanoids 5; 17
- Kume N., Cybulsky M.I. and Gimbrone M.A. Jr. (1992) Lysophosphatidylcholine, a component of atherogenic lipoproteins induces vascular adhesion molecule expression on human endothelial cells Hypertension 25; 511
- Kunitake S.T., Mendel C.M. and Hennessy K. (1992) Interconversion between apolipoprotein A-I-containing lipoproteins of pre-beta and alpha electrophoretic mobilities J Lipid Res 33; 1807
- Kurachi K. and Davie E.W. (1977) Activation of human factor XI (plasma thromboplastin antecedent) by factor XIIa (activated Hageman factor) Biochemistry 16; 5831-5839
- Kustikova O., Kramerov D., Grigorian M., Berezin V., Bock E., Lukanidin E. and Tulchinsky E. (1998) Fra-1 induces morphological transformation and increases in vitro invasiveness and motility of epithelioid adenocarcinoma cells Mol Cell Biol 18; 7095
- Kusuhara M., Chait A., Cader A. and Berk B. (1997) Oxidized LDL stimulates mitogen activated protein kinases in smooth muscle cells and macrophages Arterio Thromb 17; 141
- Kwon H.M., Sangiorgi G., Ritman E.L., McKEnna C., Holmes D.R.Jr, Schwartz R.S. and Lerman A. (1998) Enhanced coronary vasa vasorum neovascularisation in experimental hypercholesterolaemia J Clin Invest 101(8); 1551
- Langer F., Morys Wortmann, Kusters B. and Storck J. (1999) Endothelial protease-activated receptor-2 induces tissue factor expression and von Willebrand factor release Br J Haem 105; 542
- Latron Y., Chautan M., Anfosso F. et al (1991) Stimulating effect of oxidised low density lipoproteins on plasminogen activator inhibitor-1 synthesis by endothelial cells Arterioscler Thromb 11;1821
- Laue T.M., Lu R., Kreig U.C., Esmon C.T. and Johnson A.E. (1989) Ca^{2+}-dependent structural changes in bovine blood coagulation factor Va and its subunits Biochemistry 28; 4762-4771
- Lawn A. and Scott J.A. (1990) J. Lipid Res. 31, 1109-1120

- Lawson C.A. (1995) Hypoxia induced thrombosis is associated with tissue factor expression Circ 92; 804
- Le D.T., Rapaport S.I. and Rao LV (1992) Relations between factor VIIa binding and expression of factor VIIa/tissue factor catalytic activity on cell surfaces J Biol Chem 267(22);15447-54
- Lee D.M. and Alaupovic P. (1970) Studies of the composition and structure of plasma lipoproteins. Isolation, composition and immunochemical characterisation of low density lipoprotein subfractions of human plasma Biochemistry 9; 2244-2252
- Lee G.F. et al (1998) A novel soluble tissue factor variant with altered FVIIa binding interface J Biol Chem 273; 4149
- Lehr H.A., Becker M., Marklund S.L., Hubner C., Arfors K.E., Kohlschutter A. and Messmer K. (1992) Superoxide-dependent stimulation of leukocyte adhesion by oxidatively modified LDL *in vivo* Arterioscler Thromb 12; 824
- Lendon C., Davies M., Born G. and Richardson P. (1991) Atherosclerotic plaques are locally weakened when macrophage density is increased Atherosclerosis 65; 302
- Lendon C., Davies M., Born G. and Richardson P. (1991) Atherosclerotic plaques are locally weakened when macrophage density is increased Atherosclerosis 65; 302
- Lenz M.L., Hughes H., Mitchell J.R., Via D.P., Guyton J.R., Taylor A.A., Gotto A.M. and Smith C. (1990) Lipid hydroperoxy and hydroxy derivatives in copper-catalyzed oxidation of low density lipoprotein J Lipid Res 31; 1043
- Lesnik P., Dentan C., Vonica A., Moreau M. and Chapman M.J. (1995) Tissue factor pathway inhibitor activity associated with LDL is inactivated by cell- and copper-mediated oxidation Arterioscler Thromb Vasc Biol 15; 1121
- Lesnik P., Vonica A., Guerin M., Moreau M. and Chapman M.J. (1993) Anticoagulant activity of tissue factor pathway inhibitor in human plasma is preferentially associated with dense subspecies of LDL and HDL and with lp(a) Arterioscler Thromb 13; 1066
- Levin D.C. and Fallon J.T. (1982) Significance of the angiographic morphology of localised coronary stenosis: histopathologic correlations Circ 66; 316
- Levin E.G. and Santell L. (1987) Association of plasminogen activator inhibitor (PAI-1) with the growth substratum and membrane of human endothelial cells J Cell Biol 105; 2543
- Li X., Tsai P., Wieder E.D., Kribben A., Van Putten V., Schrier R.W. and Nemenoff R.A. (1994) Vascular smooth muscle cells grown on Matrigel J Biol Chem 269 (30); 19653

- Lichtlen P.R., Hugenholtz P.G., Rafflenbeul W., Hecker H., Jost S. and Deckers J.W. (1990) Retardation of angiographic progression of coronary artery disease by nifedipine. Results of International Nifedipine Trial on Anti-atherosclerotic Therapy (INTACT) Lancet 335; 1109
- Lin C.S., Penha P.D., Zak F.G. and Lin J.C. (1988) Morphodynamic interpretation of acute coronary thrombosis, with special reference to volcano-like eruption of atheromatous plaque caused by coronary artery spasm Angiology 39; 535
- Lindgren F.T., Jensen L.C., Wills R.D., and Freeman N.K. (1969) Flotation rates, molecular weight and hydrated densities of the low density lipoproteins Lipids 4; 337-344
- Lindsell C.E., Shawber C.J., Boulter J. and Weinmaster G. (1995) Jagged: a mammalian ligand that activates Notch1Cell 80; 909
- Lipp P. and Niggli E. (1996) Prog Biophys Mol Biol 65; 265-296
- Little W.C., Constantinescu M., Applegate R.J., Kutcher M.A., Burrows M.T., Kahl F.R. and Santamore W.P. (1988) Can coronary angiography predict the site of a subsequent myocardial infarction in patients with mild-to-moderate coronary artery disease? Circulation 78; 1157
- Lorand L. (1986) Activation of blood coagulation factor XIII Ann N Y Acad Sci 485; 144-158
- Lupu C., Kruithof E.K.O., Kakkar V.V. and Lupu F. (1999) Acute release of tissue factor pathway inhibitor after *in vivo* thrombin generation in baboons Thromb Haem 82; 1652
- Lusis A.J. (2000) Atherosclerosis Nature 407; 233
- MacFarlane R.G. (1964) A clotting scheme for 1964Nature 202; 498
- Mackman N., Morrisey J.H., Fowler B. and Edgington T.S. (1989) Complete sequence of the human tissue factor gene, a highly regulated cellular receptor that initiates the coagulation protease cascade Biochemistry 28;1755-1762.
- Malavasi B., Rasetti M.F., Roma P., Fogliatto R., Alevi P., Catapano A.L. and Galli G. (1992) Evidence for the presence of 7-hydroperoxycholest-5-en-3 beta-ol in oxidized human LDL Chem Phys Lipids 62; 209
- Malden L.T., Chait A., Raines E.W. and Ross R. (1991) The influence of oxidatively modified low density lipoproteins on expression of platelet-derived growth factor by human monocyte-derived macrophages JBC 266(21); 13901
- Mallat Z., Hugel B., Ohan J., Leseche G., Freyssinet J.M. and Tedgui A. (1999) Shed membrane microparticles with procoagulant potential in human atherosclerotic plaques: a role for apoptosis in plaque thrombogenicity Circ 99; 348

- Marcus A.J. and Hajjar D.P. (1993) Vascular transcellular signalling J Lipid Res 34; 2017
- Marmur J.D., Thiruvikraman S.V., Fyfe B.S., Guha A., sharma S.K., Ambrose J.A., Fallon J.T., Nemerson Y. and Taubman M.B. (1996) Identification of active tissue factor in human coronary atheroma Circ 94; 1226
- Martin N.B. et al (1993) The effect of IL-4 on TNFα induced expression of tissue factor and PAI-1 in HUVEC Thromb Haem 70(6); 1037
- Martin P. (1997) Science 276; 75
- Martin S.J., Reutelingsperger C.P.M., McGahon A.J., Rader J.A., van Schie R.C.A., LaFace D.M. and Green D.R. (1995) Early redistribution of plasma membrane phosphatidylserine is a general feature of apoptosis regardless of the initiating stimulus: inhibition by over expression of bcl-2 and abl J Exp Med 182; 1545
- Massaeli H.M.J., Austria A. and Pierce G.N. (1999) Chronic exposure of smooth muscle cells to minimally oxidised LDL results in depressed inositol 1,4,5-trisphosphate receptor density and Ca^{2+} transients Circ Res 85; 515
- Massaeli H.M.J., Austria A. and Pierce G.N. (2000) Lesions in ryanodine channels in smooth muscle cells exposed to oxidised LDL Arterio Thromb Vasc Biol 20; 328
- Masuda M., Nakamura S., Murakami T., Komiyama Y. and Takahashi H. (1996) Association of tissue factor with a γ-chain homodimer of the IgE receptor type I in cultured human monocytes Eur J Immunol 26; 2529
- McGill H.C. Jr (1984) George Lyman Duff memorial lecture. Persistent problems in the pathogenesis of atherosclerosis Arteriosclerosis 4; 443
- McMurray H.F., Parthasarathy S. and Steinberg D. (1993) Oxidatively modified low density lipoprotein is a chemoattractant for human T lymphocytes J Clin Invest 92; 1004
- Meade T.W., Mellows S., Brozovik M. et al (1986) Haemostatic function and ischaemic heart disease: principal results of the Northwick Park Heart Study Lancet 2; 533-7
- Mechtcheriakova D., Wlachos A., Holzmuller H., Binder B. and Hofer E. (1999) Vascular endothelial growth factor-induced tissue factor expression in endothelial cells is mediated by egr-1 Blood 93(11); 3811
- Meitus-Snyder M., Gown M.S. and Pitas R.E. (2000) Class A scavenger receptor up-regulation in smooth muscle cells by oxLDL; enhancement by calcium flux and concurrent cyclooxygenase-2 up-regulation JBC 275; 17661

- Melis E., Moons L., De Mol M., Herbert J-M., Mackman N., Collen D., Carmeliet P. and Dewerchin M. (2001) Targeted deletion of the cytosolic domain of tissue factor in mice does not affect development Biochem Biophys Res Comm 286; 580
- Milne R., Theolis R., Maurice R., Pease R., Weech P., Rassar E., Fruchart J.C., Scott J. and Marcel Y. (1989) J. Biol. Chem. 264, 19754-19760
- Misumi K. et al (1998) Comparison of plasma tissue factor levels in unstable and stable angina pectoris Am J Cardiol 81; 22-26
- Mitchell J.R.A. and Schwartz C.J. (1965) Arterial disease. Philadelphia, Pa: FA Davis Co; 1965
- Mitchison M.J., Hothersall D.C., Brooks P.N. and De Burbure C.Y. (1985) The distribution of ceroid in human atherosclerosis J Pathol 145; 177
- Mody R.S. and Carson S.D. (1997) Tissue factor cytoplasmic domain is multiply phosphorylated in vitro Biochemistry 36; 7869
- Moise A., Lesperance J., Theroux P., Taeymans Y., Goulet C. and Bourassa M.G. (1984) Clinical and angiographic predictors of new total coronary occlusion in coronary artery disease: analysis of 313 non-operated patients Am J Cardiol 54; 1176
- Monkovic D.D. and Tracy P.B. (1990) Activation of human factor V by factor Xa and thrombin Biochemistry 29; 1118-1128
- Monroe D.M., Roberts H.R. and Hoffman M. (1994) Platelet procoagulant complex assembly in a tissue factor-initiated system Brit J Haematol 88;314
- Mora R., Lupu F. and Simionescu N. (1987) Prelesional events in atherogenesis. Colocalization of apolipoprotein B, unesterified cholesterol and extracellular phospholipid liposomes in the aorta of hyperlipidemic rabbit Atherosclerosis 67; 143
- Morel D.W., DiCorleto P.E. and Chisholm G.M. (1984) Endothelial and smooth muscle cells alter low density lipoprotein in vitro by free radical oxidation Arteriosclerosis 4; 357
- Morel D.W., Hessler J.R. and Chisholm G.M. (1983) Low density lipoprotein cytotoxicity induced by free radical peroxidation of lipid J Lipid Res 24; 1070
- Moreno S. and Nurse P. (1990) Substrates for p34cdc2: *in vivo* veritas? Cell 61; 549
- Morrissey J.H. (2001) Tissue factor: an enzyme co-factor and a true receptor Thromb Haem 86; 66-74
- Moulton K.S., Heller E., Konerding M.A., Flynn E., Palinski W. and Folkman J. (2000) Angiogenesis inhibitors endostatin or TNP-470 reduce intimal

neovascularisation and plaque growth in apolipoprotein E-deficient mice Circ 99; 1726

- Mueller B.M. and Ruf W. (1998) Requirement for binding of catalytically active FVIIa in tissue factor-dependent experimental metastasis J Clin Invest 101; 1372
- Mueller B.M., Reisfeld R.A., Edgington T.S. and Ruf W. (1992) Expression of tissue factor by melanoma cells promotes efficient haematogenous metastasis PNAS USA 89(24);11832
- Muller Y.A., Ultsch M.H., Kelley R.F. and de Vos A.M. (1994) Structure of the extracellular domain of human tissue factor: location of the factor VIIa binding site Biochemistry 33;10864-
- Munro J.M. and Cotran R.S. (1988) Lab Invest 58; 249
- Murohara, M., R. Scalia, and A.M. Lefer (1996) Lysophosphatidylcholine promotes P-selectin expression in platelets and endothelial cells. Possible involvement of protein kinase C activation and its inhibition by nitric oxide donors. Circ. Res. 78: 780-789
- Naito K. and Fujikawa K. (1991) Activation of human blood coagulation factor XI independent of FXII. Factor XI is activated by thrombin in the presence of negatively charged surfaces J Biol Chem 266; 7353
- Nakagawa K., Zhang Y.M., Tsuji H., Yoshizuni M., Kasahara T., Nishinura H., Nawroth P.P. and Nakagawa M. (1998) The angiogenic effect of tissue factor on tumours and wounds Semin Thromb Haem 24; 207
- Narayanan S. (1999) Current concepts of coagulation and fibrinolysis Adv in Clin Chem 33; 133
- Navab M., Imes S.S., Hough G.P., Hama S.Y., Ross L.A., Bork R.W., Valente A.J., Berliner J.A., Drinkwater D.C., Laks H. and Fogelman A.M. (1991) Monocyte transmigration induced by modification of LDL in cocultures of human aortic wall cells is due to induction of monocyte chemotactic protein 1 synthesis and is abolished by HDL J Clin Invest 88; 2039-2046
- Navab M., Hough G.P., Stevenson D.C., Drinkwater H., Laks H. and Fogelman A.M. (1988) Monocyte migration into the subendothelial space of a coculture of adult human aortic and smooth muscle cells J Clin Invest 82; 1853-1863
- Neary R., Bhatnagar D., Durrington P.N., Ishola M., Arrol S. and Mackness M.I. (1992) Atherosclerosis 89; 35
- Negre-Salvaryre A., Fitoussi G., Reaud V., Pieraggi M.T., Thiers J.C. and Salvayre R. (1992) A delayed and sustained rise of cytosolic calcium is elicited by oxidised

low density lipoprotein in cultured bovine aortic endothelial cells FEBS Lett 299; 60

- Nelson C.A. and Morris M.D. (1977) The ultracentrifugal heterogeneity of serum low density lipoproteins in normal humans Biochem Med 18; 1-9.
- Nelson M.T., Cheng M., Rubart L.F., Santana A.D., Bonev A.D., Knot H.J. and Lederer W.J. (1995) Relaxation of arterial smooth muscle by calcium sparks 270; 633
- Nesheim M.E. and Mann K.G. (1979) Thrombin-catalyzed activation of single chain bovine factor V J Biol Chem 254; 1326-1334
- Neuenschwander P.F. and Morrissey J.H. (1992) Deletion of the membrane anchoring region of tissue factor abolishes autoactivation of FVII but not co-factor function. Analysis of a mutant with a selective deficiency in activity J Biol Chem 267; 14477
- Nigon F., Lesnik P., Rouis M. and Chapman M.J. (1991) Discrete subspecies of human low density lipoproteins are heterogeneous in their interaction with the cellular LDL receptor J Lipid Res 32; 1741
- Nobes C.D. and Hall A. (1995) Rho, Rac and cdc42 GTPases regulate the assembly of multimolecular focal complexes associated with actin stress fibers, lamellipodia and filopodia Cell 81; 53
- Nobuyoshi M., Tanaka M., Nosaka H. and Kimura K. (1991) Progression of coronary atherosclerosis: is coronary spasm related to progression? J Am Coll Cardiol 18; 904
- Noguchi N., Gotoh N. and Niki E. (1993) Dynamics of the oxidation of low density lipoprotein induced by free radicals Biochim Biophys Acta 1168; 348
- Odekon L.E., Sato Y. and Rifkin D.B. (1992) Urokinase type plasminogen activator mediates basic fibroblast growth factor induced bovine endothelial cell migration independent of its proteolytic activity J Cell Physiol 150; 258
- Ollivier V., Bentolila S., Chabbat J., Hakim J. and de Prost D. (1998) Tissue factor dependent vascular endothelial growth factor production by human fibroblasts in response to activated FVII Blood 91(8); 2689
- Olsson U., Camejo G., Hurt-Camejo E., Elfsber K., Wiklund O. and Bondjers G. (1997) Arterioscler. Thromb. Vasc. Biol. 17, 149-155
- Orning L., Stephens R.W., Petersen L.B., Hamers M.J.A.G., Sormorken H. and Sakariassen K.S. (1997) A peptide sequence from the EGF-2 like domain of FVII inhibits TF dependent FX activation Thromb Res 86(1);5

- Orning L., Stephens R.W., Petersen L.B., Hamers M.J.A.G., Stormorken H. and Sakariassen K.S. (1997) A peptide sequence from the EGF-2 domain of FVII inhibits TF-dependent FX activation Thromb Res 86(1);5
- Ott I., Fischer E.G., Miyagi Y., Mueller B.M. and Ruf W. (1998) A role for tissue factor in cell adhesion and migration mediated by interaction with actin-binding protein 280 J Cell Biol 140; 1241
- Ou Z., Ogano A., Guo L., Konda Y., Harigaya Y. and Nagakawa Y. (1995) Identification and quantitation of choline glycerophospholipids that contain aldehyde residues by fluorimetric high performance liquid chromatography Anal Biochem 227; 289
- Packard C.J. and Shepard J. (1997) Lipoprotein heterogeneity and apolipoprotein B metabolism Arterioscler Thromb Vasc Biol 17; 3542
- Palinski W., Rosenfeld M.E., Yla-Hertuala S., Gurtner G.C., Socher S.S., Butler S.W., Parthasarathy S., Carew d., Steinberg D. and Witzum J.L. (1989) Low density lipoprotein undergoes oxidative modification *in vivo* Proc Natl Acad Sci USA 86; 1372
- Parhami F., Fang Z.T., Fogelman A.M. and Berliner J.A. (1995) Stimulation of G_s and inhibition of G_i protein functions by minimally oxidised LDL Arterio Thromb Vasc Biol 15; 2019
- Parhami F., Fang Z.T., Fogelman A.M., Andalibi M.C., Territo M.C. and Berliner J.A. (1993) Minimally modified low density lipoprotein-induced inflammatory responses in endothelial cells are mediated by cyclic adenosine monophosphate JCI 92; 471
- Parthasarathy S. and Rankin S.M. (1992) Role of oxidised low density lipoprotein in atherogenesis Prog Lipid Res 31; 127
- Parthasarathy S., Printz D.J., Boyd D., Joy L. and Steinberg D. (1986) Macrophage oxidation of LDL generates a modified form recognised by the scavenger receptor Arteriosclerosis 3; 149-159
- Parthasarathy S., Wieland E. and Steinberg D. (1989) A role for endothelial cell lipoxygenase in the oxidative modification of low density lipoprotein PNAS USA 86; 1046
- Pasqualini M.E., Moreno L.R., Munoz S.E. and Eynard A.R. (1997) Proaggregatory and procoagulant properties of three murine mammary gland tumour cell lines with different metastatic capabilities Exp Toxicol Pathol 49; 403
- Paterson J.C. (1936) Vascularisation and haemorrhage of the intima of arteriosclerotic coronary arteries Arch Pathol 22; 313

- Patsch W.R., Ostlund I., Kuisk I., Levy R. and Schonfeld G. (1982) Characterisation of lipoprotein in a kindred with familial hypercholesterolaemia J Lipid Res 23; 1196-1205
- Pendurthi U.R., Allen K.E., Ezban M. and Rao L.V.M. (2000) Factor VIIa and thrombin induce the expression of Cyr61 and connective tissue growth factor, extracellular matrix signaling proteins that could act as possible downstream mediators in factor VIIa: tissue factor-induced signal transduction J Biol Chem 275(19); 14632
- Pendurthi U.R., Alok D. and Rao L.V.M. (1997) Binding of FVIIa to tissue factor induces alterations in gene expression in human fibroblast cells: up-regulation of poly(A) polymerase PNAS USA 94; 12598
- Peng S., Hu B. and Morin R.J. (1991) Angiotoxicity and atherogenicity of cholesterol oxides J Clin Lab Anal 5; 144
- Penn M. S., Chandrashekhar V.P., Cui M-Z., Dicorleto P.E. and Chisholm G.M. (1999) LDL increases inactive tissue factor on vascular smooth muscle cells surfaces: hydrogen peroxide activates latent cell surface tissue factor Circ 99; 1753
- Penn M.S., Cui M-Z., Winokur A.L., Bethea J., Hamilton T.A., DiCorleto P.E. and Chisholm G.M. (2000) Smooth muscle cell surface tissue factor pathway activation by oxidised low-density lipoprotein requires cellular lipid peroxidation Blood 96; 3056
- Petersen L.C. and Persson E. (1996) Effect of Ca^{2+} on the structure and function of factor VIIa Haemost 26(S1); 40
- Petersen L.C., Thastrup O., Hagel G., Sorensen B.B., Freskgard P., Rao V.M. and Ezban M. (2000) Exclusion of known protease activated receptors in factor VIIa-induced signal transduction Thromb Haemost 83; 571
- Petit L., Lesnik P., Dachet C., Moreau M. and Chapman M.J. (1999) Tissue factor pathway inhibitor is expressed by human monocyte derived macrophages-relationship to tissue factor induction by cholesterol and oxLDL Arterioscler Thromb Vasc Biol 19; 309-315
- Petterson K.S., Boberg K.M., Stabursvik A. and Prydz H. (1991) Toxicity of oxygenated cholesterol derivatives toward cultured human umbilical vein endothelial cells Arterioscler Thromb 11; 423
- Phair R.D. (1988) Cellular calcium and atherosclerosis: a brief review Cell Calcium 9;275

- Pike A.C.W. (1999) Structure of human factor VIIa and its implications for the triggering of blood coagulation PNAS USA 96;8925
- Pilcher B.K., Dumin J.A., Sudbeck B.D., Krane S.M., Welgus H.G. and Parks W.C. (1997) The activity of collagenase-1 is required for keratinocyte migration on a type I collagen matrix J Cell Biol 137; 1445
- Poole A., Gibbins J.M., Turner M., van Vugt M.J., van de Winkel J.G.J., Saito T., Tybulewicz V.L.J. and Watson S.P. (1997) The Fc receptor γ-chain and the tyrosine kinase Syk are essential for activation of mouse platelets by collagen EMBO J 16(9); 2333
- Porter V. A., Bonev A.D., Knot H.J., Heppner T.J., Stevenson A.S., Kleppisch T., Lederer W.J. and Nelson M.T. (1998) Frequency modulation of Ca^{2+} sparks is involved in regulation of arterial diameter by cyclic nucleotides Am J Physiol (Cell Physiol 43) 274; C1346
- Poulsen L.K., Jacobsen N., Sorensen B.B., Bergenhem N.C., Kelly J.D., Foster D.C., Thastrup O., Ezban M. and Petersen L.C. (1998) Signal transduction via the mitogen-activated protein kinase pathway induced by binding of coagulation factor VIIa to tissue factor J Biol Chem 273; 6228
- Pozzan T. and Rizzuto R. (2000) The renaissance of mitochondrial Ca^{2+} transport Eur J. Biohem 267; 5269
- Puurunen M., Manttari M., Manninen V., Tenkanen L., Alfthan G., Enholm C., Vaarala O., Aho K. and Palosuo T. (1994) Antibody against oxidised low density lipoprotein predicting myocardial infarction Arch Intern Med 154; 2605
- Quinn M.T., Parasarathy S. and Steinberg D. (1985) Proc Natl Acad Sci USA 82; 5949
- Quinn M.T., Parthasarathy S. and Steinberg D. (1985) Endothelial cell-derived chemotactic activity for mouse peritoneal macrophages and the effects of modified forms of low density lipoprotein PNAS USA 82; 5949
- Quinn M.T., Parthasarathy S. and Steinberg D. (1988) Lysophosphatidylcholine: a chemotactic factor for human monocytes and its potential role in atherogenesis PNAS USA 85; 2805
- Quinn M.T., Parthasarathy S., Fong L.G. and Steinberg D. (1987) Proc Natl Acad Sci USA 84; 2995
- Quinn M.T., Parthasarathy S., Fong L.G. and Steinberg G. (1987) Oxidatively modified low density lipoproteins: a potential role in recruitment and retention of monocytes/macrophages during atherogenesis PNAS USA 84; 2995

- Quirk S.M. (1998) The regulation of uterine tissue factor by oestrogen Endocrine 3; 177
- Raab G. and Klagsbrun M. (1997) Heparin-binding EGF-like growth factor Biochim Biophys Acta 133; 179
- Rajavashisth T.B., Andalibi A., Territo M.C., Berliner J.A., Navab M. and Fogelman A.M. (1990) Induction of endothelial cell expression of granulocyte and macrophage colony stimulating factors by modified low density lipoprotein Nature 344; 254
- Rajavashisth T.B., Andalibi A., Territo M.C., Berliner J.A., Navab M., Fogelman A.M. and Lusis A.J. (1990) Induction of endothelial cell expression of granulocyte and macrophage colony stimulating factor by modified low density lipoproteins Nature 344; 254
- Ramos M.A., Kuzuya M., Esaki T., Miura S., Satake S., Asai T., Kanda S., Hayashi T. and Iguchi A. (1998) Induction of macrophage VEGF in response to oxLDL and VEGF accumulation in human atherosclerotic lesions Arterio Thromb Vasc Biol 18; 1188
- Randolph G.J., Luther T., Albrecht S., Magdolen V. and Muller W.A. (1998) Role of tissue factor in adhesion of mononuclear phagocytes to and trafficking through endothelium in vitro Blood 92; 4167
- Ranganathan G., Blatti SP., Subramaniam M., Fass DN., Maihle NJ. and Getz MJ (1991) Cloning of murine tissue factor and regulation of gene expression by transforming growth factor type beta 1 J Biol Chem 266(1);496-501
- Reid V.C. and Mitchinson M.J. (1993) Toxicity of oxidised low density lipoprotein towards mouse peritoneal macrophages in vitro Atherosclerosis 10; 680
- Reinartz J., Schaefer B., Bechtel M.J. and Kramer M.D. (1996) Plasminogen activator inhibitor type-2 (PAI-2) in human keratinocytes regulates pericellular urokinase-type plasminogen activator Exp Cell Res 223; 91
- Resink T.J., Tkachuk V.A., Bernhardt J. and Buhler F.R. (1992) Arteriosclerosis Thrombosis 12; 278
- Richardson P.D., Davies M.J. and Born G.V.R. (1989a) Influence of plaque configuration and stress distribution on fissuring of coronary atherosclerotic plaques Lancet 2; 941
- Richardson P.D., Davies M.J. and Born G.V.R. (1989b) Influence of plaque configuration and stress distribution on fissuring of coronary atherosclerotic plaques in human coronary arteries Br Heart J 60; 459

- Roberts H.R., Monroe D.M., Oliver J.A., Chang J-Y. and Hoffman M. (1998) Newer concepts of blood coagulation Haemophilia 4; 331
- Romer J., Bugge T.H., Pyke C., Lund L.R., Flick M.J., Degen J.L. and Dano K. (1996) Nat Med 2; 287
- Rosenfeld M.E. and Ross R. (1990) Macrophage and smooth muscle cell proliferation in atherosclerotic lesions of WHHL and comparably hypercholesterolaemic fed rabbits Arteriosclerosis 10; 680
- Rosenfeld M.E., Palinski W., Yla-Herttuala S. and Carew T.E. (1990) Macrophages, endothelial cells, and lipoprotein oxidation in the pathogenesis of atherosclerosis Toxicol Path 18; 560
- Ross R. (1986) The pathogenesis of atherosclerosis – an update New Eng J Med 314;488
- Ross R. (1993) The pathogenesis of atherosclerosis: a perspective for the 1990s Nature 362;801
- Rothblat G.H., Mehlberg F.H., Johnson W.J. and Phillips M.C. (1992) Apolipoproteins, membrane cholesterol domains, and the regulation of cholesterol efflux J Lipid Res 33; 1901
- Rottingen J.A., Enden T., Camerer E., Iversen J-G. and Prydz H. (1995) Binding of FVIIa to tissue factor induces cytosolic Ca^{2+} signals in J82, transfected COS-1 cells, MDCK cells and in human endothelial cells induced to synthesise tissue factor JBC 270(9);4650
- Roy S., Paborsky LR. Vehar GA (1991) Self-association of tissue factor as revealed by chemical crosslinking J Biol Chem 266(8);4665-8
- Rubenstein B. (1978) Heterogeneity of human plasma low density lipoprotein Can J Biochem 56; 977-980
- Ruddock V. and Meade T.W. (1994) Factor VIIa activity and ischaemic heart disease : fatal and non-fatal events Q J Med 87; 403
- Ruf W. and Edgington T.S. (1991) An anti-tissue factor monoclonal antibody which inhibits TF.VIIa complex is a potent anticoagulant in plasma Thromb Haem 66(5); 529-33
- Ruf W., Schullek J.R., Stone and Edgington T.S. (1994) Mutational mapping of functional residues in tissue factor: identification of factor VII recognition determinants in both structural modules of the predicted cytokine receptor homology domain Biochemistry 33;1565-1572
- Ruggeri Z.M. and Zimmerman T.S. (1987) von Willebrand factor and von Willebrand disease Blood 70; 895-904

- Rye K.A. and Barter P.J. (1992) in Structure and Function of Apolipoproteins (Rosseneu, M. ed), pp 401-426, CRC Press, Boca Raton
- Sachindis A., R. Locher, T. Mengden, and W. Vetter (1990) Low-density lipoprotein elevates intracellular calcium and pH in vascular smooth muscle cells and fibroblasts without mediation of the LDL receptor. Biochem. Biophys. Res. Commun. 167: 353-359
- Sadler J.E. and Davie E.W. (1987) in The Molecular Basis of Blood Diseases (Sramatoyannopoulos G., Nienhuis A.W., Leder P. and Majerus P.W. Eds.) pp575-630, W.B. Saunders Co., Philadelphia, PA.
- Sakai A., Kume N., Ochi H., Nishi E., Moriwaki H., Tanoue K. and Kita T. (1995) P-selectin and VCAM-1 are focally expressed in hypercholesterolemic rabbits before intimal accumulation of macrophages and T lymphocytes. Circulation. 92(Suppl. 1):I558-I559. (Abstr.)
- Sasahara M., Raines E.W., Chait A., Carew T.E., Steinberg D., Wahl P.W. and Ross R. (1994) Inhibition of hypercholesterolaemia-induced atherosclerosis in the nonhuman primate by probucol. I. Is the extent of atherosclerosis related to resistance of LDL to oxidation? J Clin Invest 94; 392
- Sato Y. Asada Y., Marutsuka K., Hatakeyama K., Kamikubo Y. and Sumiyoshi A. (1997) Tissue factor pathway inhibitor inhibits aortic smooth muscle cell migration induced by TF: FVIIa complex Thromb Haem 78;1138
- Sawada M., Miyake S., Ohdama S., Matsubara O., Masuda S., Yakumaru K. and Yoshizawa Y. (1999) Expression of tissue factor in non-small cell lung cancers and its relationship to metastasis Br J Canc 79; 472
- Schaefer H.I.MP., Hold K.M., Egas-Kenniphaas J.M. and van der Laarse A. (1993) Intracellular calcium signalling after binding of low-density lipoprotein to confluent and non-confluent cultures of an endothelial cell line, EA.hy926 Cell Calcium 14; 507
- Scheidegger K.J., James R.W. and Delafontaine P. (2000) Differential effects of low density lipoproteins on IGF-1 and IGF-1 receptor expression in vascular smooth muscle cells JBC 275; 26864
- Schleef R.R., Bevilacqua M.P., Sawrey M., Gimbrone M.A. and Loskutoff D.J. (1988) Cytokine activation of vascular endothelium J Biol Chem 263; 5797
- Schullek J.R., Ruf W. and Edgington T.S. (1994) Key ligand interface residues in tissue factor contribute independently to factor VIIa binding 269(30);19399-.

- Schwatrz M.L., Pizzo S.V., Hill R.L. and McKee P.A. (1973) Human Factor XIII from plasma and platelets. Molecular weights, subunit structures, proteolytic activation, and cross-linking of fibrinogen and fibrin J Biol Chem 248; 1395-1407
- Scott-Burden, T., T.A.J. Resink, A.W.A. Hahn, U. Baur, R.J. Box, and F.R. Buhler (1989) Induction of growth-related metabolism in human vascular smooth muscle cells by low-density lipoprotein. J. Biol. Chem. 264: 12582-12589
- Sevanian A., Berliner J. and Petterson H. (1991) Uptake, metabolism, and cytotoxicity of isomeric cholesterol-5,6-epoxides in rabbit aortic endothelial cells J Lipid Res 32; 147
- Sevinsky J.R., Rao L.V.M. and Ruf W. (1996) Ligand-induced protease receptor translocation into caveolae: a mechanism for regulating cell surface proteolysis of the tissue factor dependent coagulation pathway JCB 133(2); 293
- Shen M.M.S., Krauss R.M., Lindgren F.T. and Forte T.M. (1981) Heterogeneity of serum low density lipoproteins in normal human subjects J Lipid Res 22; 236-244
- Sherman C.T., Litvack F., Grundfest W. et al (1986) Coronary angioscopy in patients with unstable angina pectoris N Engl J Med 315; 913
- Shi R-J, Wen-Zhou L., Marder V.J. and Sporn L.A. (2000) Cloning of guinea pig tissue factor cDNA: comparison of primary structure among six mammalian species Thromb Haemost 83; 455
- Shimokawa H. and Vanhoutte P.M. (1989) Impaired endothelium-dependent relaxation to aggregating platelets and related vasoactive substances in porcine coronary arteries in hypercholesterolaemia and atherosclerosis Circ 64; 900
- Shoji M., Abe K., Nawroth P.P. and Rickles F.R. (1997) Molecular mechanisms linking thrombosis and angiogenesis in cancer Trends Cardio Med 7;
- Shoji M., Hancock W.W., Abe K. et al (1998) Activation of coagulation and angiogenesis in cancer: immunohistochemical localisation in situ of clotting proteins and VEGF in human cancer Am J Pathol 152; 399
- Shoji T., Nishizawa Y., Fakumoto M., Shimamura K., Kimura J., Kanda H., Emoto M., Kawagishi T. and Morii H. (2000) Inverse relationship between circulating oxidised low density lipoprotein (oxLDL) and anti-oxLDL antibody levels in healthy subjects Atherosclerosis 148; 171
- Siegbahn A., Johnell M., Rorsman C., Ezban M., Heldin C-H. and Ronnstrand L. (2000) Binding of factor VIIa to tissue factor on human fibroblasts leads to activation of phospholipase C and enhanced PDGF-BB-stimulated chemotaxis Blood 96; 3452

- Siess W., Zangl K. J., Essler M., Bauer M., Brandl R., Corrinth C., Bittman R., Tigyi G. and Aepfelbacher M. (1999) Lysophosphatidic acid mediates the rapid activation of platelets and endothelial cells by mildly oxidized low density lipoprotein and accumulates in human atherosclerotic lesions 96(12); 6931
- Simon B.C., Cunningham L.D. and Cohen R.A. (1990) Oxidised low density lipoproteins cause contraction and inhibit endothelium-dependent relaxation in the pig coronary artery J Clin Invest 86; 75
- Slotte J.P., Oram J.F. and Bierman E.L. (1987) J Biol Chem 262; 12904
- Smalley D.M., Lin J.H.C., Curtis M.L., Kobari Y., Stemerman M.B. and Pritchard K.A. Jr. (1996) Native LDL increases endothelial cell adhesiveness by inducing intracellular adhesion molecule-1 Arterio Thromb Vasc Biol 16; 585
- Smirnov V.N. (1990) Vascular signal transduction and atherosclerosis Ann N Y Acad Sci 598; 167
- Smith C., Mitchison M.J., Aruoma O.I., and Halliwell B. (1992) Stimulation of lipid peroxidation and hydroxyl-radical generation by the contents of human atherosclerotic lesions Biochem J 286; 901
- Sommer A., Prenner E., Gorges R., Statz H., Grillhofer H., Kostner G.M., Paltauf F. and Hermetter A. (1992) Organization of phosphatidylcholine and sphingomyelin in the surface monolayer of low density lipoprotein and lipoprotein (a) as determined by time-resolved fluorometry J Biol Chem 267; 24217
- Sorensen B. et al (1999) Factor VIIa-induced p44/42 mitogen activated kinase activation requires the proteolytic activity and is independent of the tissue factor cytoplasmic domain J Biol Chem 274;21349
- Sparrow C.P. and Olszewski J. (1992) Cellular oxidative modification of low density lipoprotein does not require lipoxygenases Proc Natl Acad Sci USA 89;128
- Sparrow C.P. and Olszewski J. (1993) Cellular oxidation of low density lipoprotein is caused by thiol production in media containing transition metal ions J Lipid Res 34; 1219
- Spengers E.D. and Kluft C. (1987) Plasminogen activator inhibitors Blood 69; 381
- Sprengers E.D. and Kluft C. (1987) Plasminogen activator inhibitors Blood 69; 381
- Stabb M.E., Simari R.D., Srivatsa S.S., Hasdai D., Pompili V.J., Holmes D.R. and Schwartz R.S. (1997) Enhanced angiogenesis and unfavourable remodelling in injured porcine coronary artery lesions: effect of local basic fibroblast growth factor delivery Angiology 48(9); 753

- Stalenhoef A.F.H., Kleinveld H.A., Kosmeijer-Schuil T.G., Demacker P.N.M. and Katan M.B. (1993) *In vivo* oxidised cholesterol in atherosclerosis Atherosclerosis 98; 113
- Stary H.C. (1989) Evolution and progression of atherosclerotic lesions in coronary arteries of children and young adults Arteriosclerosis 9;1
- Stary H.C., Chandler A.B., Dinsmore R.E., Fuster V., Glagov S., Insull W., Rosenfeld M.E., Schwartz C.J., Wagner W.D. and Wissler R.W. (1995) A definition of advanced types of atherosclerotic lesions and a histological classification of atherosclerosis Circ 92; 1355
- Stary H.C., Chandler A.B., Dinsmore R.E., Fuster V., Glagov S., Insull W., Rosenfeld M.E., Schwartz C.J., Wagner W.D. and Wissler R.W. (1995) A definition of advanced types of atherosclerotic lesions and a histological classification of atherosclerosis Circ 92; 1355
- Steinberg D. (1991) Circulation 84; 1420
- Steinberg D. (1997a) Lewis A. Conner memorial lecture: oxidative modification of LDL and atherogenesis Circ 95; 1062
- Steinberg D. (1997b) Low density lipoprotein oxidation and its pathobiological significance J Biol Chem 272(34); 20963
- Steinberg D. and Witzum J.L. (1990) Lipoproteins and atherogenesis: current concepts JAMA 264; 3047
- Steinbrecher U.P., Parthasarathy S., Leake D.S., Witzum J.L. and Steinberg D. (1984) Modification of low density lipoprotein by endothelial cells involves lipid peroxidation and degradation of low density lipoprotein phospholipids Proc Natl Acad Sci USA 81; 3883
- Steinbrecher U.P., Witzum J.L., Parathsarathy S. and Steinberg D. (1987) Decrease in reactive amino groups during oxidation or endothelial cell modification of LDL. Correlation with changes in receptor-mediated catabolism Arteriosclerosis 7; 135
- Steinbrecher U.P., Zhang H.F. and Lougheed M. (1990) Role of oxidatively modified LDL in atherosclerosis Free Radical Biol Med 9; 155
- Stephens N.G., Parsons A., Schofield P.M., Kelly F., Cheeseman K., Mitchison M.J. and Brown M.J. (1996) Randomised controlled trial of vitamin E in patients with coronary disease: Cambridge Heart Antioxidant Study (CHAOS) Lancet 347; 781
- Stiko-Rahm A., Hultgardh-Nilsson A., Regnstrom J., Hamsten A. and Nilsson J. (1992) Native and oxidised LDL enhances production of PDGF AA and the surface

expression of PDGF receptors in cultured human smooth muscle cells Arterioscler Thromb 12; 1099

- Strehler E.E. (1991) Recent advances in the molecular characterisation of plasma membrane Ca^{2+} pumps J Memb Biol 120(1); 1-15
- Strehler E.E., Heim R., Carafoli E. Molecular characteristics of plasma membrane Ca^{2+} pump isoforms Adv Exp Med Biol 307; 251-261
- Strickberger S.A. et al (1988) Evidence for increased aortic plasma membrane calcium transport caused by experimental atherosclerosis in rabbits Circ Res 62; 75
- Stubbs M.T. and Bode W. (1993) A player of many parts: the spotlight falls on thrombin's structure 69;1
- Suefuji H. et al (1997) Increased plasma tissue factor levels in acute myocardial infarction Am Heart J 134; 253
- Suzuki K., Dahlback B. and Stenflo J. (1982) Thrombin-catalyzed activation of human coagulation factor V J Biol Chem 257; 6556-6564
- Taeymans Y., Theroux P., Lesperance J. and Waters D. (1992) Quantitative angiographic morphology of the coronary artery lesions at risk of thrombotic occlusion Circulation 85; 78
- Tagaki T. and Doolittle R.F. (1974) Analytical examination of oxidized free and esterified 7-ketocholesterol and related oxysterols in human plasma incubated with copper Biochemistry 13; 750-756
- Tamasawa N. and Takebe K. (1992) Tohoku J, Exp Med 168; 37
- Taniguchi T., Kakkar A.K., Tuddenham E.G.D., Williamson R.C.N. and Lemoine N.R. (1998) Enhanced expression of the urokinase receptor induced through the tissue factor: factor VIIa pathway in human pancreatic cancer Cancer Res 58; 4461
- Taubman M.B., Fallon J., Schecter A.D., Giesen P., Mendlowitz M., Fyfe B., Marmur J.D. and Nemerson Y. (1997) Thromb Haem 88; 200
- Teng B A., Sniderman R.M., Krauss P.O., Kwiterovich P.O., Milne R.W., and Marcel Y.L. (1985) Modulation of Apolipoprotein B antigen determinants in human low density lipoprotein subclasses J Biol Chem 260; 5067-5072
- Thiruvikraman S.V., Guha A., Roboz J., Taubman , Nemerson Y. and Fallon J.T. (1996) In situ localisation of tissue factor in human atherosclerotic plaques by binding of digoxigenin-labeled factors VIIa and X Lab Invest 75(4); 451
- Thomas A.C., Davies M.J., Dilly S., Dilly N. and Franc F. (1986) Potential errors in the estimation of coronary artery stenosis from clinical arteriography with reference to the shape of the coronary arterial lumen Br Heart J 55; 129

- Toole J.J., Knopf J.L., Wozney J.M., Sultzman L.A., Buecker J.L., Pittman D.D., Kaufman R.J., Brown E., Shoemaker C., Orr E.C., Amphlett G.W., Foster W.B., Coe M.L., Knutson G.J., Fass D.N. and Hewick R.M. (1984) Nature 312; 342-347
- Toshima S.I., Hasegawa A., Kurabayashi M., Itabe H., Takano T., Sugano J., Shimamura K., Kimura J., Michishita I., Suzuki T. and Nagai R. (2000) Circulating oxidised low density lipoprotein levels: a biochemical risk marker for coronary heart disease Arterio Thromb Vasc Biol 20; 2243
- Tracy P.B., Nesheim M.E. and Mann K.G. (1981) Coordinate binding of factor Va and factor Xa to the unstimulated platelet J Biol Chem 256; 743-751
- Tracy R.E., Devaney K. and Kissling G. (1985) Characteristics of the plaque under a coronary thrombus 405; 411
- Tribble D.L., Holl L.G., Wood P.D. and Krauss R.M. (1992) Variations in oxidative susceptibility among six low density lipoprotein subfractions of differing density and particle size Atherosclerosis 93; 189-199
- Tribble D.L., Van der Berg J.J.M., Motchnik P.A., Ames B.N., Lewis D.M., Chait A. and Krauss R.M. (1994) Oxidative susceptibility of low density lipoproteins subfractions is related to their ubiquinol-10 and α-tocopherol content PNAS USA 1994; 1183
- Tsuchiya S., Yamabe M., Yamaguchi Y., Kobayashi Y., Konno T. and Tada K. (1980) Establishment and characterization of a human acute monocytic leukaemia cell line (THP-1) Int J Cancer 26;171-176
- Van der Wal A.C., Becker A.E., van der Loos C.M. and Das P.K. (1994) Site of intimal rupture or erosion of thrombosed coronary atherosclerotic plaques is characterised by an inflammatory process irrespective of the dominant plaque morphology Circulation 89; 36
- Van Hinsbergh V.W.M., van Scheffer M., Havekes L. and Kempen H.J.M. (1986) Biochim Biophys Acta 878; 49
- van't Veer C., Hackeng T.M., Delahaye C., Sixma J.J., Bouma B.N. (1994) Activated FX and thrombin formation triggered by tissue factor on endothelial cell matrix in a flow model: effect of the tissue factor pathway inhibitor Blood 84; 1132
- Varadi K., Siekman J., Turecek P.L., Schwarz P. and Marder V.J. (1999) Phospholipid bound tissue factor modulates both thrombin generation and APC-mediated factor Va inactivation Thromb Haem 82; 1673
- Vehar G.A. and Davie E.W. (1980) Preparation and properties of bovine factor VIII (antihemophilic factor)Biochemistry 19; 401-410

- Vehar G.A., Keyt B., Eaton D., Rodriguez H., O'Brien D.P., Rotblat F., Oppermann H., Keck R., Wood W., Harkins R.N., Tuddenham E.G.D., Lawn R.M. and Capon D.J. (1984) Nature 312; 337
- Versteeg H.H., Hoedemaeker I., Diks S.H., Stam J.C., Spaargaren M., van Bergen en Henegouwen P.M.P., van Deventer S.J.H. and Pepperlenbosch M.P. (2000) FVIIa/tissue factor-induced signalling via activation of src-like kinases, phosphatidylinositol 3-kinase and Rac J Biol Chem 275(37); 28750
- Versteeg H.H., Hoedemaeker I., Diks S.H., Stam J.C., Spaargaren M., van Bergen en Henegouwen P.M.P., van Deventer S.J.H. and Peppelenbosch M.P. (2000) FVIIa/tissue factor-induced signaling via activation of src-like kinases, phosphatidylinositol 3-kinase and Rac J Biol Chem 275(37); 28750
- Virchow R. (1856) Phlogose und thrombose in gefassystem, gesammelte abhandlungen zur wisenschaftlichen medicin Frankfurt-am-Main, Germany: Meidinger Sohn 458
- von Rokitansky C. (1852) A manual of pathological anatomy Vol 4. Day G.E., London: Sydenham Society 261
- Vrana J.A., Stang M.T., Grande J.P. and Getz M.J. (1996) Expression of tissue factor in tumour stroma correlates with progression to invasive breast cancer: paracrine regulation by carcinoma cell-derived members of the transforming growth factor β family Canc Res 56; 5063
- Wang T., Yu W. and Powell W.S. (1992) Formation of monohydroxy derivatives of arachidonic acid, linoleic acid, and oleic acid during oxidation of low density lipoprotein by copper ions and endothelial cells J Lipid Res 33; 525
- Watanabe T., Yasuda M. and Yamamoto T. (1999) Angiogenesis by tissue factor *in vitro* and *in vivo* Thromb Res 96(3); 183
- Watson A.D., Navab M., Hama S.Y., Sevanian A., Prescott S.M., Stafforini D.M., McIntyre T.M., La Du B.N., Fogelman A.M. and Berliner J.A. (1995) J Clin Invest 95; 774-782
- Weidner N., Semple J.P., Welch W.R. and Folkman J. (1991) Tumour angiogenesis and metastasis – correlation in invasive breast cancer N Eng J Med 324; 1
- Weinberger J., Ramos L., Ambrose J.A. and Fuster V. (198?) Morphologic and dynamic changes of atherosclerotic plaque at the carotid artery bifurcation: sequential imaging by real time ultrasonography J Am Coll Cardiol 12; 1515
- Weinstein D.B., Carew T.E. and Steinberg D. (1976) Uptake and degradation of low density lipoprotein by swine arterial smooth muscle cells with inhibition of cholesterol biosynthesis Biochim Biophys Acta 424; 404

- Weis J.R., Pitas R.E., Wilson B.D. and Rodgers D.M. (1991) Oxidised low density lipoprotein increases cultured human endothelial cell tissue factor activity and reduces protein C activation FASEB J 5; 2459
- Weisser B., Locher R., Mengden T. and Vetter W. (1992) Oxidation of low density lipoprotein enhances its potential to increase intracellular free calcium concentration in vascular smooth muscle cells Arterioscler Thromb 12; 231
- Wilcox J.N., Smith K.M., Schwartz S.M., and Gordon D. (1989) Localization of tissue factor in the normal vessel wall and in the atherosclerotic plaque PNAS USA 86;2839-43
- Williams J.K., Armstrong M.L., Heistad D.D. (1988) Vasa vasorum in atherosclerotic coronary arteries: responses to vasoactive stimuli and regression of atherosclerosis Circ Res 62; 515
- Wilson I.A. (1998) The mechanism of an inhibitory antibody on TF-initiated blood coagulation revealed by the crystal structures of human tissue factor, Fab 5G9 and TF 5G9 complex J Mol Biol 275; 873-894
- Witzum J.L and Steinberg D. (1991) Role of oxidised lipoprotein in atherogenesis J Clin Invest 88; 1785
- Wojtukiewicz M.Z., Zacharski L.R., Rucinska M., Zimnoch L., Jaromin J., Rozanska-Kudelska M., Kisiel W. and Kudryk B. (1999) Expression of tissue factor and tissue factor pathway inhibitor *in situ* in laryngeal carcinoma Thromb Haem 82; 1659
- Woolf N. and Davies M.J. (1992) Interrelationship between atherosclerosis and thrombosis: In Fuster V., Verstraete M., eds. Thrombosis in cardiovascular disorders. Philadelphia: W.B. Saunders; 41
- World Health Organisation (1985) WHO Tech Rep Serv 143;1
- Yla-Herrtuala S., Lipton B.A., Rosenfeld M.E., Sarkioja T., Yoshimura T., Leonard E.J., Witzum J.L. and Steinberg D. (1991) Expression of monocyte chemoattractant protein 1 in macrophage rich areas of human and rabbit atherosclerotic lesions PNAS USA 88; 5252
- Yla-Herttuala S, Palinski W, Rosenfeld ME, Parthasarathy S, Carew TE, Butler S, Witztum JL, Steinberg D (1989) Evidence for the presence of oxidatively modified low density lipoprotein in atherosclerotic lesions of rabbit and man J Clin Invest 84; 1086
- Yla-Herttuala S., Rosenfeld M.E., Parasarathy S., Glass C.K., Sigal E., Sarkioja T., Witzum J.L. and Steinberg D. (1991) Gene expression in macrophage-rich human atherosclerotic lesions. 15-lipoxygenase and acetyl low density lipoprotein receptor

messenger RNA colocalize with oxidation specific lipid-protein adducts J Clin Invest 87; 1146

- Yla-Herttuala S., Rosenfeld M.E., Parasarathy S., Glass C.K., Sigal E., Witzum J.L. and Steinberg D. (1990) Colocalization of 15-lipoxygenase mRNA and protein with epitopes of oxidized low density lipoprotein in macrophage-rich areas of atherosclerotic lesions Proc Natl Acad Sci USA 87; 6959
- Yoshitake S., Schach B.G., Foster D.C., Davie E. W. and Kurachi K. (1985) Nucleotide sequence of the gene for human factor IX (antihemophilic factor B).Biochemistry 24; 3736
- Zhang H., Basra H.J.K. and Steinbrecher U.P. (1990) Effects of oxidatively modified LDL on cholesterol esterification in cultured macrophages J Lipid Res 31; 1361
- Zhang Y., Deng Y., Luther T., Muller M., Ziegler R., Waldherr R., Stern DM. and Nawroth PP. (1994) Tissue factor controls the balance of angiogenic and antiangiogenic properties of tumor cells in mice J Clin Invest 94(3);1320-7
- Zioncheck T.F., Roy S. and Vehar G.A. (1992) The cytoplasmic domain of tissue factor is phosphorylated by a protein kinase C-dependent mechanism J Biol Chem 267(6):3561-4
- Zucker S., Mirza H., Conner C.E., Lorenz A.F., Drews M.H., Bahou W.F. and Jesty J. (1998) Vascular endothelial growth factor induces tissue factor and matrix metalloproteinases production in endothelial cells conversion of prothrombin to thrombin results in progelatinase A activation and cell proliferation Int J Canc 75; 780
- Zumbach M., Hofmann M., Borcea V., Luther T., Kotzsch M., Muller M., Hergesell O., Andrassy K., Ritz E., Ziegler R., Wahl P. and Nawroth P.P. (1997) Tissue factor antigen is elevated in patients with microvascular complications of diabetes Exp and Clin Endo and Diab 105(4); 206 and comment Tschoepe D. (1997) Activated haemostasis in diabetic microvascular complications: a role for tissue factor? Exp and Clin Endocrin and Diab 105(4); 204
- Zwijsen R.M.L., Oudenhoven I.M.J. and de Haan L.H.J. (1992) Effects of cholesterol and oxysterols on gap junctional communication between human smooth muscle cells Eur J Pharmacol 228; 115